University of Milano-Bicocca

PhD Program in Molecular and Translational Medicine

Molecular and Functional Characterization of Cells with Stem Properties isolated by Sphere Forming Assay from Human Renal Cell Carcinoma Tissues and Cell Lines

Coordinator: Prof. Andrea Biondi

Tutor: Prof. Roberto Perego

Co-tutor: Dott.ssa Silvia Bombelli

Dott.ssa. Maria Anna ZIPETO

Matr. No. 072653

XXVI CYCLE

ACADEMIC YEAR

2012/2013

To my Family

Table of contents

Chapter 1

General Introduction

STEM CELLS

Stem cells (SCs) include totipotent, pluripotent and multipotent cell types that give rise to and are found within tissues of all multi-cellular organisms. These unique cells have two distinct functional features, specifically the capacity to undergo unlimited cell divisions and the ability todifferentiate into specialized cell types. Those specific characteristics make these cells a powerful model system to study cellular identity and early mammalian development.

SCs are used not only as an *in vitro* tool in biomedical research, but also as a cellular source for tissue regeneration and cellular replacement therapies.The inherent regenerative capacity and plasticity of these cells gives them enormous potential in the biomedical research field, and thus they have been the topic of intense scientific, cultural and political debate over the past 20 years. Moreover, SC research has greatly expanded our knowledge about tissue and organ development, cellular repair, tumor biology and has provided novel platforms for drug screening. Thus, SCs representimportant components of innovative strategies in emerging fields such as tissue engineering, gene therapy and cell-based therapeutics.

Definition and classification

SCs are conventionally defined as undifferentiated cells with the capacity for self-renewal, combined with the ability to produce at

least one type of highly differentiated progeny. Four distinct types of SCs have been described, two of which are physiological types, and exist at different stages of life – embryonic stem cells (ESCs) and somatic stem cells (SSCs). A third type of SCs is engineered, or induced from differentiated cell types, and these are known as induced pluripotent stem cells (iPSc). Finally, rare subsets of cells exhibiting some SC properties have been described in almost all cancers, and these are known as cancer stem cells (CSCs).

ESCs are undifferentiated pluripotent cells derived from the inner cell mass of a developing blastocyst. These primitive SCs harbor the unique ability to give rise to all three germ layers: ectoderm, endoderm, and mesoderm.

SSCs, also known as adult SCs, can be found throughout the body after development. Unlike ESCs, SSCs are multipotent and can only differentiate into cells of the organ they originate from, for example a blood stem cell can only differentiate into components of the blood system.

iPSCs were first described in 2006 by Takahashi and Yamanaka by reprogramming of somatic cells through virus-enforced over expression of four embryonic transcription factors Oct3/4, Sox2, c-Myc and Klf4. Similar to ESCs, iPSCs express specific pluripotency genes and surface proteins, give rise to teratomas when injected subcutaneously into immunocompromised mice, andcontribute to different tissues of the developing embryos upon blastocyst injection (Takahashi, 2006).

CSCs are defined as a subpopulation of cancer cells that can self-renew and propagate the cancer, and finally differentiate in all the types of cells found in the original tumor.

SCs can also be classified by the range of commitment options and their lineage potential (Smith, 2006) (Fig.1):

- Totipotent cells have total potential, due to their ability to differentiate not only into all three germ layers, but also into extra-embryonic tissues, such as the cells developing into the placenta. The only cells that can be classified as totipotent are the zygote and the first stages of the embryo.
- Pluripotent cells such as ESCs are derived from the inner cell mass of a pre-implantation blastocyst and have the ability to differentiate into all three germ layers as well as contribute to the germ line in an adult organism:
    - Endoderm-derived tissues includethe gut tube epithelium, the lung,the liver and the pancreas
    - Ectoderm-derived tissues include the central nervous system, the lens of the eye, the ganglia and nerves, the epidermis, hair and mammary glands.
    - Mesoderm-derived tissues includethe skeleton, skeletal muscles, the dermis of the skin, connective tissue, the heart, blood (lymph cells), kidney and spleen.

- Germ line tissues and cells include oocytes or sperm carrying the maternal or paternal genetic material, with a haploid set of chromosomes.

Unlike totipotent cells, pluripotent cells do not have the ability to form extra-embryonic tissues able to support the embryo's growth in the uterus. They can be isolated, adapted and propagated indefinitely under the right conditions in an undifferentiated state *in vitro.*

- Multipotent cells (SSCs) are found within already specialized tissues and can self-renew and differentiate into distinct cell types, but are lineage restricted.

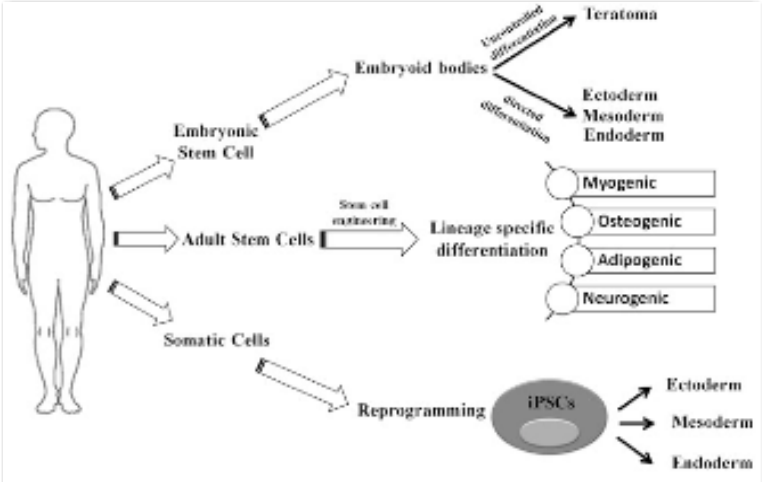

Figure 1: Schematic representation of differentiation process of embryonic stem cells (ESCs), adult stem cells (ASCs), and induced pluripotent stem cells (iPSCs): while ESCs can give rise to all three germ layers via directed differentiation, ASCs have restricted potential to generate myogenic, osteogenic, adipogenic and neurogenic lineages under specified conditions. In contrast to the unidirectional developmental pathways of ESCs and ASCs, iPSCs undergo forced dedifferentiation and then can be directed to form differentiated cells representing all three germ layers, like ESCs (Cai, 2014).

Adult stem cells

It is believed that even post-development, most adult tissues contain functional SSCs, also known as adult SCs, that have the ability to compensate for tissue damage and cell death by generating new cells (Snippert, 2011). Certain adult stem/progenitor cells, in particular bone marrow-derived stem and progenitor cells, may also be attracted to distant, extra-medullary peripheral sites following injury and participate in tissue repair by remodeling the damaged area (Mimeault, 2006). Although adult SCs have markedly less capacity for self-renewal and potency compared with primitive embryonic or pluripotent SCs, they are able to maintain tissue homeostasis throughout life. These cells are thought to be rare, largely quiescent cells capable of both self-renewal, maintenance of the stem cell pool, and differentiation, to ensure production of all mature cells within a tissue throughout the lifespan of an individual (Axelson, 2013). These properties distinguish the "stemness" of these unique cells (Mikkers, 2005). The working definition of stemness encompasses the properties of cellular immaturity, multilineage potential and self-renewal capacity, and also includes features such as functional behaviors and gene expression profiles that correlate with these properties (McCampbell, 2012).

Recent advances in stem cell research have revealed the diverse applications of these undifferentiated cells to both regenerative medicine and cancer therapy. SCs are indeed emerging as an alternative or sole option for treating a wide spectrum of diseases,

such as type I diabetes, kidney disease and a variety of malignancies. Increased understanding of features specific to adult SCs residing in mature tissues might lay the foundation for the development of new cell-based therapies for degenerative disorders. Elucidatingkey stem cell functional mechanisms that, if compromised, can give rise to pathologic conditions such as cancer, requires the ability to distinguish these cells from their differentiated progeny. Prospective isolation of SCs out of tissue samples facilitates the study of pathways that regulate the balance between SC self-renewal and differentiation.

Cancer stem cells

Cancer pathogenesis has been recognized for decades as a multi-step process at both genetic and phenotypic levels. Cytogenetic and molecular genetic analyses have shown that many types of cancer are specifically associated with defined genetic alterations (Mitelman, 2013). According to the classical, or stochastic, view of tumor initiation and progression, the initiating genetic alteration takes place and is required for the immortalization of a differentiated target cell that will subsequently acquire additional genetic hits – or aberrations such as DNA mutations, deletions, or insertions – over time. The acquisition of additional hits exacerbates the deregulated behavior of differentiated target cells, thus leading to the common clinical phenotypesthat characterize each cancer. Traditionally, this model has been relatively well accepted in the study of oncogenesis. However, it soon became clear that this model could not be applied

to all tumors, for instance in the case of Chronic Myeloid Leukemia (CML). In 1977 Fialkow et al. suggested that this disease arose from rare transformed hematopoietic SCs, since the chromosomal translocation 9;22, also known as the Philadelphia chromosome, or BCR-ABL translocation, could be found in most types of differentiated hematopoietic cells. These discoveries led to the concept that oncogenes can be directly responsible for the definition of specific characteristics of the tumor phenotype (Vicente-Duenas, 2013). These observations prompted investigations to determine why every cell within a tumor mass is not capable of initiating a new tumor. At least two alternative models have been proposed to account the cellular heterogeneity and inherent differences in tumor-regenerating capacity for individual tumor-derived cells. The first model, which is in agreement with the classical model of oncogenesis described above, postulates that all tumor cells have equal but low propensity for tumor formation (Nowell, 1976; Kruh, 2003) (Fig. 2). In contrast, the cancer stem cell (CSC) hypothesis states that tumors are organized hierarchically, with a subset of tumor cells at their apex that posses self-renewal and multilineage differentiation potential (Clarke, 2006; Vermeulen, 2008). Thus, not all the cells that form the tumor mass are equally competent for regenerating the tumor (Fig. 2). Moreover, according to the CSC theory, the phenotype of bulk tumor cells is largely genetically dictated by the initiating oncogenic event occurring in the tumor stem cell compartment.

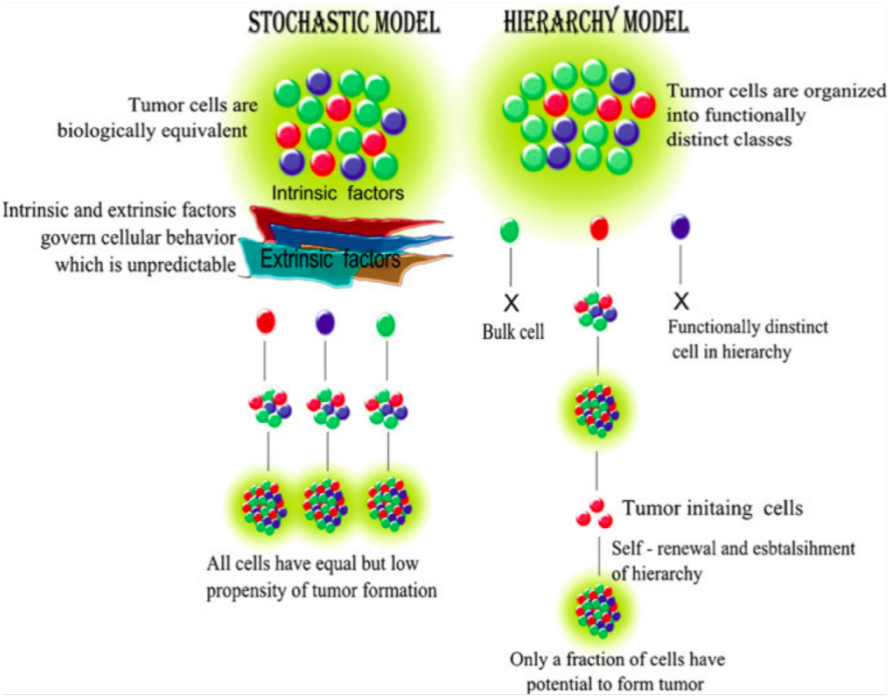

Figure 2: Schematic illustrating the two models of tumorigenesis: stochastic model and hierarchy model that accountsfor tumor cellular heterogeneity (Steinhoff, 2013).

Although SC concepts and their application to cancer were postulated many decades ago, the first evidence for the existence of CSC was provided by Dick and colleagues, in studies showing that leukemic engraftment could only be initiated from blood-derived $CD34^{+}$ $CD38^{-}$ cellular fractions (Bonnet, 1997). In 2003, Clarke and colleagues applied these concepts and experimental approaches for the first time to a solid breast cancer tumor thus leading to the observation that in xenograft assays, as few as 100 $CD44^{+}CD24^{-}$/low cells were tumorigenic, whereas tens of thousands of cells with alternate phenotypes were not (Al Haji, 2003). This paper was rapidly

followed by similar studies in other solid tumors, such as brain, prostate, colon, lung and intestinal cancer (Sing, 2004; Dalerba, 2007).

It is important to note that the cell of origin, which is the normal cell that acquires the first cancer – promoting mutation, is not necessarily related to the CSC. Indeed, although the terms “tumor-initiating cell” and “CSC” have often been used interchangeably, it is still not clear whether tumor-initiating cells are truly SCs.

Two possible origins of CSCs have been proposed. One possibility is that the cell of origin that undergoes the first oncogenic hit is a stem cell. This hypothesis seemed to be the most probable origin of CSCs since adult SCs are the only cells that persist for long periods up to several decades within a tissue, thereby allowing the accumulation of a series of mutations. Since SCs have endogenous machinery for maintaining the capacity for self-renewal, it seems logical that these cells couldsimply maintain an ongoing program, rather than turning on stem cell pathways in more mature cell types. Consequently, fewer mutational hits would be required to transform SCs compared to their mature counterparts. An example where a new tumor cell is reprogrammed, thus generating new malignant cells types instead of normal ones,is in Chronic Myeloid Leukemia (CML). Animal model studies have demonstrated that it is possible to generate tumors in mice that are very similar to the ones in humans, recapitulating their cellular heterogeneity, by restricting the oncogenic alteration only to the stem cell compartment (Perez-Caro, 2009). Alternatively, it is

possible that this process might occur in a differentiated cell that acquires the initiating oncogenic hit(s), and in the subsequent process of oncogene-mediated tumor reprogramming these aberrant cells reacquire stem cell characteristics to become a CSC. In order for this to happen, two pre-requisites are necessary: although it is a differentiated cell, it has to possess enough plasticity in order to be reprogrammable. Moreover, the alteration induced by the oncogene must be able to activate the required programs to confer functional stem cell behavior (Vicente-Duenas, 2013).
Understanding the normal cellular hierarchy within a given tissue represents an important pre-requisite to identifying the cell of origin of cancer.

Histologically, most tumors, and in particular solid tumors, are heterogeneous. This suggests that they conform to a hierarchical model. Tumor heterogeneity is indeed not only a result of the variation in distance from the afferent vasculature and the presence of various inflammatory cells and cancer associated fibroblasts. The CSC hypothesisand the clonal evolution models have been recently put forward to account for intratumoral heterogeneity and intrinsic differences in tumor-regenerating capacity. According to this Darwinian view of tumor progression, new CSCs and their progeny will prevail under selective pressure because they persist in the tumor microenvironment in the presence of therapeutic intervention or changes in nutritional or immune status (Nowell, 1976). Clonal diversity has been well described in both acute myeloid leukemia

(AML) and acute lymphoblastic leukemia (ALL), with leukemic SCs driving the generation of malignant clones, although with kinetically different repopulation abilities (Ding, 2012. Greaves, 2010). Another factor that might explain cellular heterogeneity is that stemness may not be a fixed immutable state, but rather a more fluid condition. According to this concept, SCs might be able to both acquire and lose stemness. In support of this possibility, it has been shown that the cancer-associated phenomenon known as epithelial to mesenchymal transition, induced by paracrine signaling from neighboring tumor cells and cancer associated fibroblasts, leads to the acquisition of a SC phenotype (Alison, 2011). CSCs can be also be functionally heterogeneous, as was shown by studies of colon cancer where lineage-tracing strategies followed the self-renewal of individual human primary colon cancer cells in serial transplantation assays in mice (Dieter, 2011). Although there is increasing evidence of genetic differences that contribute to heterogeneity within a tumor, the extent to which epigenetic mechanisms are involved remains unclear. However, it cannot be assumed that all tumor subclones are substained by CSCs, and some cells types could differentiate in a unidirectional mannerwhen generated by cells with only limited propagating potential.

The adaptability of CSCs as a result of genetic diversity is supported by their apparently lowered susceptibility to drug and irradiation. It is indeed often suggested that CSC are resistant to therapy in the same way that adult SCs are protected against insult. The protective

mechanisms responsible for this characteristic include enhanced quiescence, expression of ATP Binding Cassette (ABC) drug pumps, high expression of anti-apoptotic proteins and resistance to DNA damage (Zhou, 2009). For instance, Bao and colleagues showed that CD133-expressing glioma cells survive ionizing radiation better than $CD133^-$ tumor cells (Bao, 2006). Although some groups have already shown that CSC are more resistant to therapy than bulk tumor cells, the phenomenon of intrinsically therapy-resistant CSCs cannot be applied to all malignancies. For instance, the undifferentiated cells that drive testicular germ cell tumors are more sensitive to radiation than their differentiated cellular progeny (Masters, 2003). Tumor cells that escape therapy may not be intrinsically therapy-resistant, but rather could be the stochastic "winning" clones that survive the tumor cell killing process (Sikic, 2008).

Directly related to the proposed resistance of CSC to therapies, this cell population also can contribute to tumor relapse at either local or distant sites. Some studies have attempted to address whether CSC are involved in metastasis. It has been shown, for instance, that in the invasive front of pancreatic tumors, a distinct subpopulation of $CD133^+CXCR4^+$ CSC was able to determine the metastatic phenotype of the tumor. As a further confirmation of this, depletion of cells expressing these markers abrogated the metastatic potential without affecting the tumorigenic potential, thus suggesting that among CSCs there might exist different subpopulation responsible for diverse phenomena (Hehlmann, 2007). The number of studies demonstrating

the role of CSCs in relapse is still very low and this is mostly due to the lack of appropriate tools and experimental methods. Additional experimental approaches will be needed in order to conclude whether CSCs are responsible for these phenomena or not.

Self-renewal in adult and cancer stem cells

SCs, by definition have the ability to self-renew. Self-renewal is a process by which a cell divides asymmetrically or symmetrically to generate one or two daughter SCs that have a developmental potential similar to that of the parent cell. Since self-renewal is essential for both the maintenance of SCs within adult tissues and the restoration of the stem cell pool after injury, the disruption of this function can lead to developmental defects, premature aging and cancer (He, 2009).

Adult SCs possess a remarkable proliferative capacity, allowing them to engage in massive and repetitive regenerative activities in response to tissue damage. A subset of adult SCs persists in the quiescent state for prolonged periods of time. Although quiescence is not an essential characteristic that defines SCs, the dysregulation or loss of this feature often results in an imbalance in progenitor cell populations, ultimately leading to stem cell depletion. Since quiescent and proliferating stem cell pools can reside in adjacent compartments, sometimes even in the same tissue, it becomes difficult to extrapolate stemcell characteristics such as marker expression or cell cycle behavior from one tissue to another, thus

making the dual capacity for self-renewal and multipotency the only criteria for stemness (Snippert, 2011).

Two main mechanisms are responsible for asymmetric division, one relying on the asymmetric partitioning of cell components that determine the cell fate and another that involves the asymmetric placement of daughter cells relative to external cues, such as the niche. An important example of asymmetric division regulated by an intrinsic mechanism, such as different partitioning of cellular components, is provided by the *C.Elegans* zygote. During development of these organisms, asymmetric division leads to the production of a larger blastomere fated to give rise to ectoderm and one smaller blastomere that produces mesoderm, endoderm and finally germ line through a series of asymmetric cell divisions (Doe, 2001).

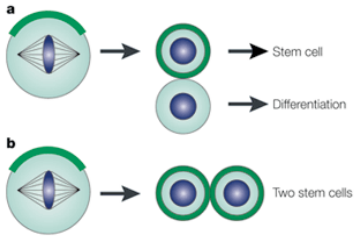

Figure 3. Schematic representation of asymmetric and symmetric division. A:during asymmetric division, spindle orientation and localization are coordinated, giving rise to a differentiating cell and a stem cell. B: During symmetric division, spindle orientation and determinant localization are not coordinated. Determinants segregate equally, giving rise to two equal stem cells

Asymmetric division represents a key mechanism for the maintenance of self-renewal potential in SCs, however it does not allow the expansion of the pool of SCs. Tight control of SCasymmetric cell divisions is important to prevent the formation of aberrant SC pools with uncontrolled proliferation, which might result in overgrowth of tissues (Verga Falzacappa, 2012). On the other hand, when the pool of SCs needs to be expanded, they can undergo symmetric division, thus generating daughter cells that are destined to acquire the same fate (Snippert, 2011). Some mammalian SCs seem to switch between asymmetric and symmetric modes of division throughout life. For instance, both neural and epidermal progenitors switch from symmetric division, typical of the embryonic developmental stage during which they need to expand their pool, to asymmetric divisions that increase the number of differentiated cells during late gestation. Althoughmost adult SCs seem to undergo only asymmetric division, they can actually switch to symmetric division as a response to depletion of the stem cell pool after physiological injuries and pathological condition, thus restoring the stem cell pool.

Cicalese and colleagues showed that states of symmetric and asymmetric division coexist in both normal and CSCs, but at different ratios: while normal SCs mostly divide asymmetrically, CSCs preferentially undergo symmetric divisions. CSCs, indeed, by dividing symmetrically, possess an unlimited replicative potential that allows them to undergo indefinite rounds of cell division, thus boosting the number of proliferating SCs in the tumor tissue (Cicalese, 2009). It is

important to note that both normal and CSCs exist in two hierarchical subpopulations: quiescent and proliferating. Absolute numbers of quiescent SCs are comparable in normal and CSCs, however, normal SCs are mainly quiescent, whereas CSCs are mainly proliferating. When normal SCs exit their quiescent state to divide, they are exposed to genotoxic damage. The accumulation of DNA damage can ultimately lead to a decline in stem cell self-renewal potential and eventual functional exhaustion (Rossi, 2007). The accumulation of DNA damage in SCs is a risk that has to be tightly regulated because potential mutations occurring in SCs can be transmitted to both progenitor and daughter SCs. In order to protect them from the accumulation of DNA damage, normal SCs are kept in a non-cycling stage. In the so-called quiescent or dormant state, adult SCs stay frozen in a semi-permanent G0 phase of the cell cycle, by slowing down their overall energy metabolism (Trumpp, 2010). It has been shown that the CDKI p21, by restricting the cell cycle of adult SCs, acts as the guardian of the quiescent state. In contrast tonormal adult SCs, CSCs hyperproliferate during tumorigenesis and are more vulnerable to DNA damage accumulation, and do not undergo pool exhaustion. It has been shown previously that the up-regulation of p21 representsa mechanism by which CSCs are able to maintain their quiescent pool, by preventing excessive accumulation of DNA damage and functional exhaustion (Viale, 2009).

Regulation of self-renewal in Cancer Stem Cells

To date, the precise mechanisms controlling stem cell self-renewal in different contextsincluding homeostasis, stress and malignancy have not been fully clarified. Stem cell self-renewal is tightly regulated by both intrinsic and extrinsic mechanisms. Integration of extrinsic cues from the microenvironment with intrinsic signaling pathways allows adult SCs to circumvent premature exhaustion of the stem cell pool, through the production of growth factors, cytokines, secreted proteins and cell-cell interactions (Verga Falzacappa, 2012). Vital intrinsic signals include developmental regulators such as Wnt, Notch and Hedgehog pathways, which are fundamental players in maintaining the balance between self-renewal and differentiation. Similarly, cell survival and cell cycle pathways, such as p53 and cyclin-dependent kinase inhibitors (CDKI) represent additional intrinsic regulatory mechanism of stem cell self-renewal (Chen, 2010). The most prevalent view is that SCs can undergo either asymmetric or symmetric division depending on whether they need to preserve or expand their pool (Fig. 3A and B) (Morrison, 2006). Asymmetrical stemcell division represents a strategy by which SCs can accomplish both self-renewal and differentiation. It results in the generation of daughter cells with different fates, which is often revealed by an uneven distribution of cell types among stem cell progeny. It is important to emphasize that most of the mechanisms that drive CSC self-renewal result from an aberrant regulation of normal SCs self-renewal. The disruption of the delicate balance between self-

renewal and differentiation in normal SCs can lead to the aberrant self-renewal properties that characterize CSCs. The identification of the mechanisms responsible for aberrant self-renewal that may be targetable by therapies, might represent an important step toward the generation of new CSC targeted therapies.

Extrinsic self-renewal regulator: the CSC niche

The niche concept was first introduced in 1978 by Schofield, who proposed that the maintenance of SCs requires association with a complement of cells, or a "niche" (Schofield, 1978). However this hypothesis was largely neglected until studies in *Drosophila* demonstrated that supporting stromal cells are important for the maintenance and self-renewal of germ-line SCs (Lin, 2002). However SC niches have also been identified in mammalian tissues such as the intestinal epithelium, epidermal structures and the bone marrow (Moore, 2006). Because SCs are usually regulated by both cellular niche-resident cells and non-cellular components, the SC niche is defined as the local tissue microenvironment that houses and maintainsSCs (Morrison, 2008). Deregulation of specificSC niches has been implicated in many diseases, including aging, cancer and degenerative diseases (Voog, 2010).

Recent data show that CSCs also rely on a niche, called the "cancer stem cell niche" that is analogous to the one where the normal SCs reside, and controls CSC differentiation and proliferation. A representative example is observed in both AML and CML, where the

expression of CD44 was shown to be essential for the homing and engraftment of CSCs to their niche. CD44-expressing leukemia SCs adhere to the niche and bind to hyaluronic acid expressed by cells on the surface of sinusoidal endothelium or endosteum in the bone marrow, and is a crucial componentof the niche's SC maintenance ability (Jin, 2006; Krause, 2006). Compared to the hematopoietic system, the study of the CSC niche in solid tumors is relatively new.

The anatomical unit of the CSC niche is complex and is composed of diverse stromal cells, such as a vascular network, mesenchymal and immune cells, extracellular matrix and soluble factors derived from niche cells (Fig.4). The involvement of the vascular network has recently been illustrated by a study showing that vascular niches within brain tumors are abnormal and this contributes to CSC self-renewal and proliferation, thus acting in contrast to the niches found in the normal tissue that usually control SC function (Calabrese, 2007). Another important micro environmental component is the extracellular matrix, which plays an essential role in anchoring CSC to the niche, thus modulating their function (Kessenbrock, 2010).

Understanding the mechanisms controlling the interaction CSCs and their niche may pave the way towards developing new strategies for cancer that can target not only CSCs directly, but also modulate the surrounding microenvironment that controls their proliferation and behavior.

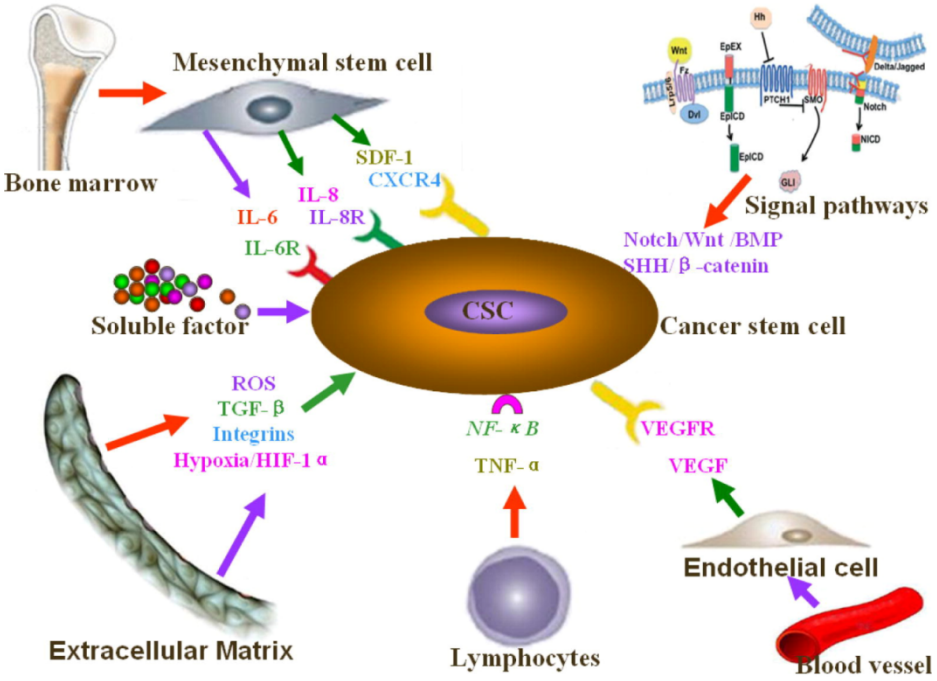

Figure 4: Schematic representation of the cancer stem cell niche. The cancer stem cell microenvironment contains multiple sources of cytokine production. The niche plays a crucial role in the maintenance of cancer stem cells functions such as pluripotency and self-renewal (Yi, 2012)

Self-renewal regulators: developmental pathways in Cancer Stem Cells

In order to better understand the nature of CSCs, as well as to identify potential therapeutic targets, it is important to achieve a better understanding of self-renewal pathways fueling CSC propagation. In many instances, CSCs appear to depend on the aberrant regulation of the same primordial cell fate regulatory pathways that regulate normal SC self-renewal (Fig.5).

Among these pathways, the **Wnt/βcatenin** pathway is a key developmental pathway and its activation in SCs is likely to be a key event of tumor initiation in many tissues, such as intestine and pituitary glands (Barker, 2009; Gaston-Massuet, 2011). Jamieson and colleagues were one of the first groups to show the importance of a self-renewal pathway in maintaining leukemia SCs. They demonstrated that aberrant Wnt/βcatenin pathway activation was the driving force in human blast crisis leukemia SC propagation (Jamieson, 2004; Abrahamsson, 2009). More recently, increased Wnt/β-catenin signaling has been implicated in the maintenance of breast CSCs and in the tumorigencity of stem-like colon cancer cells (Korkaya, 2009, Vermeulen, 2010). The importance of the Wnt pathway in the regulation of CSC self-renewal is further confirmed by the introduction of a number of small molecules targeting this pathway, that are either in the discovery stage or early phase clinical trials. A variety of small molecules are directed against various Wntreceptor interactions and cytosolic and nuclear signaling. Interestingly, many of the cell markers used to isolate CSCs, such as for instance Lgr5 and CD44 are direct Wnt targets (Takebe, 2010).

Notch signaling plays an important role in normal embryonic development, as well as in adult tissue repair. The Notch signaling pathway is highly conserved in mammals and has been implicated in several hematopoietic and solid tumors, where one or more Notch paralogs showed oncogenic activity (Miele, 2006; Leong, 2008). The strongest evidence for a role of Notch in CSCs comes from breast

cancer (Korkaya, 2007), embryonic brain tumors (Fan, 2006) and gliomas (Fan, 2010). Gamma secretase inhibitors are able to abolish the formation of mammospheres from a variety of human breast cancer cell lines as well as primary patients. Activation of the Notch pathway has been implicated also in the regulation of CSC frequency in gastrointestinal tumors (Hoey, 2009).

The **Hedgehog** pathway is a crucial mediator of normal tissue development (Ingham, 2001). Emerging data from many human human malignancies including glioma, multiple myeloma, myeloid leukemia, breast cancer and colorectal cancer have suggested that Hedgehog signaling regulates CSC function (Tazekaki, 2011; Peacock, 2007; Zhao, 2009; Clement, 2007; Varnat, 2009). These studies suggest that Hedgehog signaling might dictate CSC fate determination that includes self-renewal and differentiation.

The **JAK/STAT** pathway is another key regulator involved in cell fate, including apoptosis, differentiation and proliferation, in response to growth factors and cytokines. Evidence supporting a role forthe JAK/STAT pathway in CSCs comes from Head and Neck Squamous cell carcinoma, where $CD44^{+}ALDH^{+}$tumors exhibiting phosphorylation of STAT3 had a worse prognosis. Moreover, $CD44^{+}ALDH^{+}$ and phosphorylated STAT3cells showed increased tumorigenic potential and higher radioresistance. Pharmacological inhibition of STAT3 not only inhibited *in vitro* tumorigenicity, but also formation of spheres, resistance to radiation and Bcl-2 expression, thus showing the

importance of STAT3 activation in the maintenance of CSCs (Chen, 2007).

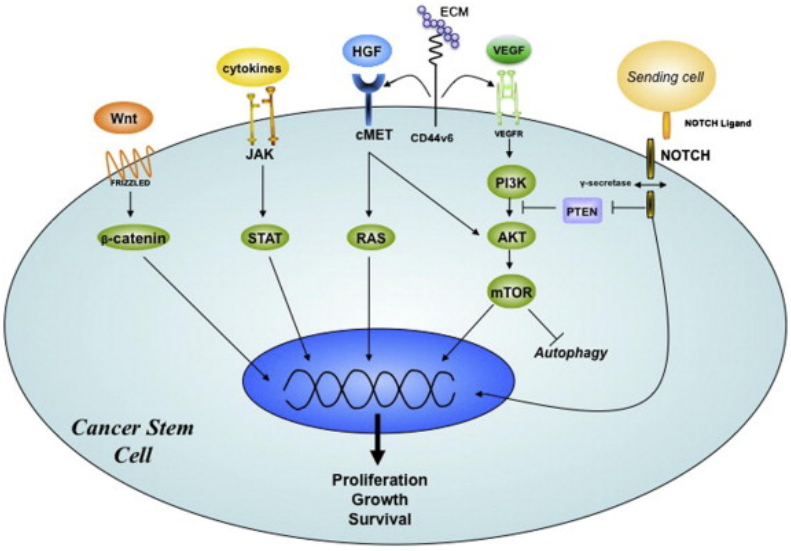

Figure 5. Main molecular pathways implicated in CSCs (Moncharmont, 2012).

Several reports have shown that **hypoxia and hypoxia inducible factors** (HIFs) are involved in the maintenance of a more stem-like state in normal tissues (Clarke, 2009; Moreno-Manzano, 2009) (Fig.6). HIFs have been shown to be crucial regulators of SC phenotypes by cross-talking with signaling pathways such as Notch and the pluripotency-associated transcription factor OCT4. Increasing experimental evidence suggest that hypoxia and HIFs regulate subpopulations of CSCs. Soeda and colleagues, for instance, demonstrated that culture in hypoxic conditions and subsequent

activation of HIFs expands the subpopulation of cells positive for the CSC marker CD133 (Soeda, 2009). Furthermore, Mc Cord and colleagues showed that hypoxia not only increased the expression of SC markers, but also enhanced the stem-like behavior of these cells by increasing sphere formation efficiency. (McCord, 2009). Interestingly, different studies have demonstrated that HIF2α, specifically, can increase the expression of SC associated genes and confer tumorigenic potential to non-SCs (Heddleston, 2009). HIf2α transcriptionally regulates OCT4, which together with NANOG, is part of the unique signature of cancer cells (Covello, 2006). Together, these studies showed that HIf2α might alter basic genetic activity of cancer cells, thus promoting a more stem-like phenotype in stem and non-stem cancer cells.

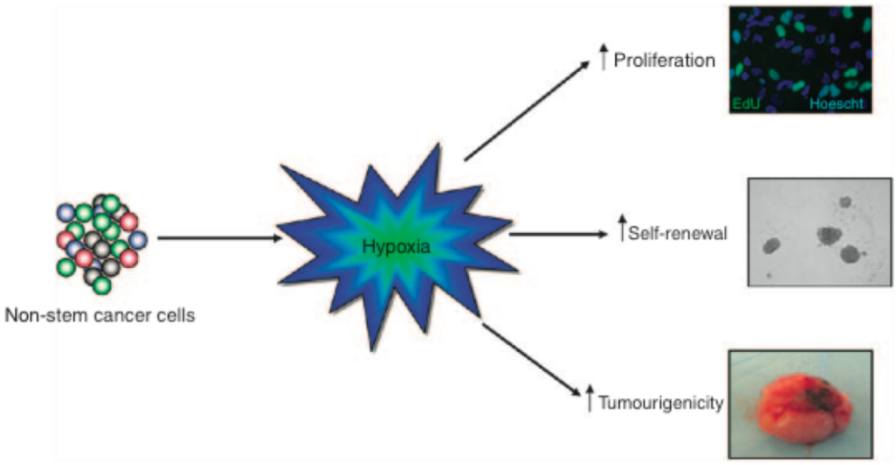

Figure 6: Hypoxia and the hypoxia inducible factors (HIFs) can promote a stem-like phenotype. Recent experimental evidence has demonstrated that HIFs have crucial roles in cancer. Following culture in low-oxygen conditions, the phenotypical non-stem cancer cells were pushed to a more stem-like state. Several important characteristics of the cancer stem cell population, such as enhanced growth, self-renewal (evidenced by spheroid formation), and tumorigenesis, have been shown to increase in the non-stem fraction of cancer cells following hypoxic culture (Heddleston et al, 2009). Non-stem cells increase their rate of proliferation above what is normally seen at 20% oxygen. This can be visualized by EdU retention (an analogue of BrdU). Hypoxia has also been shown to promote self-renewal, which can be measured by spheroid growth starting from a single cell. Non-stem cancer cells expressing constitutively active HIF2a protein have been demonstrated to have increased tumorigenicity in mouse models (Heddleston, 2010)

It has been shown that **microRNA (miRNAs)** regulate SC self-renewal and differentiation by targeting components that determine the SC fate. MiRNAs are a class of multi-functional small non-coding 22 nucleotide long single-stranded RNA. MiRNA biogenesis can be regulated at each of these steps through accessory protein to ensure proper miRNA homeostasis. The disruption of this regulation could be responsible for generation of pathological conditions. Each miRNA can target hundreds of genes and are involved in a broad range of biological processes, including embryonic development, self-renewal and differentiation of SCs, as well as cell division, initiation and progression of cancers (Liu, 2011). Mir145, for instance, have been described as regulator of self-renewalsince it directly regulates OCT4, SOX2 and KLF4, thus inhibiting SC self-renewal and inducing differentiation (Xu, 2009). Concerning CSCs, it has been shown that CSCs may display different miRNA expression profiles that vary by tumor type (Qian, 2008). A recent report define distinct miRNA expression patterns in different stem/progenitor cell populations, demonstrating the downregulation of tumor suppressor miRNAs, such as let-7 and mir34, which revealed a coordination of miRNA in regulating CSCs self-renewal and cancer cell proliferation (Liu, 2012).

Another mechanism that has been recently shown to be involved in self-renewal regulation is the Adenosine-to-inosine (A-to-I) **RNA editing.**A-to-I editing is a post-transcriptional, site-specific modification process that is catalyzed by Adenosine Deaminase Acting on RNA (ADAR) gene family members. Deletion of ADAR1 in

mice causes widespread apopotosis, defective hematopoiesis and embryonic lethality, thus suggesting that as well as the other pathways described above, it plays an essential role for embryo-development, cell proliferation and differentiation (Wang, 2004). Since, several models have highlighted the importance of ADAR1 in the regulation of pluripotent and adult SCs, it becomes clear that a disruption in this mechanism can lead to the aberrant activation of pluripotency and self-renewal (XuFeng, 2009, Qiu, 2013) Although RNA editing levels seems to be lower in cancer tissues compared to their normal counterparts, evidences of RNA editing involvement in CSCs regulation come from Chronic Myeloid Leukemia, where Jiang and colleagues showed that ADAR1 promotes Chronic Myeloid Leukemia progression. Aberrant ADAR1 activation in chronic myeloid leukemia indeed endows myeloid progenitors with self-renewal capacity thus leading to leukemia SC generation (Jiang, 2013). The study of these pathways becomes a crucial step toward a better understanding of the mechanism that fuel CSCs propagation that could represent new targets for therapies aimed to eliminate CSCs.

Identification and isolation of cancer stem cells

The identification of markers expressed by SCs is essential for their purification and their study. While adult SCs have been isolated near to homogeneity, the CSC subset appears to be increasingly more complicated, depending on the tissue analyzed. Different methodologies are used to identify and then isolate CSCs population from tissues. Most of them exploit SCs properties and include

expression of surface markers, functional assays as well as tumorigenicity evaluations (Fig.7).

Surface marker expression analysis

Due to the easier accessibility of blood forming cells, and the availability of wide-range of well characterized *in vitro* and *in vivo* functional assays, it is not surprising that the first experimental characterization of CSCs came from AML, where the surface marker phenotype $CD34^{+}CD38^{-}$ identified a small subpopulation of cells that was able to propagate leukemia, while cells expressing both CD34 and CD38 were not despite having the morphological phenotype of leukemic blasts (Bonnet, 1997). This approach was further extended to solid tumors, such as pancreas, breast, brain, prostate, lung and colorectal tumors (Li, 2007; Ricci-Vitiani, 2007; Singh, 2004; Al-Hajj, 2003) where cell surface markers of normal SCs formed the basis of CSCs identification and characterization. A phenotypic identification of CSCs exploiting normal SCs markers suggests that the identification of CSCs mainly relies on surface marker expression analysis. However, applicability of this strategy in tumors from organs such as ovary, where the normal SC signature has not been identified yet, demands an alternative strategy to identify appropriate CSC markers. The validity of the use of surface markers is not certain in all the case, since several CSC markers that are currently applied for isolation of CSCs are not known to be expressed in normal tissues, but may be present in other tissues (Kusumbe, 2009). As well as for other tissues, also in the kidney the surface markers used for the identification of

adult renal SCs (CD133) do not identify the renal CSC, which is instead characterized by the surface marker CD105. The existence of multiple and heterogeneous subpopulations of CSCs within the same tumor represents a drawback, that demands switching to functional definitions in CSC identification schemes (Visvader, 2008).

Side population analysis

Another approach that has been used to identify CSCs population is the use of the side population assay (Wu, 2007). This assay exploits the high expression level of cell membrane adenosine triphosphate (ATP)-binding cassette (ABC) transporter protein that provide a cell the ability to efflux, by using ATP, chemotherapeutic drugs and certain dyes, such as the DNA stain Hoechst (Wu, 2008). Since ABC transporters also serve to detoxify cells by expelling cytotoxic agents from cells and chemotherapy drugs are also substrate for these efflux pumps, they might be a mechanism for drug resistance in CSCs. Goodell initially described the isolation and characterization of cells by this method in 1996, using mouse bone marrow. It was observed that when entire bone marrow populations were stained using Hoechst33342 and observed simultaneously for fluorescence at two emission wavelengths, cells with maximum efflux capacity segregated as a side population next to the Hoechst bright population. The side population not only expressed SCs markers such as Sca1 but is also capable of reconstituting the bone marrow of irradiated mice upon transplantation (Challen, 2006). In tumors, the side population (SP) contained the sphere forming population and could also rapidly

initiate tumors at high frequency. Moreover, SP cells are able to undergo asymmetric division, thus giving rise to both a side population fraction and a non-side population fraction. The use of side population assay allowed the identification of CSCs in several tumors, such as bladder, endometrial, ovarian, hepatocellular, pancreatic and lung. However, the identification of putative CSCs by using the side population assay is complicated because of the inherent toxicity of the dye. Moreover, since SCs have been isolated from the non-side population cell fraction as well, the dye efflux is not sufficient to detect SCs (Bapat, 2010; Kim, 2005; Wu, 2007).

ALDH activity

ALDH is a cytosolic isoenzyme involved in the detoxification of intracellular aldheydes by oxidation and conversion of retinol to retinoic acid and it is responsible for the resistance to chemotherapeutic agents (Russo, 1988). Visus and colleagues were the first to describe the use of ALDH as putative marker in head and neck squamous cell carcinoma (Visus, 2007). High ALDH activity has been demonstrated in CSCs from tumors such as breast, colon and lung cancer and many studies have showed poorer outcome, worse overall survival and chemo radiation resistance associated with overexpression of ALDH (Ohi, 2011)

CSC isolation by clonogenic assay

The clonogenic assay is another alternative strategy for the isolation of CSCs and was first carried out on primary tumor cells with mouse

myeloma by Puck and colleagues, and later human myeloma and other tumor cells were also cultured (Puck,1956; Park, 1980, Courtenay, 1978). These clonal assays represented the breaking point for the establishment of a SC model of human tumor growth. The clonogenic assay is based on the rationale that CSCs are able to form colonies from a single cell more efficiently than their progeny (Franken, 2006). According to this protocol, colonies derived from the CSC fraction, after usually 21 days of incubation, are stained with crystal violet or nitro-blue-tetrazolium, counted and measured and these parameters are compared with the same parameters observed in colonies derived from a non-CSC fraction. It is generally observed that colonies derived from CSC show both number and size greater than colonies derived from non-CSCs. The clonogenic assay, as well as the use of surface markers and side population is, however, not fully reliable, mostly because of technical considerations, where the temperature of the agar, or proper cell dilution are examples of critical steps in order to ensure that each colony results from a single cell (Tirino, 2013).

Sphere forming assay

Another strategy for isolation and characterization of CSCs is the sphere-forming assay, which is similar to the clonogenic assay in that it requires that CSCs are able to grow in non-adherent conditions. Initially exploited for the isolation of neural SCs, this assay have subsequently been described for the isolation of normal and CSCs from various tissues, such as brain (Reynolds, 1992), breast (Dontu,

2003), pancreas (Rovira, 2010) and prostate (Lawson, 2007). Although the mechanism by which CSCs preferentially form clonal spheres is still not known, this assay is based on assessing the self-renewing populations of tumor cells that are able to grow in suspension in serum-free conditions. Although this is thought to be a characteristic of CSCs, some cell lines appear to display this ability to be ubiquitously. Also this method is laden with technical difficulties, such as the inability to distinguish the spheres from aggregates at higher cell densities as well as the ability to detect quiescent cells (Pastrana, 2011). These problems can easily be bypassed by plating a single CSC in serum free conditions. In this way, if this single cell is a true CSC, it will be able to form primary, secondary and tertiary spheres.

Tumorigenicity in animal models.

The gold standard for the demonstration of CSCs identity is their ability to grow as serially transplantable tumors in immunodeficient hosts, resembling the original tumor and giving rise to cells of different lineages that compose the tissue of origin. Even in the first studies with leukemia in 1997, the final validation of CSCs came from the transplantation of a minority of undifferentiated cells isolated based on surface markers from AML patients in Nonobese Diabetic/Severe Combined Immunodeficiency (NOD/SCID) mice. Through this transplantation, Bonnet and Dick showed that these cells were the only subset within the total population capable of reconstituting the original tumor, including a range of more

differentiated cell types (Bonnet, 1997). These studies showed that CSCs regenerate tumors with a frequency much higher and at a lower cell numbers compared to the tumor bulk cell fraction. As well as other assays, this assay also have some technical considerations: first of all, sorted and transplanted human cancer cells have not only been challenged with various experimental manipulation but have also ended up in dramatically different context compared to their original niche. Moreover, this assay is highly dependent on the linearity of the cell number/ tumor frequency relationship, strain of the murine model, lack of immune response and presence of species-specific signals (Rosen, 2009). Species barriers may impede certain crucial niche functions, such as interactions between adhesion molecules or between growth factors and their receptors. That is why, to reduce this complication, it is possible to provide human growth factors or human stroma elements (Feuring-Buske, 2003; Karnoub, 2007). Moreover, due to the importance of the association of the tumor with the microenvironment, orthotopic models, in which cells are delivered directly to a niche, may be preferred if compared to subcutaneous xenograft. Unfortunately there are no set criteria on which strain of mouse should be used for tumorigenesis assays.

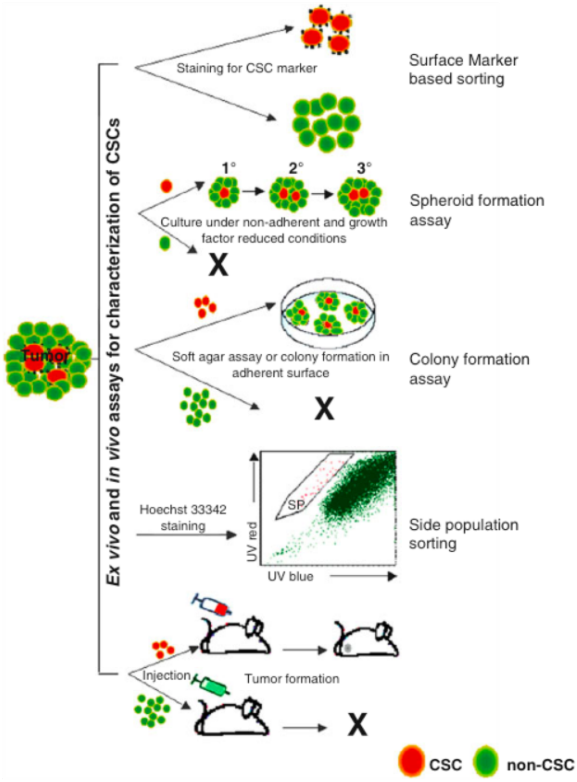

Figure 7. Schematic representing the current ex vivo and in vivo strategies adapted for character- ization of CSCs from blood cancers and diverse solid tumors. Cell surface marker expression based FACS sorting provides the most convenient tool for CSC isolation. However recent studies illustrating existence of phonotypical heterogeneity demands further validation of this approach. The non-adherent sphere assay predicts that CSC can be serially passaged for many cycles and that it generates a tumor sphere resembling the primary sphere in each case. Colony formation assays are also the readout of CSC activity. However CSCs and progenitors cannot be distinguished in these clonal assays. Side population assessment of the is based on the stemness specific functional ability of CSCs to actively efflux dyes such as Hoechst 33342 out of their cytoplasm due to the expression of MDR proteins, such as ABC transporters. The gold-standard functional assay for evaluating the presence of CSCs is transplantation of sorted subpopulations into immuno-compromised mice models (Steinhoff, 2013).

Our laboratory is involved in the study and characterization of renal cell carcinoma and normal kidney by using well-characterized primary cultures as a model. Moreover, we are interested in the isolation and characterization of both renal normal and cancer SCs by using the sphere forming assay. In this section I will summarize some biological, histologic and genetic features of renal cell carcinoma, as well as the state of art for the study of both normal and cancer SCs from human kidney.

RENAL CELL CARCINOMA

Renal cell carcinoma (RCC) accounts for 2-3% of all malignancies in the adult and it's the seventh most common cancer in men and the ninth in women. It is indeed a male predominant disease (2:1) ratio, with a typical presentation around the sixth or seventh decades of life. Patients with this cancer can present with local or systemic symptoms, although most presentations are incidental, since renal mass are incidentally identified on radiographic examination. The classical presentation of RCCs includes the triad of flank-pain, hematuria and a palpable-abdominal mass, all of which have negative prognostic implications. Other common presenting features may be not specific such as fatigue, weight loss or anemia. Despite an increased early detection of incidental renal masses with cross-sectional imaging and subsequent removal with surgery, mortality has increased, thus suggesting that advanced and metastatic disease still predominantly account for the mortality rate in patients with RCC

(Hollingsworth, 2006). An important concept in the study of RCC is that the disease is not one entity but rather a collection of different types of tumors, each derived from the various parts of the nephron and possessing distinct genetic characteristics, histological features and sometimes clinical phenotypes. In 1996 Heidelberg proposed a classification method for RCC according to which it is possible to identify three different histological subtypes: the most common is the clear cell disease that accounts for 70-80% of all RCC, followed by papillary disease 10-15%, the chromophobe 4-5%) and the carcinoma of collecting duct (Kovacs, 1997).

As well as other tumors, such as colon and breast cancer, RCC can be both sporadic tumor and familial. Only about 2-3% of cases are familial and several autosomal dominant syndromes have been described as associated to RCC. Among them the most notable is the Von Hippel Lindau syndrome. The study of familial RCC was really helpful in the understanding mechanism of transformations responsible also for the most common sporadic forms (Linehan, 2003).

Clear cell carcinoma

The most common type of RCC is the clear cell (RCCcc), so named because the high lipid content in the cytoplasm is dissolved during histological preparation methods leaving a clear cytoplasm. At the histological level, RCCcc is characterized by cells with a clear cytoplasm and a compact-alveolar or acinar growth pattern

interspersed with intricate, arborizing vasculature. Moreover, a variable portion of cells with granular eosinophilic cytoplasm may be present (Cheville, 2003). At a genetic level, RCCcc is characterized by complex chromosomal alterations. The most important loss in this tumor type involves 2p, 4q, 6q, 13q, 14q, e Xq chromosome, but the most common genetic aberration involves 3q chromosome (Moch, 2002). Familial cases can be associated by several autosomal dominant syndromes and among them the most notable is the Von-Hippel Lindau syndrome, a highly penetrant disorder that is characterized by the development of several vascular tumor, including clear cell renal cell carcinoma (Lonser, 2003). The tumor suppressor gene responsible for this disease, the Von Hippel Lindau (VHL) gene, is located on chromosome 3. Patients with the Von Hippel Lindau disease inherit a defect on one of the alleles of the gene and RCC arise from the inactivation or silencing of the remaining VHL allele. It is important to underline that VHL defects happen also in the 60% of the sporadic cases, but while familial cases tend to be early onset and multifocal, sporadic RCCcc tend to be late onset and unifocal (Rini, 2009). Another demonstration of the tumor suppressor role of VHL comes from a study showing that the re-introduction of this gene into cultures of renal-cell carcinoma led to the inhibition of the growth (Gnarra, 1996). The identification of this gene as responsible for most of RCCcc case has been really useful not only for the diagnosis and prognosis of this tumor, but in particular for the study of its pathogenesis.

The VHL protein by inhibiting Hypoxia inducible genes, including several encoding proteins such as vascular endothelial growth factor (VEGF), transforming growth factor α (TGF-α) , GLUT-1 transporter and carbonic anhydrase IX (CAIX) regulates important cellular processes such as angiogenesis,cellular growth, glucose uptake and pH regulation. When VHL protein is lost, as a result of the bi-allelic inactivation these proteins are over-expressed, thus creating a microenvironment favorable for the epithelial cell growth and proliferation. When VHL is absent, cells behave as they would do in hypoxic conditions, thus accumulating Hypoxia Inducible Factors (HIFs) and subsequently aberrantly producing growth factors such as the already mentioned VEGF and GLUT-1. The continue action of these growth factors might induce the neoplastic transformation of tubular cells (Linhean, 2003).

The VHL protein, by forming a complex with elonghin proteins C and B, can bind Cul-2 protein, which shows an activity as ubiquitin ligase. This complex is able to promote the ubiquitination and destruction of proteins such as, for instance, hypoxia inducible factor 1α and 2α (HIF1α and HIF2α), that are key regulators of the hypoxic response in the organisms. Recent research on VHL-defective RCC cell lines and on RCCs from patients with VHL disease, suggested that the deregulation of HIFα and especially HIF2α plays an important role in the RCCcc carcinogenesis. It has been shown that VHL-/- RCC cell lines seem to produce both HIF1α and HIF2α or HIF2α alone (Maxwell, 1999). Moreover, the elimination of HIF2α is sufficient to

suppress VHL-/- tumor growth *in vitro* (Kondo, 2003) In addition, it is becoming clear that HIf-1α, more than HIf2α can undergo proteosomal degradation in VHL-/- RCC cells because of either alternative ubiquitin ligase or a direct interaction with the proteasome (Kong, 2007). Finally, tumor suppression by VHL can be overridden by HIF2α but not by HIF1α. These studies, together with examination of kidney tumors from VHL patients suggest that HIF2α is more oncogenic than HIF1α (Mandriota, 2002). Studies of transcriptional selectivity, have indeed identified exclusive HIF1α targets, exclusive HIF2α target genes and genes that are responsive to both HIF1α and HIF2α. Interestingly, Raval et colleagues showed that pro-tumorigenic genes, such as cyclin D1, TGFα and VEGF respond exclusively to HIF2α, while proapoptotic genes responds negatively to HIF2α but positively to HIF1α(Raval, 2005). Moreover, it has been shown that HIF1α and HIF-2α differentially cross-talk with collateral signaling pathways, such as C-MYC and OCT4, that are activated by HIF2α and respectively antagonized and not affected at all by HIF1α (Gordan, 2006,2008). In addition to VHL, other genetic abnormalities on chromosome 3 have been shown to be involved in the pathogenesis of RCC, such as for instance the translocation of chromosome 3p at a fragile site at 3p1 (Cohen, 1979).

Papillary RCC

Papillary renal cell carcinoma (RCCp) represents a small fraction of renal tumors and originates from the proximal convoluted tubule

epithelium (Baldewijns, 2008). This tumor has been further divided into type 1 and type 2 on the bases of hystopathological features. Type 1 tumors are papillary lesions covered with small cells with pale cytoplasm and small nuclei with indistinct nucleoli, while type 2 tumors are papillary lesions covered by large cells with abundant eosinophilic cytoplasm, larger spherical nuclei and well defined nucleoli (Cohen, 2005).

Chromofobe RCC

The chromophobe RCC (RCCcr), originates from the epithelium of distal tubule and its histology show large, polygonal cells with finely reticulated cytoplasm, distinct cell borders and atypical nuclei with perinuclear halo. Moreover, cells from RCCcr can present with intensely eosinophilic cytoplasm. This type of RCC is mostly associated with loss of chromosomes 1, 2, 6, 10, 13, 17 and 21 (Kovacs, 1997; Rini, 2009)

Normal and Cancer Stem Cells in the Kidney

The increasing interest in the potential of adult SCs in regenerative medicine has led to numerous studies focused on the identification of endogenous adult renal SCs within the mature mammalian kidney. A varied experimental armamentarium, such as pulse chase labeling of slow cycling cells by BrDU, Hoechst exclusion, expression of surface markers, has been used to identify the putative renal SC Oliver and colleagues isolated from rodents' renal papilla quiescent cells with a high BrDU signal that showed stem properties. These cells expressed both epithelial and mesenchymal markers and were able to give rise to spheres and had the capability to proliferate after injection upon renal injury, thus restoring the original tissue (Oliver, 2004). The same approach has been used by three different groups to isolate and characterize cells with stem properties from adult human kidney (Iwatani, 2004; HIshikawa, 2005; Challen, 2006). Another approach used in the hunt for renal SCs exploits the expression of previously proposed SC markers. Bussolati and colleagues isolated potential progenitors from human kidney based on the expression of the SC marker CD133 (Bussolati, 2005). These cells, did not only lack the expression of hematopoietic markers, but did express a renal embryonic marker, PAX2, thus suggesting a renal origin. In this model, clones deriving from a single $CD133^{+}$ cells were able to expand *in vitro* as well as to both differentiate and self-renew. Moreover, once injected into the veins of SCID mice with glycerol-induced tubulonecrosis, these cells were able to migrate and

regenerate tubules (Bussolati, 2005). Another group identified, by using a combination of CD133 and CD24 markers, a subpopulation able to self-renew and differentiate into tubular cells, osteocytes and adipocites, in the subpareietal area of glomeruli. These cells were able to regenerate tubular structures in different sites of the nephron upon tubular damage (Sagrinati, 2006). The sphere forming assay in the kidney was employed for the first time by Buzhor and colleagues. This group, by using high density culture conditions, was able to obtain 3D spheroid aggregates lacking clonal self-renewal capability and showing only tubulogenic potential (Buzhor, 2011). However, Bombelli and colleagues were able to isolate from adult kidney a pure population of SCs with self-renewal and multipotency capacity. This study showed that markers such as CD133 and CD24 both in combination and alone were not able to identify a pure population of adult renal SCs. On the opposite, the combination of both PKH^{high} status and $CD133^{+}/C24^{-}$ expression, allowed the identification of a SC population never identified before with both self-renewal and multipotency capacity, thus providing a more accurate definition of the resident renal SC population (Bombelli, 2013). Based on the hierarchical view of the tumor generation due to mutations of the stem/progenitor cell compartment, a better understanding of the cellular biology of adult renal SCs, might become not only a useful tool for regenerative medicine, but could also represent an important step toward a better comprehension of the molecular basis of renal pathologies, as well as to the origin of renal cell carcinoma according to the CSC theory.

Several studies investigated the existence of CSCs in RCC, their characterization and their possible analogy with normal renal progenitor/SCs. As for CSCs from other tumors, different approaches have been used to isolate CSCs from renal cell carcinoma. Bussolati and colleagues identified a population of tumor-initiating cells by means of cell sorting with the mesenchymal marker CD105. These cells, that represented less than 10% of the tumor mass, not only displayed tumor-initiating ability at a minimum of 100 cells but could be serially transplanted and recapitulate the histological pattern of tumor. Moreover, these cells were able to give rise to clonal spheres, as well as express SC markers such as CD44, CD90, NANOG and OCT4 (Bussolati, 2008). Notably, these cells did not express the marker of renal adult SCs CD133, which on the opposite was expressed by cells within the renal cell carcinoma that did not show any tumorigenic potential but were probably involved in the regulation of angiogenesis and tumor support (Bruno, 2006). Addla and colleagues identified cells belonging to the side population within renal tumors, by using the cytofluorimetric evaluation of Hoechst dye uptake. Cells from the side population showed a higher proliferative potential as well as the ability to give rise to spheres. This study confirmed that CD133 was absent in the side population, while cells did express CD105. (Addla, 2008). Another group identified a side population in the RCC cell line 769P. These cells showed CSC properties, such as self-renewal, differentiation, resistance to chemotherapy and high tumorigenic capability (Huang, 2013). Since the identification of selective markers may be difficult, the sphere-forming assay could be

really useful to enrich CSCs by exploiting their ability to give rise to spheres. Zhong and colleagues, were able to select cells from the RCC cell line SK-RC-42 with the ability to grow in suspension and form spheres that show stemness features, such as high tumorigenicity, expression of stemness genes and resistance to chemotherapeutic agents (Zhong, 2010). Concerning the origin of CSCs the data are still discordant. Mutation or epigenetic alterations occurring into embryonic SCs may explain the pediatric malignancy Wilm's tumor, while the different histological variants of RCC might derive from mutations in the adult SC compartment of the kidney. The identification of CSCs from RCCcc lacking of CD133 expression, does not allow association of CSCs with renal adult SCs. Since RCC CSCs express CD105 but lack the expression of CD133, they could derive from an earlier unidentified mesenchymal population which is ahead the expression of the renal progenitor marker CD133. Another alternative explanation might involve a dedifferentiation process at either renal progenitor or tubular terminally differentiated cells (Fig.8) (Bussolati, 2011). These studies together suggest the existence of renal CSCs, although a definitive selective marker for their isolation is still lacking. Moreover, different subpopulations with SC properties may be present in this heterogeneous tumor and be responsible of the different phenomena such as tumor initiation and resistance to therapy.

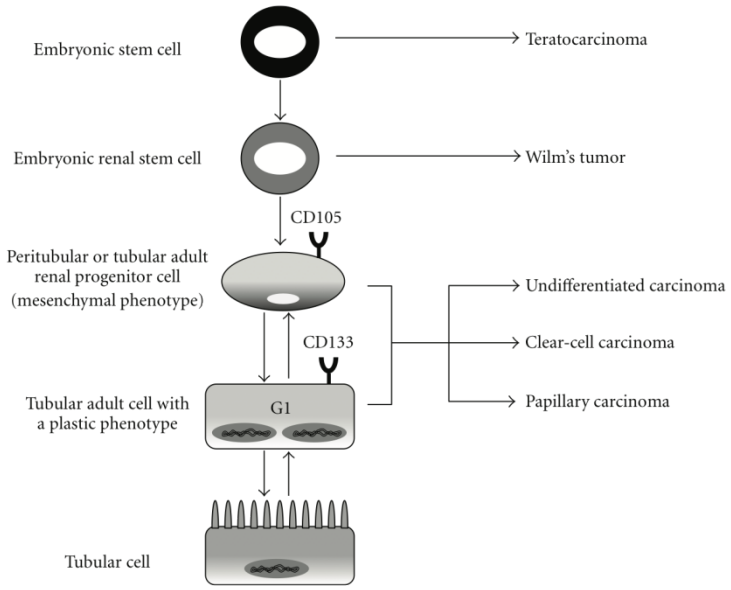

Figure 8. Possible stem cell origin of renal CSCs. Pediatric malignancy Wilm's tumor might originate from mutations/epigenetic alterations of the renal embryonic stem cells. Different histologic types of renal carcinomas might be the result of mutation occurring in the stem cell compartment of adult kidney. Since renal CSCs lack the expression of CD133, marker of adult renal progenitors, CSCs might origin from a yet unidentified mesenchymal population, which is ahead of CD133+ renal progenitors in the differentiation lineage. Alternatively, they might originate from a process of de-differentiation of renal progenitors or mature cells (Bussolati, 2011).

AIMS OF THE THESIS

High cancer mortality rates underscore the necessity for improved diagnostic techniques for early cancer detection and advanced therapeutic treatment to prevent disease relapse. CSCs are a rare subset of malignant cells that constitute a reservoir of tumor-initiating cells with the ability to both self-renew and differentiate into bulk tumors. Since this unique population harbors the potential to drive cancer progression and relapse, it represents an attractive target for therapy. As well as for other tumors (Al Hajii, 2003; Dalerba, 2007), CSCs, with their resistance to therapies and their tumor initiating ability, may play a relevant role in the pathogenesis of RCC. Only few studies have described the existence of CSCs in RCC by using different approaches such as side population (Addla, 2008; Huang, 2013) and use of surface marker expression (Bussolati, 2008). However, a definitive selective marker for the isolation and targeting of RCC CSCs is still lacking, thus suggesting to further investigate this field. It is still unclear whether CSCs are the results of oncogenic hits happening into the population of residing adult SCs within an organ or into terminally differentiated cells that undergo dedifferentiation thus acquiring stemness hallmarks (Bussolati, 2011). Whether CSCs derive from adult SCs or not, the understanding of mechanism of self-renewal and of the pathways that control it might represent a useful tool for the comprehension of mechanisms that regulate CSCs.

As described in chapter 2, we obtained a population enriched with adult renal SCs through the sphere forming assay adapted to human renal tissues. These spheres significantly upregulated SC and pluripotency markers and cell subpopulations within them showed the ability to both self-renew and differentiate. The isolation of these renal SCs represents an important step for a better understanding of RCC CSCs.

In order to understand CSCs it becomes also crucial to study the bulk tumor biology and the mechanisms that regulate its growth.

As described in chapter 3, we established RCC primary cultures that maintain both genetic and phenotypic features of the parental tumor. RCC primary cultures represent indeed a reliable model for the study of RCC and a really useful tool for the identification, through a direct comparison, of the features that distinguish CSCs from the whole tumor population.

Since CML represents an important paradigm for distinguishing the sequence and cellular framework of genetic and epigenetic events involved in the CSC production, as well as one of the best characterized at the level of molecular pathways involved in the regulation of self-renewal, we decided to move to this model in order to better understand mechanisms that regulates CSC self-renewal. We identified the RNA editing enzyme ADAR1 as a novel crucial player in BC LSC generation, as well as in the regulation of self-renewal of LSCs.

These data are described in chapter 4 and in the chapter "preliminary results" that provide data obtained in the same model. It is intriguing

the hypothesis that the ADAR1 enzyme might play a role in the regulation of CSCs also in other tumors.

The study of both normal adult stem cells and renal cell carcinoma primary cultures, as well as the identification of new regulators of self-renewal in CSCs from CML set the basis for the study of CSCs in human RCC. Based on these premises, the specific aims of chapter 5 are:

- To evaluate the existence of cells able to give rise to spheres and thus holding SC properties within human RCC cell lines and RCC tissues
- To characterize at a molecular level spheres from human RCC cell linesand tissues in order to identify pathways that distinguish these cells from the bulk tumor and might represent target for therapies
- To evaluate cell cycle and cell division properties of cells within the spheres by using different tools
- To evaluate the existence of cells with different ability to self-renew within the spheres and to characterize them at a phenotypical level
- To evaluate the tumorigenic potential of cells within the spheres

The identification of cells with stem properties within RCC, as well as the elucidation of self-renewal pathways that distinguish them from the bulk tumor represent an important step for the development of CSC targeted therapies for RCC.

REFERENCES

Addla, S. K., M. D. Brown, C. A. Hart, V. A. Ramani and N. W. Clarke (2008). "Characterization of the Hoechst 33342 side population from normal and malignant human renal epithelial cells." Am J Physiol Renal Physiol**295**(3): F680-687.

Al-Hajj, M., M. S. Wicha, A. Benito-Hernandez, S. J. Morrison and M. F. Clarke (2003). "Prospective identification of tumorigenic breast cancer cells." Proc Natl Acad Sci U S A**100**(7): 3983-3988.

Alison, M. R., S. M. Lim and L. J. Nicholson (2011). "Cancer stem cells: problems for therapy?" J Pathol**223**(2): 147-161.

Axelson, H. and M. E. Johansson (2013). "Renal stem cells and their implications for kidney cancer." Semin Cancer Biol**23**(1): 56-61.

Bao, S., Q. Wu, R. E. McLendon, Y. Hao, Q. Shi, A. B. Hjelmeland, M. W. Dewhirst, D. D. Bigner and J. N. Rich (2006). "Glioma stem cells promote radioresistance by preferential activation of the DNA damage response." Nature**444**(7120): 756-760.

Bapat, S. A. (2010). "Human ovarian cancer stem cells." Reproduction**140**(1): 33-41.

Barker, N., R. A. Ridgway, J. H. van Es, M. van de Wetering, H. Begthel, M. van den Born, E. Danenberg, A. R. Clarke, O. J. Sansom and H. Clevers (2009). "Crypt stem cells as the cells-of-origin of intestinal cancer." Nature**457**(7229): 608-611.

BI, S. (2008). "Natural and acquired resistance to cancer therapies " The molecular bases of cancer 583-592.

Bombelli, S., M. A. Zipeto, B. Torsello, G. Bovo, V. Di Stefano, C. Bugarin, P. Zordan, P. Vigano, G. Cattoretti, G. Strada, C. Bianchi and R. A. Perego (2013). "PKH(high) cells within clonal human nephrospheres provide a purified adult renal stem cell population." Stem Cell Res**11**(3): 1163-1177.

Bonnet, D. and J. E. Dick (1997). "Human acute myeloid leukemia is organized as a hierarchy that originates from a primitive hematopoietic cell." Nat Med**3**(7): 730-737.

Bruno, S., B. Bussolati, C. Grange, F. Collino, M. E. Graziano, U. Ferrando and G. Camussi (2006). "CD133+ renal progenitor cells contribute to tumor angiogenesis." Am J Pathol**169**(6): 2223-2235.

Bussolati, B., A. Brossa and G. Camussi (2011). "Resident stem cells and renal carcinoma." Int J Nephrol**2011**: 286985.

Bussolati, B., A. Brossa and G. Camussi (2011). "Resident stem cells and renal carcinoma." Int J Nephrol**2011**: 286985.

Bussolati, B., S. Bruno, C. Grange, S. Buttiglieri, M. C. Deregibus, D. Cantino and G. Camussi (2005). "Isolation of renal progenitor cells from adult human kidney." Am J Pathol**166**(2): 545-555.

Bussolati, B., S. Bruno, C. Grange, U. Ferrando and G. Camussi (2008). "Identification of a tumor-initiating stem cell population in human renal carcinomas." FASEB J**22**(10): 3696-3705.

Buzhor, E., O. Harari-Steinberg, D. Omer, S. Metsuyanim, J. Jacob-Hirsch, T. Noiman, Z. Dotan, R. S. Goldstein and B. Dekel (2011). "Kidney spheroids recapitulate tubular organoids leading to enhanced tubulogenic potency of human kidney-derived cells." Tissue Eng Part

A**17**(17-18): 2305-2319.

Cai, W. (2014). Engineering in Translational Medicine London.

Challen, G. A., I. Bertoncello, J. A. Deane, S. D. Ricardo and M. H. Little (2006). "Kidney side population reveals multilineage potential and renal functional capacity but also cellular heterogeneity." J Am Soc Nephrol**17**(7): 1896-1912.

Challen, G. A., I. Bertoncello, J. A. Deane, S. D. Ricardo and M. H. Little (2006). "Kidney side population reveals multilineage potential and renal functional capacity but also cellular heterogeneity." J Am Soc Nephrol**17**(7): 1896-1912.

Chen, Y. W., K. H. Chen, P. I. Huang, Y. C. Chen, G. Y. Chiou, W. L. Lo, L. M. Tseng, H. S. Hsu, K. W. Chang and S. H. Chiou (2010). "Cucurbitacin I suppressed stem-like property and enhanced radiation-induced apoptosis in head and neck squamous carcinoma--derived CD44(+)ALDH1(+) cells." Mol Cancer Ther**9**(11): 2879-2892.

Chen, Y. W., K. H. Chen, P. I. Huang, Y. C. Chen, G. Y. Chiou, W. L. Lo, L. M. Tseng, H. S. Hsu, K. W. Chang and S. H. Chiou (2010). "Cucurbitacin I suppressed stem-like property and enhanced radiation-induced apoptosis in head and neck squamous carcinoma--derived CD44(+)ALDH1(+) cells." Mol Cancer Ther**9**(11): 2879-2892.

Cheng, T., N. Rodrigues, H. Shen, Y. Yang, D. Dombkowski, M. Sykes and D. T. Scadden (2000). "Hematopoietic stem cell quiescence maintained by p21cip1/waf1." Science**287**(5459): 1804-1808.

Cheville, J. C., C. M. Lohse, H. Zincke, A. L. Weaver and M. L. Blute (2003). "Comparisons of outcome and prognostic features among

histologic subtypes of renal cell carcinoma." Am J Surg Pathol**27**(5): 612-624.

Cicalese, A., G. Bonizzi, C. E. Pasi, M. Faretta, S. Ronzoni, B. Giulini, C. Brisken, S. Minucci, P. P. Di Fiore and P. G. Pelicci (2009). "The tumor suppressor p53 regulates polarity of self-renewing divisions in mammary stem cells." Cell**138**(6): 1083-1095.

Clarke, L. and D. van der Kooy (2009). "Low oxygen enhances primitive and definitive neural stem cell colony formation by inhibiting distinct cell death pathways." Stem Cells**27**(8): 1879-1886.

Clarke, M. F., J. E. Dick, P. B. Dirks, C. J. Eaves, C. H. Jamieson, D. L. Jones, J. Visvader, I. L. Weissman and G. M. Wahl (2006). "Cancer stem cells--perspectives on current status and future directions: AACR Workshop on cancer stem cells." Cancer Res**66**(19): 9339-9344.

Clement, V., P. Sanchez, N. de Tribolet, I. Radovanovic and A. Ruiz i Altaba (2007). "HEDGEHOG-GLI1 signaling regulates human glioma growth, cancer stem cell self-renewal, and tumorigenicity." Curr Biol**17**(2): 165-172.

Cohen, A. J., F. P. Li, S. Berg, D. J. Marchetto, S. Tsai, S. C. Jacobs and R. S. Brown (1979). "Hereditary renal-cell carcinoma associated with a chromosomal translocation." N Engl J Med**301**(11): 592-595.

Courtenay, V. D., P. J. Selby, I. E. Smith, J. Mills and M. J. Peckham (1978). "Growth of human tumour cell colonies from biopsies using two soft-agar techniques." Br J Cancer**38**(1): 77-81.

Covello, K. L., J. Kehler, H. Yu, J. D. Gordan, A. M. Arsham, C. J. Hu, P. A. Labosky, M. C. Simon and B. Keith (2006). "HIF-2alpha regulates Oct-4:

effects of hypoxia on stem cell function, embryonic development, and tumor growth." Genes Dev**20**(5): 557-570.

Dalerba, P., S. J. Dylla, I. K. Park, R. Liu, X. Wang, R. W. Cho, T. Hoey, A. Gurney, E. H. Huang, D. M. Simeone, A. A. Shelton, G. Parmiani, C. Castelli and M. F. Clarke (2007). "Phenotypic characterization of human colorectal cancer stem cells." Proc Natl Acad Sci U S A**104**(24): 10158-10163.

Dieter, S. M., C. R. Ball, C. M. Hoffmann, A. Nowrouzi, F. Herbst, O. Zavidij, U. Abel, A. Arens, W. Weichert, K. Brand, M. Koch, J. Weitz, M. Schmidt, C. von Kalle and H. Glimm (2011). "Distinct types of tumor-initiating cells form human colon cancer tumors and metastases." Cell Stem Cell**9**(4): 357-365.

Ding, L., T. J. Ley, D. E. Larson, C. A. Miller, D. C. Koboldt, J. S. Welch, J. K. Ritchey, M. A. Young, T. Lamprecht, M. D. McLellan, J. F. McMichael, J. W. Wallis, C. Lu, D. Shen, C. C. Harris, D. J. Dooling, R. S. Fulton, L. L. Fulton, K. Chen, H. Schmidt, J. Kalicki-Veizer, V. J. Magrini, L. Cook, S. D. McGrath, T. L. Vickery, M. C. Wendl, S. Heath, M. A. Watson, D. C. Link, M. H. Tomasson, W. D. Shannon, J. E. Payton, S. Kulkarni, P. Westervelt, M. J. Walter, T. A. Graubert, E. R. Mardis, R. K. Wilson and J. F. DiPersio (2012). "Clonal evolution in relapsed acute myeloid leukaemia revealed by whole-genome sequencing." Nature**481**(7382): 506-510.

Doe, C. Q. and B. Bowerman (2001). "Asymmetric cell division: fly neuroblast meets worm zygote." Curr Opin Cell Biol**13**(1): 68-75.

Fan, X., L. Khaki, T. S. Zhu, M. E. Soules, C. E. Talsma, N. Gul, C. Koh, J.

Zhang, Y. M. Li, J. Maciaczyk, G. Nikkhah, F. Dimeco, S. Piccirillo, A. L. Vescovi and C. G. Eberhart (2010). "NOTCH pathway blockade depletes CD133-positive glioblastoma cells and inhibits growth of tumor neurospheres and xenografts." Stem Cells**28**(1): 5-16.

Fan, X., W. Matsui, L. Khaki, D. Stearns, J. Chun, Y. M. Li and C. G. Eberhart (2006). "Notch pathway inhibition depletes stem-like cells and blocks engraftment in embryonal brain tumors." Cancer Res**66**(15): 7445-7452.

Feuring-Buske, M., B. Gerhard, J. Cashman, R. K. Humphries, C. J. Eaves and D. E. Hogge (2003). "Improved engraftment of human acute myeloid leukemia progenitor cells in beta 2-microglobulin-deficient NOD/SCID mice and in NOD/SCID mice transgenic for human growth factors." Leukemia**17**(4): 760-763.

Franken, N. A., H. M. Rodermond, J. Stap, J. Haveman and C. van Bree (2006). "Clonogenic assay of cells in vitro." Nat Protoc**1**(5): 2315-2319.

G, S. (2013). "Regenerative Medicine: From Protocol to Patient." Springer Science + Business Media Dodrdrecht.

Gaston-Massuet, C., C. L. Andoniadou, M. Signore, S. A. Jayakody, N. Charolidi, R. Kyeyune, B. Vernay, T. S. Jacques, M. M. Taketo, P. Le Tissier, M. T. Dattani and J. P. Martinez-Barbera (2011). "Increased Wingless (Wnt) signaling in pituitary progenitor/stem cells gives rise to pituitary tumors in mice and humans." Proc Natl Acad Sci U S A**108**(28): 11482-11487.

Gnarra, J. R., D. R. Duan, Y. Weng, J. S. Humphrey, D. Y. Chen, S. Lee, A. Pause, C. F. Dudley, F. Latif, I. Kuzmin, L. Schmidt, F. M. Duh, T.

Stackhouse, F. Chen, T. Kishida, M. H. Wei, M. I. Lerman, B. Zbar, R. D. Klausner and W. M. Linehan (1996). "Molecular cloning of the von Hippel-Lindau tumor suppressor gene and its role in renal carcinoma." Biochim Biophys Acta**1242**(3): 201-210.

Gordan, J. D., P. Lal, V. R. Dondeti, R. Letrero, K. N. Parekh, C. E. Oquendo, R. A. Greenberg, K. T. Flaherty, W. K. Rathmell, B. Keith, M. C. Simon and K. L. Nathanson (2008). "HIF-alpha effects on c-Myc distinguish two subtypes of sporadic VHL-deficient clear cell renal carcinoma." Cancer Cell**14**(6): 435-446.

Gordan, J. D., C. B. Thompson and M. C. Simon (2007). "HIF and c-Myc: sibling rivals for control of cancer cell metabolism and proliferation." Cancer Cell**12**(2): 108-113.

Greaves, M. (2010). "Cancer stem cells: back to Darwin?" Semin Cancer Biol**20**(2): 65-70.

He, S., D. Nakada and S. J. Morrison (2009). "Mechanisms of stem cell self-renewal." Annu Rev Cell Dev Biol**25**: 377-406.

Heddleston, J. M., Z. Li, J. D. Lathia, S. Bao, A. B. Hjelmeland and J. N. Rich (2010). "Hypoxia inducible factors in cancer stem cells." Br J Cancer**102**(5): 789-795.

Heddleston, J. M., Z. Li, R. E. McLendon, A. B. Hjelmeland and J. N. Rich (2009). "The hypoxic microenvironment maintains glioblastoma stem cells and promotes reprogramming towards a cancer stem cell phenotype." Cell Cycle**8**(20): 3274-3284.

Hehlmann, R., A. Hochhaus, M. Baccarani and L. European (2007). "Chronic myeloid leukaemia." Lancet**370**(9584): 342-350.

Hishikawa, K., T. Marumo, S. Miura, A. Nakanishi, Y. Matsuzaki, K. Shibata, T. Ichiyanagi, H. Kohike, T. Komori, I. Takahashi, O. Takase, N. Imai, M. Yoshikawa, T. Inowa, M. Hayashi, T. Nakaki, H. Nakauchi, H. Okano and T. Fujita (2005). "Musculin/MyoR is expressed in kidney side population cells and can regulate their function." J Cell Biol**169**(6): 921-928.

Hoey, T., W. C. Yen, F. Axelrod, J. Basi, L. Donigian, S. Dylla, M. Fitch-Bruhns, S. Lazetic, I. K. Park, A. Sato, S. Satyal, X. Wang, M. F. Clarke, J. Lewicki and A. Gurney (2009). "DLL4 blockade inhibits tumor growth and reduces tumor-initiating cell frequency." Cell Stem Cell**5**(2): 168-177.

Hollingsworth, J. M., D. C. Miller, S. Daignault and B. K. Hollenbeck (2006). "Rising incidence of small renal masses: a need to reassess treatment effect." J Natl Cancer Inst**98**(18): 1331-1334.

Huang, B., Y. J. Huang, Z. J. Yao, X. Chen, S. J. Guo, X. P. Mao, D. H. Wang, J. X. Chen and S. P. Qiu (2013). "Cancer stem cell-like side population cells in clear cell renal cell carcinoma cell line 769P." PLoS One**8**(7): e68293.

Ingham, P. W. and A. P. McMahon (2001). "Hedgehog signaling in animal development: paradigms and principles." Genes Dev**15**(23): 3059-3087.

Iwatani, H., T. Uzu, M. Kakihara, Y. Nakayama, K. Kanasaki, M. Yamato, Y. Hirai, K. Umimoto and A. Yamauchi (2004). "A case of Wegener's granulomatosis with pulmonary bleeding successfully treated with double filtration plasmapheresis (DFPP)." Clin Exp Nephrol**8**(4): 369-

374.

Jamieson, C. H., L. E. Ailles, S. J. Dylla, M. Muijtjens, C. Jones, J. L. Zehnder, J. Gotlib, K. Li, M. G. Manz, A. Keating, C. L. Sawyers and I. L. Weissman (2004). "Granulocyte-macrophage progenitors as candidate leukemic stem cells in blast-crisis CML." N Engl J Med**351**(7): 657-667.

Jiang, Q., L. A. Crews, C. L. Barrett, H. J. Chun, A. C. Court, J. M. Isquith, M. A. Zipeto, D. J. Goff, M. Minden, A. Sadarangani, J. M. Rusert, K. H. Dao, S. R. Morris, L. S. Goldstein, M. A. Marra, K. A. Frazer and C. H. Jamieson (2013). "ADAR1 promotes malignant progenitor reprogramming in chronic myeloid leukemia." Proc Natl Acad Sci U S A**110**(3): 1041-1046.

Jin, L., K. J. Hope, Q. Zhai, F. Smadja-Joffe and J. E. Dick (2006). "Targeting of CD44 eradicates human acute myeloid leukemic stem cells." Nat Med**12**(10): 1167-1174.

Karnoub, A. E., A. B. Dash, A. P. Vo, A. Sullivan, M. W. Brooks, G. W. Bell, A. L. Richardson, K. Polyak, R. Tubo and R. A. Weinberg (2007). "Mesenchymal stem cells within tumour stroma promote breast cancer metastasis." Nature**449**(7162): 557-563.

Kessenbrock, K., V. Plaks and Z. Werb (2010). "Matrix metalloproteinases: regulators of the tumor microenvironment." Cell**141**(1): 52-67.

Kim, C. F., E. L. Jackson, A. E. Woolfenden, S. Lawrence, I. Babar, S. Vogel, D. Crowley, R. T. Bronson and T. Jacks (2005). "Identification of bronchioalveolar stem cells in normal lung and lung cancer." Cell**121**(6): 823-835.

Kondo, K., W. Y. Kim, M. Lechpammer and W. G. Kaelin, Jr. (2003). "Inhibition of HIF2alpha is sufficient to suppress pVHL-defective tumor growth." PLoS Biol**1**(3): E83.

Kong, X., B. Alvarez-Castelao, Z. Lin, J. G. Castano and J. Caro (2007). "Constitutive/hypoxic degradation of HIF-alpha proteins by the proteasome is independent of von Hippel Lindau protein ubiquitylation and the transactivation activity of the protein." J Biol Chem**282**(21): 15498-15505.

Korkaya, H., A. Paulson, E. Charafe-Jauffret, C. Ginestier, M. Brown, J. Dutcher, S. G. Clouthier and M. S. Wicha (2009). "Regulation of mammary stem/progenitor cells by PTEN/Akt/beta-catenin signaling." PLoS Biol**7**(6): e1000121.

Kovacs, G., M. Akhtar, B. J. Beckwith, P. Bugert, C. S. Cooper, B. Delahunt, J. N. Eble, S. Fleming, B. Ljungberg, L. J. Medeiros, H. Moch, V. E. Reuter, E. Ritz, G. Roos, D. Schmidt, J. R. Srigley, S. Storkel, E. van den Berg and B. Zbar (1997). "The Heidelberg classification of renal cell tumours." J Pathol**183**(2): 131-133.

Krause, D. S., K. Lazarides, U. H. von Andrian and R. A. Van Etten (2006). "Requirement for CD44 in homing and engraftment of BCR-ABL-expressing leukemic stem cells." Nat Med**12**(10): 1175-1180.

Kruh, G. D. (2003). "Introduction to resistance to anticancer agents." Oncogene**22**(47): 7262-7264.

Kusumbe, A. P. and S. A. Bapat (2009). "Cancer stem cells and aneuploid populations within developing tumors are the major determinants of tumor dormancy." Cancer Res**69**(24): 9245-9253.

Lawson, D. A., L. Xin, R. U. Lukacs, D. Cheng and O. N. Witte (2007). "Isolation and functional characterization of murine prostate stem cells." Proc Natl Acad Sci U S A**104**(1): 181-186.

Leong, K. G. and W. Q. Gao (2008). "The Notch pathway in prostate development and cancer." Differentiation**76**(6): 699-716.

Li, C., D. G. Heidt, P. Dalerba, C. F. Burant, L. Zhang, V. Adsay, M. Wicha, M. F. Clarke and D. M. Simeone (2007). "Identification of pancreatic cancer stem cells." Cancer Res**67**(3): 1030-1037.

Lin, H. (2002). "The stem-cell niche theory: lessons from flies." Nat Rev Genet**3**(12): 931-940.

Linehan, W. M., M. M. Walther and B. Zbar (2003). "The genetic basis of cancer of the kidney." J Urol**170**(6 Pt 1): 2163-2172.

Liu, C., K. Kelnar, A. V. Vlassov, D. Brown, J. Wang and D. G. Tang (2012). "Distinct microRNA expression profiles in prostate cancer stem/progenitor cells and tumor-suppressive functions of let-7." Cancer Res**72**(13): 3393-3404.

Liu, C. and D. G. Tang (2011). "MicroRNA regulation of cancer stem cells." Cancer Res**71**(18): 5950-5954.

Mandriota, S. J., K. J. Turner, D. R. Davies, P. G. Murray, N. V. Morgan, H. M. Sowter, C. C. Wykoff, E. R. Maher, A. L. Harris, P. J. Ratcliffe and P. H. Maxwell (2002). "HIF activation identifies early lesions in VHL kidneys: evidence for site-specific tumor suppressor function in the nephron." Cancer Cell**1**(5): 459-468.

Masters, J. R. and B. Koberle (2003). "Curing metastatic cancer: lessons from testicular germ-cell tumours." Nat Rev Cancer**3**(7): 517-525.

Maxwell, P. H., M. S. Wiesener, G. W. Chang, S. C. Clifford, E. C. Vaux, M. E. Cockman, C. C. Wykoff, C. W. Pugh, E. R. Maher and P. J. Ratcliffe (1999). "The tumour suppressor protein VHL targets hypoxia-inducible factors for oxygen-dependent proteolysis." Nature**399**(6733): 271-275.

McCampbell, K. K. and R. A. Wingert (2012). "Renal stem cells: fact or science fiction?" Biochem J**444**(2): 153-168.

McCord, A. M., M. Jamal, U. T. Shankavaram, F. F. Lang, K. Camphausen and P. J. Tofilon (2009). "Physiologic oxygen concentration enhances the stem-like properties of CD133+ human glioblastoma cells in vitro." Mol Cancer Res**7**(4): 489-497.

Miele, L., H. Miao and B. J. Nickoloff (2006). "NOTCH signaling as a novel cancer therapeutic target." Curr Cancer Drug Targets**6**(4): 313-323.

Mikkers, H. and J. Frisen (2005). "Deconstructing stemness." EMBO J**24**(15): 2715-2719.

Mimeault, M. and S. K. Batra (2006). "Concise review: recent advances on the significance of stem cells in tissue regeneration and cancer therapies." Stem Cells**24**(11): 2319-2345.

Mitelman F, J. B., Mertens F (2013). "Mitelman Database of Chromosome Aberrations and Gene Fusions in Cancer."

Moch, H. and M. J. Mihatsch (2002). "Genetic progression of renal cell carcinoma." Virchows Arch**441**(4): 320-327.

Moore, K. A. and I. R. Lemischka (2006). "Stem cells and their niches." Science**311**(5769): 1880-1885.

Moreno-Manzano, V., F. J. Rodriguez-Jimenez, J. L. Acena-Bonilla, S.

Fustero-Lardies, S. Erceg, J. Dopazo, D. Montaner, M. Stojkovic and J. M. Sanchez-Puelles (2010). "FM19G11, a new hypoxia-inducible factor (HIF) modulator, affects stem cell differentiation status." J Biol Chem**285**(2): 1333-1342.

Morrison, S. J. and J. Kimble (2006). "Asymmetric and symmetric stem-cell divisions in development and cancer." Nature**441**(7097): 1068-1074.

Morrison, S. J. and A. C. Spradling (2008). "Stem cells and niches: mechanisms that promote stem cell maintenance throughout life." Cell**132**(4): 598-611.

Nowell, P. C. (1976). "The clonal evolution of tumor cell populations." Science**194**(4260): 23-28.

Ohi, Y., Y. Umekita, T. Yoshioka, M. Souda, Y. Rai, Y. Sagara, Y. Sagara, Y. Sagara and A. Tanimoto (2011). "Aldehyde dehydrogenase 1 expression predicts poor prognosis in triple-negative breast cancer." Histopathology**59**(4): 776-780.

Oliver, J. A., O. Maarouf, F. H. Cheema, T. P. Martens and Q. Al-Awqati (2004). "The renal papilla is a niche for adult kidney stem cells." J Clin Invest**114**(6): 795-804.

Park, C. H., M. Amare, M. A. Savin, J. W. Goodwin, M. M. Newcomb and B. Hoogstraten (1980). "Prediction of chemotherapy response in human leukemia using an in vitro chemotherapy sensitivity test on the leukemic colony-forming cells." Blood**55**(4): 595-601.

Pastrana, E., V. Silva-Vargas and F. Doetsch (2011). "Eyes wide open: a critical review of sphere-formation as an assay for stem cells." Cell

Stem Cell**8**(5): 486-498.

Peacock, C. D., Q. Wang, G. S. Gesell, I. M. Corcoran-Schwartz, E. Jones, J. Kim, W. L. Devereux, J. T. Rhodes, C. A. Huff, P. A. Beachy, D. N. Watkins and W. Matsui (2007). "Hedgehog signaling maintains a tumor stem cell compartment in multiple myeloma." Proc Natl Acad Sci U S A**104**(10): 4048-4053.

Perez-Caro, M., C. Cobaleda, I. Gonzalez-Herrero, C. Vicente-Duenas, C. Bermejo-Rodriguez, M. Sanchez-Beato, A. Orfao, B. Pintado, T. Flores, M. Sanchez-Martin, R. Jimenez, M. A. Piris and I. Sanchez-Garcia (2009). "Cancer induction by restriction of oncogene expression to the stem cell compartment." EMBO J**28**(1): 8-20.

Puck, T. T. and P. I. Marcus (1956). "Action of x-rays on mammalian cells." J Exp Med**103**(5): 653-666.

Qiu, W., X. Wang, M. Buchanan, K. He, R. Sharma, L. Zhang, Q. Wang and J. Yu (2013). "ADAR1 is essential for intestinal homeostasis and stem cell maintenance." Cell Death Dis**4**: e599.

Raval, R. R., K. W. Lau, M. G. Tran, H. M. Sowter, S. J. Mandriota, J. L. Li, C. W. Pugh, P. H. Maxwell, A. L. Harris and P. J. Ratcliffe (2005). "Contrasting properties of hypoxia-inducible factor 1 (HIF-1) and HIF-2 in von Hippel-Lindau-associated renal cell carcinoma." Mol Cell Biol**25**(13): 5675-5686.

Reynolds, B. A. and S. Weiss (1992). "Generation of neurons and astrocytes from isolated cells of the adult mammalian central nervous system." Science**255**(5052): 1707-1710.

Ricci-Vitiani, L., D. G. Lombardi, E. Pilozzi, M. Biffoni, M. Todaro, C.

Peschle and R. De Maria (2007). "Identification and expansion of human colon-cancer-initiating cells." Nature**445**(7123): 111-115.

Rini, B. I., S. C. Campbell and B. Escudier (2009). "Renal cell carcinoma." Lancet**373**(9669): 1119-1132.

Rosen, J. M. and C. T. Jordan (2009). "The increasing complexity of the cancer stem cell paradigm." Science**324**(5935): 1670-1673.

Rossi, D. J., D. Bryder, J. Seita, A. Nussenzweig, J. Hoeijmakers and I. L. Weissman (2007). "Deficiencies in DNA damage repair limit the function of haematopoietic stem cells with age." Nature**447**(7145): 725-729.

Rovira, M., S. G. Scott, A. S. Liss, J. Jensen, S. P. Thayer and S. D. Leach (2010). "Isolation and characterization of centroacinar/terminal ductal progenitor cells in adult mouse pancreas." Proc Natl Acad Sci U S A**107**(1): 75-80.

Russo, J. E. and J. Hilton (1988). "Characterization of cytosolic aldehyde dehydrogenase from cyclophosphamide resistant L1210 cells." Cancer Res**48**(11): 2963-2968.

Sagrinati, C., G. S. Netti, B. Mazzinghi, E. Lazzeri, F. Liotta, F. Frosali, E. Ronconi, C. Meini, M. Gacci, R. Squecco, M. Carini, L. Gesualdo, F. Francini, E. Maggi, F. Annunziato, L. Lasagni, M. Serio, S. Romagnani and P. Romagnani (2006). "Isolation and characterization of multipotent progenitor cells from the Bowman's capsule of adult human kidneys." J Am Soc Nephrol**17**(9): 2443-2456.

Schofield, R. (1978). "The relationship between the spleen colony-forming cell and the haemopoietic stem cell." Blood Cells**4**(1-2): 7-25.

Singh, S. K., C. Hawkins, I. D. Clarke, J. A. Squire, J. Bayani, T. Hide, R. M. Henkelman, M. D. Cusimano and P. B. Dirks (2004). "Identification of human brain tumour initiating cells." Nature**432**(7015): 396-401.

Smith, A. (2006). "A glossary for stem cell biology." Nature**441**(1060).

Snippert, H. J. and H. Clevers (2011). "Tracking adult stem cells." EMBO Rep**12**(2): 113-122.

Soeda, A., M. Park, D. Lee, A. Mintz, A. Androutsellis-Theotokis, R. D. McKay, J. Engh, T. Iwama, T. Kunisada, A. B. Kassam, I. F. Pollack and D. M. Park (2009). "Hypoxia promotes expansion of the CD133-positive glioma stem cells through activation of HIF-1alpha." Oncogene**28**(45): 3949-3959.

Steinhoff, G. (2013). Regenerative Medicine From Protocol to Patient. Dordrecht, Springer.

Takahashi, K. and S. Yamanaka (2006). "Induction of pluripotent stem cells from mouse embryonic and adult fibroblast cultures by defined factors." Cell**126**(4): 663-676.

Takebe, N., P. J. Harris, R. Q. Warren and S. P. Ivy (2011). "Targeting cancer stem cells by inhibiting Wnt, Notch, and Hedgehog pathways." Nat Rev Clin Oncol**8**(2): 97-106.

Takezaki, T., T. Hide, H. Takanaga, H. Nakamura, J. Kuratsu and T. Kondo (2011). "Essential role of the Hedgehog signaling pathway in human glioma-initiating cells." Cancer Sci**102**(7): 1306-1312.

Tirino, V., V. Desiderio, F. Paino, A. De Rosa, F. Papaccio, M. La Noce, L. Laino, F. De Francesco and G. Papaccio (2013). "Cancer stem cells in solid tumors: an overview and new approaches for their isolation and

characterization." FASEB J**27**(1): 13-24.

Trumpp, A., M. Essers and A. Wilson (2010). "Awakening dormant haematopoietic stem cells." Nat Rev Immunol**10**(3): 201-209.

Varnat, F., A. Duquet, M. Malerba, M. Zbinden, C. Mas, P. Gervaz and A. Ruiz i Altaba (2009). "Human colon cancer epithelial cells harbour active HEDGEHOG-GLI signalling that is essential for tumour growth, recurrence, metastasis and stem cell survival and expansion." EMBO Mol Med**1**(6-7): 338-351.

Verga Falzacappa, M. V., C. Ronchini, L. B. Reavie and P. G. Pelicci (2012). "Regulation of self-renewal in normal and cancer stem cells." FEBS J**279**(19): 3559-3572.

Vermeulen, L., E. M. F. De Sousa, M. van der Heijden, K. Cameron, J. H. de Jong, T. Borovski, J. B. Tuynman, M. Todaro, C. Merz, H. Rodermond, M. R. Sprick, K. Kemper, D. J. Richel, G. Stassi and J. P. Medema (2010). "Wnt activity defines colon cancer stem cells and is regulated by the microenvironment." Nat Cell Biol**12**(5): 468-476.

Vermeulen, L., M. R. Sprick, K. Kemper, G. Stassi and J. P. Medema (2008). "Cancer stem cells--old concepts, new insights." Cell Death Differ**15**(6): 947-958.

Viale, A., F. De Franco, A. Orleth, V. Cambiaghi, V. Giuliani, D. Bossi, C. Ronchini, S. Ronzoni, I. Muradore, S. Monestiroli, A. Gobbi, M. Alcalay, S. Minucci and P. G. Pelicci (2009). "Cell-cycle restriction limits DNA damage and maintains self-renewal of leukaemia stem cells." Nature**457**(7225): 51-56.

Vicente-Duenas, C., I. Romero-Camarero, C. Cobaleda and I. Sanchez-

Garcia (2013). "Function of oncogenes in cancer development: a changing paradigm." EMBO J**32**(11): 1502-1513.

Visus, C., D. Ito, A. Amoscato, M. Maciejewska-Franczak, A. Abdelsalem, R. Dhir, D. M. Shin, V. S. Donnenberg, T. L. Whiteside and A. B. DeLeo (2007). "Identification of human aldehyde dehydrogenase 1 family member A1 as a novel CD8+ T-cell-defined tumor antigen in squamous cell carcinoma of the head and neck." Cancer Res**67**(21): 10538-10545.

Visvader, J. E. and G. J. Lindeman (2008). "Cancer stem cells in solid tumours: accumulating evidence and unresolved questions." Nat Rev Cancer**8**(10): 755-768.

Voog, J. and D. L. Jones (2010). "Stem cells and the niche: a dynamic duo." Cell Stem Cell**6**(2): 103-115.

W, C. (2014). "Engineering in Translational Medicine,." Springer-Verlag London.

Wang, Q., M. Miyakoda, W. Yang, J. Khillan, D. L. Stachura, M. J. Weiss and K. Nishikura (2004). "Stress-induced apoptosis associated with null mutation of ADAR1 RNA editing deaminase gene." J Biol Chem**279**(6): 4952-4961.

Wu, C. and B. A. Alman (2008). "Side population cells in human cancers." Cancer Lett**268**(1): 1-9.

Wu, C., Q. Wei, V. Utomo, P. Nadesan, H. Whetstone, R. Kandel, J. S. Wunder and B. A. Alman (2007). "Side population cells isolated from mesenchymal neoplasms have tumor initiating potential." Cancer Res**67**(17): 8216-8222.

Xu, N., T. Papagiannakopoulos, G. Pan, J. A. Thomson and K. S. Kosik (2009). "MicroRNA-145 regulates OCT4, SOX2, and KLF4 and represses pluripotency in human embryonic stem cells." Cell**137**(4): 647-658.

XuFeng, R., M. J. Boyer, H. Shen, Y. Li, H. Yu, Y. Gao, Q. Yang, Q. Wang and T. Cheng (2009). "ADAR1 is required for hematopoietic progenitor cell survival via RNA editing." Proc Natl Acad Sci U S A**106**(42): 17763-17768.

XuFeng, R., M. J. Boyer, H. Shen, Y. Li, H. Yu, Y. Gao, Q. Yang, Q. Wang and T. Cheng (2009). "ADAR1 is required for hematopoietic progenitor cell survival via RNA editing." Proc Natl Acad Sci U S A**106**(42): 17763-17768.

Yi, S. Y., Y. B. Hao, K. J. Nan and T. L. Fan (2013). "Cancer stem cells niche: a target for novel cancer therapeutics." Cancer Treat Rev**39**(3): 290-296.

Zhong, Y., K. Guan, S. Guo, C. Zhou, D. Wang, W. Ma, Y. Zhang, C. Li and S. Zhang (2010). "Spheres derived from the human SK-RC-42 renal cell carcinoma cell line are enriched in cancer stem cells." Cancer Lett**299**(2): 150-160.

Zhou, B. B., H. Zhang, M. Damelin, K. G. Geles, J. C. Grindley and P. B. Dirks (2009). "Tumour-initiating cells: challenges and opportunities for anticancer drug discovery." Nat Rev Drug Discov**8**(10): 806-823.

Chapter 2

PKH^{high} cells within clonal human nephrospheres provide a purified adult renal stem cell population

Silvia Bombelli[a], Maria Anna Zipeto[a]†, Barbara Torsello[a]†, Giorgio Bovo[b], Vitalba Di Stefano[a], Cristina Bugarin[c], Paola Zordan[d], Paolo Viganò[e], Giorgio Cattoretti[b], Guido Strada[e], Cristina Bianchi[a], Roberto A Perego[a]*

[a]Department of Health Sciences, University of Milano-Bicocca, Monza, Italy
[b]Anatomo-Pathology Unit, University of Milano-Bicocca, San Gerardo Hospital, Monza, Italy
[c]Pediatric Department, Laboratory of Cytometry, University of Milano-Bicocca, San Gerardo Hospital, Monza, Italy
[d]Division of Regenerative Medicine, Stem Cells and Gene Therapy, S. Raffaele Scientific Institute, Milano, Italy
[e]Urology Unit, Bassini ICP Hospital, Milano, Italy

† MAZ and BT have contributed equally to this work and both have to be considered second author

Stem Cell Research, Volume 11, Issue 3, November 2013; Pages 1163-1177

Abstract

The existence and identification of adult renal stem cells is a controversial issue. In this study, renal stem cells were identified from cultures of clonal human nephrospheres. The cultured nephrospheres exhibited the activation of stem cell pathways and contained cells at different levels of maturation. In each nephrosphere, the presence of 1.12-1.25 cells mirroring stem cell properties was calculated. The nephrosphere cells were able to generate three-dimensional tubular structures in 3D cultures and in vivo. In clonal human nephrospheres a PKH^{high} phenotype was isolated using PKH26 epifluorescence, which can identify quiescent cells within the nephrospheres. The PKH^{high} cells capable of self-renewal and of generating the differentiated epithelial, endothelial and podocityc progeny, can also survive in vivo maintaining the undifferentiated status. The PKH^{high} status, together with a CD133+/CD24- phenotype, identified a homogeneous cell population displaying in vitro self-renewal and multipotency capacity. The resident adult renal stem cell population isolated from nephrospheres can be used for the study of mechanisms that regulate self-renewal and differentiation in adult renal tissue as well as in renal pathological conditions.

Keywords: Adult renal stem cells; Human kidney; Nephrosphere; Self-renewal; Multipotency

Introduction

Most adult tissues are believed to contain adult stem cells that are able to compensate for tissue loss by generating new cells. In renal pathologies, the presence and function of adult renal stem cells may have clinical relevance. In recent years, sources of renal stem/progenitor cells have been suggested to be localized in different portions of the nephron,based on CD133 alone (Bussolati *et al.*, 2005) or coupled with the CD24 surface marker (Sagrinati *et .55al.*, 2006), or based on the aldehyde dehydrogenase (ALDH) activity (Lindgren *et al.*, 2011). However, markers can fall victim to their promiscuity. In fact, they may be expressed either by stem or more differentiated cells, and often they do not permit the identification of a homogeneous stem cell population. Moreover, for medical applications, it is also crucial to understand the physiological behavior of renal stem cells to appreciate how they change in specific pathological situations, such as renal cell carcinoma. Therefore, it is necessary to source a purified stem cell population. Recent reviews (Snippert and Clevers, 2011; McCampbell and Wingert, 2012) have stressed the importance of selecting the correct approach for the identification of adult stem cells. They proposed that the dual capacity of self-renewal and multipotency should be the only criteria used for stem cell definition, instead of an exclusive initial use of surface markers or signatures. The capacity of self-renewal and multipotency can be evidenced by in vitro clonal growth of cellular spheres from individual stem cells. The sphere-forming assay has

already been described for the isolation of normal and cancer stem cells from various tissues, such as brain (Reynolds and Weiss, 1992), breast (Dontu *et al.*, 2003), pancreas (Rovira *et al.*, 2010) and prostate (Lawson *et al.*, 2007). The model has also been applied to embryonic renal murine cells obtaining clonal spheres that, however, were not able to differentiate towards an epithelial lineage. The same authors never obtained nephrospheres from postnatal murine kidney (Lusis *et al.*, 2010). The sphere-forming assay has also been applied to adult human renal cells, obtaining aggregation of epithelial cells in 3D spheroids unable to display clonal self-renewal and with only tubulogenic potency (Buzhor *et al.,* 2011). Starting from these data, the aim of this paper was to obtain a population enriched with adult renal stem cells through the formation of clonal spheres with an adaptation of sphere-forming assay to human renal tissue. Within the clonal spheres, the quiescent cells have been evidenced by using PKH26 lyophilic fluorescent dye that is retained by the less dividing cells (Cicalese *et al.*, 2009; Pece *et al.*, 2010). Among these cells, a subpopulation displaying self-renewal and multipotency has been identified. This approach, exploiting the functional feature of asymmetrical division that define stem cells, permitted the isolation of a purified, homogeneous and more defined human renal stem cell population. These isolated stem cells might become a tool for regenerative medicine in kidney diseases and could represent an important step for a better comprehension of the cellular and molecular basis of renal pathologies, including renal cell carcinoma, according to the cancer stem cell theory.

Materials and methods

Tissues

Normal kidney tissue was obtained after nephrectomy from 44 patients with localized renal tumors. The renal parenchyma opposite to the tumor was considered as normal. All procedures were performed after written consent from the patients and in accordance with recommendations of the Local Ethical Committee.

Dissociation of Renal Tissue and Nephrosphere Culture

To obtain a single cell suspension for nephrosphere culture, normal renal tissues were mechanically and enzymatically dissociated as described (Bianchi *et al*., 2010). The cells and structures obtained after digestion were sieved through a 250µm cell strainer and then passed through a pipette syringe to obtain a single cell suspension that represented the bulk renal cell population. Red blood cells were removed by hemolysis with 0.8% NH_4Cl solution. The single cell suspension was allowed to adhere for 24-48 hours in SC medium containing DMEM-F12 (Sigma Aldrich), supplemented with B27 (Invitrogen), ITS supplement (5 µg/ml Insulin, 5 µg/ml Transferrin, 5 ng/ml sodium selenite), 36ng/ml Hydrocortisone, 40pg/ml Triiodothyronine (all from Sigma Aldrich), 20ng/ml EGF, 20ng/ml bFGF (Tebu Bio). The adherence passage permitted the loss of hematopoietic cells and fibroblasts (Pece *et al.*, 2010) and thus the selection of the bulk epithelial population. 20,000 bulk renal cells or trypsinized bulk epithelial cells were plated in a well of 6-well plate (10,000 cells/ml) with SC medium on poly-Hema (Sigma Aldrich)

coated dishes in non-adherent conditions for the formation of floating nephrospheres. After 10-12 days, the sphere-forming efficiency (SFE) was calculated as the number of obtained nephrospheres divided by the number of plated cells and expressed as a percentage. Nephrospheres were collected and then dissociated enzymatically for 5 minutes in TrypLE Express (Invitrogen) and mechanically by repetitive pipette syringing until single cell suspension was reached. The single cell suspension was used for successive analysis or was re-plated in the sphere-forming conditions to obtain secondary spheres and so on. Renal differentiated primary cell cultures were used as control and were obtained as described (Bianchi *et al.*, 2010).

PKH26 and PKH2 Assays

The single cell suspension of epithelial renal cells obtained after 24-48 hours of adhesion was stained for 5 minutes with red PKH26 or green PKH2 dye (dilution 1:250; Sigma Aldrich) following manufacturer's instructions, and plated to obtain nephrospheres. The cell suspension obtained from PKH26-stained secondary nephrospheres was FACS sorted with a FACSAria flow cytometer (Becton & Dickinson) on the basis of PKH fluorescence intensity. It was possible to isolate a cellular population with the highest PKH fluorescence (PKH^{high}) chosen on the basis of the SFE percentage. Cells without PKH fluorescence represented the PKH^{neg} population and the cells with intermediate fluorescence represented the PKH^{low}

population. An average sorting rate of 500-1000 events per second at a sorting pressure of 20psi with a 100µm nozzle was maintained.

Differentiation Assays

Single cell suspensions obtained from the dissociation of secondary nephrospheres or from sorted cells were plated on coverslip or dishes. Cells were grown in DMEM supplemented with 10% FBS (Euroclone) for epithelial differentiation, and in VRADD medium for podocytic differentiation as described (Lasagni *et al.*, 2010). Endothelial differentiation was induced as described (Bussolati *et al.*, 2005) by culturing cells on endothelial cell attachment factor (Sigma) in Endothelial Basal Medium (EBM) (Cambrex Bio Science) with 10ng/ml VEGF (Miltenyi Biotec) and 10% FBS. Immunofluorescence or FACS analysis with the appropriate antibodies was performed, and cellular lysates were used for western blot. For 3D cultures 20,000 cells were resuspended in 100 µL of Matrigel or 4mg/ml neutralized type 1 Collagen and plated in wells of a 24-well plate. The substrates with the cells were allowed to stiffen at 37°C for 30 minutes and then were incubated with DMEM supplemented with 10% FCS for 5-7 days. The 3D structures obtained were formalin-fixed and embedded in paraffin to perform immunohistochemistry (IHC).

Immunofluorescence on Cells and FACS Analysis

Immunofluorescence (IF) on cells grown on coverslips and FACS analysis were performed as described (Bianchi *et al*, 2010). Immunofluorescence on floating nephrospheres was also performed by fixing the spheres in 4% paraformaldehyde for 20 minutes,

blocking for 20 minutes with PBS with 0.1% BSA (Sigma Aldrich) and 0.3% Triton X-100, then incubating with the specific primary antibody for 2 hours at room temperature. Spheres were then incubated with Alexa Fluor 488 or 555 conjugated anti-mouse or Alexa Fluor 594 or 488 conjugated anti-rabbit IgG antibodies (Molecular Probes Invitrogen) for 1 hour and then resuspended with ProLong Gold Antifade with DAPI (Molecular Probes). The slides where then mounted. Immunofluorescence micrographs were obtained at x400 magnification using a Zeiss LSM710 confocal microscope and Zen2009 software (Zeiss).

FACS analysis was performed with a FACSCanto instrument and FACS Diva software; the acquisition process was stopped when 20,000 events were collected in the population gate. PKH^{high} cells were sorted, on the basis of CD133 and CD24 expression, with the FACSAria flow cytometer. An average sorting rate of 500-1000 events per second at a sorting pressure of 20psi with a 100µm nozzle was maintained. The antibodies used and their source and working concentrations are summarized in Table S3.

Aldefluor Assay

To evaluate the rate of ALDH enzymatic activity in nephrosphere cells, the ALDEFLUOR kit (STEMCELL Technologies Inc.) was used. Nephrosphere cells and primary cell culture cells were suspended in ALDEFLUOR assay buffer containing ALDH substrate (BAAA, 1µM for 10^6 cells) and incubated for 45 minutes at 37°C. In each experiment, a sample of cells was incubated with 50mM of specific ALDH inhibitor

diethylaminobenzaldehyde (DEAB) as negative control. FACS analysis was performed using a FACSCanto instrument and FACS Diva software (Becton Dickinson).

cDNA Synthesis and TaqMan Low Density Array (TLDA) and TaqMan Assays

Total RNA was extracted with TRIZOL (Invitrogen) from secondary nephrospheres and differentiated primary cell cultures established from 4 patients. 2μg of RNA were reverse transcribed using the High-Capacity cDNA Reverse Transcription Kit (Applied Biosystems). Expression of 96 genes (Table S1A) represented in TaqMan® Human Stem Cell Pluripotency Panel Array (Applied Biosystems) was profiled according to the manufacturer's instructions. 100ng of cDNA from each sample were loaded on each port of a TLDA card (Applied Biosystems). PCR amplification was performed for 40 cycles of 2 minutes at 50°C, 10 minutes at 94.5°C, 30 seconds at 97°C and 1 minute at 59.7°C using an ABI Prism 7900HT sequence detection system (Applied Biosystems). Notch pathway was evaluated using the TaqMan Gene Expression Assays (Applied Biosystems) reported in table S1B and GAPDH (Hs99998805_m1) as an endogenous control. PCR amplification was performed as described (Perego *et al.*, 2005a) using 50ng of cDNA for each reaction run in duplicate on an ABI PRISM® 7900HT Sequence Detector System (Applied Byosystems). The ΔCt was calculated as the Ct value of the gene minus the CT value of the endogenous control (GAPDH). The expression fold-change between primary cultures and nephrospheres was calculated as $2^{-\Delta\Delta Ct}$

(Bianchi *et al.*, 2010) always using the primary cultures as a calibrator. The minimum and maximum levels of $2^{-\Delta\Delta Ct}$ were calculated as described in the User Bulletin #2 issued by Applied Biosystems. For TLDA analysis, the genes that did not show expression in at least 2 samples were excluded, so 56 out 96 genes constituted the statistical analysis. The ΔCt values of the 56 analyzed genes were plotted on a heat map using the TIGR Multiple Experiment Viewer (TMEV v4.1) and clusterized on the basis of the samples. Statistical analysis was performed on the ΔCt values and $p<0.05$ was considered significant.

Xenotransplantation under the Renal Capsule

All animal experiments described in this study were conducted in agreement with the stipulations of the local Animal Care and Use Committee. $5x10^3$ nephrosphere cells or PKH sorted cells were resuspended in 35µl of collagen solution and allowed to stiffen at 37°C for 30 minutes. The collagen pellets were then incubated with DMEM supplemented with 10% FBS for a maximum of 24 hours before xenograft into 5 week-old CD1 nude mice (Charles River). For subrenal transplantation, an abdominal wall incision above the right kidney was made, and the kidney exteriorized. The kidney capsule was raised from the parenchyma and collagen gel was sandwiched between them (Eirew *et al.*, 2008). The incisions were then sutured. Mice were mated 14 days after surgery, the kidneys were removed and then frozen to perform successive analyses.

Immunohistochemistry on Paraffin-Embedded Sections and Immunofluorescence on Frozen Sections

Paraffin-embedded sections (2µm thick) of three-dimensional structures grown in collagen and Matrigel were labeled with the primary antibodies against Cytokeratin 7, pan-Cytokeratin, CD10, Vimentin (Table S3). The stainings were performed using antibody dilutions (Table S3) and antigen retrieval techniques indicated by the manufacturers. AEC and DAB (Zymed) were used as substrates for Streptavidin Peroxidase. All slides were counterstained with hematoxylin.

Frozen sections (5µm thick) were fixed in acetone at 4°C. Blocking was performed by incubating the slides with PBS containing 2% BSA and 0.1% Triton X-100. The slides were then incubated for 2 hours with mouse monoclonal anti-HLA-ABC or anti-E-Cadherin and rabbit monoclonal anti-Cytokeratin 18 or rabbit polyclonal anti-N-Cadherin (Table S3). The slides were then incubated for 1 hour with the secondary antibodies as described above. Nuclear counterstaining and image acquisitions were obtained as described above.

Hematoxylin/Eosin staining was performed on both paraffin-embedded and frozen sections.

Statistics

The unpaired two-tail Student's t-test was used to analyze statistical differences and $p<0.05$ was considered significant.

Results

Establishment and Growth Characteristics of Nephrospheres

Single-cell suspensions of human normal renal cells were grown at low density with defined serum-free medium and in conditions that do not allow cell adherence. As in the case of mammary cells (Dontu *et al.*, 2003), under these culture conditions, most of the renal cells underwent apoptosis, while only a small number of cells survived and grew as spherical floating colonies (Figure1A), termed as nephrospheres. Nephrosphere formation was achieved with renal samples from 42 out of 44 patients (95.4%), and nephrospheres reproducibly contained 130.1±23.4 (mean±SD) cells per sphere after 10-12 days in culture. Before plating, renal cells were labeled with red PKH26 or green PKH2 dyes and then mixed and cultured together, but this never gave rise to the coexistence of red and green cells in the same nephrosphere (Figure1B), suggesting a clonal origin of the spheres. New nephrospheres formed after their dissociation into isolated cells and cultivation in sphere-forming conditions. Nephrosphere cultures were propagated in excess of 11 passages and maintained in culture for at least 6 months. The sphere-forming efficiency (SFE) of renal cells to form primary nephrospheres was 0.69% starting from the bulk renal population. Starting from the bulk epithelial population grown in adhesion for 24-48 hours, the SFE was 0.87% which was approximately maintained among the different passages (Table S2). This indicated that the sphere-initiating cells and the total number of spheres were stable over time (Figure 1C), and

suggested a stable presence of one sphere-initiating cell in each nephrosphere. The estimated frequency of sphere-initiating cells in bulk renal cells was 1 out of 145 cells. In bulk epithelial cells and in the different nephrosphere passages, this frequency was in the range of 1 out 116-104 cells (Table S2). These data permitted to calculate that 1.12-1.25 cells in each nephrosphere (~130 cells/sphere) were able to self-renew and to generate new spheres.

Cellular Characterization of Nephrospheres

To assess the cellular composition, secondary nephrospheres were immunostained after 10 days in culture using specific markers (Figure 2). Nephrosphere cells were positive for renal embryonic marker Pax2, thus demonstrating the renal origin of sphere cells (Figure 2A and S1A). Not all sphere-composing cells expressed the epithelial marker Cytokeratin, as demonstrated by immunofluorescence and FACS analysis, while some cells expressed the proximal tubular marker N-Cadherin and the distal tubular marker E-Cadherin. Interestingly, E-Cadherin and N-Cadherin were expressed in the same cells inside the spheres, as shown by the yellow signal, and were not mutually exclusive as they appear instead in adult renal tissue and in primary cell cultures, identifying the distal and proximal tubular cells respectively (Nouwen *et al.*, 1993; Prozialeck *et al.*, 2004; Keller *et al.*, 2012). Some cells of the spheres also expressed the podocytic marker Synaptopodin (Figure 2A, arrows).The expression of Synaptopodin and Podocin has been proved also by western blot of nephrosphere cell lysates (Figure S2). ALDH activity has been recently described as a

marker for stem/progenitor cells in different tissues (Armstrong *et al.*, 2004; Corti *et al.*, 2006), even of renal origin (Lindgren *et al.*, 2011). Aldefluor assay was performed on nephrosphere cells evidencing a statistically higher aldefluor positive (ALDE+) population if compared to the differentiated renal primary cell cultures (Figure 2B), which may suggest that nephrospheres are enriched with cells possessing stem/progenitor properties.

All these data demonstrated that there are different cellular phenotypes at different stages of differentiation in nephrospheres.

Molecular Characterization of Nephrospheres

In nephrosphere cells obtained from 4 different patients and in corresponding differentiated renal primary cell cultures, the expression of 96 genes of a Stem Cell Pluripotency Panel (Applied Biosystems) (Table S1A), and the Notch pathway genes (Table S1B) have been analyzed by Real Time PCR (Figure 3). 35 of the 96 analyzed genes were not expressed in the renal samples and were thus excluded from the analysis. Among those not expressed, there were markers of differentiation of non-renal lineages, indicating a tissue specificity of our cellular models. By clustering the samples in a heat map on the basis of the 56 expressed genes, it was possible to observe two different groups belonging to nephrosphere cultures or to differentiated primary cell cultures (Figure 3A). This can be explained by the statistical difference of 29 genes in nephrospheres compared to differentiated primary cell cultures. Among the genes overexpressed in nephrospheres, 12 are classified as stem cell

markers (Table S1A), and 4 as markers for maintenance of pluripotency, namely *GABRB3, NANOG, OCT4, SOX2*. Three extracellular matrix (ECM) genes of the laminin family were found statistically upregulated in the nephrospheres, supporting the possibility of sphere-composing cells to produce ECM components (Dontu *et al.*, 2003, Lusis *et al.*, 2010, Buzhor *et al.*, 2011). Moreover, 3 Notch receptors (Notch1, Notch2 and Notch 3), 2 Notch ligands (Jag1 and Dll1) and 2 Notch targets (Hes1 and Hey1) were statistically up-regulated in nephrospheres, thus indicating an activation of the Notch pathway (Figure 3B).

The nephrospheres obtained from human normal renal tissues expressed high levels of pluripotency and stem cell genes and showed an activation of the Notch pathway involved in the stem cell fate decision. Also *LGR5* gene, known to be expressed in human embryonic kidney (Baker *et al*., 2012), is expressed in our nephrospheres but not in our differentiated primary cell cultures (data not shown). All the analyzed genes with corresponding ΔCt and $2^{-\Delta\Delta Ct}$ values are summarized in supplemental tables 1A and 1B.

Identification and Isolation of Stem Cells within the Nephrospheres

Before plating, cells were labeled with PKH26 and then cultured to allow for nephrosphere growth. PKH26 is a fluorescent dye that binds to the phospholipid membrane and is diluted in actively replicating cells mirroring the properties of progenitor cells, while PKH26 concentration is maintained in quiescent cells mirroring the properties of stem cells, known to represent a quiescent population

within the tissue (McCampbell *et al.*, 2012; Terskikh *et al.*, 2012). Even in the spheres other authors evidenced the quiescence of stem cells, demonstrating their asymmetrical division and a consequent minor number of replications (Cicalese *et al.,* 2009; Pece *et al.,* 2010). Very few cells within the nephrospheres retained strong epifluorescence, suggesting that in the nephrospheres there is only a small number of quiescent cells that may possess the stem properties needed to maintain the nephrosphere culture (Figure 4A). On the basis of PKH26 epifluorescence, which reflects the cell proliferation history, 3 different cell populations were sorted from secondary nephrospheres: quiescent/slow-replicating PKH^{high} cells, medium-replicating PKH^{low} cells and high-replicating PKH^{neg} cells. PKH^{high} cells were the most brightly-stained PKH-positive cells and they were gated as 0.8-1% of the total population, corresponding to the usual SFE obtained, which represents the fraction of self-renewing cells. PKH^{low} cells, with intermediate fluorescence, were gated as 15-20% of the total cell population, and the PKH^{neg} cells, without fluorescence, as 60-70% of the total cell population. After re-plating the three subpopulations in sphere-forming conditions, the PKH^{low} and PKH^{neg} cells generated small aggregates not capable of further propagation in culture; only PKH^{high} cells were able to generate tertiary and their successive filial nephrospheres (Figure 4B). Moreover, PKH^{high} cells sorted and re-plated at a density of 1 cell/well in sphere-forming conditions could generate clonal nephrospheres, but only if they were cultured in the conditioned medium in which secondary spheres grew (Figure 4C). These sorted PKH^{high} cells demonstrated an

SFE of about 47%, and 1 out of 2.1 cells was able to generate a new nephrosphere. This indicated that in the PKH^{high} sorted population there was a 69 fold enrichment of cells with stem properties with respect to the bulk renal population (Table S2). However, it must be noted that the FACS procedure has a damaging effect on cells which affects their capacity to form nephrospheres. This effect has also been described by others (Pece *et al.*, 2010), and in the sorted cells of this current study, the sphere-forming capacity is reduced to 65.24% of its maximum capacity. Based on this FACS effect, the calculated SFE of the PKH^{high} cells might be about 72%, with a frequency of cells able to generate new nephrospheres of 1 out of 1.4 and an enrichment of stem cells of about 104 fold in the PKH^{high} population (Table S2).

Therefore, the quiescent PKH^{high} population was the only cellular subpopulation within the nephrosphere that illustrated a self-renewal capacity, able to generate new clonal nephrospheres, and that can be considered as harboring the stem-like properties. Nephrosphere culture media seem to contain factors able to promote the sphere formation from 1 single PKH^{high} cell.

Cells from Nephrospheres and PKH^{high} Cells are Capable of Differentiation along Multiple Lineages

When a stem cell divides, it is able to both self-renew and to differentiate. In this study, nephrosphere-derived cells and PKH-sorted cells were tested for the capacity to differentiate toward epithelial, podocytic and endothelial lineages.

Epithelial differentiation of nephrosphere-derived cells was induced, and after two days the cells grew as oloclones, while at day 7 they reached confluence as a monolayer with a typical polygonal shape (Figure 5A). A phenotypical characterization of these differentiated cells was performed using markers known to be expressed in proximal and distal tubular cells (Perego *et al.*, 2005; Bianchi *et al.*, 2010). Almost all cells expressed epithelial Cytokeratin and in addition Vimentin that is usually expressed by tubular cells only in vitro (Perego *et al*,2005; Forino *et al*, 2006; Bianchi *et al*, 2010) (Figure 5B, 5C). About 60% of cells exhibited an expression of the proximal tubular marker CD13 (Baer *et al.*, 1997; Keller *et al.*, 2012) (Figure 5B). In these Cytokeratin positive differentiated nephrosphere cells, there was co-expression of proximal tubular marker N-Cadherin and CD13, and distal tubular marker E-Cadherin and Calbindin D (Hemmingsen et al., 2000) (Figure 5C). The N-Cadherin and E-Cadherin expression was mutually exclusive (Figure 5C), as observed also when the PKH^{high} and $PKH^{low/neg}$ subpopulation were cultured in epithelial differentiating medium (Figure 5E). All these data evidenced the capability of nephrosphere cells to give rise to a mixed differentiated population of proximal and distal tubular cells that mimic the phenotype of differentiated primary epithelial cell cultures obtained directly from renal tissues (Bianchi *et al.*, 2010).

Podocytic differentiation was obtained by culturing the nephrosphere-derived cells in VRADD medium. After 7-10 days in culture, the cells reached confluence but with difficultly. They

displayed a different morphology with respect to the epithelial differentiated cells and did not express the epithelial marker cytokeratin (Figure 5D). The podocytic markers Synaptopodin, Nestin, alpha-Actinin and Podocin were expressed on podocytic-differentiated nephrosphere cells (Figure 5D) and not on the epithelial-differentiated cells (Figure S1B). The Synaptopodin and Podocin expression has been proved by western blot of podocytic-differentiated nephrosphere cell lysates (Figure S2). When PKH-sorted cells were cultured in podocytic culture conditions, only PKH^{high} cells displayed a podocytic phenotype with a positive expression of Synaptopodin and no expression of Cytokeratin (Figure 5F).

Only PKH^{high} cells that differentiated into the endothelial lineage had a typical von Willebrand factor (vWF) expression pattern and did not express Cytokeratin, while $PKH^{low/neg}$ cells expressed Cytokeratin and not vWF (Figure 5G). The total nephrosphere cells submitted to endothelial differentiation exhibited a vWF pattern completely different from that of HUVEC cells, which were used as a positive control. In these endothelial-differentiated total nephrosphere cells the vWF and Cytokeratin profile was similar to renal primary cell cultures used as a negative control (Figure S1C).

To assess the ability to generate three-dimensional structures, nephrosphere-derived cells were cultured in semisolid substrates such as type 1 collagen and matrigel. After 7-10 days, it was possible to observe the formation of spherical and tubular-like structures.

Once these structures were formalin-fixed, paraffin-embedded and hematoxylin/eosin stained, it was possible to observe a hollow conformation expressing Cytokeratin and proximal CD10 or distal Cytokeratin 7 tubular markers. Interestingly, they did not express Vimentin, evidencing that nephrosphere-derived cells had the capacity to generate three-dimensional structures able to mimic the in vivo tubular behavior (Figure 6A and S1D).

In Vivo Behavior of Nephrosphere Cells and PKH Sorted Cells

To evaluate the ability to generate three-dimensional structures in vivo, nephrosphere cells and PKH-sorted cells were embedded in a collagen pellet and transplanted under the renal capsule of CD1 nude mice. After 20 days, the kidneys with the pellet were removed and analyzed. Nephrosphere cells in the pellet raised tubular-like structures expressing human leucocyte antigen (HLA) as confirmation of human origin, Cytokeratin 18 as confirmation of epithelial lineage, and mutually exclusive E-Cadherin or N-Cadherin as confirmation of a differentiated tubular nature. No structures were found with PKH^{high} cells in the pellet, but the parenchyma just under the capsule presented some infiltrated cells. Morphologically these cells were not of inflammatory origin, did not express macrophage markers, were morphologically different with respect to the surrounding cells and were not organized in tubule- or glomerular-like structures. The immunofluorescence analysis of mice parenchyma demonstrated the presence of some HLA positive cells, suggesting that PKH^{high} cells could be migrated toward the parenchyma; these cells maintained

the negative expression of Cytokeratin (Figure 6B) as the PKH^{high} cells did in the nephrosphere (Figure 6C). $PKH^{low/neg}$ cells were neither able to generate structures within the pellet nor able to migrate into the parenchyma (Figure 6B).

CD133 and CD24 Expression Defines Different subpopulations in PKH^{high} Cells

In the past, the marker CD133 alone or together with CD24 has been used to evidence the presence of cells with stem/progenitor properties in adult human kidney (Bussolati *et al.*, 2005; Sagrinati *et al.*, 2006). In the total nephrosphere cell population there is a trend, although not significant, toward a percentage increment of $CD133^+/CD24^-$ and $CD133^+/CD24^+$, and a decrement of $CD133^-/CD24^-$ cellular phenotypes with respect to differentiated primary cell cultures (Figure 7A) that are not able to generate nephrospheres. The distribution of the two markers among the PKH subpopulations was also investigated. $CD133^+/CD24^+$ cells were detectable in all three PKH subpopulations with no statistical differences among them. Moreover, an enrichment of $CD133^+/CD24^-$ population in PKH^{high} cells was observed that was significant with respect to the PKH^{neg} cells, the total nephrosphere cell population, and the differentiated primary cell cultures (Figure 7B). In PKH^{high} cells, the $CD133^-/CD24^-$ phenotype reached the minimum level and the $CD133^-/CD24^+$ phenotype was expressed in very few. Considering that in the nephrospheres the only cells with self-renewal capacity were the PKH^{high} cells, these cells were sorted on the basis of the expression of the two markers to

assess whether there was a cell phenotype preferentially able to self-renew when plated in sphere-forming conditions. It was not possible to isolate the $CD133^-/CD24^+$ phenotype because of its scarcity in PKH^{high} cell population and, among the three sortable, filial spheres could only be obtained from the $CD133^+/CD24^-$ and $CD133^+/CD24^+$ subpopulation (Figure 7C). Moreover epithelial, podocytic and endothelial differentiation on these three subpopulations was induced (Figure 7D and Figure S3). Only CD133+/CD24-/PKH^{high} phenotype possessed the capacity to differentiate into all the three lineages. This subpopulation presented proximal (Cytokeratin and CD13) or distal (Cytokeratin and Calbindin-D) tubular epithelial markers, protrusions and podocytic (Synaptopodin and Podocin) markers, and the endothelial (von Willebrand factor) marker with its typical pattern (Figure S1C), when cultured in epithelial, podocytic and endothelial specific media respectively. CD133+/CD24+/PKH^{high} and CD133-/CD24-/PKH^{high} phenotypes were both able to differentiate into epithelial lineage and only into podocytic or endothelial lineages respectively.

Therefore, in the model of this study, the combination of the PKH^{high} status with the CD133+/CD24- phenotype enabled the identification of cells that in vitro displayed stem properties. These cells represented a ~ 72% cluster of the total PKH^{high} population and this percentage was similar to the SFE of PKH^{high} cells corrected for FACS effect (about 72%) (Table S2).

Discussion

Attempts to identify a resident adult stem cell in kidney have led to the identification of $CD133^+/CD24^+$ cells in the Bowman's capsule (Sagrinati *et al.*, 2006) or $CD133^+$ cells in the renal cortex (Bussolati *et al.*, 2005) and in the renal inner medulla (Bussolati *et al.*, 2012). However, it is now accepted that an accurate identification of adult stem cells should be performed not only on the basis of surface markers but also on functional features that define a stem cell (Snippert *et al.*, 2011) such as self-renewal and multipotency. In this study, the sphere-forming assay was used to exploit the functional characteristics of stem cells and allowed the isolation from adult kidney of a purified stem population with self-renewal and multipotency capacity. The nephrospheres described in this current study were demonstrated to be of clonal origin and can be propagated for several passages without increasing the total sphere number. Compared to the non-clonal spheroids obtained from adult renal cells described by others (Buzhor *et al.*, 2011) our model is different because of culture media and plating cellular density; high densities are suggested to promote aggregation rather than clonal growth (Singec *et al.*, 2006; Jessberger *et al.*, 2007; Lusis *et al.*, 2010). The maintenance of the total sphere number is an indication that in the dissociated nephrosphere there is just one cell able to perform an asymmetric division and self-renew and thus to generate a filial sphere. The expression of the renal embryonic marker Pax2, normally not expressed in adult renal cells, the coexistence of proximal and

distal tubular markers N-Cadherin and E-Cadherin in the same cell, as well as the expression of Synaptopodin and Podocin might indicate the spheres as a dynamic environment and a primitive renal cellular model in which self-renewal is maintained, and commitment toward different lineages is ongoing.

In the nephrospheres, as compared to corresponding differentiated primary cell cultures, the gene expression analysis evidenced a significant upregulation of stem cell and pluripotency markers. In addition there was an activation of Notch pathway, which is known to influence the stem/progenitor cell decisions to self-renew or differentiate (Mizutani *et al.*, 2007; Blanpain *et al.*, 2007; Fortini *et al.*, 2009), and to be involved in podocytic differentiation of adult renal progenitors (Lasagni *et al.*, 2010). These data suggest that these spheres are not an in vitro growth adaptation but may contain a stem cell population. It may also suggest which genes could be involved in stem cell maintenance and differentiation processes in adult kidney. Notch signaling is expressed throughout the development of nephrons (Sharma *et al.*, 2011; Sirin and Susztak, 2012) and the Notch receptors (Notch1 and Notch2) and ligand (Jagged1) involved in kidney development (McCright, 2003; Surendran *et al.*, 2010) are the same as those found upregulated in our nephrospheres. Moreover, the overexpression of genes of the Laminin family confirm that sphere cells may produce ECM components, thus aiding in the formation of a specific niche (Dontu *et al.*, 2003; Lusis *et al.*, 2010; Buzhor *et al.*, 2011).

The present work demonstrated the identification and the isolation of a subpopulation with stem abilities within the nephrospheres, exploiting the asymmetrical self-renewal capacity evidenced by the PKH assay. Only the brightest fluorescent PKH^{high} cell population, representative of a quiescent status, likely due to asymmetrical division, contained the cells able to generate nephrospheres by self-renew and thus possible stem cells.

Besides self-renewal, the other aspect that defines an adult stem cell is the capability to differentiate into the various cell types that compose an adult tissue (Alison and Islam, 2009). Within the nephrospheres, there are cells able to differentiate into an epithelial, podocytic, and endothelial lineage, and to form three-dimensional structures very similar to in vivo proximal or distal tubules. The ability to selectively differentiate into the three lineages is maintained by the isolated PKH^{high} cells when cultured in vitro. However, $PKH^{low/neg}$ subpopulations maintained only the epithelial differentiative capacity, maybe because they were already committed toward the epithelial lineage. The orthotopic transplantation of whole nephrosphere cells under the murine renal capsule showed their capability to organize in vivo eliciting tubular-like structures. The isolated PKH^{high} cells had an unexpected behavior. In fact, although they did not form structures, they survived and their presence in the parenchyma may suggest a possible migration toward the parenchyma maintaining an undifferentiated status, as if in vivo PKH^{high} cells alone were following a homing gradient. Therefore, it

seems that PKH^{high} cells can generate structures only when transplanted as a whole nephrosphere cell population in the presence of PKH^{low} and PKH^{neg} cells. However, these aspects need to be more investigated, even though this behavior seems similar to that of the Lgr5+ intestinal stem cells, which form in vitro organoids with high efficiency only if they are cultured together with their niche-supporting Paneth cells (Sato *et al.*, 2011). It has to be also remembered that stem cell progeny can provide important and diversified feedback mechanisms to regulate their stem cell parents and participate in the creation of a unique microenvironment to host the stem cells (Hsu and Fuchs, 2012).

The model of this current study showed that CD133 and CD24 markers, as a single or combined expression, are so promiscuous that are not able to identify a pure population of adult renal stem cells. In PKH^{high} cells, the only cell population presenting self-renew and an in vitro multipotency capacity, it was possible to identify three subpopulations with different phenotypes and behaviors on the basis of CD133 and CD24 expression. The CD133+/CD24-/PKH^{high}phenotype identified the only cells exhibiting self-renewal and multipotency for all the three lineages analyzed. The CD133+/CD24+/PKH^{high} phenotype had only a bipotent capacity although self-renewal is still maintained. It looks like the bipotent mammary progenitors that have clonogenic capacity (Zhao et al 2012) even though it decreases through each passage (Dontu et al 2003). The CD133-/CD24-/PKH^{high} phenotype differentiated only as epithelium or endothelium and lost

the self-renewal capacity, probably because of the lack of CD133, as described for adult renal progenitor cells (Sallustio et al 2013) and for cancer stem cells (Lan et al 2013; Li et al 2013). Therefore the combination of PKH^{high} status and CD133+/CD24- expression identify a stem population, never described before, that the in vitro assays suggest having self-renewal and multipotency capacity toward proximal and distal tubular, podocytic, and endothelial lineages. This cell population that gathered about 72% of the total PKH^{high} cells, according to the calculated SFE of PKH^{high} cells (about 72%), might be a candidate adult resident renal stem cell population. The PKH^{high} status probably hides a molecular profile that, until now, has not been disclosed. Further studies are needed to better characterize these cells, and a wide-range expression profiling is needed to find a specific signature able to identify them and their localization and fate on renal tissue.

In conclusion, the clonal nephrospheres described provided a homogeneous resident renal stem cell population more precisely defined with respect to those obtained using surface markers (Bussolati *et al*, 2005; Sagrinati *et al*, 2006), and permitted to isolate it with purity. It may represent a useful tool to better understand both the mechanisms that regulate self-renewal and differentiation in the adult renal tissues as well as the mechanisms that may be altered in nephropathies or renal cancer.

Acknowledgements

We thank E. Dugnani for useful advices; M Quinn for editing revision. This research was supported by MIUR Grants (PRIN, FAR) and in part by Associazione Gianluca Strada Onlus. The funders had no role in study design and preparation of the manuscript. S.B. was recipient of a Postdoctoral Fellowship and M.A.Z of a PhD fellowship from MIUR; V.D.S was recipient of a Postdoctoral Fellowship from Regione Lombardia – Fondazione Cariplo grant.

Conflict of interest

The authors declare that they have no conflict of interest

Figure legends

Figure 1: Growth Characteristics of Nephrospheres

(A) Representative phase-contrast image of a nephrosphere population. (B) Evaluation of nephrospheres clonality. Nephrospheres obtained from cells stained with red PKH26 alone, with green PKH2 alone, and from cells stained with PKH26 or PKH2 before mixing these two populations together. (C) Growth curve of nephrosphere culture. The curves represent the number of spheres/well against the different passages obtained from 4 different patients. For each passage, $2x10^4$ cells obtained from the previous passage were plated onto a well. The continuous line represents the average. Bars, 100μm. See also Table S2.

Figure 2: Immunophenotypical Characterization of Nephrospheres

(A) IF and FACS analysis of nephrospheres with the antibodies indicated. For PAX2 stained nephrospheres the DAPI signal is in the

insert. The arrows show Synaptopodin positivity. Blue: DAPI. Yellow: colocalization of red and green signals of E-Cadherin and N-Cadherin (400x; Bars, 50µm). Results are typical and representative of three independent experiments. FACS analysis data for Cytokeratin are also referred to three independent experiments, mean±SD of positive cells is reported. (B) Representative FACS analysis of nephrosphere cells and primary cell culture cells after ALDEFLUOR assay. Cells incubated with ALDEFLUOR substrate and DEAB, were used to set the baseline fluorescence (ALDE-) and to define the ALDEFLUOR-positive region (ALDE+). Incubation of cells with ALDEFLUOR substrate alone induces a shift of fluorescence in ALDE+ region, defining the ALDEFLUOR-positive cell population that is higher in nephrosphere cells. The data are referred to three independent experiments (mean±SD). NS: Nephrospheres. PCC: primary cell cultures. *$p<0.01$.

Figure 3: Stem Cell TLDA Profile and Notch Pathway Expression in Nephrospheres

(A) TMEV heat map showing the 56 analyzed genes expressed in nephrospheres and primary cell cultures established from four different patients. Samples were clustered on the basis of the gene expression evaluated as ΔCt. Green: lowest level of ΔCt, highest level of expression. Red: highest level of ΔCt, lowest level of expression. (B) Expression level of pluripotency genes, ECM genes and Notch pathway genes in nephrospheres with respect to primary cell cultures. The values are expressed as $2^{-\Delta\Delta Ct}$ which represent the expression fold change in nephrospheres in respect to the

differentiated primary cell cultures. The differences are all significant, see also Table S1A and S1B. The error bars represent the maximum and minimum $2^{-\Delta\Delta Ct}$. ECM: extracellular matrix. NS: nephrospheres. PCC: primary cell cultures.

Figure 4: Identification and Isolation of PKH^{high} Stem-Like Cells in the Nephrospheres

(A) Typical and representative images of red PKH26 distribution in all obtained nephrospheres. (B) Typical FACS profile of a PKH26-labeled nephrosphere cell population with gated populations (left) and suspension cultures in sphere-forming conditions of FACS-sorted PKH^{high}, PKH^{low} and PKH^{neg} cells at day 12 (right). (C) A single PKH^{high} cell monitored for clonal growth at specific indicated time points. The image is Representative of 3 different clonal sortings performed. Bars, 100µm. See also Table S2.

Figure 5: Differentiation Ability of Nephrosphere-Derived Cells or PKH-Sorted Cells

Epithelial differentiation of nephrosphere-derived cells. (A) Representative phase-contrast morphology of nephrosphere cells cultured in epithelial differentiation medium at 2 or 7 days; Bars, 100µm. (B) Typical FACS profile of tubular markers in nephrosphere cells differentiated into epithelium, mean±SD of 3 independent experiments. (C) IF analysis of epithelial-differentiated nephrosphere cells with indicated antibodies; Bars, 20µm. (D) Podocytic differentiation of nephrosphere cells, IF analysis with the indicated antibodies; Bars, 20µm. See also Figure S1B.

PKH^{high} (top) and $PKH^{low/neg}$ (bottom) sorted cells, IF analysis with the indicated antibodies; Bars, 20µm. (E) Epithelial differentiation. (F) Podocytic differentiation. (G) Endothelial differentiation

ECAD: E-Cadherin; NCAD: N-Cadherin; CD13: Aminopeptidase-N; CALB: Calbindin D; CK: pan-Cytokeratin; Syn: Synaptopodin; vWf: von Willebrand factor; Blue: DAPI.

Figure 6: In Vitro and in Vivo Formation of Three-Dimensional Tubular-Like Structures

(A) Three-dimensional tubular-like structures grown from nephrosphere cells in collagen type I (top) or matrigel (bottom). From the left: representative phase-contrast micrographs of structures (200x; bars, 100µm); hematoxylin-eosin staining (H&E), immunohistochemical analysis with the indicated antibodies (600x; bars, 20µm). (B) In vivo evaluation of nephrosphere, PKH^{high} and $PKH^{low/neg}$ cells (from top to bottom). On the left: representative hematoxylin-eosin staining of renal parenchyma of nude mice after transplantation under capsule of collagen pellet with total nephrosphere (NS)-derived cells (top), PKH^{high} sorted cells (middle), $PKH^{low/neg}$ sorted cells (bottom). The structure formed (arrowheads) and the infiltration of cells just under the pellet (arrow) are shown. On the right: IF analysis, with the indicated antibodies, of structures formed by nephrosphere cells (top), of infiltrated PKH^{high} cells (middle), and $PKH^{low/neg}$ cells (bottom) (400x; bars, 20µm). (C) Representative IF analysis of the different distribution of Cytokeratin

(green) with respect to PKH26 (red) in nephrospheres (400x; bar, 50µm).

Blue: DAPI; CK: pan cytokeratin; CD10: CD10; CK7: Cytokeratin 7; VIM: Vimentin; HLA: Human Leucocyte Antigen; CK18: Cytokeratin 18; NCAD: N-Cadherin; ECAD: E-Cadherin.

Figure 7: Expression of CD133 and CD24 markers in the spheres

(A) Representative FACS profile of CD133 and CD24 markers in differentiated primary cell cultures (PCC), nephrosphere cells (NS), and PKH^{neg}, PKH^{low},PKH^{high}-sorted cell subpopulations. Mean±SD of 4 independent experiments. (B) Percentage of CD133+/CD24- cells among the different cell populations. Mean±SD of 4 independent experiments; *$p<0.05$. (C) Sorted CD133+/CD24-/PKH^{high}, CD133+/CD24+/PKH^{high} and CD133-/CD24-/PKH^{high} cell populations plated in sphere-forming conditions. Representative phase-contrast images (100x). (D) Epithelial, podocytic and endothelial differentiation of sorted CD133+/CD24-/PKH^{high}, CD133+/CD24+/PKH^{high} and CD133-/CD24-/PKH^{high} cell populations, IF analysis with the indicated antibodies; representative images of 3 independent experiments. Bars, 20µm. For the staining of CK/SYN on podocytic-differentiated cells two different fields are shown. See also Figure S3 for negative controls. CD13: Aminopeptidase-N; CALB: Calbindin D; CK: pan-Cytokeratin; Syn: Synaptopodin; vWf: von Willebrand factor; Blue: DAPI.

Supplementary data to this article can be found online at http://dx.doi.org/10.1016/j.scr.2013.08.004.

Figure 1

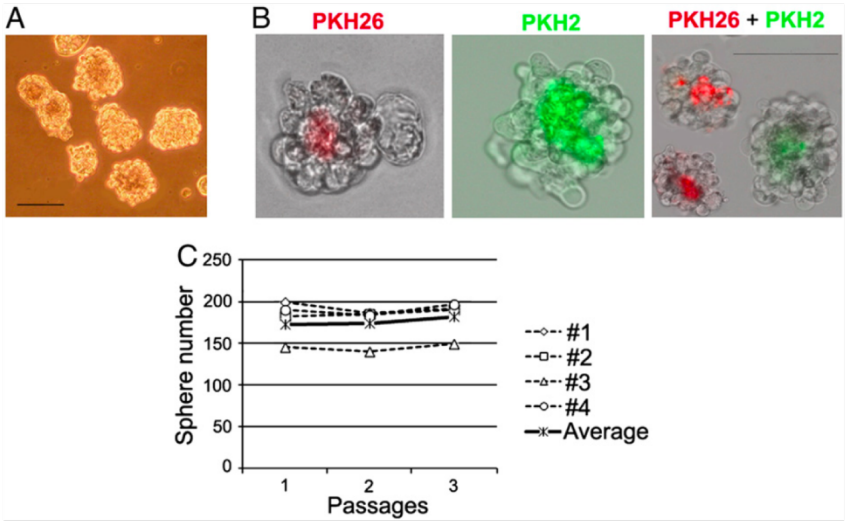
A
B
PKH26
PKH2
PKH26 + PKH2
C
Sphere number
250
200
150
100
50
0
1
2
3
Passages
#1
#2
#3
#4
Average

Figure 2

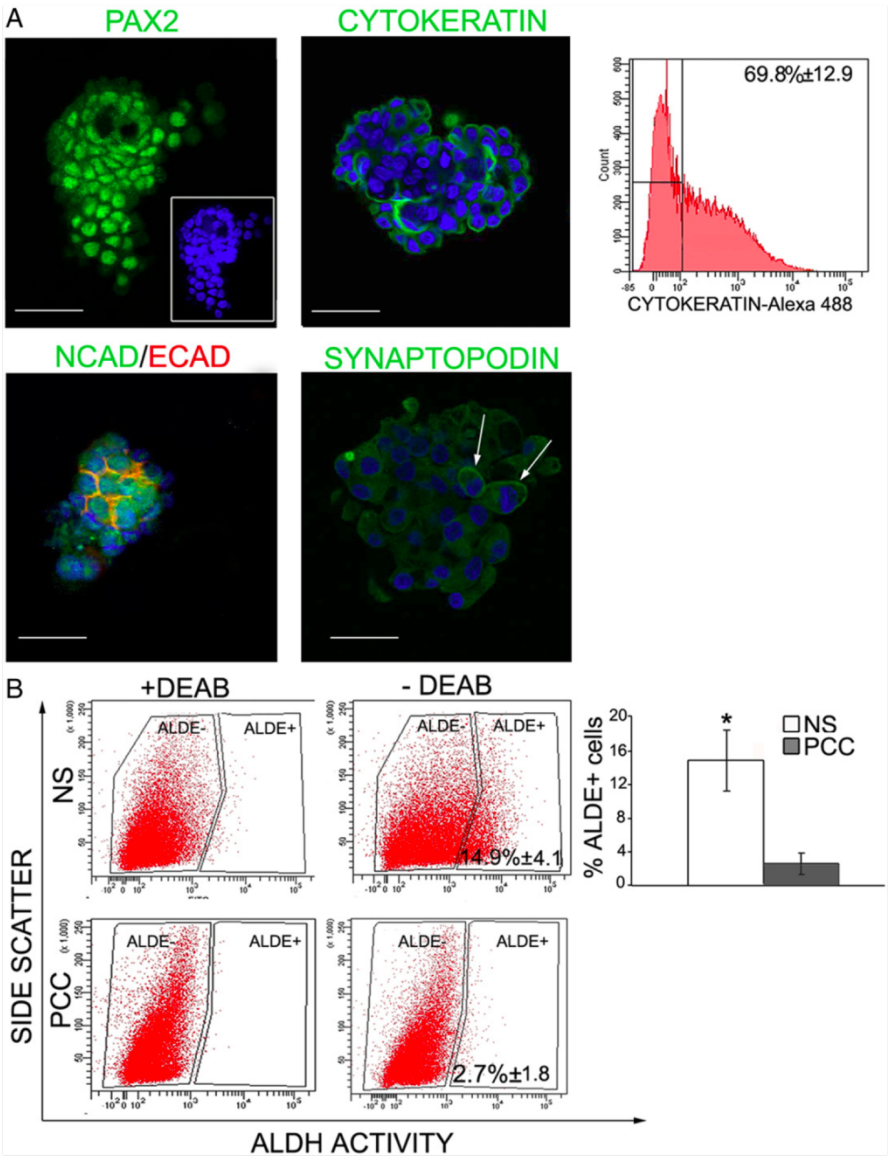
A
PAX2
CYTOKERATIN
69.8%±12.9
Count
CYTOKERATIN-Alexa 488
NCAD/ECAD
SYNAPTOPODIN
B
+DEAB
- DEAB
NS
PCC
ALDE-
ALDE+
14.9%±4.1
2.7%±1.8
% ALDE+ cells
NS
PCC
SIDE SCATTER
ALDH ACTIVITY

Figure 3

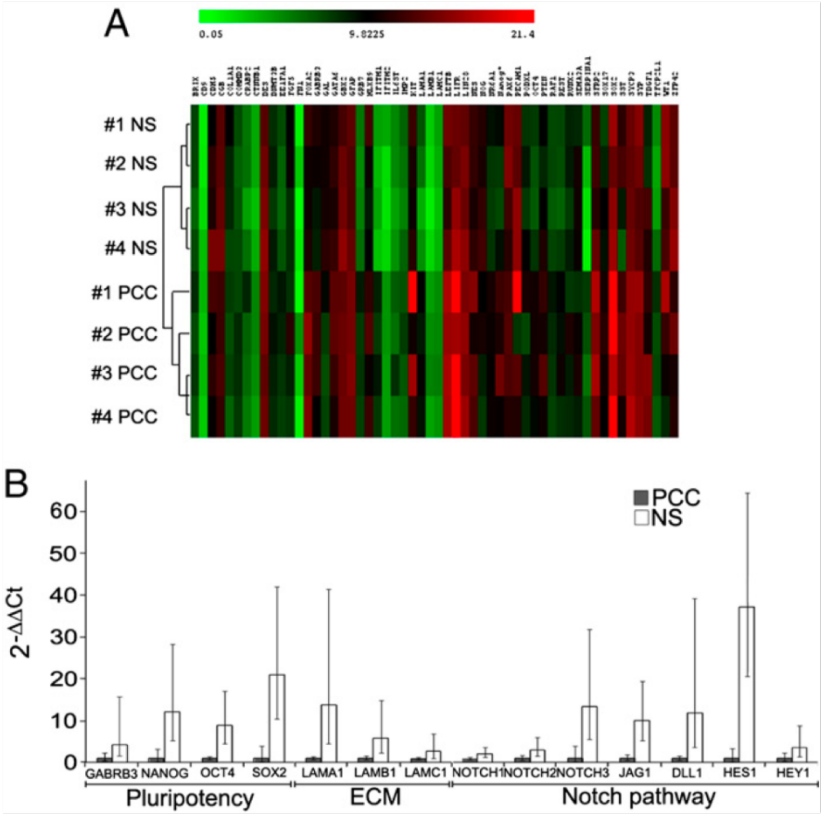
A
0.05
9.0225
21.4
#1 NS
#2 NS
#3 NS
#4 NS
#1 PCC
#2 PCC
#3 PCC
#4 PCC
B
PCC
NS
2-ΔΔCt
0
10
20
30
40
50
60
GABRB3
NANOG
OCT4
SOX2
LAMA1
LAMB1
LAMC1
NOTCH1
NOTCH2
NOTCH3
JAG1
DLL1
HES1
HEY1
Pluripotency
ECM
Notch pathway

Figure 4

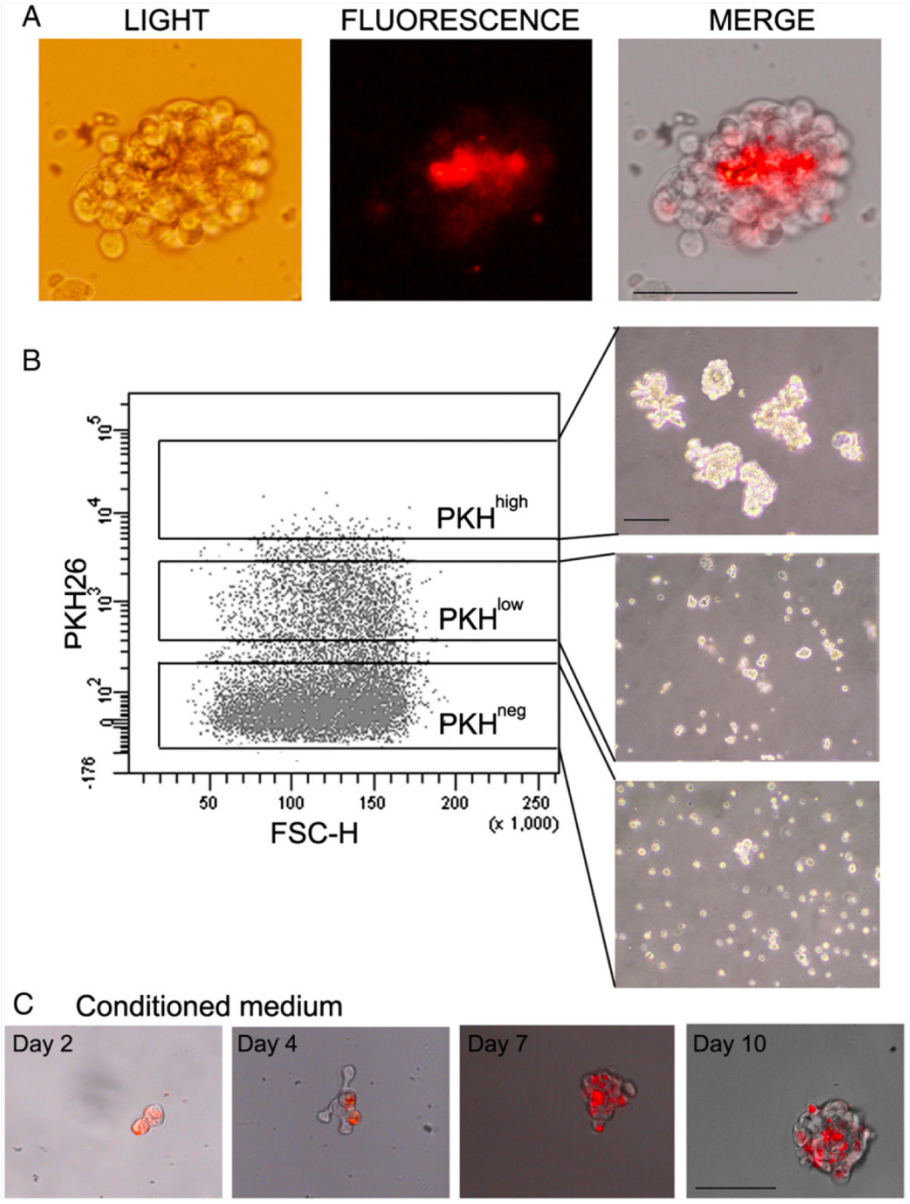
A
LIGHT
FLUORESCENCE
MERGE
B
PKH26
PKH^high
PKH^low
PKH^neg
FSC-H
(x 1,000)
C
Conditioned medium
Day 2
Day 4
Day 7
Day 10

Figure 5

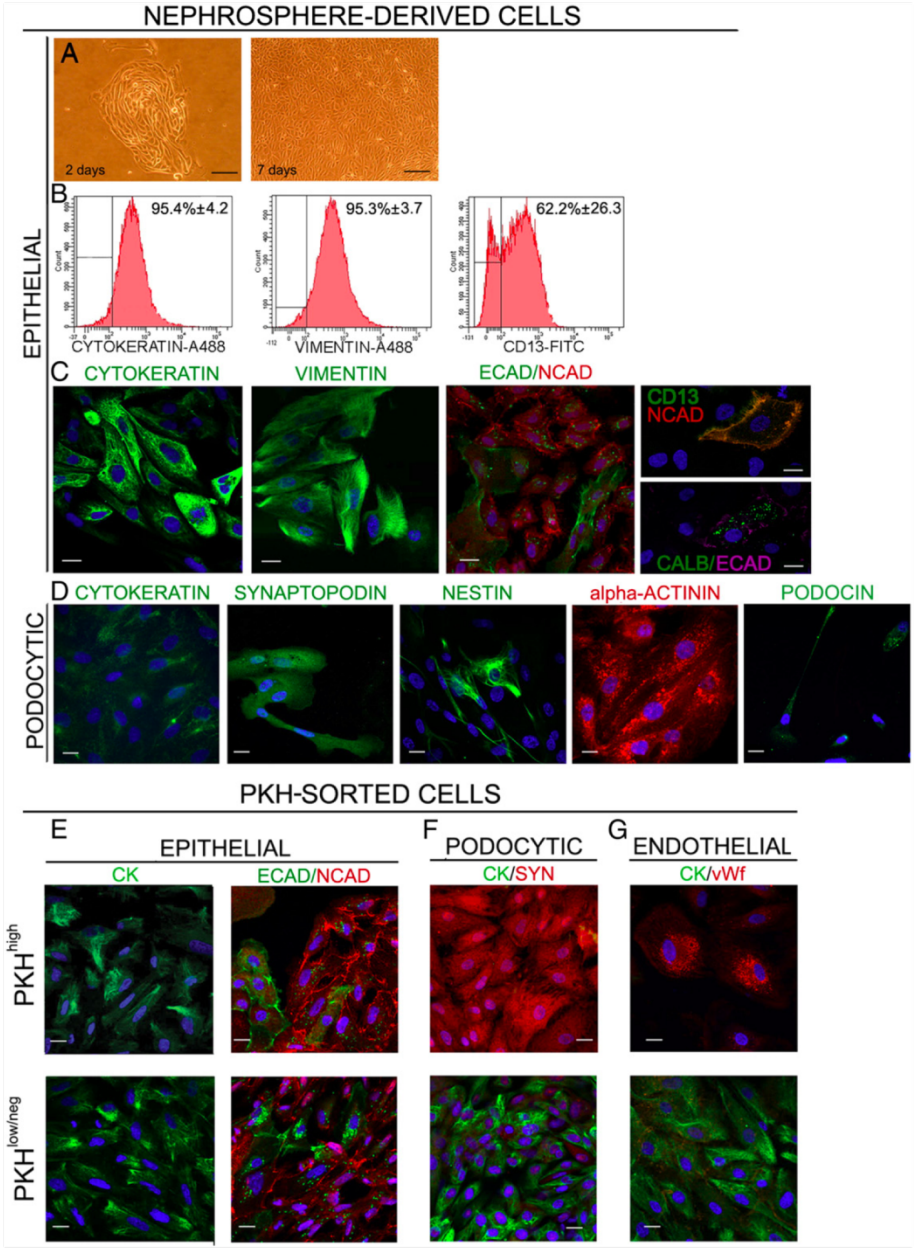
NEPHROSPHERE-DERIVED CELLS
A
2 days
7 days
EPITHELIAL
B
95.4%±4.2
95.3%±3.7
62.2%±26.3
CYTOKERATIN-A488
VIMENTIN-A488
CD13-FITC
C
CYTOKERATIN
VIMENTIN
ECAD/NCAD
CD13
NCAD
CALB/ECAD
D
CYTOKERATIN
SYNAPTOPODIN
NESTIN
alpha-ACTININ
PODOCIN
PODOCYTIC
PKH-SORTED CELLS
E
EPITHELIAL
CK
ECAD/NCAD
F
PODOCYTIC
CK/SYN
G
ENDOTHELIAL
CK/vWf
PKH high
PKH low/neg

Figure 6

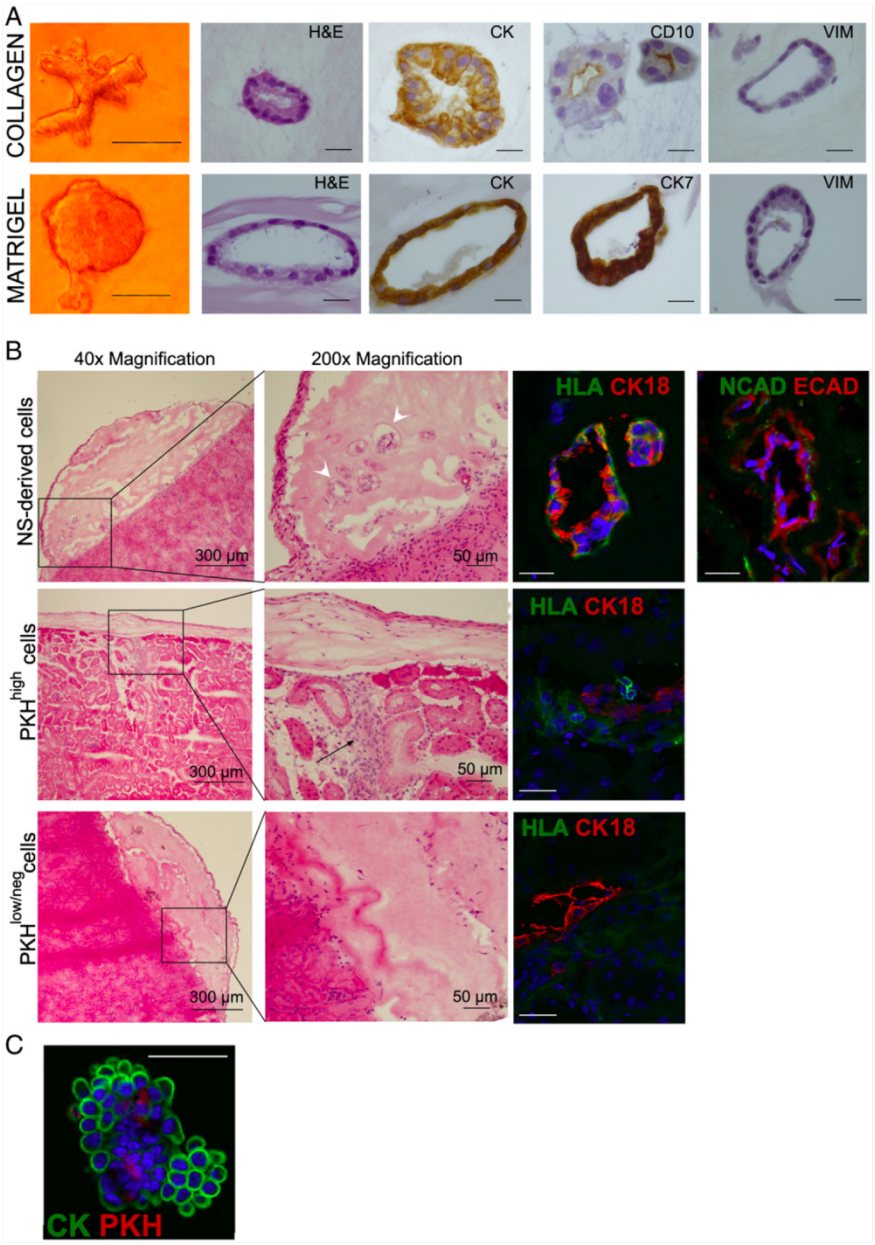
A
COLLAGEN
MATRIGEL
H&E
CK
CD10
VIM
H&E
CK
CK7
VIM
B
40x Magnification
200x Magnification
NS-derived cells
PKH high cells
PKH low/neg cells
300 µm
50 µm
HLA CK18
NCAD ECAD
HLA CK18
HLA CK18
C
CK PKH

Figure 7

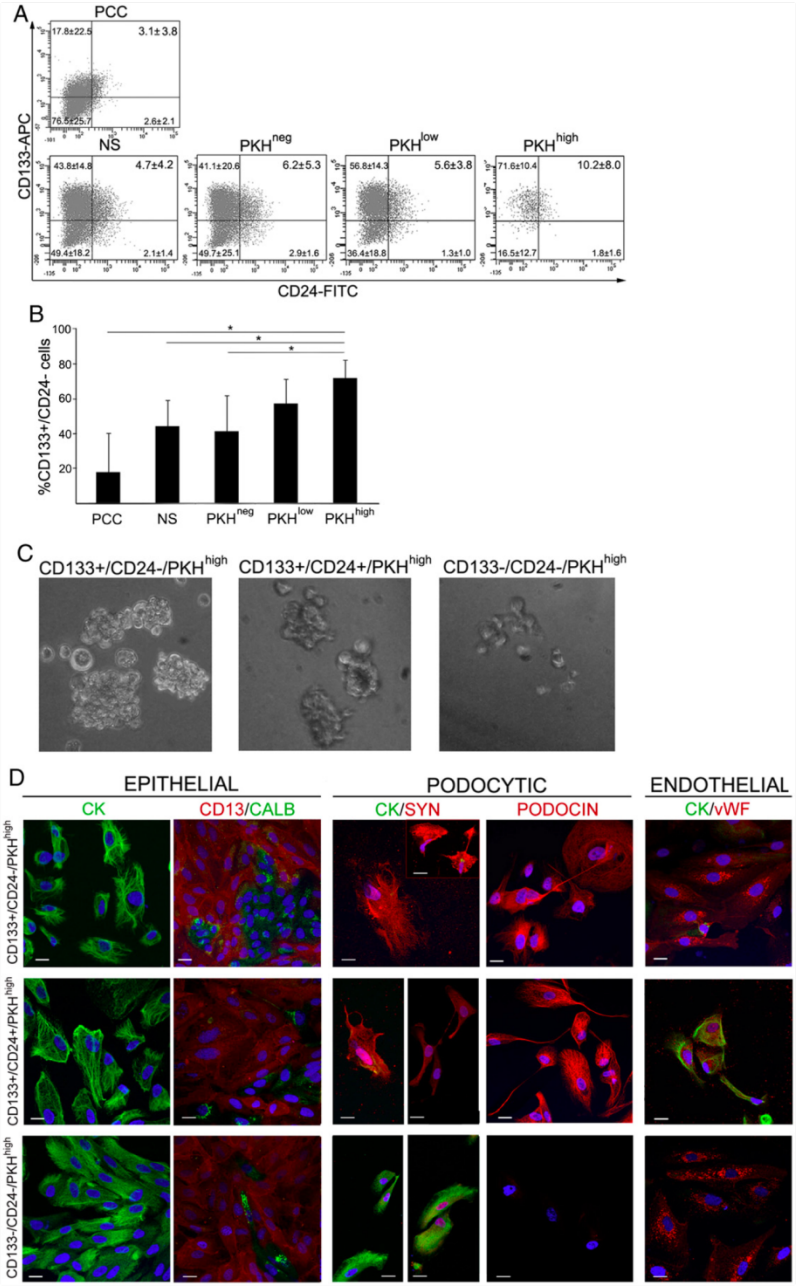
A
PCC
NS
PKH^neg
PKH^low
PKH^high
CD133-APC
CD24-FITC
B
%CD133+/CD24- cells
PCC
NS
PKH^neg
PKH^low
PKH^high
C
CD133+/CD24-/PKH^high
CD133+/CD24+/PKH^high
CD133-/CD24-/PKH^high
D
EPITHELIAL
PODOCYTIC
ENDOTHELIAL
CK
CD13/CALB
CK/SYN
PODOCIN
CK/vWF
CD133+/CD24-/PKH^high
CD133+/CD24+/PKH^high
CD133-/CD24-/PKH^high

References

Alison, M.R., Islam, S., 2009. Attributes of adult stem cells. J.Pathol. 217(2), 144-160.

Armstrong, L., Stojkovic, M., Dimmick, I., Ahmad, S., Stojkovic, P., Hole, N., et al., 2004. Phenotypic characterization of murine primitive hematopoietic progenitor cells isolated on basis of aldehyde dehydrogenase activity. Stem Cells. 22(7), 1142-1151.

Baer, P.C., Nockher, W.A., Haase, W., Scherberich, J.E., 1997. Isolation of proximal and distal tubule cells from human kidney by immunomagnetic separation. Kidney International. 52(5), 1321-1331.

Barker, N., Rookmaaker, M.B., Kujala, P., Ng, A., Leushacke, M., Snippert, H., van de Wetering, M., et al., 2012. Lgr5(+ve) stem/progenitor cells contribute to nephron formation during kidney development. Cell Rep. 2(3), 540-552.

Bianchi, C., Bombelli, S., Raimondo, F., Torsello, B., Angeloni, V., Ferrero, S., et al., 2010. Primary cell cultures from human renal cortex and renal-cell carcinoma evidence a differential expression of two spliced isoforms of Annexin A3. Am. J. Pathol. 176(4), 1660-1670.

Blanpain, C., Horsley, V., Fuchs, E., 2007. Epithelial stem cells: Turning over new leaves. Cell. 128(3), 445-458.

Bussolati, B., Bruno, S., Grange, C., Buttiglieri, S., Deregibus, M.C., Cantino, D., et al., 2005. Isolation of renal progenitor cells from adult human kidney. Am.J.Pathol. 166(2), 545-555.

Bussolati, B., Moggio, A., Collino, F., Aghemo, G., D'Armento, G., Grange, C., et al., 2012. Hypoxia modulates the undifferentiated phenotype of human renal inner medullary CD133+ progenitors through Oct4/miR-145 balance. Am.J.Renal Physiol. 302(1), F116-28.

Buzhor, E., Hararri-Steinberg, O., Omer, D., Metsuyanim, S., Jacob-Hirsch, J., Noiman, T., et al., 2011. Kidney spheroids recapitulate tubular organoids leading to enhanced tubulogenic potency of human kidney-derived cells. Tissue Eng.Part A. 17(17-18), 2305-2319.

Corti, S., Locatelli, F., Papadimitriou, D., Donadoni, C., Salani, S., Del Bo, R., et al., 2006. Identification of a primitive brain-derived neural stem cell population based on aldheyde dehydrogenase activity. Stem Cells. 24(4), 975-985.

Cicalese, A., Bonizzi, G., Pasi, C., Faretta, M., Ronzoni, S., Giulini, B., et al., 2009. The tumor suppressor p53 regulates polarity of self-renewing divisions in mammary stem sells. Cell. 138(6), 1083-1095.

Dontu, G., Abdallah, W.M., Foley, J.M., Jackson, K.W., Clarke, M.F., Kawamura, M.J., et al., 2003. In vitro propagation and trascriptional profiling of human mammary stem/progenitor cells. Genes Dev. 17(10), 1253-1270.

Eirew, P., Stingl, J., Raouf, A., Turashvili, G., Aparicio, S., Emerman, J.T., et al., 2008. A method for quantifying normal human mammary epithelial stem cells with in vivo regenerative ability. Nat.Med. 14(12), 1384-1389.

Forino, M., Torregrossa, R., Ceol, M., Murer, L., Delle Vella, M.,Del Prete, D., et al., 2006. TGFbeta1 induces epithelial-mesenchymal transition, but not myofibroblast transdifferentiation of human kidney tubular epithelial cells in primary culture. Int.J.Exp.Path. 87(3), 197-208.

Fortini, M.E., 2009. Notch signalling: The core pathway and its posttraslational regulation. Dev.Cell. 16(5), 633- 647.

Hemmingsen, C., 2000. Regulation of renal calbindin-D28K.Pharmaciol. Toxicol. 87, Suppl. 3, 5-30.

Hsu, Y.C., Fuchs, E., 2012. A family business: stem cell progeny join the niche to regulate homeostasis. Nat.Rev.Mol. Cell Biol. 13(2), 103-114.

Jessberger, S., Clemenson, Jr G.D., Gage, F.H., 2007. Spontaneous fusion and nonclonal growth of adult neural stem cells. Stem Cells. 25(4), 871-874.

Keller, C., Kroening, S., Zuehlke, J., Kunath, F., Krueger, B., Goppelt-Struebe, M., 2012. Distinct mesenchymal alterations in N-cadherin and E-cadherin positive primary renal epithelial cells. PLoS One. 7(8), e43584.

Lan, X., Wu, XZ., Wang, Y., Wu, FR., Zang, CB., Tang, C., et al.,CD133 silencing inhibits stemness properties and enhances chemoradiosensitivity in CD133-positive liver cancer stem cells. Int. J. Mol. Med.. 31(2), 315-324.

Lasagni, L., Ballerini, L., Angelotti, M.L., Parente E., Sagrinati, C., Mazzinghi B., et al., 2010. Notch activation differentially regulates renal progenitors proliferation and differentiation toward the podocyte lineage in glomerular disorders. Stem Cells. 28(9), 1674-1685.

Lawson, D.A., Xin, L., Lukacs, R.U., Cheng, D., Witte, O.N., 2007. Isolation and functional characterization of murine prostate stem cells. Proc. Natl.Acad.Sci.USA. 104(1), 181-186.

Li, Z., 2013. CD133: a stem cell biomarker and beyond. Exp. Hematol. Oncol. 2(1), 17-24.

Lindgren, D., Bostrom, A.K., Nilsson, K., Hansson, J., Sjolund, J., Moller, C., et al., 2011. Isolation and characterization of progenitor-like cells from human renal proximal tubules. Am.J.Pathol. 178(2), 828-837.

Lusis, M., Li, J., Ineson, J., Christensen, M.E., Rice, A., Little, M.H., 2010. Isolation of clonogenic, long-term self renewing embryonic renal stem cells. Stem Cell Research. 5(1), 23-39.

McCampbell, K.K., Wingert, R.A., 2012. Renal stem cells: fact or science fiction? Biochem. J. 444(2), 153-168.

McCright, B., 2003. Notch signaling in kidney development. Curr.Opin.Nephrol. Hypertens. 12(1), 5-10.

Mizutani, K., Yoon, K., Dang, L., Tokunaga, A., Gaiano, N., 2007. Differential Notch signaling distinguishes neural stem cells from intermediate progenitors. Nature. 449(7160), 351-355.

Nouwen, E.J., Dauwe, S., van der Biest, I., De Broe, M.E., 1993. Stage- and segment-specific expression of cell-adhesion molecole N-CAM, A-CAM, and L-CAM in the kidney. Kidney Int. 44(1), 47-58.

Pece, S., Tosoni, D., Confalonieri, S., Mazzarol, G., Vecchi, M., Ronzoni, S., et al., 2010. Biological and molecular heterogeneity of breast cancers carrelates with their cancer stem cell content. Cell. 140(1), 62-73.

Perego, R.A., Bianchi C., Corizzato, M., Eroini, B., Torsello, B., Valsecchi, C., et al., 2005. Primary cell cultures arising from normal kidney and renal cell carcinoma retain the proteomic profile of corresponding tissues. J.Proteome Res. 4(5), 1503-1510.

Perego, R.A., Corizzato, M., Bianchi C., Eroini, B., Bosari, S., 2005a. N- and C-terminal isoforms of arg quantified by real-time PCR are specifically espressed in human normal and neoplastic cells, in neoplastic cell lines, and in HL-60 cell differentiation. Mol.Carcinog. 42(4), 229-239.

Prozialeck, W.C., Lamar, P.C., Appelt, D.M., 2004. Differential expression of E-cadherin, N-cadherin and beta-catenin in proximal and distal segments of the rat nephron. BMC Physiol. 4,10.

Reynolds, B.A., Weiss, S., 1992. Generation of neurons and astrocytes from isolated cells of the adult mammalian central nervous system. Science. 255(5052), 1707-1710.

Rovira, M., Scott, S.G., Liss, A.S., Jensen, J., Thayer, S.P., Leach, S.D., 2010. Isolation and characterization of centroacinar/terminal ductal progenitor cells in adult mouse pancreas. Proc.Natl.Acad.Sci.USA. 107(1), 75-80.

Sallustio, F., Serino, G., Costantino, V., Curci, C., Cox, SN., De Palma, G., et al., 2013. miR-1915 and miR-1225-5p regulate the expression of CD133, PAX2 and TRL2 in adult renal progenitor cells. PLoS One. 8(7), e68296.

Sangrinati, C., Netti, G.S., Mazzinghi, B., Lazzeri, E., Liotta, F., Frosali, F., et al., 2006. Isolation and characterization of multipotent progenitor cells from the Bowman's capsule of adult human kidneys. J.Am.Soc.Nephrol. 17(9), 2443-2456.

Sato, T., Van, H.S., Sato, T., van Es, J.H., Snippert, H.J., Stange, D.E., et al., 2011. Paneth cells constitute the niche for Lgr5 stem cells in intestinal crypts. Nature. 469(7330), 415-418.

Sharma, S., Sirin, Y., Susztak, K., 2011. The story of Notch ancd chronic kidney disease. Curr.Opin.Nephrol.Hypertens. 20(1), 56-61.

Singec, I., Knoth, R., Meyer, R.P., Maciaczyk, J., Volk, B., Nikkhah, G., et al., 2006. Defining the actual sensitivity and specificity of the neurosphere assay in stem cell biology. Nat.Meth. 3(10), 801-806.

Sirin, Y., Susztak, K., 2012. Notch in the kidney: development and disease. J.Pathol. 226(2), 394-403.

Snippert, H.J., Clevers, H., 2011. Tracking adult stem cells. EMBO Rep. 12(2), 113-122.

Surendran, K., Boyle, S., Barak, H., Kim, M., Stomberski, C., McCright, B., et al., 2010. The contibution of Notch1 to nephron segmentation in the developing kidney is revealed in a sensitized Notch2 background and can be augmented by reducing Mint dosage. Dev.Biol. 337(2), 386-395.

Terkikh, V.V., Vasilev, A.V., Vorotelyak, E.A., 2012. Label retaining cells and cutaneous stem cells. Stem Cell Rev. and Rep. 8(2), 414-425.

Zhao, X., Malhotra, GK., Band, H., Band, V., 2012. Derivation of myoepithelial progenitor cells from bipotent mammary stem/progenitor cells. PLoS One. 7(4), e35338.

Chapter 3

Renal cell carcinoma primary cultures maintain genomic and phenotypic profile of parental tumor tissues

BMC Cancer 2011, 11:244

Ingrid Cifola[1]*, Cristina Bianchi [2]*, Eleonora Mangano[1], Silvia Bombelli[2], Fabio Frascati[1], Ester Fasoli[3], Stefano Ferrero[3], Vitalba Di Stefano[2], Maria Anna Zipeto[2], Fulvio Magni[2], Stefano Signorini[4], Cristina Battaglia[5§], Roberto A. Perego[2§]

*equally contributing

1 Institute for Biomedical Technologies (ITB), National Research Council (CNR), Milan, Italy

2 Department of Experimental Medicine, University of Milano-Bicocca, Milan, Italy

3 Department of Medicine, Surgery and Dentistry, Pathological Anatomy Unit, University of Milan, San Paolo Hospital and "Ospedale Maggiore Policlinico" Foundation, Milan, Italy

4 Department of Laboratory Medicine, Desio Hospital, University of Milano-Bicocca, Milan, Italy

5 Dipartimento di Scienze e Tecnologie Biomediche, Università degli Studi di Milano, Milan, Italy

Abstract

Background

Clear cell renal cell carcinoma (ccRCC) is characterized by recurrent copy number alterations (CNAs) and loss of heterozygosity (LOH), which may have potential diagnostic and prognostic applications. Here, we explored whether ccRCC primary cultures, established from surgical tumor specimens, maintain the DNA profile of parental tumor tissues allowing a more confident CNAs and LOH discrimination with respect to the original tissues.

Methods

We established a collection of 9 phenotypically well-characterized ccRCC primary cell cultures. Using the Affymetrix SNP array technology, we performed the genome-wide copy number (CN) profiling of both cultures and corresponding tumor tissues. Global concordance for each culture/tissue pair was assayed evaluating the correlations between whole-genome CN profiles and SNP allelic calls. CN analysis was performed using the two CNAG v3.0 and Partek softwares, and comparing results returned by two different algorithms (Hidden Markov Model and Genomic Segmentation).

Results

A very good overlap between the CNAs of each culture and corresponding tissue was observed. The finding, reinforced by high whole-genome CN correlations and SNP call concordances, provided evidence that each culture was derived from its corresponding tissue and maintained the genomic alterations of parental tumor. In addition, primary culture DNA profile remained stable for at least 3 weeks, till to third passage. These cultures showed a greater cell

homogeneity and enrichment in tumor component than original tissues, thus enabling a better discrimination of CNAs and LOH. Especially for hemizygous deletions, primary cultures presented more evident CN losses, typically accompanied by LOH; differently, in original tissues the intensity of these deletions was weaken by normal cell contamination and LOH calls were missed.

Conclusions

ccRCC primary cultures are a reliable *in vitro* model, well-reproducing original tumor genetics and phenotype, potentially useful for future functional approaches aimed to study genes or pathways involved in ccRCC etiopathogenesis and to identify novel clinical markers or therapeutic targets. Moreover, SNP array technology proved to be a powerful tool to better define the cell composition and homogeneity of RCC primary cultures .

Background

The clear cell subtype of renal cell carcinoma (ccRCC) accounts for 85% of all RCCs and occurs as familial or, more often, sporadic forms. It is characterized by recurrent genetic anomalies, like copy number alterations (CNAs) and loss of heterozygosity (LOH), that involve specific chromosomes (chrs) and result in deletions with LOH on chrs 3p (often involving the von Hippel Lindau (*VHL*) locus in 3p26-p25), 6q, 8p, 9p and 14q, and duplications of chrs 5q and 7 [1-3]. Evidences suggest that this peculiar pattern of genomic instability represents a tumor-specific molecular fingerprint useful for diagnostic and prognostic applications [3-5]. However, more work still needs to

completely clarify the complex molecular pathogenesis of ccRCC. Although the involvement of the *VHL* tumor suppressor gene has been demonstrated in all familial and in 80-90% sporadic ccRCCs, the remaining 10-20% harbors wild-type *VHL*[6, 7], suggesting that, despite their identical histological phenotype, these tumors have an intrinsic molecular heterogeneity that still needs to be unraveled [6, 8]. The recognition of this molecular heterogeneity might improve the selection of patients for targeted therapies and allow the identification of specific oncogenes and tumor suppressor genes to be used as novel clinical markers or therapeutic targets.

The current availability of high-throughput platforms to assess molecular changes at genome-wide level might provide an opportunity to achieve this goal. Presently a comprehensive and detailed genomic profiling of DNA alterations is possible by using the single nucleotide polymorphism (SNP) array technology. Unlike CGH technique, the SNP array platform allows the simultaneous analysis of both chromosomal and allelic imbalances [9] and the distinction between LOH associated with CN changes (such as hemizygous deletions) and CN neutral status (often termed as uniparental disomy) [10]. In addition, this technology is able to provide information about the fraction of normal and tumor cell present in the tumor tissue samples [11]. This allows a more complete definition of the complex genetic rearrangements associated with cancer pathologies. Moreover, since the regions of LOH accompanied by deletion (representing the second hit of Knudson's hypothesis) are of

particular interest because they may contain genes involved in tumor etiology, the assessment of deletion/LOH areas represents a useful approach to identify regions potentially harboring novel tumor suppressor genes [12]. Accordingly, in a previous study, we used the SNP array technology to characterize the whole-genome DNA profile of a collection of ccRCC tissue samples to find novel chromosomal regions and genes potentially interesting as candidate tumor markers [13].

However, in ccRCC specimens, as in most solid tumor tissues, the molecular analyses may be affected by tissue heterogeneity due to the presence of necrotic areas and non-tumor cells, such as tumor-infiltrating leukocytes, endothelial cells and fibroblasts [14]. With the purpose to increase the quality of data by minimizing this "background noise, several different technical approaches have been explored [15]. Tissue heterogeneity must be considered also when evaluating which are the most appropriate computational tools to process and analyze array-based CN data [11, 16].

Thus, to overcome the problem of tissue heterogeneity and to prospectively perform *in vitro* functional studies aimed to better understand ccRCC molecular pathogenesis, it is necessary to have a viable and more homogeneous cell material retaining the phenotypic and genomic profile of original tissue. A possible strategy to face these requirements is to adapt fresh ccRCC tissue specimens to grow *in vitro* as primary cell cultures, which provide a good quality, homogeneous and well-characterized cellular material, enriched with tumor cell component [17] and retaining at the first passages the

phenotypic and proteomic profile of the corresponding tissues from which they derive [15, 18, 19]. Hence, primary cultures represent a better *in vitro* tumor model than stable cell lines, that can be even very different from the original tissues and thus not at all representative [6]. Anyway, the reliability of data obtained from primary cultures strictly depends on their careful cytological characterization, especially regarding possible cell contaminations that might influence data interpretation with misleading effects.

In this study, we investigated whether ccRCC primary cultures, established from surgical tumor specimens and phenotypically well-characterized, maintain the DNA profile of parental tumor tissues and allow a better discrimination of CNAs and LOH with respect to original tissues. Till now, the comparison of DNA profile between tumor primary cultures and parental tissues has been reported, with discordant results, in melanoma [20], neuroblastoma [21] and glioblastoma [22], using either SNP array or array-CGH techniques, and in RCC [23] only using traditional CGH on metaphase spreads and short-term primary cultures not extensively characterized.

Methods

ccRCC primary culture preparation and immunophenotypic characterization

Nine ccRCC primary cultures were established from corresponding surgical tissue specimens of ccRCC cases (Table 1). Patients were enrolled in the research project at Policlinico Hospital (University of

Milan, Italy) and provided informed consent for the research use of leftover material. Study protocol and procedures were approved by the local ethic committee. All RCC cases were diagnosed as “clear cell” subtype independently by two pathologists with expertise in kidney cancer. Prior to surgery, a whole blood sample was collected for each case and stored at –20°C. Immediately after surgical removal of the kidney, sections of fresh tissue samples enriched in tumor component by needle dissection were both stored at -80°C and collected in cold DMEM medium supplemented with 10% fetal calf serum (FCS), 1% penicillin/streptomycin, 1% amphotericin and 1% glutamine (Culture Medium) and kept at 4°C until processing (within 24 hrs). After removal of adipose and necrotic areas, tumor tissues were mechanically minced in 1 mm^3-fragments and digested with 25 mg/ml collagenase type IV (Sigma-Aldrich, St Louis, MO, USA) in DMEM medium for 2 hrs at 37°C, vigorously vortexing every 15 minutes. Then, samples were washed three times in PBS at 4°C and plated in 60 mm-Petri dishes or on glass cover slips in the Culture Medium and incubated at 37°C in 5% CO_2. Medium was changed twice weekly and cells were 1:3 splitted when reaching 90% confluence. Cell morphology was observed in contrast phase, at 100X magnification, by Olympus CK40 inverted microscope (Olympus Corporation, Tokyo, Japan).

For immunofluorescence microscopy, ccRCC cells grown on glass cover slips were fixed for 30 min in 4% paraformaldehyde PBS buffer, pH 7.2, at 37°C, rinsed with PBS, pre-incubated for 15 min in GDB buffer (0.02 mol/l sodium phosphate buffer, pH 7.4, with 0.45 mol/l

NaCl and 0.5% BSA) containing 0.3% Triton X-100, and incubated with mouse monoclonal antibodies (mAbs) against pan-cytokeratin (clone MNF-116, Dako, Glostrup, Denmark; dilution 1:200), vimentin (clone V9, Dako; dilution 1:200), carbonic anhydrase IX (CA9) (clone M75, dilution 1:50; a gift from Prof. Pastorekova, Institute of Virology, Slovak Academy of Sciences, Bratislava, Slovak Republic) and FITC-conjugated mAb against CD13 (clone CBL 169F, Chemicon, Billerica, MA, USA; dilution 1:25) for 2 hrs at room temperature. After washing in PBS, cover slips were incubated for 1 hr with goat anti-mouse Alexa-Fluor488-conjugated IgG secondary antibody (Molecular Probes, Invitrogen Life Technologies, Carlsbad, CA, USA; dilution 1:100). Nuclear counterstaining was performed by incubation for 5 min with 1 μM DAPI (Sigma-Aldrich) in PBS buffer. Immunofluorescence micrographs were obtained using a Zeiss Axiovert 200 inverted microscope (Zeiss Inc., Oberkochen, Germany), at 400X magnification, equipped with a CoolSNAP HQ camera driven by Metamorph software. For flow-cytometry analysis, cells at the first confluence (p1) were detached from plates with 0.25% trypsin-EDTA (Sigma-Aldrich), rinsed and incubated for 15 min in PBS with 5% FCS. For CD13 and CA9 staining, cells were incubated for 15 min at room temperature with the specific mouse mAbs. Cytokeratin and vimentin staining was performed using the specific mouse mAbs after permeabilization with IntraStain solution (Dako). Cells were then incubated with goat anti-mouse Alexa-Fluor488-conjugated IgG secondary antibody (Molecular Probes, Invitrogen Life Technologies) for 30 min at 4°C and counted by the FACSCalibur flow cytometer and

CellQuest software (BD Biosciences) until 30,000 events were acquired.

Western Blot analysis

For each case, cells plated in a 6mm-Petri dish were lysated when at the first confluence (p1), and the extracted proteins quantified by the Bio-Rad microassay (BioRad, Hercules, CA, USA), as previously described [18]. 30 µg proteins were separated on NuPage 4-12% Bis-Tris pre-cast gels (Invitrogen Life Technologies) and blotted onto nitrocellulose membranes probed in 10mM Tris-HCl, pH 8, and 3% BSA, with mouse mAb against CA9 (clone M75, dilution 1:50). Detection was performed using a secondary antibody coupled with horseradish peroxidase for 1 hr at room temperature and the SuperSignal West Pico detection system (Pierce, Rockford, IL, USA).

DNA extraction and target preparation for Affymetrix SNP Arrays

The genomic studies were performed on all ccRCC primary cultures at first confluence (p1); in addition, for 80MLa and 81BPG cases also cultures at second confluence (p2) or at second (p2) and third (p3) confluences were characterized. Genomic DNA was extracted from primary cell cultures by QIAmp DNA Mini kit (Qiagen, Hilden, Germany), according to manufacturer's cultured cell protocol. DNA from tumor tissues and autologous whole blood samples, used as normal control, was extracted using a standard proteinase K cell lysis and phenol-chloroform procedure. Samples were quantified by ND-1000 spectrophotometer (NanoDrop Technologies, Wilmington, DE, USA) and checked by electrophoresis on 0.8% agarose gel. Starting from 250 ng, DNA samples were processed using the GeneChip®

Human Mapping 50K Hind Assay kit (Affymetrix, Santa Clara, CA, USA), according to manufacturer's protocol, and hybridized onto GeneChip® Human Mapping 50K Hind Arrays. Intensity signals were acquired by Affymetrix GeneChip® Scanner 3000 7G and quantified by GTYPE v4.1 software (Affymetrix), using the BRLMM algorithm to assign SNP calls and to generate CHP files. A SNP call rate greater than 95% was considered as "good quality" threshold.

Genome-wide copy number and LOH profiling in ccRCC primary cultures and tumor tissues

To assess copy number alterations (CNAs) and loss of heterozygosity (LOH), two different software CNAG (version 3.0) and Partek Genomics Suite (version 6.5) were applied. CNAG is a well known software commonly used to analyze SNP array derived-CN data in tumor samples [24]. The AsCNAR (allele-specific copy-number analysis using anonymous reference) algorithm was applied to perform a "self-reference paired analysis", by comparing each culture and corresponding tumor tissue to the matched blood sample. All resulting profiles (global log ratio CN profiles; allele log ratio CN profiles; Hidden Markov Model (HMM)-inferred CN state; HMM-inferred LOH) were visually inspected to identify regions affected by aberrations. To increase data reliability, we chose to include only CNAs longer than 2 Mb (resolution limit of 50K SNP array platform). CNAG software was also used to obtain a genome-wide map of LOH events occurring in each culture or tumor tissue with respect to matched blood. Only the LOH events defined as statistically significant by CNAG (with LOH likelihood higher than 30, as default

threshold, and thus visualized in the HMM-LOH track) and covering regionslonger than 2 Mb were considered.

The same paired analysis was performed using Partek Genomics Suite software (Partek Inc., St Louis, MO, USA), starting from CEL intensity files and applying the two alternative algorithms Hidden Markov Model (HMM, the same used by CNAG) and Genomic Segmentation (GS). For HMM analysis, default parameters were adopted; for GS analysis, the default window of 10 contiguous SNPs was maintained, Signal to noise ratio at 0.5 and p-value at 0.001 were also adopted.

To estimate the global concordance between the genomic profile of each primary culture and its parental tissue, a paired whole-genome CN correlation was calculated, starting from the CNAG "HMM-CN state" data (SNP copy number status inferred by HMM), and applying Spearman's regression method. SNP call concordance index and Spearman's correlation between the CNAG SNP allelic calls of two matched samples were also calculated. For SNP call concordance, a contingency table of the counts for each combination of the four genotype categories (AA, AB, BB, NoCall) for culture (in row) and matched tissue (in column) was accomplished. The concordance index was calculated as a ratio between the sum of principal diagonal counts and 56,859 (total number of real informative SNPs on 50K Hind arrays), multiplied by 100. A SNP call concordance higher than 60% for two related samples was adopted as threshold. All statistical analysis were performed in R environment.

Results

Phenotypic characterization of ccRCC primary cultures

The nine ccRCC primary cultures established from surgical tissue specimens reached the first confluence (p1) in 8.0 ± 2.1 days. They grew well till reaching the fourth confluence, and then began to slow down their growth rate. In particular, 80MLa and 81BPG cultures reached the second confluence (p2) after 13 days, and 81BPG culture reached the third confluence (p3) after 20 days. Cells exhibited heterogeneous epithelioid morphology, were able to form foci and presented cytoplasmic vacuoles frequent in clear cell RCC subtype during *in vitro* growth (Figure 1a). Cytoplasmic staining specific for the epithelial cytokeratin and for vimentin, a mesenchymal marker expressed also in the epithelial RCC cells, both *in vivo* and *in vitro*[18, 25], and specific expression of the proximal tubular marker CD13 was present in more than 90% of cells, as evaluated by immunofluorescence and FACS analysis (Figure 1b) and according to the proximal tubular origin of ccRCC. Immunofluorescence and FACS analysis were performed also with the monoclonal antibody against the transmembrane carbonic anhydrase IX (CA9) protein, one of the most used biomarkers for ccRCC [26, 27]. Our ccRCC primary cultures showed the typical pattern of membrane fluorescence and more than 60% of cells were positive for CA9 (Figure 1b). Moreover, protein lysates analyzed by Western Blot with anti-CA9 antibody showed the expected doublet at about 55 kDa in all samples, except

for 73PG culture (Figure 1c). On the whole, these results confirmed the neoplastic phenotype of our tubular primary cultures.

Genome-wide assessment of CNAs and LOH in ccRCC primary cultures

The Affymetrix 50K SNP Array platform was used to perform the whole-genome SNP profiling of 12 samples from ccRCC primary cultures, nine at the first confluence (p1), two at the second confluence (p2), and one at the third confluence (p3). In addition, 9 samples from the corresponding original tumor tissues and 9 autologous blood samples were analyzed. We obtained an average SNP call rate equal to 98.54%, ranging from 95.79% to 99.67%, and all arrays were included in the analyses. Using CNAG v3.0 software, we performed the genome-wide profiling of CNAs in each tumor primary culture at p1. Globally, the typical “clear cell RCC” genomic signature was confirmed, including deletions on chr 3p and amplifications on chrs 5q and 7 (see Additional File 1), the same signature that we previously described in another set of ccRCC tissue samples [13].

Genome-wide comparison of DNA profile of primary cultures and original tumor tissues

Our main purpose was to assess if ccRCC primary cultures reflected the genomic profile of tumor tissues from which they were derived. First of all, for each tumor primary culture/ tissue pair, we calculated the global correlation coefficient (by Spearman regression) between their whole-genome CN profiles. Starting from the HMM-CN state data generated by CNAG, we obtained a mean CN correlation value equal to 0.73 (rang 0.30 - 0.99) (Table 2). This wide range of variation

was due essentially to 66SML sample, which presented the lowest CN correlation coefficient (Spearman0.30). On the other hand, both the concordance index and the Spearman's correlation calculated on CNAG SNP allelic calls gave very high values for all cases (SNP call concordance indexes from 94% to 98% and Spearman's coefficients from 0.87 to 0.96), thus indicating a strong correlation between cultures and corresponding tissues at SNP genotype level, also for the 66SML case (Table 2).

Looking at the individual CN profiles produced by CNAG for each sample, 7 out 9 primary cultures exactly maintained all the DNA alterations presented by the corresponding tumor tissues, or retained the normal CN profile as observed in the original tissue (73PG case) (Figure 2). The remaining two cultures presented the DNA profile of parental tissues except for one CNA: 59RG culture did not show the chr 16p amplification and 66SML culture did not show the chr 1p deletion observed in the corresponding tissues. Moreover, four primary cultures presented additional CNAs on one or two chromosomes, not found in original tissues: 50PC and 60CC cultures had an additional amplification on chr 22q, 59RG showed amplification of chrs 2 and 7, whereas 81BPG showed deletion with LOH on chrs 8p and 14q (Figure 2).

Concerning LOH profile, 60CC culture exactly maintained all the allelic imbalances, with corresponding CN status, found in the original tumor tissue, while 50PC, 61FG and 73PG cultures confirmed the absence of LOH observed in parental tissues (Figure 2). The remaining five primary cultures presented a total of 11 LOH regions

that were not detected by CNAG in original tissues because not reaching the LOH likelihood threshold to be classified as statistically significant by the software and thus visualized in the HMM-LOH track. Viceversa, we did not found LOH events occurring in tumor tissues and not confirmed in corresponding cultures.

Additionally, we performed the whole-genome DNA profiling of 80MLa culture also at second (p2) confluence (see Additional File 2) and of 81BPG culture at second (p2) and third (p3) confluences (Figure 3). In both cases, all the CNAs and LOH observed at p1 were exactly maintained at p2 and p3, and no other alterations occurred along passages. Even the deletions on chrs 8p and 14q found in 81BPG culture at p1, but not in original tissue, were confirmed at p2 and p3 (Figure 3). On the whole, these results indicated that the genomic profile of ccRCC primary cultures highly reflected that of parental tissues and remained stable during the early passages, thus suggesting that these well-characterized primary cultures may be a good *in vitro* model of original tumor tissues.

Moreover, when looking more in detail at the CN profiles calculated by CNAG, we observed that in six primary cultures (59RG, 61FG, 66SML, 70LS, 80MLa, 81BPG) the CN values of aberrant regions were more definite in cultures than in parental tissues and this phenomenon prevalently affected CN loss events. In the 66SML case, this situation was particularly evident. The primary culture presented 4 wide CN loss regions on chrs 2q, 3p, 9 and 14q. As shown in Figure 4 for chr 3p deletion, in primary culture the CNA region was defined by pronounced negative CN values, easily classified by CNAG

software as statistically significant CN loss. This deletion was present also in the parental tissue and was visible in the CN profile. However, because of its less pronounced CN values it did not reach the software threshold to be signed as statistically significant and did not appear in the HMM-CN state track. In Additional File 3 we reported other CN loss regions for 66SML case and two other representative samples: calculating the mean CN values corresponding to each of these deletions, we always observed values more negative in culture than in corresponding parental tissue. This situation reflected also on LOH profiles. In fact, all the 11 LOH events previously mentioned as detected in primary cultures but not in parental tissues occurred in such deleted regions presenting weak CN loss values in tissues. As represented in Figure 4 for chr 3p in 66SML, the software still detected the presence of heterozygous SNP calls in parental tissue (green bars below chromosome ideogram), thus indicating that the hemizygous deletion does not occur in all cells and suggesting the presence of contaminating diploid cells. In all these cases, LOH likelihood consequently decreased below statistical significance threshold and these events were missed to be visualized by CNAG in the HMM-LOH track, as illustrated in Figure 4 (see Additional File 3 for LOH likelihoods of the other deleted regions). Thus, it can be concluded that the increased cell homogeneity of primary cultures, in term of tumor component, in comparison with their parental tumor tissues, enabled a better discrimination of CNAs and LOH.

Lastly, we performed the same paired analysis between tumor primary culture and parental tissue using Partek Genomics Suite

software, which allows to choose between two alternative CN algorithms. Globally, using the HMM-based algorithm (the same used by CNAG), Partek returned results overlapping with CNAG analysis. Differently, when applying the GS algorithm, Partek was able to retrieve all those CN losses missed to be classified as statistically significant in tissue samplesby the CNAG HMM algorithm. This is illustrated for 66SML case in Additional File 4. These results confirmed that in tissue samples these deletions were really present even if less visible than in cultures due to sample heterogeneity, and they did not arise *de novo* in primary cultures.

Discussion

In this study, we investigated whether the *in vitro* model of ccRCC primary cell cultures, established from surgical tumor specimens, well reproduces the DNA profile of parental tumor tissues, thus allowing a more confident CNAs and LOH discrimination with respect to the original tissues. Tumor cells from ccRCC surgical specimens may be adapted to *in vitro* growth with high efficiency, independently from any clinico-pathological characteristic of patients, as we previously confirmed also in a wide series of well-characterized samples [18, 19]. The growth and survival rate of our ccRCC cultures were in agreement with those reported by other authors [14] and proved that our primary cultures grow for the first four passages without difficulties [18]. The cellular composition of our cultures was very homogeneous: more than 90% of cultured cells were of proximal

tubular origin, with morphological characteristics typical of ccRCC, and more than 60% of cells were positive for CA9, a biomarker present in almost all ccRCC cases and expressed in most, although not all, of the malignant clear cells of each single positive case [26, 28]. When evaluated by Western Blot, CA9 expression was quite strong in all samples, except for 73PG culture where it was undetectable. Notably, about this latter culture, we found an identical normal genomic profile in primary culture and parental tissue in terms of both CNAs and LOH (with the resolution power of the 50K SNP array platform), although the tumor tissue sample, unlike primary culture, showed a CA9 expression by immunohistochemistry (data not shown). This finding is in agreement with another paper reporting a ccRCC case which expressed CA9 in the surgical tissue sample but not in the corresponding primary culture [15]. Moreover, in our experience with a wide series of samples [19], we observed other few ccRCC cases showing a CA9 positivity at tissue level but not in corresponding primary cultures. Excluding tissue sampling mistakes, this behavior might be due to a transitory expression of CA9 during tissue excision.] In fact, it is known that surgical conditions, like tissue ischemia after renal artery clamping and subsequent hypoxia, may up-regulate the expression of downstream targets of HIF-1 (hypoxia inducible factor 1), including CA9, that conversely it should not be induced under normoxic conditions like those applied for primary cultures, [29]. On the other hand, the outgrowth of normal tubular epithelial cells in 73PG culture

is unlikely based on the extensive phenotypic characterization we performed on all our cultures [19].

Up to now, karyotypic characterization of RCC primary cultures has been performed only by classical cytogenetic G-banding [30] or CGH techniques [23]. In our knowledge, this is the first study applying the Affymetrix SNP array technology to assess at genome-wide level both CNAs and LOH in ccRCC primary cultures. Globally, our cultures confirmed the typical ccRCC genomic signature [13, 23, 30]. These cultures typically showed alterations on at most 4 or 5 chromosomes. Only two samples made exception: 73PG culture did not show alterations in both CN and LOH profiles, while 60CC showed CNAs on all chromosomes. In particular, 60CC primary culture, as well as its corresponding tissue, showed an atypical ccRCC genomic profile more similar to that of chromophobe subtype (characterized by wide losses on chrs 1, 2, 6, 10, 13, 17 and 21), notwithstanding its typical "clear cell" histology.

It should also be noted that while 73PG specimen derived from a small in size tumor, suggestive of an early stage of neoplastic progression, 60CC specimen derived from thelargest one, probably associated with a more advance stage of tumor progression characterized by an aberrant and "clear cell" atypical genomic profile [2].

Up today, very few genomic comparisons between short-term primary cultures and parental tumor tissues have been performed. In glioblastoma, for example, the genomic profile of primary cultures, assessed by array-CGH, resulted considerably different from that of

parental tumors, with changes progressively occurring already after 2 weeks of culture, resulting in an inconsistent representation of tumor biology [22]. In melanoma [20] and neuroblastoma [21], instead, using SNP array technology, primary cultures showed to encompass the spectrum of significant alterations present in primary tumors, thus providing a genetically appropriate *in vitro* model for functional genomics characterizations.

Concerning RCC, up till now the comparisons between primary cultures and tumor tissues mainly regarded phenotypic characterizations and proteomic profiling [15, 18, 31]. A comparison of the genomic profile between primary cultures and parental tissues has been reported only by Sanjmyatav et al. by using traditional CGH [23]. Their DNA profiling showed a poor overlap of CNAs between ccRCC primary cultures and parental tumor tissues. In fact, only 3 out 8 ccRCC cultures exactly showed the same DNA alterations present in the corresponding tissues. In addition, other 3 cultures did not show any of the CNAs found in the corresponding tissue samples and resulted diploid. Probably, the poor overlap of CNAs obtained by Sanjmyatav et al. [23] was due both to the low sensitivity and resolution level of the technique used (i.e. CGH on metaphase chromosome spreads) and to the not extensive cytological characterization of primary cultures. These findings highlight the importance of a careful phenotypic characterization of primary cultures for a correct interpretation of genomic results.

Globally, these few genomic comparison studies between primary cultures and parental tissues point out that the use of tumor primary

cultures as *in vitro* model for genetic analysis or functional studies must be distinctively evaluated tumor by tumor and that in any case it depends on the level of phenotypic characterization of primary cultures.

Looking at the genome-wide CN profiles, our results indicated that 7 out of 9 well-characterized primary cultures exactly reproduced the DNA profile of the corresponding tumor tissues. The other two cultures (59RG and 66SML) maintained all but one the CNAs showed by the original tissues. These findings are in agreement with Lin *et al.* who evidenced that in melanoma, some significant alterations present in original tissues (as a deletion on chr 13q) were almost undetectable in cultured cells despite the landscape of genomic alterations was strikingly similar [20]. However, it must be pointed out that even if primary cultures might have lost some genomic alterations present in original tumor tissues, they probably correspond to some "passenger mutations", that do not confer selective growth advantage to tumor cells and thus might be lost in cultured cells, and not to "driver mutations" [32].

Although the good overlap of CN profiles between each our primary culture and corresponding tissue, we obtained a CN correlation mean value equal to 0.73 (by Spearman regression method), a value just a little higher than that reported for glioblastoma cultures and tissues (Pearson mean 0.62) [22]. The reason is in the wide range of variance we obtained among our 9 cases (range 0.30-0.99), mainly due to the contribution of one case (66SML) on the mean. Although this variability seems too high for conclusive messages from, it must be

noted that in our series it essentially depends on a software issue. In fact, we used the CNAG “HMM-CN state” data, that is the SNP copy number status inferred by HMM algorithm and visualized in the HMM-CN state track. However, in the presence of a high sample heterogeneity, as in the case of 66SML tissue (illustrated in Figure 4), the HMM-CN state data missed to detect CN aberrations, even if present, because their CN values did not reach the software threshold for a statistical significance. For this reason, the 66SML sample had the lowest CN correlation coefficient between culture and tissue (Spearman0.30), a value that does not really reflect a poor overlap but only a software constraint.

Similarly to those found in neuroblastoma [21], the SNP call concordance indexes and the Spearman’s correlation coefficients calculated on CNAG SNP allelic calls indicated a strong correlation at SNP genotype level between our cultures and parental tissues, 66SML sample included, thus confirming that each primary culture really derived from its corresponding tissue.

Notably, in six samples, CNAs were more evident and better discriminated in primary cultures than in corresponding tumor tissues. This phenomenon principally occurred in deleted regions and it is due to the different cellular composition of the two samples and it was also observed in neuroblastoma tissues and derived cell lines [21]. Tumor tissues are heterogeneous and comprise a mixture of tumor and normal cells (endothelial cells, leukocytes, fibroblasts). For this reason, the copy number values corresponding to DNA alterations of tumor cells are inevitably “diluted” by the diploid

values coming from normal cells. Differently, primary cultures were more homogeneous in terms of tumor component, as shown by their phenotypic characterization, and thus presented better defined CNAs. Tumor tissue heterogeneity reflects also on LOH detection. In fact, the software used in the analysis not only detected the allele retained by the tumor, but also the second allele still present in normal cells; in these cases the LOH call will be missed [33]. In our ccRCC primary cultures, instead, hemizygous deletions were accompanied by LOH calls, confirming the great sample homogeneity that enables to discriminate CNAs and LOH. Thus, the presence of LOH calls in deleted regions could be adopted as a parameter to evaluate the degree of tumor sample purity and the level of normal cell contamination and consequently the origin of cultured cells, highlighting the power of SNP array technology with respect to CGH technique. Such an evidence appears more important taking into account that since today there is not a single universally applied method able to certainly make these evaluations [34].

The high cell homogeneity observed in our ccRCC cultures might explain also the additional CNAs found in 4 of them but not in original tissues. The acquisition of these alterations *de novo* during *in vitro* growth is unlikely since cultures were analyzed at first confluence. Moreover, the genomic analysis of some cultures at second and third confluences provided evidence that these cultures did not accumulate further alterations during passages and remained stable for at least 3 weeks. We could therefore conclude that these alterations might fail to be seen in the heterogeneous tumor tissues

because present in a very small number of cells (<20%), thus resulting undetectable for CN analysis algorithms [11, 24].

Actually, the true picture of genomic alterations occurring in a tumor can be obtained only performing a genomic analysis directly on tumor cells isolated, for example, by laser capture microdissection, which allows a >90% of purity [35] and circumvents the problem of DNA alteration "dilution" due to tissue heterogeneity. However, such a useful technical approach has the not negligible inconvenience of providing cellular material not exploitable for eventual subsequent functional studies.

Conclusions

By performing the genome-wide copy number profiling of a collection of ccRCC primary cultures and corresponding tumor tissues, we demonstrated that these well-characterized primary cultures maintained the genomic alterations of parental tumors. Moreover, their DNA profile remained stable for at least 3 weeks, till to third confluence. Importantly, RCC primary cultures provided greater cell homogeneity and enrichment in tumor component than parental tissues, as proved also by phenotypic characterization, thus enabling a better discrimination of DNA alterations. In this context, SNP array technology demonstrated to be a powerful tool able to confirm the origin of cultured cells and to evaluate sample homogeneity and normal cell contamination. The observation that ccRCC primary cultures retain not only the phenotypic features and the proteomic profile of original tumor tissues but also their genomic

profile proves that these short-term cultures are a reliable *in vitro* model that well represents ccRCC genetics and biology and that prospectively, could be usedfor functional approaches.

Competing interests

The authors declare that they have no competing interests.

Authors' contributions

IC carried out microarray experiments and bioinformatic analyses. EM and FF performed statistical and bioinformatic analyses. CB, SB, VDS and MAZ prepared primary cultures and performed phenotypic characterizations. EF and SF carried out histological classification of clinical cases and prepared DNA from tissue samples. SS prepared DNA from blood samples.

FM participated in the study design. CB and RAP coordinated and supervised the study and, together with IC and CB, wrote the manuscript. All authors read and approved the final manuscript.

Acknowledgements

A special thank to Dr. Paola Brambilla (Dept. Experimental Medicine, University of Milano-Bicocca), Dr. Paolo Mocarelli (Desio Hospital, University of Milano-Bicocca), Dr. Silvano Bosari (Dept. Medicine, Surgery and Dentistry, San Paolo Hospital, University of Milan), Dr. Valentina Usuelli (Dept. Specialistic Surgical Sciences, Urology Unit, Ospedale Maggiore Policlinico" Foundation, University of Milan) and we also thank Danila Coradini for scientific editing of the manuscript.

This work was supported by grants from the Italian Ministry of University and Research: FIRB 2003 (n. RBLA03ER38_004), PRIN 2006 (n. 69373), FIRB 2007 (Rete nazionale per lo studio del proteoma umano, n. RBRN07BMCT).

Additional files can be found online at

http://www.biomedcentral.com/1471-2407/11/244/additional

Figure Legends

Figure 1 Phenotypic characterization of ccRCC primary cultures.

(a) Representative cellular morphology during *in vitro* growth. 100X magnification. (b) Representative micrographs of immunofluorescence staining (top) and FACS analysis (bottom) of pan-cytokeratin, vimentin, CD13 and CA9. DAPI counterstains nuclei in blue. 400X magnification. The positivity percentages for the different markers are reported in the FACS analysis as mean value (± SD) of the nine cultures. (c) Western blot analysis of CA9 in all ccRCC primary cultures. B-actin was used as internal control.

Figure 2 - Copy number alterations and LOH events in ccRCC primary cultures and parental tissues, as calculated by CNAG v3.0 software.

On each chromosomal arm (p, short arm; q, long arm), amplifications (↑) and deletions (↓) and LOH events are reported for all samples. Color labels distinguish CN alterations (CNAs) detected by CNAG and signed in the color-coded "HMM-CN state" track (red for amplifications and dark green for deletions), and CNAs resulting

below threshold to be visualized in the software HMM-CN track (light green for deletions). Only LOH events reaching significant likelihood to be signed by CNAG in the HMM-LOH track are reported.

Figure 3 – Whole-genome view of copy number profile in 81BPG primary culture at first (p1), second (p2) and third (p3) confluences, and in corresponding tumor tissue, using CNAG v3.0 software.

Analysis was performed using CNAG v3.0 software, comparing primary culture at each passage and parental tumor tissue to the autologous blood sample, as described in Methods section. Chromosomes are represented horizontally, from 1 to 22 in different colors, separated by vertical bars. For each sample, the three tracks represent (on log scale): a) “copy number plot”: copy number log ratio values of single SNPs; b) “copy number average”: copy number log ratio values locally averaged on 10 contiguous SNPs; c) “allele-based analysis”: copy number log ratio values for each allele (red and green lines).

Figure 4 - Visualization of chr 3 in 66SML primary culture (upper panel) and parental tissue (lower panel) using CNAG v3.0 software.

Chromosome 3 is shown from p to q end (from left to right). The upper two graphs represent single SNP copy number data on log2 scale (red dots) and copy number values locally averaged on 10 contiguous SNPs (blue line), whereas copy number values for each allele (red and green lines) are shown below. Green bars in the middle represent heterozygous SNP calls detected by the software comparing each sample to autologous blood. The three bars at the bottom represent the color-coded visualization of Hidden Markov

Model-copy number state (HMM-CN state: yellow, diploidy; pink, amplification; light blue, deletion) and of HMM-LOH state (blue, significant LOH; yellow, no LOH), with LOH likelihood indicated by the thickness of the third blue bar. Boxes on the left report mean CN log2ratio values and mean LOH likelihoods calculated for the whole deleted region in primary culture and tissue, respectively .

Figure 1

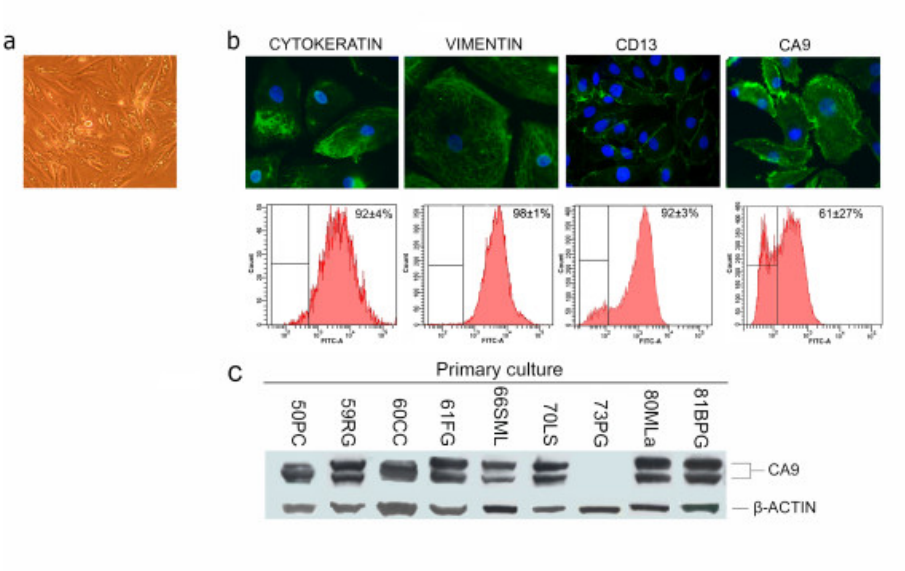

Figure 2

Figure 3

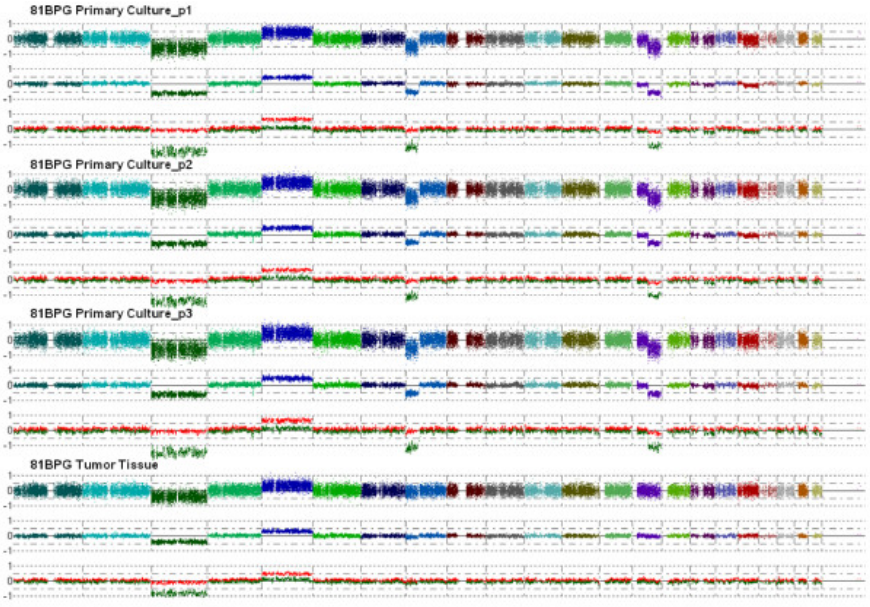

Figure 4

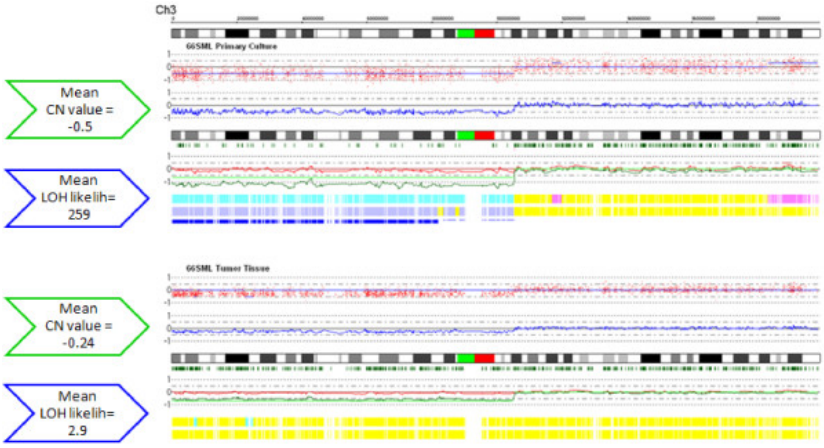
Ch3
665ML Primary Culture
Mean CN value = -0.5
Mean LOH likelih= 259
665ML Tumor Tissue
Mean CN value = -0.24
Mean LOH likelih= 2.9

References

1. Kovacs G, Akhtar M, Beckwith BJ, Bugert P, Cooper CS, Delahunt B, Eble JN, Fleming S, Ljungberg B, Medeiros LJ, Moch H, Reuter VE, Ritz E, Roos G, Schmidt D, Srigley JR, Storkel S, van den Berg E, Zbar B: **The Heidelberg classification of renal cell tumours**. *J Pathol* 1997, **183**(2):131-133.

2. Hoglund M, Gisselsson D, Soller M, Hansen GB, Elfving P, Mitelman F: **Dissecting karyotypic patterns in renal cell carcinoma: an analysis of the accumulated cytogenetic data**. *Cancer Genet Cytogenet* 2004, **153**(1):1-9.

3. Klatte T, Rao PN, de Martino M, LaRochelle J, Shuch B, Zomorodian N, Said J, Kabbinavar FF, Belldegrun AS, Pantuck AJ: **Cytogenetic profile predicts prognosis of patients with clear cell renal cell carcinoma**. *J Clin Oncol* 2009, **27**(5):746-753.

4. Gunawan B, Huber W, Holtrup M, von Heydebreck A, Efferth T, Poustka A, Ringert RH, Jakse G, Fuzesi L: **Prognostic impacts of cytogenetic findings in clear cell renal cell carcinoma: gain of 5q31-qter predicts a distinct clinical phenotype with favorable prognosis**. *Cancer Res* 2001, **61**(21):7731-7738.

5. Perego RA, Corizzato M, Brambilla P, Ferrero S, Bianchi C, Fasoli E, Signorini S, Torsello B, Invernizzi L, Bombelli S, Angeloni V, Pitto M, Battaglia C, Proserpio V, Magni F, Galasso G, Mocarelli P: **Concentration and microsatellite status of plasma DNA for monitoring patients with renal carcinoma**. *Eur J Cancer* 2008, **44**(7):1039-1047.

6. Beroukhim R, Brunet JP, Di Napoli A, Mertz KD, Seeley A, Pires MM, Linhart D, Worrell RA, Moch H, Rubin MA, Sellers WR, Meyerson

M, Linehan WM, Kaelin WG, Jr., Signoretti S: **Patterns of gene expression and copy-number alterations in von-hippel lindau disease-associated and sporadic clear cell carcinoma of the kidney**. *Cancer Res* 2009, **69**(11):4674-4681.

7. Young AC, Craven RA, Cohen D, Taylor C, Booth C, Harnden P, Cairns DA, Astuti D, Gregory W, Maher ER, Knowles MA, Joyce A, Selby PJ, Banks RE: **Analysis of VHL Gene Alterations and their Relationship to Clinical Parameters in Sporadic Conventional Renal Cell Carcinoma**. *Clin Cancer Res* 2009, **15**(24):7582-7592.

8. Gordan JD, Lal P, Dondeti VR, Letrero R, Parekh KN, Oquendo CE, Greenberg RA, Flaherty KT, Rathmell WK, Keith B, Simon MC, Nathanson KL: **HIF-alpha effects on c-Myc distinguish two subtypes of sporadic VHL-deficient clear cell renal carcinoma**. *Cancer Cell* 2008, **14**(6):435-446.

9. Dutt A, Beroukhim R: **Single nucleotide polymorphism array analysis of cancer**. *Curr Opin Oncol* 2007, **19**(1):43-49.

10. Bacolod MD, Schemmann GS, Giardina SF, Paty P, Notterman DA, Barany F: **Emerging paradigms in cancer genetics: some important findings from high-density single nucleotide polymorphism array studies**. *Cancer Res* 2009, **69**(3):723-727.

11. Goransson H, Edlund K, Rydaker M, Rasmussen M, Winquist J, Ekman S, Bergqvist M, Thomas A, Lambe M, Rosenquist R, Holmberg L, Micke P, Botling J, Isaksson A: **Quantification of normal cell fraction and copy number neutral LOH in clinical lung cancer samples using SNP array data**. *PLoS One* 2009, **4**(6):e6057.

12. Balmain A, Gray J, Ponder B: **The genetics and genomics of cancer**. *Nat Genet* 2003, **33 Suppl**:238-244.

13. Cifola I, Spinelli R, Beltrame L, Peano C, Fasoli E, Ferrero S, Bosari S, Signorini S, Rocco F, Perego R, Proserpio V, Raimondo F, Mocarelli P, Battaglia C: **Genome-wide screening of copy number alterations and LOH events in renal cell carcinomas and integration with gene expression profile**. *Mol Cancer* 2008, **7**:6.

14. Tan X, Zhai Y, Chang W, Hou J, He S, Lin L, Yu Y, Xu D, Xiao J, Ma L, Wang G, Cao T, Cao G: **Global analysis of metastasis-associated gene expression in primary cultures from clinical specimens of clear-cell renal-cell carcinoma**. *Int J Cancer* 2008, **123**(5):1080-1088.

15. Craven RA, Stanley AJ, Hanrahan S, Dods J, Unwin R, Totty N, Harnden P, Eardley I, Selby PJ, Banks RE: **Proteomic analysis of primary cell lines identifies protein changes present in renal cell carcinoma**. *Proteomics* 2006, **6**(9):2853-2864.

16. Hagenkord JM, Monzon FA, Kash SF, Lilleberg S, Xie Q, Kant JA: **Array-based karyotyping for prognostic assessment in chronic lymphocytic leukemia: performance comparison of Affymetrix 10K2.0, 250K Nsp, and SNP6.0 arrays**. *J Mol Diagn* 2010, **12**(2):184-196.

17. Heinzman JM, Brower SL, Bush JE, Silverman JF: **Ex vivo enrichment of malignant carcinoma cells in primary culture**. *Pathology* 2007, **39**(5):491-494.

18. Perego RA, Bianchi C, Corizzato M, Eroini B, Torsello B, Valsecchi C, Di Fonzo A, Cordani N, Favini P, Ferrero S, Pitto M, Sarto C, Magni F, Rocco F, Mocarelli P: **Primary cell cultures arising from normal kidney and renal cell carcinoma retain the proteomic profile of corresponding tissues**. *J Proteome Res* 2005, **4**(5):1503-1510.

19. Bianchi C, Bombelli S, Raimondo F, Torsello B, Angeloni V, Ferrero S, Di Stefano V, Chinello C, Cifola I, Invernizzi L, Brambilla P, Magni F, Pitto M, Zanetti G, Mocarelli P, Perego RA: **Primary cell cultures from human renal cortex and renal-cell carcinoma evidence a differential expression of two spliced isoforms of Annexin A3**. *Am J Pathol* 2010, **176**(4):1660-1670.

20. Lin WM, Baker AC, Beroukhim R, Winckler W, Feng W, Marmion JM, Laine E, Greulich H, Tseng H, Gates C, Hodi FS, Dranoff G, Sellers WR, Thomas RK, Meyerson M, Golub TR, Dummer R, Herlyn M, Getz G, Garraway LA: **Modeling genomic diversity and tumor dependency in malignant melanoma**. *Cancer Res* 2008, **68**(3):664-673.

21. Volchenboum SL, Li C, Li S, Attiyeh EF, Reynolds CP, Maris JM, Look AT, George RE: **Comparison of primary neuroblastoma tumors and derivative early-passage cell lines using genome-wide single nucleotide polymorphism array analysis**. *Cancer Res* 2009, **69**(10):4143-4149.

22. De Witt Hamer PC, Van Tilborg AA, Eijk PP, Sminia P, Troost D, Van Noorden CJ, Ylstra B, Leenstra S: **The genomic profile of human malignant glioma is altered early in primary cell culture and preserved in spheroids**. *Oncogene* 2008, **27**(14):2091-2096.

23. Sanjmyatav J, Schubert J, Junker K: **Comparative study of renal cell carcinoma by CGH, multicolor-FISH and conventional cytogenic banding analysis**. *Oncol Rep* 2005, **14**(5):1183-1187.

24. Yamamoto G, Nannya Y, Kato M, Sanada M, Levine RL, Kawamata N, Hangaishi A, Kurokawa M, Chiba S, Gilliland DG, Koeffler HP, Ogawa S: **Highly sensitive method for genomewide detection of allelic composition in nonpaired, primary tumor**

specimens by use of affymetrix single-nucleotide-polymorphism genotyping microarrays. *Am J Hum Genet* 2007, **81**(1):114-126.

25. Young AN, Amin MB, Moreno CS, Lim SD, Cohen C, Petros JA, Marshall FF, Neish AS: **Expression profiling of renal epithelial neoplasms: a method for tumor classification and discovery of diagnostic molecular markers**. *Am J Pathol* 2001, **158**(5):1639-1651.

26. Li G, Cuilleron M, Cottier M, Gentil-Perret A, Lambert C, Genin C, Tostain J: **The use of MN/CA9 gene expression in identifying malignant solid renal tumors**. *Eur Urol* 2006, **49**(2):401-405.

27. Patard JJ, Fergelot P, Karakiewicz PI, Klatte T, Trinh QD, Rioux-Leclercq N, Said JW, Belldegrun AS, Pantuck AJ: **Low CAIX expression and absence of VHL gene mutation are associated with tumor aggressiveness and poor survival of clear cell renal cell carcinoma**. *Int J Cancer* 2008, **123**(2):395-400.

28. Li G, Passebosc-Faure K, Lambert C, Gentil-Perret A, Blanc F, Oosterwijk E, Mosnier JF, Genin C, Tostain J: **The expression of G250/mn/CA9 antigen by flow cytometry: its possible implication for detection of micrometastatic renal cancer cells**. *Clin Cancer Res* 2001, **7**(1):89-92.

29. Signoretti S, Regan M, Atkins M: **Carbonic anhydrase IX as a predictive biomarker of response to kidney cancer therapy**. *BJU Int* 2008, **101 Suppl 4**:31-35.

30. Kovacs G, Szucs S, De Riese W, Baumgartel H: **Specific chromosome aberration in human renal cell carcinoma**. *Int J Cancer* 1987, **40**(2):171-178.

31. Shi T, Dong F, Liou LS, Duan ZH, Novick AC, DiDonato JA: **Differential protein profiling in renal-cell carcinoma**. *Mol Carcinog* 2004, **40**(1):47-61.

32. Bozic I, Antal T, Ohtsuki H, Carter H, Kim D, Chen S, Karchin R, Kinzler KW, Vogelstein B, Nowak MA: **Accumulation of driver and passenger mutations during tumor progression**. *Proc Natl Acad Sci U S A* 2010, **107**(43):18545-18550.

33. Lo KC, Bailey D, Burkhardt T, Gardina P, Turpaz Y, Cowell JK: **Comprehensive analysis of loss of heterozygosity events in glioblastoma using the 100K SNP mapping arrays and comparison with copy number abnormalities defined by BAC array comparative genomic hybridization**. *Genes Chromosomes Cancer* 2008, **47**(3):221-237.

34. Ochs RL, Fensterer J, Ohori NP, Wells A, Gabrin M, George LD, Kornblith P: **Evidence for the isolation, growth, and characterization of malignant cells in primary cultures of human tumors**. *In Vitro Cell Dev Biol Anim* 2003, **39**(1-2):63-70.

35. Nishidate T, Katagiri T, Lin ML, Mano Y, Miki Y, Kasumi F, Yoshimoto M, Tsunoda T, Hirata K, Nakamura Y: **Genome-wide gene-expression profiles of breast-cancer cells purified with laser microbeam microdissection: identification of genes associated with progression and metastasis**. *Int J Oncol* 2004, **25**(4):797-819.

Chapter 4

Since Chronic Myeloid Leukemia (CML) was the first neoplasm to be shown to be initiated at a CSCs level, it represents an important paradigm to understand the molecular mechanism and the combination of genetic and epigenetic events involved in the production of CSCs. Moreover, it can represent a good model to screen for novel sel-renewal regulators that can be responsible for disease relapse and resistance to therapies. In order to study and develop a new model of CSCs, such as in our experience RCC CSCs, the CML represents a good model to refer to. The following section includes the publication derived from a collaboration with a laboratory highly specialized in the cancer stem cell field at Sanford Consortium for Regenerative Medicine in San Diego. Moreover we obtained preliminary results as a follow up of the same project, that are described at the end of this chapter.

ADAR1 Promotes Malignant Progenitor Reprogramming in Chronic Myeloid Leukemia

PNAS, 2013 VOL.110 N.3 1041-1046

Qingfei Jiang,[1] Leslie A. Crews,[1] Christian L. Barrett,[2]Hye-Jung Chun,[3] Angela C. Court,[1] Jane M. Isquith,[1, 4] Maria A. Zipeto,[1, 5] Daniel J. Goff,[1] Mark Minden,[6] Anil Sadarangani,[1] Jessica M. Rusert,[7] Kim-Hien T. Dao,[8] Sheldon R. Morris,[1] Lawrence S. B. Goldstein,[7] Marco A. Marra,[3] Kelly A. Frazer,[2] and Catriona H. M. Jamieson[1, a]

[1]Department of Medicine, Stem Cell Program and Moores Cancer Center, University of California, San Diego, La Jolla, CA 92093, USA

[2]Department of Pediatrics, Division of Genome Information Sciences, University of California, San Diego, La Jolla, CA 92093, USA

[3]Canada's Michael Smith Genome Sciences Centre, BC Cancer Agency, Vancouver, BC, Canada

[4]Department of Animal Science, California Polytechnic State University, San Luis Obispo, CA

[5]Department of Experimental Medicine, University of Milano-Bicocca, Milan, Italy

[6]Princess Margaret Hospital, Toronto, ON, Canada

[7]Department of Cellular and Molecular Medicine, University of California, San Diego and Howard Hughes Medical Institute

[8]Oregon Health and Science University Knight Cancer Institute, Portland, Oregon

Abstract

The molecular etiology of human progenitor reprogramming into self-renewing leukemia stem cells (LSC) has remained elusive. While DNA sequencing has uncovered spliceosome gene mutations that promote alternative splicing and portend leukemic transformation, isoform diversity may also be generated by RNA editing mediated by adenosine deaminase acting on RNA (ADAR) enzymes that regulate stem cell maintenance. In this study, whole transcriptome sequencing of normal, chronic phase (CP) and serially transplantable blast crisis (BC) chronic myeloid leukemia (CML) progenitors revealed increased interferon-γ pathway gene expression in concert with BCR-ABL amplification, enhanced expression of the interferon responsive ADAR1 p150 isoform and a propensity for increased A-to-I RNA editing during CML progression. Lentiviral overexpression experiments demonstrate that ADAR1 p150 promoted expression of the myeloid transcription factor PU.1 and induced malignant reprogramming of myeloid progenitors. Moreover, enforced ADAR1 p150 expression was associated with production of a mis-spliced form of GSK3β implicated in LSC self-renewal. Finally, functional serial transplantation and shRNA studies demonstrate that ADAR1 knockdown impaired *in vivo* self-renewal capacity of BC CML progenitors. Together these data provide a compelling rationale for developing ADAR1-based LSC detection and eradication strategies

Introduction

While advanced malignancies are diverse in phenotype, they often exhibit stem cell properties including enhanced survival, differentiation, quiescence and self-renewal potential (1, 2). Early insights into the molecular pathogenesis of cancer stemmed from the discovery of the Philadelphia chromosome (Ph^+) and its constitutively active BCR-ABL1 tyrosine kinase in chronic myeloid leukemia (CML) (3-5). Tyrosine kinase inhibitor (TKI) therapy targeting BCR-ABL1 suppresses CML during the chronic phase (CP) of the disease in most patients able to tolerate long-term therapy (6). While the CP stage of CML can often be controlled for long periods of time with standard TKI therapies, subsequent genetic and epigenetic alterations promote progenitor expansion and the generation of self-renewing leukemia stem cells (LSC) that fuel disease progression and blast crisis (BC) transformation along with TKI resistance (7, 8). Furthermore, TKI discontinuation usually results in CML resurgence, suggesting that quiescent progenitors persist despite therapy (9-12).

Mutations in spliceosome genes and alternative splicing of coding and non-coding RNAs are emerging as important drivers of transcriptomic diversity that fuel leukemic progression and therapeutic resistance(7, 8, 13). Moreover, previous studies reveal extensive RNA editing in the human transcriptome (14-17), primarily in primate-specific Alu sequences (18-20), which promotes splice isoform diversity. RNA editing activity is mediated by the adenosine deaminase acting on double-stranded (ds) RNA (ADAR) family of editases (21), which includes ADAR1 (also known as ADAR), ADAR2 (ADARB1), and ADAR3 (ADARB2). ADAR1 and ADAR2 are active in

embryonic cell types (18), and ADAR3 may play a non-enzymatic regulatory role in RNA editing activity (22). ADAR enzymes regulate fetal and adult hematopoietic stem cell (HSC) maintenance and stem cell responses to inflammation (23-26). ADAR-mediated adenosine-to-inosine (A-to-I) RNA editing in Alu-sequence containing double-stranded RNA hairpin structures (14, 20)can generate alternative donor or acceptor splice sites(27, 28), alter RNA structure (21), modulate regulatory RNAs and gene silencing activities (29), and introduce codon sequence alterations (29). Interestingly, ADAR deregulation has been implicated in a variety of malignant cell types (30, 31). However, the functional effects of RNA editing in leukemia have not been elucidated. Here we examined the role of ADAR1-mediated RNA editing in malignant reprogramming of myeloid progenitors into LSC that drive BC transformation in CML.

Whole transcriptome sequencing coupled with qRT-PCR analysis demonstrated increased interferon (IFN)-responsive ADAR1 expression in LSC from primary BC CML patient samples compared with CP CML and normal cord blood progenitors. This coincided with enhanced expression of inflammatory pathway genes during CP to BC progression. Moreover, ADAR1 p150 mRNA expression correlated with BCR-ABL amplification and increased A-to-I editing with differential expression of ADAR target genes in BC CML. Lentiviral ADAR1 p150 expression induced PU.1 expression that promotes expansion of myeloid progenitors, and was associated with production of a mis-spliced form of glycogen synthase kinase (GSK)-3β that has been implicated in LSC self-renewal (7). Lentiviral ADAR1 knockdown also reduced BC LSC self-renewal capacity in RAG2$^{-/-}\gamma c^{-/-}$ mice. These data shed new light on the contribution of ADAR1-

mediated RNA editing to malignant progenitor reprogramming driving leukemic progression.

Results

Inflammatory Mediator Driven RNA Editing Portends Blastic Transformation

To investigate the mechanisms driving malignant reprogramming of myeloid progenitors into LSC, we performed whole transcriptome sequencing (RNA-Seq) on fluorescence-activated cell sorting (FACS)-purified $CD34^{+}CD38^{+}Lin^{-}$ progenitor cells isolated from primary CML patient samples (Table S1). We identified 2228 differentially expressed genes in BC compared to CP progenitors, and pathway analysis demonstrated overrepresentation of inflammatory IFN-related and proteoglycan-related pathways involved in hematological development (Fig. 1A) in BC versus CP CML. Among the significantly affected networks identified using Ingenuity Pathway Analysis (IPA), IFN-γ, cytokine and tumor necrosis factor (TNF) signaling pathways (Fig. S1A) along with self-renewal and reprogramming factors (KLF family and LEF1, Fig. S1B) were found to be enriched for differentially expressed genes in BC compared to CP CML.

Analysis of inflammatory mediator splice isoform expression revealed up-regulation of numerous inflammation-associated receptors and signaling molecules (Fig. S2A). The most significantly upregulated transcripts included an LSC marker, IL-3Rα (CD123); IFN receptors (IFNAR); and TNF receptors (TNFRSF) (Fig. S2A).Notably, transcription of the IFN-responsive isoform of ADAR1 has been shown to be stimulated by a variety of inflammatory molecules (32, 33). Because of known functional differences between ADAR1 p150 and p110

which are not evident by whole gene expression studies, we performed a sensitive qRT-PCR analysis in $CD34^{+}CD38^{+}Lin^{-}$ progenitor cells from primary CML patient samples (Table S1) using splice isoform-specific primers (Table S2). Expression levels of the inflammation-responsive ADAR1 p150 isoform were increased approximately eight-fold in CML BC progenitors in comparison with normal cord blood (Fig. S1C), while levels of the constitutively active p110 isoform were not significantly different among groups (Fig. S1D). Analysis of the ratio of p150/p110 showed a relative enrichment of the p150 ADAR1 isoform associated with CML progression (Fig. 1B) and BCR-ABL amplification in BC CML progenitors (Fig. 1C). We observed similar patterns of increased ADAR1 p150 expression in the granulocyte/macrophage progenitor (GMP) fraction of primary CML samples (Fig. S1E), which expands during CML progression (Fig. S1F) (34). To confirm sensitivity of HSC to inflammatory-mediator induced ADAR1 p150 expression, qRT-PCR analysis was performed on $CD34^{+}$ cord blood cells treated with IFNγ or TNFα, and results showed a two-fold upregulation of ADAR1 p150 (Fig. S1G).

Additional analysis of ADAR family gene expression in the RNA-Seq data demonstrated that while total ADAR1 (ADAR) expression was detectable in all samples, ADAR2 and ADAR3 were expressed below detection thresholds (Fig. S2B). This is consistent with previous reports showing that ADAR1 is the most highly expressed RNA editing enzyme in tumor cells (35, 36), and suggests that ADAR1 is likely the primary functional A-to-I RNA editase in CML LSC.

To investigate the contribution of ADAR1 upregulation to RNA editing during CML progression, RNA-Seq analysis of CML CP and BC

$CD34^{+}CD38^{+}Lin^{-}$ progenitors was compared to the genomic coordinates of putative A-to-I editing sites identified in a previously published dataset (35). In 8 CP and 8 BC CML primary patient samples, the fraction of sites that contained guanosine bases (representing inosine substitution) compared with adenosine bases was calculated for each patient sample. This revealed a striking enrichment of A-to-G changes in ADAR target sites in BC compared to CP progenitors (Fig. 1D), demonstrating a shift towards increased RNA editing during CML progression. Furthermore, volcano plot analysis of editing at ADAR target sites revealed approximately 16-fold more editing sites with significantly increased editing ratios during BC transformation (Fig. 1E). A total of 274 sites exhibited significantly different editing rates (Dataset S1), and were predominantly located within Alu repeat sequences (Fig. 1F). These data suggest that RNA editing activity is not only cell type and context-specific but also disease stage specific and therefore could be a harbinger of disease progression.

By examining the relative levels of ADAR target gene (35) transcripts, we found that 175 of 1,293 putative ADAR target genes were differentially expressed in BC compared with CP progenitors (Fig. 1G). Differential expression of a subset of ADAR target genes clearly distinguished BC from CP or cord blood progenitors (Fig. 1G). In addition, non-negative matrix factorization, using 200 random start sites, recapitulated these major groupings (Fig. S1H). Finally, cophenetic correlation coefficients calculated using this human myeloid progenitor dataset, compared with a randomized dataset, also supported three major groupings in the data (Fig. S1I).

To investigate whether there was evidence of a link between aberrant RNA editing and alternative splice isoform expression in BC versus CP CML, editing ratios at ADAR target sites were calculated for transcripts that were differentially expressed (Fig. S2C,D). Editing ratios were found to be increased for significantly differentially expressed transcripts (Fig. S2C). Moreover, differential isoform expression of ADAR target genes revealed distinct clustering of CML BC versus CP (Fig. S2D). Thus, the shift in transcriptional patterns associated with increased RNA editing may reflect malignant reprogramming of progenitors in CML.

BCR-ABL Expression Enhances Inflammatory Mediator Gene Expression

Since qRT-PCR analyses revealed that ADAR1 p150 expression correlated with BCR-ABL levels in BC CML (Fig. 1C), we sought to investigate the potential mechanisms driving ADAR1 induction in BC CML and the relationship between ADAR1 p150 and BCR-ABL. Both qRT-PCR analyses and RNA-Seq studies were performed with $CD34^+$ cord blood transduced with lentivirus expressing BCR-ABL p210 tagged with GFP or vector control (Fig. 2A,B). Increased phosphorylation of the BCR-ABL substrate Crkl by nanoproteomics analysis confirmed functional BCR-ABL activation (Fig. 2C). These analyses suggested that BCR-ABL may indirectly regulate ADAR1. In support of this possibility, RNA-Seq analyses of lenti-BCR-ABL transduced cord blood compared to vector-transduced controls identified 45 differentially expressed genes (Fig. 2D). BCR and ABL1 were upregulated along with inflammatory mediators such as TNFRSF9 (Fig. 2D). Other differentially expressed genes included

factors involved in extracellular matrix (ECM) function or intercellular junctions (Fig. 2D). Since TNF pathways, receptors and other inflammatory mediators were also upregulated during CML progression (Figs. 1A, S1A and S2A), it is conceivable that BCR-ABL regulates ADAR1 p150 through the induction of inflammatory receptor expression.

ADAR1 Promotes Malignant Myeloid Progenitor Expansion and Alternative Splicing

Lentiviral ADAR1 overexpression and shRNA knockdown studies were performed to examine the functional consequences of ADAR1 p150 upregulation. Transduction efficiency of lentiviral vectors driving human ADAR1 (p150) overexpression (lenti-ADAR1) or ADAR1-targeting shRNA (lenti-shADAR1) was validated in normal cord blood (Fig. S3A-D). Myeloid lineage skewing was observed in colony forming assays performed with $CD34^{+}CD38^{+}Lin^{-}$ cord blood progenitors transduced with lenti-ADAR1 p150, as demonstrated by increased macrophage (M) colony numbers and a corresponding decrease in erythroid burst-forming unit (BFU-E) colony numbers (Fig. 3A). This myeloid lineage bias coincided with upregulation of PU.1 – a myeloid transcription factor, and downregulation of GATA1 – an erythroid transcription factor, in colonies from cord blood progenitors transduced with ADAR1 p150 lentivirus (Fig. 3B,C) and in CML BC progenitor-derived colonies (Fig. 3D,E). RNA-Seq analyses demonstrated an increase in the PU.1/GATA1 ratio in BC versus CP progenitors (Fig. 3F). Additionally, network analysis of RNA-Seq data revealed downregulation of genes involved in GATA1-dependent processes (Fig. 3G).

Short-term culture of normal progenitors transduced with lenti-ADAR1 at increasing multiplicity of infection (MOI) confirmed a positive correlation between PU.1 and ADAR1 expression, while the levels of GATA1 expression remained constant (Fig. 3H). The ADAR1-mediated myeloid lineage skewing recapitulates qRT-PCR data reported with aged human HSC (37) and the expansion of GMP (34) during progression of CML from CP to BC (Fig. S1F). Since we have previously identified production of a mis-spliced form of GSK3β lacking exons 8 and 9 (7) associated with GMP expansion in CML BC, and activation of ADAR1 might promote alternative splicing (27), we performed splice isoform specific qRT-PCR for GSK3β variants in individual colonies derived from lenti-ADAR1 transduced cord blood or CML CP progenitors. While GSK3β exon 8-9del was undetectable in cord blood progenitors, in CML CP samples mRNA levels of this variant were increased relative to the exon 9del form, which represents a predominant GSK3β transcript in normal hematopoietic tissues (7) (Fig. 3I). Together, these results demonstrate that ADAR1 overexpression drives hematopoietic differentiation towards the myeloid lineage, coincident with PU.1 upregulation and alternative splicing of GSK3β in CML progenitors.

ADAR1 Knockdown Impairs Malignant Myeloid Progenitor Self-Renewal

Previous reports demonstrate that ADAR1 mediates mouse HSC maintenance (23, 24), however the relative effects of down-modulating ADAR1 expression in human LSC versus normal HSC have not been established. In support of a favorable therapeutic index for ADAR1 inhibitory strategies in CML progenitors versus normal cord

blood, shRNA knockdown and colony assay experiments showed that lenti-shADAR1 knockdown in normal cord blood progenitors did not affect hematopoietic differentiation (Fig. S3E), while CML CP progenitors transduced with lenti-shADAR1 produced fewer macrophage colonies coupled with increased numbers of BFU-E colonies (Fig. S3F).

To examine the role of ADAR1 in CML progenitor survival and self-renewal capacity *in vivo*, $CD34^+$ human BC CML progenitors were transduced with lenti-shADAR1 or shRNA backbone (lenti-shControl) and transplanted intrahepatically into neonatal $RAG2^{-/-}\gamma c^{-/-}$mice (Fig. 4A). In addition, qRT-PCR analysis was performed to confirm ADAR1 p150 knockdown. Similar to experiments in normal cord blood (Fig. S3B), ADAR1 p150 levels prior to transplant were reduced by approximately 50% in CML BC progenitors transduced with lenti-shADAR1 compared with vector controls (Fig. 4A).

By 10 weeks post-transplant, robust leukemic engraftment was detectable in hematopoietic tissues by FACS analysis of human $CD45^+$ cells (Fig. 4B). Similar levels of human hematopoietic cell engraftment were detected in bone marrow from mice transplanted with lenti-shADAR1-transduced BC progenitors compared with lenti-shControl (Fig. 4C,D). Quantitative RT-PCR analysis confirmed that pooled human progenitors from primary transplant recipient bone marrow maintained reduced levels of ADAR1 p150, consistent with continued activity of the ADAR1 shRNA after primary engraftment (Fig. 4A). We transplanted equal numbers of human $CD34^+$ progenitors derived from the bone marrow of primary recipients of lenti-shControl or lenti-shADAR1-transduced cells into secondary recipient mice and the bone marrow was analyzed for human cell engraftment and

$CD34^+CD38^+Lin^-$ progenitors by FACS (Fig. 4E,F). Notably, this revealed a significant reduction of serial engraftment potential of shADAR1-transduced CML BC progenitors (~20%) compared with shControls (~50%) (Fig. 4E). While leukemic burden was not significantly diminished, the LSC self-renewal capacity was irrevocably reduced by ADAR1 knockdown, suggesting that ADAR1 plays a pivotal role in the propagation of leukemia driven by self-renewing malignant progenitors.

Discussion

Activation of IFN-responsive ADAR1 p150 in primary CML progenitors correlated with increased A-to-I RNA editing following blastic transformation. Full transcriptome RNA-Seq analyses suggest that upregulation of ADAR1 p150 in BC CML may be related to activation of inflammatory pathways such as cytokines and TNF in advanced disease. Hematopoietic progenitor studies demonstrated that lentivirally enforced ADAR1 p150 expression promotes human myeloid differentiation fate. Lentiviral-shRNA knockdown of ADAR1 in a xenotransplantation model impaired self-renewal capacity of BC LSC. Together, these data suggest that an inflammatory mediator driven isoform switch favoring ADAR1 p150 expression drives expansion of malignant progenitors and contributes to CML progression.

ADAR-mediated RNA editing can regulate myriad molecular processes including RNA interference (29), microRNA function (38), and RNA stability, localization, nuclear retention, degradation, and alternative splicing (27, 39-41).Moreover, high levels of ADAR-

mediated RNA editing activity may reflect a reversion to a primitive transcriptional program typical of embryonic stem cells (18). A previous study demonstrated that ADAR1 was among the top 5% of genes expressed in the mutational evolution of lobular breast cancer (36), indicating that activation of ADARs may correlate with disease progression in multiple malignant cell types (31). While previous studies have shown ADAR1 p110 upregulation in a murine leukemia model (42) and in pediatric acute leukemias (43), it should be emphasized that human hematopoietic tissues undergo dramatic changes during aging (44, 45) that are caused in part by increased inflammation and genomic instability (46).

Our data suggest that inflammatory cues may facilitate selective upregulation of the IFN-responsive ADAR1 p150 isoform in hematologic malignancies. Using whole transcriptome sequencing analysis, we found that inflammatory signaling receptors were differentially expressed in BCR-ABL-expressing cord blood. Inflammatory cytokines such as IFN, TNFα and other interleukins have been shown to stimulate ADAR1 p150 expression (32, 33), and IFN regulates HSC quiescence (47). Together, BCR-ABL mediated upregulation of inflammatory pathway receptors could sensitize hematopoietic progenitors to inflammatory stimuli that drive ADAR1 expression and promote CML LSC self-renewal.

Whole transcriptome-based RNA editing analyses revealed that CML progression is accompanied by differential RNA editing. Recent in-depth transcriptomic studies have shown that genes with predicted A-to-I editing events are significantly enriched in cancer-related pathways (35). ENREF 32The present study provides further evidence supporting a role for ADAR-directed RNA editing in splice

isoform diversity in cancer and demonstrates activation of inflammation-associated RNA editing during the progression of hematologic malignancies. Our results suggest that ADAR1 p150 upregulation may contribute to blastic transformation of CML driven by the $CD34^{+}CD38^{+}Lin^{-}$ progenitor and GMP subpopulations. Since ADAR-mediated RNA editing occurs primarily in primate-specific Alu repeat sequences (14, 19, 20), in human cells the activation of RNA editases may fuel species-specific malignant reprogramming of progenitors to adopt a more primitive stem cell fate under pathological conditions.

Myeloid lineage skewing was observed in response to enforced ADAR1 p150 expression, concomitant with PU.1 activation. While a previous study in an *in vitro* model implicated PU.1 in the regulation of murine ADAR1 expression (48), cell type and niche-specific stimuli may have differential effects on RNA editing, and our studies in human cells – where 90% of RNA editing occurs in primate-specific Alu sequences – suggest that the converse may also occur. It is conceivable that ADAR1 directly controls PU.1 through RNA editing-dependent effects or via potential transcriptional regulation related to its Z-DNA binding function (41, 49). In support of the former possibility, a database (50) compiling RNA editing sites from multiple publications (DARNED) reports that transcripts of *Spi1* (gene encoding PU.1; chr11, Start: 47379732, End: 47400127) showed evidence of A-to-I RNA editing at 28 sites (14). Future gene expression analyses and identification of *de novo* RNA editing sites through analysis of whole genome and transcriptome DNA-RNA differences (15) in normal HSC harboring enforced ADAR1 p150

expression and LSC will be necessary to further dissect the link between ADAR1 activation PU.1 expression.

In addition to up-regulation of PU.1 in response to ADAR1 p150 overexpression, we also detected production of a mis-spliced GSK3β variant in colonies derived from CML CP progenitors transduced with lentiviral ADAR1 p150. We have previously shown that this particular form of GSK3β harbors reduced activity, and promotes LSC self-renewal via activation of β-catenin (7). In support of a role for ADAR1 in CML LSC self-renewal, we showed in humanized CML xenograft mouse models that ADAR1 knockdown reduced CML BC LSC serial transplantation potential. Given that these CML BC progenitors expressed significantly higher levels of ADAR1 p150 compared to normal cord blood progenitors, we expect that LSC are relatively more dependent on IFN-responsive ADAR1 activity (24). Together these data suggest that inflammation-dependent activation of the ADAR1 p150 editase promotes CML progression. Aberrant ADAR1 activation in CML endows myeloid progenitors with self-renewal capacity leading to LSC generation. Thus, inhibition of ADAR1 activity could represent an effective strategy to prevent LSC-driven relapse in CML while sparing normal HSC populations. Furthermore, ADAR1-mediated RNA editing activation could prove to be a novel diagnostic and prognostic indicator of disease progression with important implications for other cancer stem cell-driven malignancies.

Materials and Methods

Detailed methods are available in *SI Methods*. http://www.pnas.org/content/suppl/2012/12/28/1213021110.DCSupplemental/pnas.201213021SI.pdf

ACKNOWLEDGMENTS

This work was supported by CIRM grants RN2-00910-1 (CHMJ) and DR1-01430 (CHMJ), CIRM training grant TG2-01154 (QJ), CIRM SEED grant RS1-00228-1, a Cancer Stem Cell Consortium with funding from the Government of Canada through Genome Canada and the Ontario Genomics Institute (OGI-047), and through the Canadian Institute of Health Research (CSC-105367). The authors wish to thank: Wenxue Ma, Alice Shih, and Heather Leu (all from Moores UC San Diego Cancer Center) for assistance with *in vivo* experiments; Sa Li (BC Cancer Agency) for performing SNV analysis; Jonathan Lee (Moores UCSD Cancer Center) for assistance with figures; Guanming Wu for providing the mapping information of pathway-to-gene relationships; and the Genome Sciences Centre Library Construction, Sequencing and Bioinformatics teams (BC Cancer Agency).

Conflict of Interest Statement

The authors declare no competing financial interests.

Figure Legends

Figure 1. Inflammatory mediator driven RNA editing portends blastic transformation. (A) Clustering of 2228 differentially expressed genes in BC (n=8) versus CP (n=8) CML progenitors. (B) Human ADAR1 p150 and p110 were analyzed in $CD34^{+}CD38^{+}Lin^{-}$ progenitors from normal cord blood (n=8), CML CP (n=6) and CML BC (n=7) by qRT-PCR. Ratios of p150/p110 were determined (overall P=0.0067, *P<0.05 compared to normal cord blood and **P<0.05 compared to CML CP by one way ANOVA with post hoc Tukey test). (C) Pearson correlation analysis of ADAR1 isoforms and BCR-ABL mRNA levels in CML BC (n=6) progenitors. (D) RNA-Seq-based analysis of A-to-G (=I) changes at putative editing sites (35) in CML BC (n=8) versus CP progenitors (n=8) (P<0.05 by unpaired two-tailed Student's t-test). For each site, the percentage of reads that contained G versus A bases was calculated for each sample. The differences between average percentages were computed between disease stages (BC-CP). Data were reported as the number of sites showing significantly different editing ratios. (E) Volcano plot analysis showing enrichment of more highly edited sites in CML BC (n=8) compared to CP progenitors (n=8). (F) Differential editing at ADAR target sites in CML BC (n=8) versus CP (n=8). All sites shown were significantly different (P<0.05 by Student's t-test, Dataset S1). (G) 175 putative ADAR target genes were differentially expressed in CP (n=8) versus BC (n=8). Unsupervised hierarchical clustering (see *SI Methods*) separated CP and BC samples. A select subset of genes (insets) discriminated BC from cord blood (n=3).

Figure 2. BCR-ABL expression enhances inflammatory mediator gene expression. (A) Diagram of the BCR-ABL1 p210 lentivirus vector construction. (B) Bright field (BF) and fluorescent microscopy showing cord blood-derived colonies transduced with lentiviral vector backbone control (pCDH) or lentivirus expressing BCR-ABL p210 and green fluorescent protein (GFP). (C) Nanoproteomics analysis of phosphorylated (p)-Crkl levels in BCR-ABL transduced CD34+ cells from cord blood (n=3). $P<0.05$ by Student's t-test. (D) CD34+ cord blood (n=3) cells were transduced with lenti-BCR-ABL or vector control and processed for RNA-Seq analysis. 45 genes were differentially expressed in BCR-ABL expressing cells compared to vector controls ($P<0.05$ by DESeq).

Figure 3. ADAR1 promotes malignant myeloid progenitor expansion.(A) Lentiviral overexpression of ADAR1 p150 in FACS-purified $CD34^{+}38^{+}Lin^{-}$ normal progenitors (n=3) reduced erythroid (BFU-E) colony formation and increased Macrophage (M) colony forming units (CFU) compared with vector (ORF) controls. (B-E) Pearson correlation analysis of HPRT-normalized ADAR1 mRNA levels and PU.1 or GATA1 in individual colonies derived from normal progenitors (n=3) transduced with lenti-ADAR1 p150 (B, C) or CML BC progenitor-derived colonies (D, E). (F) Ratio of PU.1 to GATA1 expression levels by RNA-Seq in CP (n=8) versus BC (n=8) CML. (G) RNA-seq based IPA network analysis of GATA1 associated genes in BC CML (n=8) compared with CP (n=8). (H) Pearson correlation analysis of HPRT-normalized ADAR1 mRNA levels and PU.1 (r^2=0.9252) or GATA1 (r^2=0.2210) in cord blood (n=2) progenitors transduced (48 hrs) with ADAR1 p150 lentivirus at increasing MOI. (I) qRT-PCR of

GSK3β splice variants in individual colonies derived from lenti-ADAR1 transduced cord blood (n=3) or CML CP (n=3) progenitors compared to vector-transduced controls. *P<0.05 and **P<0.01 compared to vector-transduced controls or CP progenitors by Student's t-test. r^2 values were calculated using Pearson correlation analysis.

Figure 4. ADAR1 knockdown impairs malignant myeloid progenitor self-renewal.(A) Diagrammatic scheme of *in vivo* experimental design. Before and after primary transplant, qRT-PCR was performed in human progenitors, confirming ADAR1 knockdown. (B) Representative FACS plots showing human $CD45^+$ engraftment in hematopoietic organs of primary $RAG2^{-/-}\gamma c^{-/-}$ transplant recipients, or untransplanted control mouse bone marrow (BM). (C, D) FACS analysis of $CD45^+$ human cell engraftment and progenitor cells in the BM of mice transplanted with BC progenitors transduced with lenti-shControl (n=3) or lenti-shADAR1 (n=5). (E, F)FACS analysis of human cells in mouse BM (shControl n=7 and shADAR1 n=8) after serial transplantation of BM $CD34^+$ cells pooled from primary transplant recipient mice. *P<0.05 compared to vector-transduced controls by Student's t-test.

Supplementary Information

Supplemental information includes supplementary Materials and Methods, three supplementary figures with corresponding figure legends, two supplementary tables and one supplementary dataset.

http://www.pnas.org/content/suppl/2012/12/28/1213021110.DCSupplemental/pnas.201213021SI.pdf

Figure 1

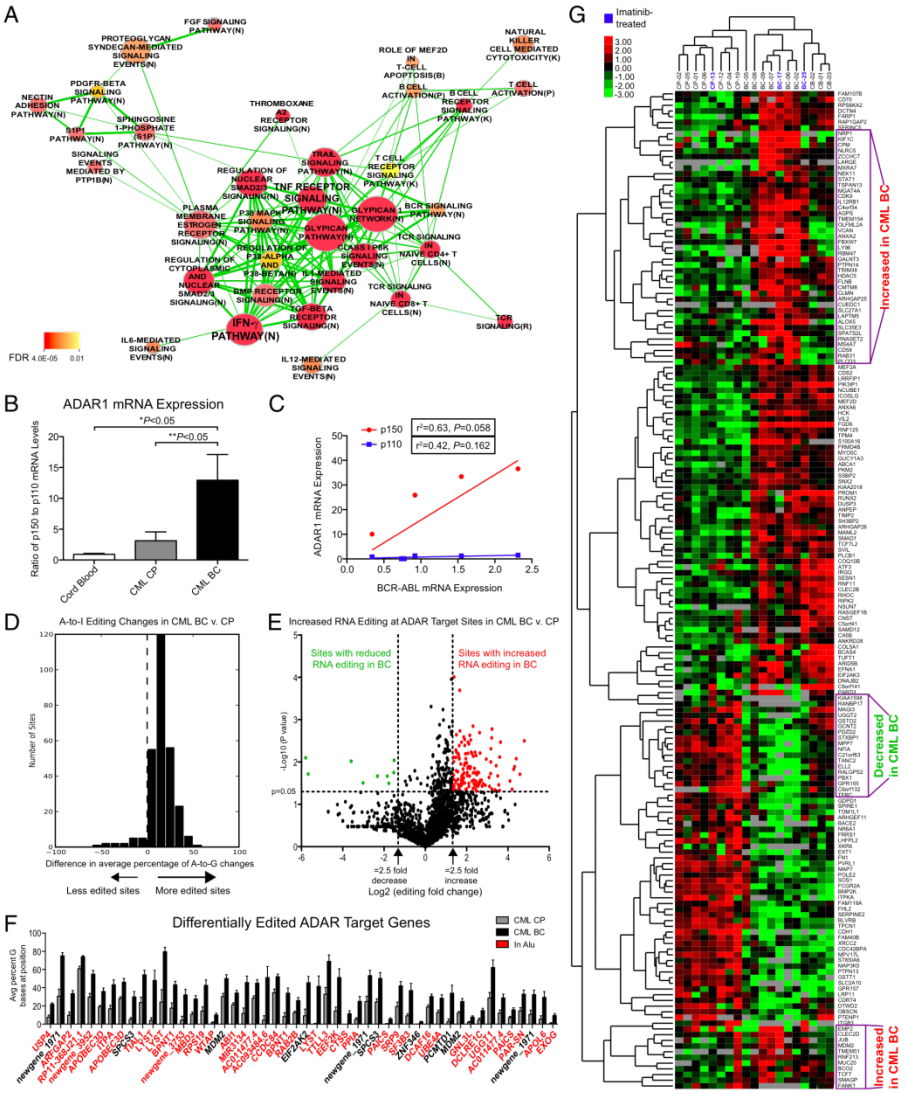
A
FGF SIGNALING PATHWAY(N)
PROTEOGLYCAN SYNDECAN-MEDIATED SIGNALING EVENTS(N)
NATURAL KILLER CELL MEDIATED CYTOTOXICITY(K)
ROLE OF MEF2D IN T-CELL APOPTOSIS(B)
PDGFR-BETA SIGNALING PATHWAY(N)
NECTIN ADHESION PATHWAY(N)
THROMBOXANE A2 RECEPTOR SIGNALING(N)
B CELL ACTIVATION(P)
T CELL ACTIVATION(P)
B CELL RECEPTOR SIGNALING PATHWAY(K)
SPHINGOSINE 1-PHOSPHATE (S1P) PATHWAY(N)
S1P1 PATHWAY(N)
SIGNALING EVENTS MEDIATED BY PTP1B(N)
TRAF SIGNALING PATHWAY(N)
T CELL RECEPTOR SIGNALING PATHWAY(K)
REGULATION OF NUCLEAR SMAD2/3 SIGNALING(N)
TNF RECEPTOR SIGNALING PATHWAY(N)
PLASMA MEMBRANE ESTROGEN RECEPTOR SIGNALING(N)
P38 MAPK SIGNALING PATHWAY(N)
GLYPICAN 1 NETWORK(N)
BCR SIGNALING PATHWAY(N)
GLYPICAN PATHWAY(N)
TCR SIGNALING
REGULATION OF P38-ALPHA AND P38-BETA(N)
CLASS I PI3K SIGNALING EVENTS(N)
IFN-MEDIATED SIGNALING EVENTS(N)
NAIVE CD4+ T CELLS(N)
REGULATION OF CYTOPLASMIC AND NUCLEAR SMAD2/3 SIGNALING(N)
TGF-BETA RECEPTOR SIGNALING(N)
NAIVE CD8+ T CELLS(N)
IFN-γ PATHWAY(N)
TCR SIGNALING(R)
IL6-MEDIATED SIGNALING EVENTS(N)
IL12-MEDIATED SIGNALING EVENTS(N)
FDR 4.0E-05 0.01
B
ADAR1 mRNA Expression
*P<0.05
**P<0.05
Ratio of p150 to p110 mRNA Levels
Cord Blood
CML CP
CML BC
C
p150
p110
r²=0.63, P=0.058
r²=0.42, P=0.162
ADAR1 mRNA Expression
BCR-ABL mRNA Expression
D
A-to-I Editing Changes in CML BC v. CP
Number of Sites
Difference in average percentage of A-to-G changes
Less edited sites
More edited sites
E
Increased RNA Editing at ADAR Target Sites in CML BC v. CP
Sites with reduced RNA editing in BC
Sites with increased RNA editing in BC
-Log10 (P-value)
p=0.05
=2.5 fold decrease
=2.5 fold increase
Log2 (editing fold change)
F
Differentially Edited ADAR Target Genes
CML CP
CML BC
In Alu
Avg percent G base at position
G
Imatinib-treated
3.00
2.00
1.00
0.00
-1.00
-2.00
-3.00
Increased in CML BC
Decreased in CML BC
Increased in CML BC

Figure 2

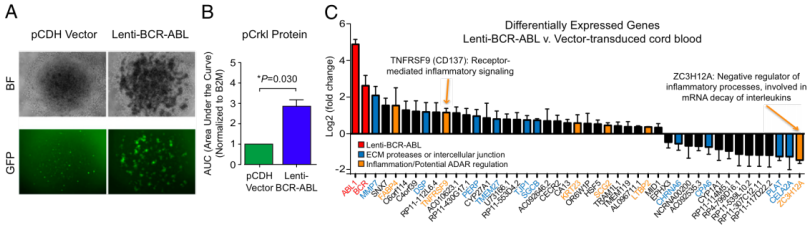

Figure 3

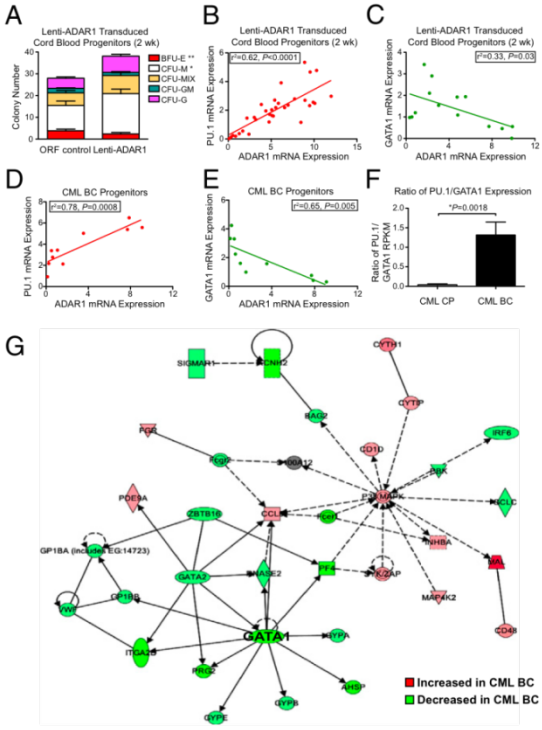

Figure 4

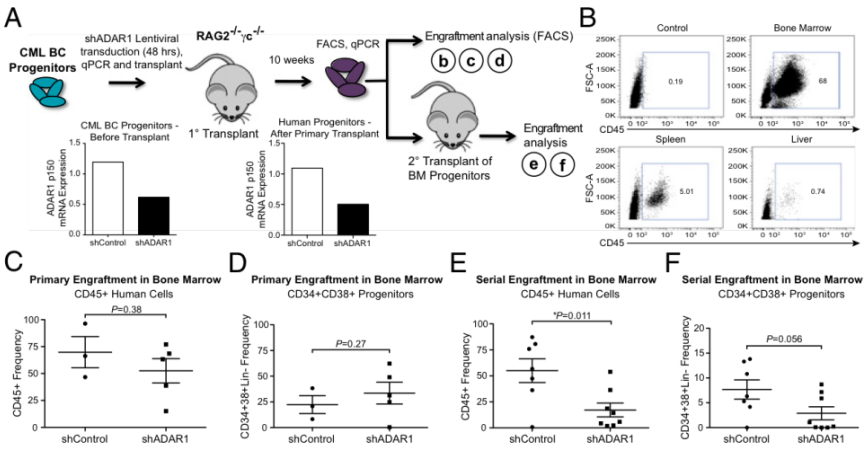
A
CML BC Progenitors
shADAR1 Lentiviral transduction (48 hrs), qPCR and transplant
RAG2-/-γc-/-
1° Transplant
10 weeks
FACS, qPCR
Engraftment analysis (FACS)
b c d
2° Transplant of BM Progenitors
Engraftment analysis
e f
CML BC Progenitors - Before Transplant
Human Progenitors - After Primary Transplant
ADAR1 p150 mRNA Expression
shControl
shADAR1
B
Control
Bone Marrow
Spleen
Liver
FSC-A
CD45
0.19
68
5.01
0.74
C
Primary Engraftment in Bone Marrow
CD45+ Human Cells
P=0.38
CD45+ Frequency
D
Primary Engraftment in Bone Marrow
CD34+CD38+ Progenitors
P=0.27
CD34+38+Lin- Frequency
E
Serial Engraftment in Bone Marrow
CD45+ Human Cells
*P=0.011
CD45+ Frequency
F
Serial Engraftment in Bone Marrow
CD34+CD38+ Progenitors
P=0.056
CD34+38+Lin- Frequency

References

1. Jamieson C (2009) The MLLgnant consequences of reverting to an embryonic transcriptional program. *Cell Stem Cell* 4(2):97-98.
2. Eppert K*, et al.* (2011) Stem cell gene expression programs influence clinical outcome in human leukemia. *Nat Med* 17(9):1086-1093.
3. Ben-Neriah Y, Daley GQ, Mes-Masson AM, Witte ON, & Baltimore D (1986) The chronic myelogenous leukemia-specific P210 protein is the product of the bcr/abl hybrid gene. *Science* 233(4760):212-214.
4. Rowley JD (1973) Letter: A new consistent chromosomal abnormality in chronic myelogenous leukaemia identified by quinacrine fluorescence and Giemsa staining. *Nature* 243(5405):290-293.
5. Shtivelman E, Lifshitz B, Gale RP, & Canaani E (1985) Fused transcript of abl and bcr genes in chronic myelogenous leukaemia. *Nature* 315(6020):550-554.
6. Hughes TP*, et al.* (2003) Frequency of major molecular responses to imatinib or interferon alfa plus cytarabine in newly diagnosed chronic myeloid leukemia. *N Engl J Med* 349(15):1423-1432.

7. Abrahamsson AE*, et al.* (2009) GSK3β missplicing contributes to leukemia stem cell generation. *Proc Natl Acad Sci U S A* 106(10):3925-3929.

8. Perrotti D, Jamieson C, Goldman J, & Skorski T (2010) Chronic myeloid leukemia: mechanisms of blastic transformation. *J Clin Invest* 120(7):2254-2264.

9. Copland M*, et al.* (2006) Dasatinib (BMS-354825) targets an earlier progenitor population than imatinib in primary CML but does not eliminate the quiescent fraction. *Blood* 107(11):4532-4539.

10. Jamieson CH, Barroga CF, & Vainchenker WP (2008) Miscreant myeloproliferative disorder stem cells. *Leukemia* 22(11):2011-2019.

11. Jorgensen HG, Allan EK, Jordanides NE, Mountford JC, & Holyoake TL (2007) Nilotinib exerts equipotent antiproliferative effects to imatinib and does not induce apoptosis in CD34+ CML cells. *Blood* 109(9):4016-4019.

12. Huang X, Cortes J, & Kantarjian H (2012) Estimations of the increasing prevalence and plateau prevalence of chronic myeloid leukemia in the era of tyrosine kinase inhibitor therapy. *Cancer* 118(12):3123-3127.

13. Perrotti D & Neviani P (2007) From mRNA metabolism to cancer therapy: chronic myelogenous leukemia shows the way. *Clin Cancer Res* 13(6):1638-1642.

14. Kim DD*, et al.* (2004) Widespread RNA editing of embedded alu elements in the human transcriptome. *Genome Res* 14(9):1719-1725.

15. Ramaswami G*, et al.* (2012) Accurate identification of human Alu and non-Alu RNA editing sites. *Nat Methods*.

16. Peng Z*, et al.* (2012) Comprehensive analysis of RNA-Seq data reveals extensive RNA editing in a human transcriptome. *Nat Biotechnol*.

17. Levanon EY*, et al.* (2004) Systematic identification of abundant A-to-I editing sites in the human transcriptome. *Nat Biotechnol* 22(8):1001-1005.

18. Osenberg S*, et al.* (2010) Alu sequences in undifferentiated human embryonic stem cells display high levels of A-to-I RNA editing. *PLoS One* 5(6):e11173.

19. Eisenberg E*, et al.* (2005) Is abundant A-to-I RNA editing primate-specific? *Trends Genet* 21(2):77-81.

20. Athanasiadis A, Rich A, & Maas S (2004) Widespread A-to-I RNA editing of Alu-containing mRNAs in the human transcriptome. *PLoS biology* 2(12):e391.

21. Bass BL & Weintraub H (1988) An unwinding activity that covalently modifies its double-stranded RNA substrate. *Cell* 55(6):1089-1098.

22. Chen CX*, et al.* (2000) A third member of the RNA-specific adenosine deaminase gene family, ADAR3, contains both

single- and double-stranded RNA binding domains. *RNA* 6(5):755-767.

23. Hartner JC, Walkley CR, Lu J, & Orkin SH (2009) ADAR1 is essential for the maintenance of hematopoiesis and suppression of interferon signaling. *Nat Immunol* 10(1):109-115.

24. XuFeng R*, et al.* (2009) ADAR1 is required for hematopoietic progenitor cell survival via RNA editing. *Proc Natl Acad Sci U S A* 106(42):17763-17768.

25. Wang Q (2011) RNA editing catalyzed by ADAR1 and its function in mammalian cells. *Biochemistry (Mosc)* 76(8):900-911.

26. Wang Q, Khillan J, Gadue P, & Nishikura K (2000) Requirement of the RNA editing deaminase ADAR1 gene for embryonic erythropoiesis. *Science* 290(5497):1765-1768.

27. Rueter SM, Dawson TR, & Emeson RB (1999) Regulation of alternative splicing by RNA editing. *Nature* 399(6731):75-80.

28. Lev-Maor G*, et al.* (2007) RNA-editing-mediated exon evolution. *Genome Biol* 8(2):R29.

29. Nishikura K (2006) Editor meets silencer: crosstalk between RNA editing and RNA interference. *Nat Rev Mol Cell Biol* 7(12):919-931.

30. Galeano F, Tomaselli S, Locatelli F, & Gallo A (2012) A-to-I RNA editing: The "ADAR" side of human cancer. *Semin Cell Dev Biol* 23(3):244-250.

31. Cenci C*, et al.* (2008) Down-regulation of RNA editing in pediatric astrocytomas: ADAR2 editing activity inhibits cell migration and proliferation. *J Biol Chem* 283(11):7251-7260.

32. Meltzer M*, et al.* (2010) The RNA editor gene ADAR1 is induced in myoblasts by inflammatory ligands and buffers stress response. *Clinical and translational science* 3(3):73-80.

33. Yang JH*, et al.* (2003) Widespread inosine-containing mRNA in lymphocytes regulated by ADAR1 in response to inflammation. *Immunology* 109(1):15-23.

34. Jamieson CH*, et al.* (2004) Granulocyte-macrophage progenitors as candidate leukemic stem cells in blast-crisis CML. *N Engl J Med* 351(7):657-667.

35. Bahn JH*, et al.* (2012) Accurate identification of A-to-I RNA editing in human by transcriptome sequencing. *Genome Res* 22(1):142-150.

36. Shah SP*, et al.* (2009) Mutational evolution in a lobular breast tumour profiled at single nucleotide resolution. *Nature* 461(7265):809-813.

37. Pang WW*, et al.* (2011) Human bone marrow hematopoietic stem cells are increased in frequency and myeloid-biased with age. *Proc Natl Acad Sci U S A* 108(50):20012-20017.

38. Yang W*, et al.* (2006) Modulation of microRNA processing and expression through RNA editing by ADAR deaminases. *Nat Struct Mol Biol* 13(1):13-21.

39. Heale BS, Keegan LP, & O'Connell MA (2009) ADARs have effects beyond RNA editing. *Cell Cycle* 8(24):4011-4012.

40. Heale BS*, et al.* (2009) Editing independent effects of ADARs on the miRNA/siRNA pathways. *EMBO J* 28(20):3145-3156.

41. Herbert A, Wagner S, & Nickerson JA (2002) Induction of protein translation by ADAR1 within living cell nuclei is not dependent on RNA editing. *Mol Cell* 10(5):1235-1246.

42. Ma CH*, et al.* (2011) [Expression of ADAR1 isoforms in murine acute T-ALL leukemia model]. *Zhongguo Shi Yan Xue Ye Xue Za Zhi* 19(3):566-569.

43. Ma CH*, et al.*(2011) Abnormal expression of ADAR1 isoforms in Chinese pediatric acute leukemias. *Biochem Biophys Res Commun* 406(2):245-251.

44. Morrison SJ, Wandycz AM, Akashi K, Globerson A, & Weissman IL (1996) The aging of hematopoietic stem cells. *Nat Med* 2(9):1011-1016.

45. Wang LD & Wagers AJ (2011) Dynamic niches in the origination and differentiation of haematopoietic stem cells. *Nat Rev Mol Cell Biol* 12(10):643-655.

46. Chambers SM*, et al.* (2007) Aging hematopoietic stem cells decline in function and exhibit epigenetic dysregulation. *PLoS biology* 5(8):e201.

47. Essers MA*, et al.* (2009) IFNα activates dormant haematopoietic stem cells in vivo. *Nature* 458(7240):904-908.

48. Wu T, Zhao Y, Hao Z, Zhao H, & Wang W (2009) Involvement of PU.1 in mouse adar-1 gene transcription induced by high-dose esiRNA. *Int J Biol Macromol* 45(2):157-162.

49. Herbert A*, et al.* (1997) A Z-DNA binding domain present in the human editing enzyme, double-stranded RNA adenosine deaminase. *Proc Natl Acad Sci U S A* 94(16):8421-8426.

50. Kiran A & Baranov PV (2010) DARNED: a DAtabase of RNa EDiting in humans. *Bioinformatics* 26(14):1772-1776.

Other preliminary results on CML model

ADAR1 contributes to Blast crisis leukemia stem cells generation by modulation of microRNA expression level.

Background and central hypothesis

Novel stem cell-based diagnostic and therapeutic strategies able to predict and prevent cancer progression and relapse represent compelling unmet medical needs. Chronic Myeloid Leukemia (CML) is a clonal myeloproliferative neoplasm and represents an important paradigm for understanding the molecular evolution of cancer since it was one of the first human malignancies to be shown to initiate from CSC level (Geron, 2008). The malignancy arises from the acquisition of translocation t(9:22) that encodes the constitutively active tyrosine kinase, BCR-ABL, targeted by therapy with tyrosine kinase inhibitors (TKI) (O'Hare, 2012).

We have recently shown that blast crisis CML Leukemic Stem Cell (LSC) harbors high expressions of inflammation-responsive ADAR1 enzyme involved in RNA-editing which regulates both LSC differentiation and self-renewal as demonstrated by *in vivo* humanized xenograft CML BC model (Jiang, 2013). MicroRNA (miRNA) represent one of the primary targets of RNA-editing. The stem-loop structures predicted for all miRNA precursors are reminiscent of the partially double-stranded fold-back structures of known editing substrates (Bass,2002) thus making them favorable

targets of ADARs-driven RNA editing, which usually triggers their degradation through interaction with Dicer and Drosha miRNA processing machinery (Tomaselli, 2013). This suggests that miRNA alterations introduced at pri-mRNA or pre-mRNA level by adenosine (A) -to- inosine (I) editing represent a source of epigenetic mutagenesis that may be responsible for broad changes in the transcriptome that drives cancer stem cell (CSC) initiation and expansion. Abnormal expression of certain miRNA is associated with CML bulk tumor and contributes to the disease progression and resistance to therapeutic treatment. However, the overall change in edited miRNA profiles at early stages of CML leukemia stem cells (LSC) initiation and disease progression is unclear. Our previous findings showed that ADAR1 contributes to malignant progenitor reprogramming (Jiang, 2013) The emerging evidences of a role for ADAR1 in the modulation of miRNA expression raised the hypothesis, evaluated in this preliminary study, that ADAR1 contributes to BC LSC generation by modulating the expression level of miRNA involved in the regulation of self-renewal, cell-cycle and differentiation. The possibility to evaluate this hypotesis even in different solid tumor models, like RCC, may help to better understand the characteristics of CSC and their heterogeneity in malignant cell population.

Methods

Primary Patient Samples, Normal Human Progenitors, and Processing. A collection of CML patient samples has been obtained from consenting patients at the University of California San Diego,

Stanford University, the University of Toronto Health Network, MD Anderson and the University of Bologna according to Institutional Review Board approved protocols. Peripheral blood mononuclear cells (PBMC) were extracted from peripheral blood following Ficoll density centrifugation. $CD34^+$cells was purified by magnetic bead separation (MACS; Miltenyi, Bergisch Gladbach, Germany) and aliquots frozen in liquid nitrogen for subsequent analyses. Normal human progenitor control cells for all experiments proposed include both cord blood and adult peripheral blood $CD34^+$ progenitors (AllCells).

FACS Aria Sorting. Primary CML patient samples and normal progenitor cells were stained with lineage specific fluorescent-conjugated antibodies and propidium iodide as previously described (Jiang, 2013) Following staining, cells were identified and sorted, using a FACS Aria II (UCSD Stem Cell Core facility), directly into lysis buffer to isolate both miRNA and total RNA (RNeasy Micro Kit; Qiagen). Human HSC were identified as $CD34^+CD38^-Lin^-$ and LSC will be identified based on $CD34^+CD38^+Lin^-$ staining. The treshold was set by using appropriate isotype and no antibody controls as well as normal cord and adult peripheral blood (AllCells) $CD34^+$ cells.

Quantitative RT-PCR (qRT-PCR). Human-specific primers to quantify the relative amount of the LSC-associated ADAR expression in mRNA isolated from normal progenitors, LSC and a variety of normal adult tissues. qRT-PCR was performed with SYBR GreenER two-step qRT-PCR Kit (Invitrogen) as previously described and

quantitative analyses were performed using routine methods (Abrahamsson, 2009).

Quantitative RT-PCR miRNA Array (qRT-PCR). cDNA was prepared in a reverse-transcription reaction using miScript RTII kit (QIAGEN) and it served as a template to profile the expression of the 84 most abundantly expressed and best characterized miRNAs by using miScript miRNA PCR Array (QIAGEN), which contains miRNA specific miScript primer assays. qRT-PCR was performed with SYBR Green Kit (QIAGEN). qRT-PCR for the validation of array results was performed by using miRNA specific primer assays and SYBR Green Kit (QIAGEN). MiScript primer control RNU6_2 and SNORD44 (Qiagen) were used as housekeeping.

Lentivirus Transduction. We have developed and characterized a lentiviral human ADAR1 vector in the pCDH-EF1-T2A-GFP lentiviral vector (System Biosciences). Vector control is the pCDH-GFP backbone. Lentivirus shRNA plasmids specific to human ADAR were purchased from Thermo-Dharmacon. We have previously validated virus efficiency (Jiang, 2013).Lentivirus production was performed according to previously established methods and a multiplicity of infection (MOI) of 50-200 was used for the transduction.

Statistical Methods. Two tail, paired Student's t-test was used to calculate changes in miRNA expression levels in CML LSC versus normal human progenitor cells, in ADAR1-transduced normal progenitors and CP LSC versus control vector-transduced cells.

Preliminary results

miRNA expression profile changes during progression of chronic myeloid leukemia from cronic phase to blast crisis.

In order to identify changes in miRNA expression during CML progression, we performed new miRNA expression qPCR array studies on primary human hematopoietic stem and progenitor cells from cord blood, CP CML and BC CML. In general, there was a trend towards increased levels of miRNA expression in CD34+ cells from CP CML compared with normal cord blood. On the opposite, we observed a decrease in the expression of 35 out of 90 miRNAs analyzed compared with CP CML (Table 1). Validation of the array results confirmed a general decrease in the expression level of 13 miRNA in BC CML compared with CP CML, with several of the let-7 family members being among these (Fig.1)

Lentivirus-enforced human ADAR1 expression broadly downregulates miRNA expression in normal and CP HSPC.

In previous report we identified the RNA editing gene ADAR1 is a key regulator of myeloid cell fate determination and LSC self-renewal in leukemic progression. Since we found that ADAR1 is upregulated during blastic transformation of CML and we observed a decrease of 13 miRNA in BC LSC compared to CP LSC we evaluated whether this change in miRNA expression level was ADAR1-dependent or not. Emerging evidences have indeed shown that ADAR1 can deregulate miRNA function through direct editing of precursor miRNA species.

Based on these premises, we sought to determine the effects of enforced ADAR1 overexpression on miRNA expression profiles. QRT-PCR analysis showed that lentiviral overexpression of ADAR1 in cord blood-derived CD34+ cells led to significant downregulation of 16 miRNAs (Fig. 2A). Interestingly, BC CD34+ cells showed the downregulation of 12 miRNA compared to CP CD34+ (Fig 2B). Among these 7 are in common with CB cells overexpressing ADAR1.

Moreover, transduction of CP CML-derived CD34+ cells with lenti-ADAR1 resulted in the statistically significant downregulation of 10 miRNAs (Fig.3A).

Similarly all these miRNA were downregulated in BC CML-derived CD34+ cells compared to CP CD34+ cells (Fig 3B).

Summary

In summary, lentivirus-enforced expression of ADAR1 recapitulates the miRNA expression changes characteristic of specific stages of CML progression. These preliminary data support a role for ADAR1 in the regulation of miRNA expression profile during CML progression from CP to BC (Fig.4). Most of the differentially expressed miRNA are involved in the regulation of self-renewal and differentiation (e.g. let-7 family, miR155) (Yu, 2007; Chen, 2013) and in the regulation of the cell-cycle.

Further experiments will evaluate whether the differential expression of miRNA is the result of actual editing from ADAR1 or if other

mechanisms occur, such as for example the direct binding of ADAR1 to pri-miRNA and pre-miRNA that could affect miRNA processing. Finally, since solid tumor carcinomas, such as breast and brain cancer, have been already associated with aberrant A-to-I editing activity, this study could represent a platform for miRNA biomarker discovery that could serve as a diagnostic and prognostic tool in other diseases, such as RCC.

Figure legends

Table 1: Differentially expressed microRNA between Cord Blood, Cronic Phase and Blast Chrisis CD34+ cells as resulted from the array. microRNA are generally upregulated in chronic phase, compare to cord blood (left), while there is a general down-regulation in Blast Chrisis compared to Chronic Phase.

Figure 1: Validation of microRNA expression profile in cord blood vs cronic phase vs blast chrisis CML.

Figure 2: A: Statistically significant downregulated microRNA in CB after lentiviral enforced ADAR1 overexpression B: microRNA commonly downregulated in cord blood overexpressing ADAR1 and Blast chrisis CML (red circles).

Figure 3: A: Statistically significan down-regulated microRNA in CP after lentiviral enforced ADAR1 overexpression B: microRNA commonly downregulated in chronic phase overexpressing ADAR1 and Blast Chrisis CML (red circles).

Figure 4: Schematic representation of hypothesis of disease progression: during chronic myeloid leukemia progression from

chronic phase to blast chrisis CML RNA editing activity increases, due to the overexpression of ADAR1. Enhanced RNA editing activity leads to downregulation of microRNA, thus affecting gene expression levels.

Table 1

Genes Over-Expressed in CP vs CB		
Position	**Mature ID**	**Fold Regulation**
A01	hsa-miR-142-5p	17.9179
A02	hsa-miR-9-5p	12.4092
A04	hsa-miR-27b-3p	10.3627
A09	hsa-miR-26a-5p	4.3873
A11	hsa-miR-26b-5p	8.4757
B01	hsa-miR-30c-5p	8.187
B04	hsa-miR-142-3p	9.6688
B11	hsa-miR-30b-5p	6.7427
B12	hsa-miR-21-5p	19.3376
C01	hsa-miR-30e-5p	5.9518
C02	hsa-miR-200c-3p	20.0195
C03	hsa-miR-15b-5p	32.2971
C04	hsa-miR-223-3p	30.5549
C06	hsa-miR-210	6.0769
C10	hsa-miR-99a-5p	5.0747
C11	hsa-miR-28-5p	8.359
D01	hsa-miR-125a-5p	4.0652
D02	hsa-miR-29b-3p	32.5218
D03	hsa-miR-29a-3p	6.6962
D05	hsa-miR-19a-3p	11.5782
D06	hsa-miR-18a-5p	20.0195
D07	hsa-miR-374a-5p	7.9631
D09	hsa-let-7a-5p	5.9932
D10	hsa-miR-124-3p	10.2912
D12	hsa-miR-23a-3p	9.1472
E01	hsa-miR-25-3p	13.4855
E02	hsa-let-7e-5p	4.6697
E04	hsa-miR-126-3p	25.1648
E06	hsa-miR-424-5p	8.594
E07	hsa-miR-30a-5p	7.5336
E09	hsa-miR-151a-5p	5.6699
E10	hsa-miR-195-5p	6.8844
E12	hsa-miR-30d-5p	5.0049
F01	hsa-miR-191-5p	6.5584
F06	hsa-miR-19b-3p	12.9361
F09	hsa-miR-186-5p	6.9323
F12	hsa-miR-22-3p	6.8369
G03	hsa-miR-29c-3p	14.6551
G06	hsa-let-7f-5p	8.0743
G07	hsa-miR-122-5p	38.408
G08	hsa-miR-20a-5p	6.7896
G09	hsa-miR-106b-5p	5.2537
G10	hsa-miR-7-5p	80.6349

Genes Under-Expressed in BC vs CP		
Position	**Mature ID**	**Fold Regulation**
A03	hsa-miR-150-5p	-8.8766
A06	hsa-let-7d-5p	-18.3792
A09	hsa-miR-26a-5p	-13.6422
A10	hsa-miR-32-5p	-4.8568
A11	hsa-miR-26b-5p	-30.2738
B02	hsa-miR-96-5p	-129.7868
B06	hsa-miR-155-5p	-22.9433
B12	hsa-miR-21-5p	-41.9326
C02	hsa-miR-200c-3p	-230.7201
C03	hsa-miR-15b-5p	-56.493
C04	hsa-miR-223-3p	-97.6806
C05	hsa-miR-194-5p	-6.2333
C06	hsa-miR-210	-12.042
C12	hsa-miR-320a	-13.0864
D01	hsa-miR-125a-5p	-36.0019
D04	hsa-miR-141-3p	-35.261
D09	hsa-let-7a-5p	-88.0347
D10	hsa-miR-124-3p	-86.2229
D12	hsa-miR-23a-3p	-27.4741
E01	hsa-miR-25-3p	-12.5533
E02	hsa-let-7e-5p	-238.8564
E03	hsa-miR-376c-3p	-96.3358
E04	hsa-miR-126-3p	-39.1245
E05	hsa-miR-144-3p	-17.5087
E08	hsa-miR-23b-3p	-10.4107
E11	hsa-miR-143-3p	-9.3179
F01	hsa-miR-191-5p	-9.5137
F03	hsa-miR-302a-3p	-324.0337
F05	hsa-let-7b-5p	-8.2249
F10	hsa-miR-196b-5p	-4.1989
G02	hsa-let-7c	-33.1285
G06	hsa-let-7f-5p	-72.0037
G07	hsa-miR-122-5p	-430.539
G10	hsa-miR-7-5p	-31.125
G11	hsa-miR-100-5p	-26.1729

Figure 1

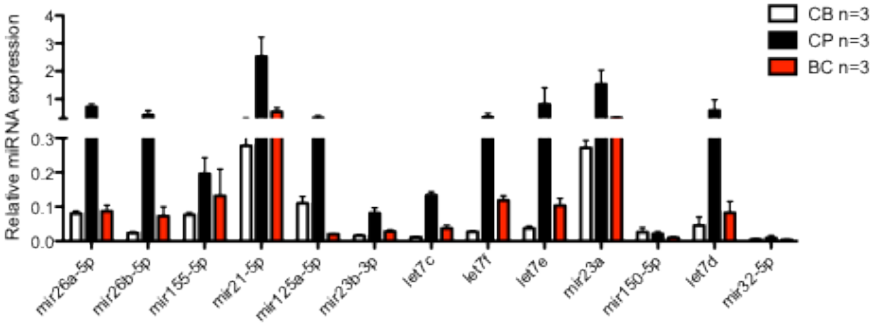

Figure 2

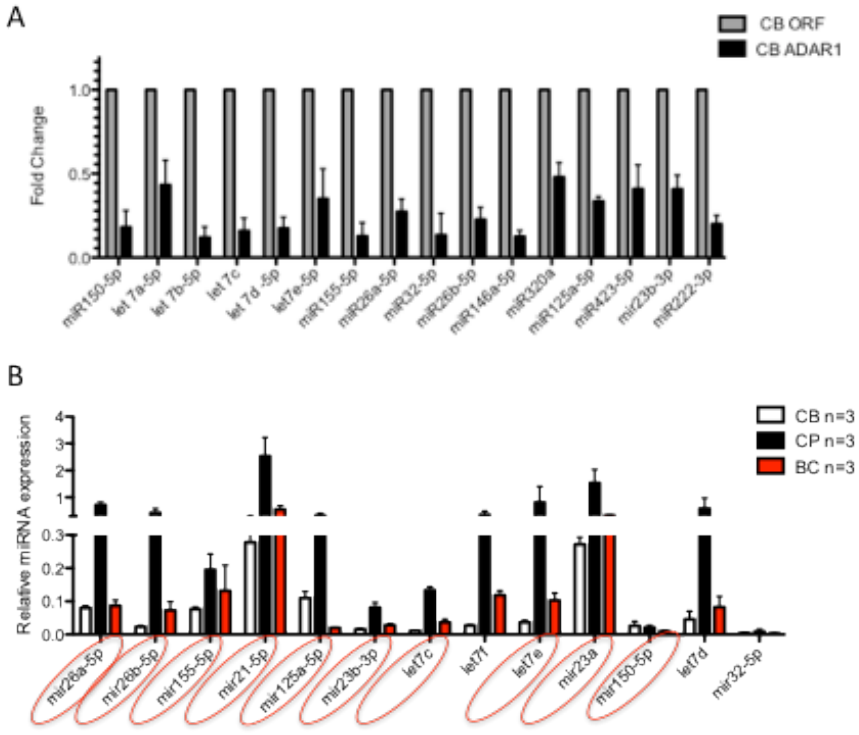

Figure 3

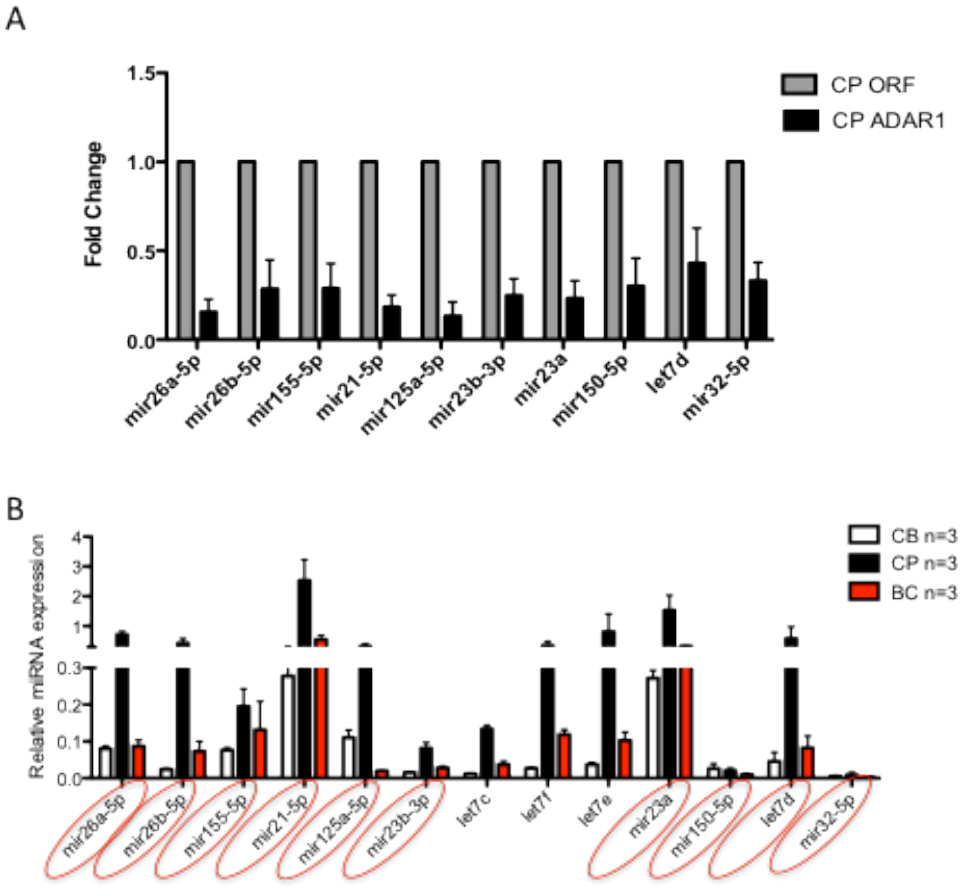
A
Fold Change
1.5
1.0
0.5
0.0
CP ORF
CP ADAR1
mir26a-5p
mir26b-5p
mir155-5p
mir21-5p
mir125a-5p
mir23b-3p
mir23a
mir150-5p
let7d
mir32-5p
B
Relative miRNA expression
CB n=3
CP n=3
BC n=3
mir26a-5p
mir26b-5p
mir155-5p
mir21-5p
mir125a-5p
mir23b-3p
let7c
let7f
let7e
mir23a
mir150-5p
let7d
mir32-5p

Figure 4

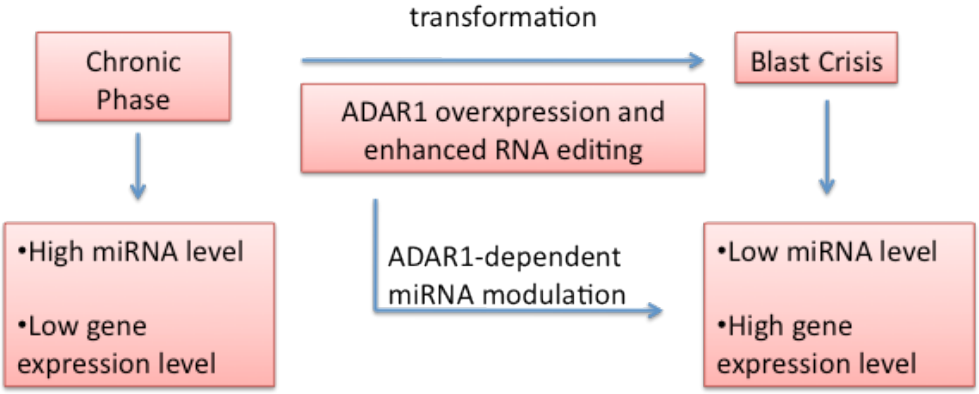
transformation
Chronic Phase
Blast Crisis
ADAR1 overxpression and enhanced RNA editing
•High miRNA level
•Low gene expression level
ADAR1-dependent miRNA modulation
•Low miRNA level
•High gene expression level

References

Bass, B. L. (2002). RNA editing by adenosine deaminases that act on RNA. *Annu Rev Biochem, 71*, 817-846. doi: 10.1146/annurev.biochem.71.110601.135501

Chen, Y., Siegel, F., Kipschull, S., Haas, B., Frohlich, H., Meister, G., & Pfeifer, A. (2013). miR-155 regulates differentiation of brown and beige adipocytes via a bistable circuit. *Nat Commun, 4*, 1769. doi: 10.1038/ncomms2742

Geron, I., Abrahamsson, A. E., Barroga, C. F., Kavalerchik, E., Gotlib, J., Hood, J. D., . . . Jamieson, C. H. (2008). Selective inhibition of JAK2-driven erythroid differentiation of polycythemia vera progenitors. *Cancer Cell, 13*(4), 321-330. doi: 10.1016/j.ccr.2008.02.017

Jiang, Q., Crews, L. A., Barrett, C. L., Chun, H. J., Court, A. C., Isquith, J. M., Jamieson, C. H. (2013). ADAR1 promotes malignant progenitor reprogramming in chronic myeloid leukemia. Proc Natl Acad Sci U S A, 110(3), 1041-1046. doi: 10.1073/pnas.1213021110

O'Hare, T., Zabriskie, M. S., Eiring, A. M., & Deininger, M. W. (2012). Pushing the limits of targeted therapy in chronic myeloid leukaemia. *Nat Rev Cancer, 12*(8), 513-526. doi: 10.1038/nrc3317

Tomaselli, S., Bonamassa, B., Alisi, A., Nobili, V., Locatelli, F., & Gallo, A. (2013). ADAR enzyme and miRNA story: a nucleotide that can make the difference. *Int J Mol Sci, 14*(11), 22796-22816. doi: 10.3390/ijms141122796

Yu, F., Yao, H., Zhu, P., Zhang, X., Pan, Q., Gong, C., . . . Song, E. (2007). let-7 regulates self renewal and tumorigenicity of breast cancer cells. *Cell*

Chapter 5

Molecular and Functional Characterization of Cells with Stem Properties Isolated by Sphere Forming Assay from Human Renal Cell CarcinomaTissues and Cell Lines

Maria Anna Zipeto[a,b], Silvia Bombelli[a], Qingfei Jiang[b],Leslie Crews[b], Vitalba Di Stefano[a], Barbara Torsello[a],Giorgio Bovo[c], Guido Strada[d], Cristina Bianchi[a], Catriona HM Jamieson[b] and Roberto A Perego[a]

Manuscript in Preparation

[a]Department of Health Sciences, University of Milano-Bicocca, Monza, Italy
[b]Department of Medicine, Stem Cell Program and Moores Cancer Center, University of California, San Diego, La Jolla, CA 92093, USA
[c]Anatomo-Pathology Unit, University of Milano-Bicocca, San Gerardo Hospital, Monza, Italy
[d]Urology Unit, Bassini ICP Hospital, Milano, Italy

Abstract

Cancer stem cells (CSC) are a rare subset of malignant cells that constitute a reservoir of tumor-initiating cells with the ability to both self-renew and differentiate into bulk tumors. As well as for other tumors, also in Renal Cell Carcinoma (RCC) the identification of CSCs might represent a step toward the development of therapies able to totally eradicate the disease. In the present study, cells with stem properties were identified from cultures of clonal tumor spheres obtained from RCC tissues after standardization of sphere-forming assay on RCC 786-0 cell line. Spheres obtained from the cell line and from RCC tissues were similar in term of phenotypic features, growth kinetics and sphere forming efficiency (SFE).

These spheres exhibited the expression of pluripotency genes as well as the activation of self-renewal pathways, when compared to the cultures representative of the bulk tumor population. Moreover they overexpressed the adenosine deaminase acting on RNA (ADAR1 and ADAR2) that might be involved in the regulation of self-renewal as demonstrated by the increase of SFE after overexpression in 786-0 cell line. When injected in immunocompromised mice, cells from spheres had a higher ability to give rise to tumor. Moreover tumor spheres from RCC tissues, as well as from 786-0, showed a heterogeneous composition, with different cell subpopulations, displaying diverse self-renewal ability. These subpopulations were identified on the basis of the different intensity of fluorescence of the PKH26 dye, able to discriminate quiescent cells within a proliferating

population. The ability to self-renew of the different PKH populations depended on the grading of the tumor. Although not distinguishing CSCs from the bulk tumor, surface marker expression in combination with PKH assay further confirmed the heterogeneity of cells within the spheres and allowed to identify an enrichment of $CD105^{+}$ and $CD133^{+}CD105^{+}$ cells in the self-renewing PKH^{high} population. In this study, by characterizing for the first time molecular pathways, such as Notch, JAK/STAT and RNA editing, that distinguish spheres, enriched in putative CSCs, from the bulk tumor, represented by primary cell cultures, we provided possible targets for new therapies that need to be further characterized in order to discern their role. Moreover, the combination of PKH assay and surface markers might be helpful for a better definition of the CSC population within RCC.

Introduction

Renal cell carcinoma (RCC) accounts for 3.8% of all malignancies in the adult and its incidency is annually increasing. With a male predominancy, it represents the seventh most common cancer in men and the ninth in women (Hollingsworth, 2006). According to Heidelberg classification it is possible to distinguish different histological RCC subtypes including from the most common, clear cell carcinoma (RCCcc), papillary (RCCp) and chromophobe (RCCc) (Kovacs, 1997). RCC is characterized by high metastatic index at diagnosis and high rate of relapse because of its resistance to both radio and chemotherapies. RCC is a tumor of unpredictable presentation and poor clinical outcome, despite the expansion of treatment possibilities that include tyrosine kinase inhibitors and mTor inhibitors (Hollingsworth, 2006). After the demonstration of the existence of a hierarchy within AML with at its apex cells with self-renewal and multilineage potential named cancer stem cells (CSCs) (Bonnet, 1997), several studies showed the presence of this cell subpopulation in several solid tumors, such as breast, brain, colon, pancreatic, prostate and ovary cancer (Al HAjii, 2003; Dalerba, 2007, Sing, 2004). As well as for other tumors, CSCs, with their resistance to therapies and their tumor initiating ability, may play a relevant role in the pathogenesis and prognosis of RCC. Only few studies have described the existence of CSCs in RCC by using different approaches for their isolation. Huang and colleagues recently showed the existence of a side population in769P RCC cell line capable of self-

renewal and differentiation (Huang, 2013). Side population studies allowed the identification of a renal CSC population in mice as well (Addla, 2008). Bussolati and colleagues demonstrated that only a 10% of the cells within human RCC, those expressing the mesenchymal marker CD105, could be serially transplanted and recapitulate the histological pattern of the primary tumor (Bussolati, 2008). Although these studies proved the existence of CSCs in RCC, a definitive selective marker for their isolation and targeting is still lacking, thus suggesting the necessity to further investigate this field. The sphere-formingassay allowsevidencing the self-renewal potential of CSCs. This assay has been already described as a functional approach to isolate and characterize normal and cancer stem cells from several tissues. The sphere-forming assay has been applied for the isolation of cells with stem properties from the RCC cell line SK-RC42 by Zhong (Zhong, 2010). No studies report the use of this assay for the identification and characterization of cells with stem properties from human RCC tissues. We have already established and characterized RCC primary cultures, able to maintain the phenotypic characteristics (Perego, 2005, Bianchi, 2010) and the genetic alterations (Cifola, 2011) of the primary tumors, and identified renal stem cells by using sphere forming assay (Bombelli, 2013). Moreover, by studying chronic myeloid leukemia stem cells (CML LSC), that represent an important paradigm for distinguishing the sequence and cellular framework of genetic and epigenetic events involved in the CSC production, we were able to identify novel regulators of self-renewal (Jiang, 2013) that might be responsible for the regulation of

CSCs in solid tumor as well, such as, for instance, RCC CSCs. Based on these premises, **the aim of this paper is to identify a population with stem properties within human RCC tissues by using the sphere forming assay establishing the method on RCC cell lines first.** Moreover, we aim to identify, by characterizing at a molecular level spheres from both RCC cell lines and tissues, the pathways that distinguish these cells from the bulk tumor and that could represent new therapeutic targets. We were able to identify cells with stem properties within human RCC cell lines and tissues and to discern developmental pathways that make them acquire hallmark of stemness. RCC spheres might represent a useful tool for the development of drugs targeted to pathways responsible for the stem phenotype and able to inhibit self-renewal potential of these cells.

Methods

Cell line and tissues

Human RCC cell lines were obtained from American Type Culture Collection (ATCC): 786-0, A498 and CAKI2 (ATTC) were derived from a primary renal cell carcinoma, CAKI-1 (ATTC) were derived from a metastatic lesion. 786-0 cells were cultured in adhesion in RPMI-1640 (Euroclone) medium supplemented with heat-inactivated (30'min, 56°C) 10% Fetal Bovine Serum (FBS) and 100 U/mL penicillin and 100 υg streptomycin (Euroclone). CAKI-1, CAKI-2, CAKI-1 cells were cultured in adhesion in DMEM Low Glucose (Euroclone) supplemented with heat-inactivated (30' min, 56°C) FBS (Euroclone)

and 100 U/mL penicillin and 100 υg streptomycin (Euroclone). Cells were grown in a humidified atmosphere at 5% CO2 at 37°C. RCC tissues were obtained after tumorectomy or nephrectomy from 44 patients. All procedures were performed after written consent from the patients and in accordance with recommendations of the Local Ethical committee.

Dissociation of RCC tissues, establishment of primary RCC tumor spheres and primary cell cultures and cell line cultures.

To obtain single cell suspension, human RCC tissues were mechanically and enzymatically dissociated as previously described (Bianchi, 2010). In order to obtain a single cell suspension, containing bulk tumor cells, the cells and the structures obtained after collagenase (type IV, Sigma-Aldrich) digestion were sieved through a 250 υm cell strained and subsequently passed through a pipette syringe. Red blood cells removal was performed by hemolysis with 0.8% NH4Cl solution. The single cell suspension was allowed to adhere for 24-48 h in SC medium composed of DMEM-F12 (Sigma-Aldrich), ITS supplement (5 υg/ml insulin, 5 υg/ml Transferrin, 5 ng/ml sodium selenite), 36 ng/ml Hydrocortisone, 40 pg/ml Triiodothyronine (all from Sigma Aldrich), 20 ng/ml EGF, 20 ng/ml bFGF (Tebu Bio). This passage in adherence was necessary to obtain a pure bulk tumor population by loosing all hematopoietic cells. In order to form floating spheres, 20000 cells from the bulk tumor were plated on a poly-Hema (Sigma-Aldrich) coated well of 6-well plates at a concentration of 10000 cells/ml with SC medium. The sphere

forming efficiency was calculated after 10-12 days as the ratio between the number of spheres obtained and the number of plated cells and expressed as percentage. Spheres were subsequently dissociated, first enzimatically by using TrypLE Express (Invitrogen) for 5 minutes and then mechanically by repetitive pipette syringing until single cell suspension was reached. The single cell suspension was used for further analysis or re-plated in the sphere forming conditions to obtain filial secondary tumor spheres. RCC differentiated primary cultures were used as control and obtained as described (Bianchi, 2010).

Cells from RCC 786-0, A498, CAKI-1 and CAKI-2 cell lines were trypsinized and passed through a pipette syringe to obtain a single cell suspension. 20000 cells from each cell line were plated in a well of 6-well plate at 10000 cells/ml density with SC medium on Poly-Hema coated dishes in non-adherent conditions for the formation of floating nephrospheres.

Clonality of spheres from cell line by single cell plating

In order to show that each sphere from cell lines is derived from a single cell and is therefore clonal, 786-0, A498 and CAKI-1 human cell line were serially diluted in SC medium and 1 cell/well was plated in each well of Poly-Hema coated 96-well plates in SC medium. After plating, each well containing a single cell was marked and the growth of the sphere was daily monitored by using the Olympus CK40

inverted phase-contrast microscope and images were acquired with Olympus Digital camera C-4040ZOOM.

PKH26 and PKH2 assays

The single cell suspension obtained by trypsinization of RCC epithelial cells after 24-48h of growth in adherence was stained for 5 minutes with either green PKH2 or red PKH26 dye (dilution 1:250; Sigma-Aldrich) according to the manufacturer's instructions and plated to obtain tumorspheres as described above. PKH-26 primary tumorspheres were dissociated and the obtained cell suspension was FACS sorted with a FACSAria flow cytometer (BD) on the basis of PKH fluorescence intensity at an average sorting rate of 500-1000 events per second at a sorting pressure of 20 psi with a 100 μm noozle. Three populations were identified on the basis of the PKH fluorescence intensity: a population with the highest PKH fluorescence (PKH^{high}), gated on the base of the sphere forming efficiency, another one with an intermediate fluorescence intensity (PKH^{low}) and the last one without any fluorescence (PKH^{neg}).

RNA extraction, cDNA synthesis and qPCR

Cells from RCC primary cultures and secondary tumorspheres established from 4 patients were collected in TRIZOL (Invitrogen) for total RNA extraction and 2 mg of cDNA were reverse transcribed with the High-Capacity cDNA Reverse Transcription Kit (Applied Byosistems). 100 ng of cDNA from each sample was loaded on each port of a TLDA card (Applied Biosystem) to perform the profiling of 96

genes included in TaqMan Human Stem Cell Pluripotency Panel Array (Applied Biosystems). PCR amplification was performed according to manufacturer's instructions using an ABI Prism 7900HT sequence detection system (Applied Biosystems). RNA extraction and cDNA reverse transcription were performed in both cells from adherent and spheres obtained from 786-0 cell line as previously described. Human specific primers for the following genes were designed to detect NOTCH1, NOTCH2, NOTCH3, NOTCH4, JAGGED 1, JAGGED 2, DLL1, DLL 3, DLL4, HES1, JAK2, STAT1, STAT3, STAT5, MCL1L, MCL1S, BCL2L, BCL2S, BFL1L, BFL1S, BCLXL,BCLXS, CYCLIN D1, CYCLIN D3, CYCLIN E1, MDM2, CDKN1A, ADAR1, ADAR2in both 786-0 spheres and monolayer and primary (Supplemental Table 1)RCC tumor spheres and primary cultures (Supplemental Table 1). qRT-PCR was performed in duplicate on iCycler using SYBR GreenER Super Mix (Invitrogen), 5 ng of template mRNA, and 0.4 mM of each forward and reverse primer. β-Actin and 18S mRNA transcript levels were used to normalize each gene. The ΔCt value was calculated as the difference between the average of the Ct value of the target gene and the average Ct value of the housekeeping gene used as control. The expression fold change between primary cultures and tumor spheres was calculated as $2^{-\Delta\Delta Ct}$ by dividing $2^{-\Delta Ct}$ of the target gene in the tumor spheres by the $2^{-\Delta Ct}$ of the same gene in the corresponding primary cultures used as calibrator and put equal to 1. For TLDA analysis, after exclusion of all the genes that did not show expression in at least 2 samples, the statistical analysis were performed on 42

out of 96 genes. The ΔCt value of the 42 analyzed genes were plotted on a heat map using TIGR Multiple Experiment Viewer (TMEV) and clusterized on the basis of the samples. Statistic was performed on the $2^{-\Delta Ct}$ values and $p<0.05$ was considered significant.

microRNA extraction and qRT-PCR

Cells from 786-0 spheres and monolayer were collected in buffer RLT (Qiagen) and RNA was extracted by RNeasy microKit (Qiagen). cDNA was prepared in a reverse-transcription reaction using miScript RTII kit (Qiagen) and served as a template to profile the expression of the 84 most abundantly expressed and best characterized miRNAs by using miScript miRNA PCR array (Qiagen), which contain miRNA specific miScript primer assays. qRT-PCR was performed by using miScript SYBR green kit (Qiagen). qRT-PCR with specific miScript primers detecting the mature miRNA (Qiagen) was performed to validate the miRNA resulted differentially expressed from the array. RNU_6 and SNORD-44 were used as housekeeping miRNA.

Subcutaneous xenotransplantation in immuno-deficient mice

Preliminary animal experiments were conducted in agreement with the stipulations of the local Animal Care and Use Committee. RCC tumorspheres were collectecd by centrifugation at 1300 rpm for 10 minutes and enzimatically and mechanically dissociated by respectively TrypleX (Invitrogen) and a syringe. Cells from bulk tumor primary cultures were trypsinized. The cells were divided into two

groups: cells from dissociated tumor spheres and cells from primary cultures and five nude mice were used. 100 μl of cell suspension composed of cells in SC media and Matrigel (ratio 1:1) were injected subcutaneously in each mouse with different cell numbers $1x10^6$, $1x10^5$, $1x10^4$, $1x10^3$, $1x10^2$. Masses could be observed after 1 week and their size was weekly measured. Tumor volume was calculated as $(width)^2$ x length/2 and expressed in mm^3.

Lentiviral production and transduction

Fluorescent ubiquitination-based cell cycle indicator (FUCCI) constructs were developed as previously described (Sakaue-Sawano, 2011) and kindly donated by Atsushi Miyawaki. The constructs expressing mCherry-hCdt1(30/120) and mVenus-hGem(1/110) were respectively named FUCCI-R and FUCCI-M. For lentivirus production, $20x10^6$ human embryonic kidney 293T cell lines were plated on poly-Lisine coated T175 flasks for 24 hours in order to reach 80% confluence by the following day. The second day, co-transfection of either FUCCI-R or FUCCI-M vector and the three helper vectors pVSVG, pREV and pMDL was performed by using Lipofectamine2000 (Invitrogen). After 8 hours of incubation, fresh DMEM supplemented with 10% FBS was replaced to bypass lipofectamine toxicity. Culture media was collected and replaced with fresh media every day for the following three days. After the third day of collection, collected media was centrifuged by Optima L-80 XP Ultracentrifuge at 4°C for 2 hours at 19500 rpm, maximum acceleration and deceleration. The virus was re-suspended and stored in StemPro Media at -80°C. The

titer was determined by infecting 293T cells with several dilutions of the virus (Multiplicity on infection (MOI) approximately 100) and by analyzing the GFP+ cells by FACS after 48 h. 786-0 cells underwent two rounds of lentiviral transduction with both lenti-FUCCI-R and lenti-FUCCI-M at a MOI of 20. 50000 cells were transduced with lenti-FUCCI-R and expanded. mCherry fluorescent cells were sorted with a FacsAria (Beckton Dickinson) and subsequently transduced with lenti-FUCCI-M with a MOI of 20. After expansion, cells were sorted on the basis of m-Venus fluorescence by FACSAria (BD), thus obtaining the double transduced population FUCCI-RM. Confocal and time lapse images were taken using a computer-assisted Olympus Fluoview FV10i fluorescence microscope (Olympus America, Center Valley, PA). For time lapse imaging, cells were plated into 35mm, 14mm microwell with no. 1.5 coverglass (0.16-0.19mm) poly-Hema (Sigma-Aldrich) coated culture dishes (MatTek Corporation, Ashland, MA). Images were taken at 5 minute intervals, for varied amounts of time no less than 24 hours to ensure documentation of cell division.

Lentiviral vector plasmids expressing ADAR1 or GFP-expressing backbone were purchased from Open Bioscience (Thermo Fisher) and lentiviruses production was performed as described above. 786-0 cells were trasnduced with lenti-ADAR1 with a MOI of 20. Enforced expression of ADAR1 was analyzed by qRT-PCR. Lenti ADAR1 conferred approximately two- to three fold higher expression than endogenous human ADAR1 level.

One-dimensional electrophoresis and Western blotting

Cells from primary cultures and RCC tumor spheres were lysed at 4˚C in buffer containing 50 mM Tris pH 7.4, 1% Nonidet P40, 0.25% Deoxycholate, 150 mM NaCl, 1 mM EDTA, Protease inhibitor Cocktail and Phosphatase Inhibitor Cocktail 1 and 2 (Sigma-Aldrich) and subjected to nuclear lysis in ice by sonic treatment for 3 s at 30 W with a probe-sonicator Vibra Cell (Sonics Materials) in order to get the total homogenate. The concentration of extracted proteins was quantified with BCA microassay (Sigma-Aldrich). Equal amounts of protein were separated on NuPage 4% to 12% pre-cast gels (Invitrogen) and analyzed by Western Blot as described before (Bianchi, 2013). Mouse monoclonal antibodies against HIF-1α (dilution 1:500, clone 54, Becton Dickinson), OCT4 (dilution 1:70, clone 40/Oct-3, Becton Dikinson), HIF2α (dilution 1:500, clone ep190b, Novus Biologicals) were used to detect protein of interest. Rabbit polyclonal antibody against β-actin (dilution 1:1000, Sigma-Aldrich) was used to normalize protein levels.

Aldefluor Assay

Cell derived from RCC primary cultures and RCC dissociated spheres were stained with ALDEFLUOR™ reagent from the ALDEFLUOR™ assay kit (Stem Cell Technologies, Vancouver, BC, Canada) according to the manufacturer's protocol. Briefly, cells from RCC primary cultures and dissociated RCC spheres were resuspendend in ALDEFLUOR™ buffer containing 1υM/10^6 cells ALDH substrate and incubated for 45 minutes at 37°C. Negative control was obtained by

incubating a sample of cells from each condition with 50 mM of specific ALDH inhibitor diethylaminobenzaldheyde (DEAB) and was used to set the gates. FACS analyses were performed on a FACSCanto (BD).

FACS analysis

After dissociation of tumor spheres, cells were washed with PBS and incubated for 15 minutes with PBS supplemented with 5% heat inactivated calf serum to block non-specific sites. Cells were subsequently stained with the specific antibody appropriately diluted. We used all monoclonal antibody produced in mouse: FITC-CD24 (20 µl, Biolegend), APC-CD133 (10 µl, Miltenyi Biotech), FITC-CD105 (10 µl, R&D). FACS analysis was performed with a FACSCAnto instrument and FACSDiva software; the acquisition was stopped when the population gated reached 20000 events.

Cell cycle FACS analysis of FUCCI-transduced 786-0 cell line

FUCCI-RM transduced 786-0 adherent cultures and dissociated spheres were washed with PBS and the expression of either mVenus or mCherry was analyzed by FACSCanto. Cells were gated on the basis of the fluorochromes signals as described: $mCherry^{+}mVenus^{-}$ represented the G1 population, $mCherry^{+}mVenus^{+}$ the G1/S transiting cells, $mCherry^{-}mVenus^{-}$ the G0 and $mCherry^{-}mVenus^{+}$ the G2 fraction.

Statistical analysis

Statistical differences were analyzed by unpaired two-tail Student's t-test and the significance was set for $p < 0.5$

Results

Establishment and clonality of spheres from human RCC cell lines and primary tumors

To determine whether a subpopulation of self-renewing cells exists within cultured human RCC cell lines, 4 different cell lines, CAKI-1, CAKI-2, A498 and 786-0 were grown at low density with defined serum-free medium in non-adherent conditions. After 3 days, spheres appeared from CAKI-1, A498 and 786-0 but not from CAKI-2 (Fig.1A) reaching their maximum size at 10 days. As previously described for mammospheres (Dontu, 2003) and for adult renal stem cells (Bombelli, 2013) these culture conditions lead most of the cells to apoptosis, thus selecting for only a small number of cells that can survive and grow as spheres. Spheres from the different cell lines showed similar sizes as well as comparable sphere forming efficiencies SFE (Fig. 1B). Comparable SFE were observed after dissociation and re-plating of cells, thus suggesting that cells were able to self-renew (data not shown). In order to prove that spheres from cell lines originated from a single cell and could be defined clonal, cells were stained before plating with either PKH2 (green) or PKH26 (red) and subsequently mixed and plated together. Since spheres from these cell lines appeared to be sticky with a high

tendency to form aggregates, this experiment did not allow us to determine their clonality (Fig.1C). On the opposite, by plating single cells through serial dilutions into poly-Hema coated 96 well plates in SC medium, we were able to show that CAKI-1, A498 and 786-0 gave rise to clonal spheres (FIG.1D).3 out of 4 RCC tested cell lines contain a population of cells able to give rise to clonal spheres that can be propagated for different passages.

Establishment, growth properties and clonalty of tumorspheres from primary human RCC.

According to the sphere-forming assay protocol, RCC cells were grown in non-adherent conditions, at low density in SC medium (Fig.2A). 34 out of 44 RCC (77,2%), gave rise to spheres that could be observed in 10-12 days of culture in sphere-forming conditions. These spheres were constantly and reproducibily composed of 133 ± 33 (Mean ± SD) cells. Moreover they could be dissociated and replated to form filial spheres up to a maximum of 5 times and maintained in culture for a maximum of 2 months (Supplementary table 2). We verified the clonal origin of primary tumor spheres by staining cells with either green PKH2 or red PKH26 and then plating together a mix of these cells. Since we never observed the contemporary existence of red and green cells within the same sphere (Fig.2B) we showed that our spheres were not just cell aggregates, but originated from a single cell instead. Analysis of growth properties of 4 different RCC spheres showed a significant decrease in SFE during the second passage to then significantly

increase again in most of the samples in the third passage. This behavior, might show that sphere-composing cells can alternate asymmetric and symmetric division thus modulating the number of stem cells within the spheres (Fig.2C).

Molecular characterization of pathways involved in the regulation of self-renewal in 786-0 RCC cell line

Due to the genotipic and functional similarities with primary patient samples (Jiang, 2003) 786-0 cell line was chosen to undergo further characterization as well as to screen molecular pathways that might be responsible for self-renewal, as already described for other models (Alison, 2012). In order to better characterize at a molecular level tumor spheres from 786-0, we evaluated by qRT-PCR the expression of 28 genes in spheres from 786-0 obtained by performing sphere forming assay in 3 different times and compared them to their corresponding monolayer cultures. Genes of interest were chosen on the base of evidences and reported in literature showing their involvement in the regulation of self-renewal pathways. Among them, some members of Notch pathway, genes involved in the regulation of cell-cycle and asymmetric division, members of the JAK/STAT pathway, as well as ADAR1. qRT-PCR analysis showed the overexpression of two Notch receptors (Notch1 and Notch2), and two Notch ligands (JAGGED2 and DLL3) in 786-0 tumorspheres compared to the corresponding monolayer cultures. Moreover, STAT3, but not its upstream regulator JAK2, resulted to be overexpressed in 786-0 compared to the monolayer, thus suggesting

that an activation of this pathway may occurr in a JAK2 independent manner. Spheres from 786-0 did also overexpressed the prosurvival gene MCL1L as well as the inhibitor of the cell cycle progression CDKN1A. Although we did not observe a significant transcriptional upregulation of Notch targets, such as for example Hes1, we cannot exclude an activation of Notch pathway, since CDKN1A and CYCLIN D, both overexpressed in the spheres, have been described as Notch targets in cancer (Borggrefe, 2008).

Moreover, we observed a statistically significant upregulation of the RNA editing enzymes ADAR1 and ADAR2. Notably RNA editing enzymes expression levels are generally low in bulk tumor, in comparison with normal tissues (Paz, 2007), thus suggesting that the enhanced expression of these enzymes is a peculiarity of cells with stem properties within the tumor. These data together showed that spheres from 786-0 modulate the expression of genes involved in the regulation of self-renewal, survival and cell division in comparison with the monolayer, and might represent a useful tool for the identification of putative pathways that might be involved in the regulation of self-renewal in spheres from primary RCC (Fig.3).

Spheres from 786-0 show differential expression of putative ADARs miRNA target compared to the monolayer cultures

Since we observed a statistically significant upregulation of both ADAR1 and ADAR2 in 786-0 spheres compared to their corresponding primary cultures we investigated whether the enhanced RNA editing

activity might affect the regulation of microRNA. It has already been demonstrated that ADAR enzymes, by editing primary and precursor microRNA, can modulate the levels of mature miRNAs by affecting the maturation process. Suggestion of the effect of ADAR1 on miRNA levels comes also from our study in the leukemia stem cells model. To identify differentially expressed miRNAs we performed miSCRIPT miRNA qPCR array on both spheres and monolayer from 786-0. Array analysis showed the statistically significant upregulation of anti-apoptotic miRNAs, and the downregulation of 7 miRNAs including members of the let-7 family of reprogramming miRNAs and miRNAs involved in the regulation of self-renewal (Data not shown). To validate some of these miRNA, we performed single qRT-PCR analyses by using specific primers in both 786-0 spheres and monolayer from three different experiments. We did not observe any significance difference in the expression of let-7 family miRNA between speheres and monolayer. On the contrary, 3 miRNA were confirmed to be statistically modulated: miR-155-5p resulted upregulated, while miR-376-3p and miR-7-5p resulted downregulated (Fig.4). Notably both miR376-3p and miR-7-5p can be target of RNA editing by ADAR2, thus suggesting that the modulation of miRNA we observed could depend on the enhanced expression of RNA editing enzymes.

RCC primary tumorspheres overexpress pluripotency and self-renewal regulators genes

In order to better characterize at a molecular level spheres obtained from primary RCC samples and to validate the differentially expressed genes observed in 786-0 tumor spheres, we evaluated gene expression in tumor sphere cells obtained from 4 different patients and their corresponding differentiated tumor primary cultures, considered as a mirror of the bulk tumor population. The expression of 96 genes of a Stem Cell pluripotency Panel (Applied Biosystems), as well as the Notch, Jak/STAT, RNA editing and cell cycle genes was evaluated by qRT-PCR. Only 42 genes out of the 96 in the Panel were expressed in the tumor samples. The remaining genes, mainly specifically involved in the differentiation into a non-renal lineages were excluded from the analysis. We observed the overexpression of 5 genes out of the 42 analyzed in primary RCC tumor spheres compared to their primary cultures. Among them, we found 3 genes, GABRB3, NANOG and OCT4 that have been classified as markers for maintenance of pluripotency (Fig.5A). By performing cluster analysis on gene expression we observed that most of the RCC primary cultures clustered distinctly from RCC spheres (Fig. 5B).

Specific qRT-PCR performed to validate the genes differentially expressed in the cell lines showed that Notch1 receptor and JAGGED1 ligand were upregulated in the spheres compared to the corresponding primary cultures, thus showing that, in agreement with what shown in 786-0 spheres, some member of Notch pathway

are overexpressed in primary RCC tumorspheres. Moreover, we observed the overexpression of both STAT3 and STAT5, as well as their upstream regulator JAK2 and the cell cycle regulator CDKN1A. As well as for 786-0 spheres, in RCC tumor spheres we could not observe the upregulation of Notch targets such as Hes1. However, we cannot exclude the activation of Notch due to the overexpression of CDKN1A, which has been shown to be a transcriptional target of Notch (Borgrrefe, 2009). The upregulation of these genes suggest the activation of pathways of self-renewal and an aberrant regulation of the cell-cycle where CDKN1A overexpression has been shown to be important in non-renal CSCs for the regulation of DNA damage repair necessary to maintain the expanding pool of CSCs (Viale, 2009). Interestingly, differently from 786-0 spheres, RCC tumor spheres overexpress only one of the RNA editing enzymes, ADAR2 (Fig.5C). Taken together these data showed that primary RCC spheres contain cells that overexpress pluripotency genes, as well as genes involved in the regulation of self-renewal and cell cycle regulation. Moreover, these data suggest that 786-0 tumor spheres represent a good starting model for the study of cells with stem properties in RCC, since several consistencies have been found between the two models.

RCC primary spheres overexpress Hif2α and OCT4 at a protein level

Since Hif2α and Hif1α are not only key genes in RCC but have also been shown to be master regulators of stemness and HIf2α is a direct upstream regulator of OCT4 (Covello, 2006), we performed western

blot analysis to evaluate its expression levels in spheres compared to their corresponding primary cultures. Moreover, we analyzed the protein level of OCT4, to evaluate whether this gene was overexpressed both at a transcriptional and a protein level. Western blot analysis performed on primary spheres and corresponding primary cultures showed that spheres overexpressed both Hif1α and Hif2α compared to their primary cultures. 786-0 cells have been used as a positive control. However, we observed an overexpression of HIf2α also in the spheres from 786-0 compared to their monoloayers (Data not shown). Moreover, we could observe the overexpression of OCT4 in the primary sphere population, thus confirming the data already observed in the transcriptomic analysis (Fig.6). These results suggested that althoug constituitvely active in RCC, Hif1α and Hif2α seem to be even more expressed in spheres compared to their corresponding primary cultures, thus suggesting that they regulate stemness. Moreover, as already described in literature, also in our model the overexpression of HIF2α is combined with the overexpression of OCT4.

Lentiviral overexpression of ADAR1 increase sphere forming efficiency of 786-0 cell line.

In order to evaluate whether ADAR1 overexpression could affect sphere forming efficiency 786-0 cells were transduced with either lenti-ADAR1 or control vector (ORF) and cells were sorted on the base of GFP signal. ADAR1 overexpressing cells were plated in sphere forming conditions and SFE was calculated. ADAR1 overexpressing

cells formed spheres with a statistically significant higher SFE compared to the control vector (Fig.7). These data suggest that ADAR1 might be involved in the regulation of self-renewal in 786-0.

Fluorescent ubiquitination cell cycle indicator allows the spatiotemporal visualization of tumor spheres growth.

After undergoing two different transduction rounds, we obtained a stably transduced FUCCI-RM cell line that allowed the visualization of cell cycle changes and cell division in spheres as described in fig.8A. Imaging analysis showed that most of the cells within the spheres were in G1 phase and dividing cells were localized on the outer side of the spheres. Imaging data were further confirmed by FACS analyses that showed that most of the cells within the spheres were in G1, while only a smaller portion was in G2/M or G0 phase. 786-0 cells grown as monolayers and used for a comparison showed the presence of cells in all the phases of the cell cycle (Fig.8B)

In order to visualize how spheres were growing we performed a Z-Stack/Time lapse imaging for 24 h, taking pictures every 5 minutes. By analyzing different layers it was possible to observe that spheres undergo growth by replication of cells localized on the outer part of the spheres, as shown by the arrow in the picture (Fig.8C). Due to the necessity to undergo two rounds of transduction, it was not possible to obtain stably transduced FUCCI-RM RCC primary cells to monitor their growth.

Cells with different self-renewal abilities coexist within the spheres

In order to evaluate whether eventual quiescent cells exist within the spheres, cells were stained before plating with the lypophilic dye PKH26 and subsequently allowed to grow in sphere-forming conditions. PKH26 is a lypophilic dye that stains the plasma membrane and it is progressively diluted at each cell division the cells undergo to. PKH26 labeled cells that are actively replicating and undergo several cell division rounds, dilute the dye and thus show a less intense epifluorescence. On the opposite, more quiescent PKH26-labeled cells retain the dye and appear more epifluorescent. PKH26 has been shown to be an effective approach for the definition of cell cycle properties within spheres, since it allows to discriminate between quiescent and more actively replicating cells in different models. In both 786-0 spheres (Fig.S1) and our RCC tumor spheres obtained from primary samples, only few cells within the spheres showed a strong epifluorescence, suggesting that only a small percentage of the cells within the spheres were quiescent (Fig.9A). FACS analyses performed on cells obtained from dissociated spheres allowed us to identify three different populations on the basis of PKH26 epifluorescence intensity. The population with the strongest epifluorescence, that represented about the 1% of the whole primary RCC sphere forming cells, on the basis of the calculated SFE, was named PKH^{high}, the one with intermediate epifluorescence, 60-70% of the total, was named PKH^{low}, while the one with the least or none epifluorescence was named PKH^{neg}. The identification of these three different populations as well as our previous experience on spheres

from normal kidney (Bombelli, 2013) brought us to evaluate whether all the PKH populations showed similar self-renewal capability or not. The three PKH26 subpopulations sorted from primary tumor spheres or 786-0 spheres were plated in non-adherent conditions at low density (10000 cells/well) in 12 well plates coated with Poly-Hema. 10-12 days after plating both PKH^{high} and PKH^{low} cells from 786-0 spheres were able to form filial spheres (Fig S1). In spheres obtained from primary RCC, instead, we did observe two different behaviors: either only PKH^{high} cells or both PKH^{high} and PKH^{low} cells were able to form secondary filial spheres. In order to better understand the reason why primary samples did behave in different way, we stratified the samples on the basis of clinical features. We observed that, among the 4 experiment performed, in spheres deriving from two G1 RCC patients only the PKH^{high} population was able to form spheres, while in those derived from two G2 RCC patients both PKH^{high} and PKH^{low} populations gave rise to secondary filial tumor spheres (Fig.9B). These observations suggested that depending on tumor grading, cells could undergo asymmetric and symmetric division at a different extent. This result might also suggest that higher grade tumors contain a higher percentage of cells able to divide symmetrically compared to lower grade tumors.

ALDH activity does not distinguish RCC primary tumor spheres from their corresponding primary cultures

ALDH activity has been recently proposed as a stemness marker in both normal and cancer stem cells from several tissues. Moreover,

we have recently shown that spheres obtained from adult kidney have a higher ALDH activity compared to their corresponding primary cultures. In order to understand whether this marker can be applied to RCC tumor spheres as well, we performed FACS analysis to compare ALDH activity in tumor spheres and primary cultures. Our data showed that there are no differences in the % of cells with high ALDH activity level between RCC tumor spheres and primary cultures (Fig.10 A and B). Since we did observe a percentage of cells with higher ALDH activity, although very low, we evaluated whether those cells represented the more quiescent PKH^{high} population. We observed that cells with high levels of ALDH activity were randomly distributed between the different PKH populations (Data not shown) Taken together, these data showed that ALDH activity does not allow neither to discriminate tumor spheres from primary cultures, but nor to functionally distinguish different PKH populations.

PKH populations express potential CSC markers at different levels

Surface markers have been extensively used, with already described limitations, for discriminating cancer stem cells from the bulk tumor. In order to evaluate whether our spheres had different marker expression profiles, we performed FACS analysis of the expression levels of CD133 and CD105 in both spheres from 786-0 and RCC and their corresponding monolayers and primary cultures. We could not observe enrichment in the expression of stem markers in spheres from 786-0 cell line compared to the monolayer (Fig. S2 A and B). A similar trend was observed in RCC tissues were we observed that

these markers were not able to distinguish RCC tumor spheres from their corresponding primary cultures (Fig.11A). However, based on the observation that PKH populations have different self-renewal potential, we better characterized the phenotype of each population by evaluating the expression of the same markers. The evaluation of the surface markers expression level in the different PKH populations in spheres from 786-0 cell line, showed that both $CD133^{+}CD105^{-}$ and $CD133^{-}CD105^{+}$ cells were enriched in the PKH^{high} population, compared to the PKH^{low} and PKH^{neg}. Notably, there were no $CD133^{+}CD105^{+}$ cells and no differences were observed in the enrichment for $CD133^{-}CD105^{-}$ cells among the three different populations (Fig.S2 C and D). FACS analysis on spheres from RCC tissues showed a statistically significant enrichment of $CD133^{+}CD105^{+}$ in PKH^{high} population compared to both PKH^{low} and PKH^{neg}. A same trend was observed in the $CD133^{-}CD105^{+}$ population that was statistically significant enriched in PKH^{high} population in comparison to both PKH^{low} and PKH^{neg}. On the opposite, $CD133^{-}CD105^{-}$ cells were enriched in PKH^{neg} cells and decreasing in the PKH^{low} up until reaching the minimum in PKH^{high}, although not in a significant way (Fig. 11B and C). These analysis showed that the PKH^{high} population is characterized by the expression of CD105 and CD133 markers, while the PKH^{low} population seems to appear more heterogeneous. These findings, may suggest that depending on the extent of $CD105^{+}$ cells PKH^{low} can have different self-renewal potential.

Xenograft

To evaluate whether sphere forming assay enriched for cells not only with enhanced stem properties but also with a higher tumorigenic potential, we performed a preliminary xenograft assay, that is considered the gold standard for the definition of CSC population. Cells from both primary tumors and primary RCC tumor spheres were subcutaneously injected in combination with Matrigel respectively into each flanks of nude mice. As shown in the growth curve, few days after the injection a visible mass started to show up in the mouse injected with $1x10^6$ cells on the sphere side, but not on the primary culture. On the opposite, a mass could be observed in the same mouse on the primary culture side only after 6 weeks and when the mass from the spheres has already almost reached 1 cm diameter. These preliminary data showed that at least $1x10^6$ cells from the whole spheres are able to give rise to tumors that arise already few days after the injection and grow fast enough to reach 1 cm diameter within 7 weeks (Supplementary table 3). On the opposite the same number of cells from the primary cultures require a longer time to develop a tumor (Fig.12). Due to logistic problems, we were not able to recover tumors and thus check their histological features.

Discussion

Several studies have investigated the existence of renal cancer stem cells, by exploiting different approaches, such as surface marker

expression (Bussolati, 2008), Hoechst exclusion (Addla, 2008; Huang, 2013) and the sphere-forming assay (Zhong, 2010). However, although these studies demonstrated the existence of CSCs within RCC, a definitive marker for their identification is still lacking.

In this study, we characterized at a molecular and functional level cells with stem properties obtained from RCC tissues, after having established the sphere-forming assay on RCC cell lines. Although this assay has already been employed for the isolation of cells with stem properties from the human RCC cell line SK-RC-42 (Zhong, 2010), we adapted it to primary human RCC tissues for the first time, starting from our experience in the establishment of nephrosphere cultures from normal adult kidney (Bombelli, 2013). We were able to obtain tumor spheres from 3 out of 4 RCC cell line tested. Out of these, we decided to exclude from any further characterization CAKI-1, since it was derived from a metastatic site and A498, since less similar to primary tumors compared to 786-0 that represented our model for the establishment of the method. Concerning human RCC tissues, it is interesting to note that although we obtained tumor spheres with a high percentage of success, not all the tumors were able to give rise to spheres. This difference might be due to technical problems or to genetic or cellular issues we were not able to define; anyway this phenomenon has been already described for other solid tumors (Ponti et al. Cancer Res 2005). However, we demonstrated that tumor spheres obtained from both RCC cell lines and tissues were of clonal origin, thus originating from a single cell. Morever, RCC tumor spheres could be propagated for several passages and maintained in culture for up to six months. Differently from normal nephrospheres

(Bombelli, 2013) the number of spheres among the different passages was not constant, thus suggesting that the self-renewal capability might be a mutating property of sphere composing cells by modulating the number of cells with stem properties within the spheres by alternating symmetric and asymmetric divisions. Since one of the feature that defines stem cells is the ability of self-renewal, in this study we characterized self-renewal both at a molecular level, by evaluating pathways involved in its regulation, and at a functional level by the PKH assay.

Since tumor cells are known to appropriate normal cellular mechanisms for growth, survival and proliferation, no large leap of faith is required to hypothesize that embryonic signaling pathways are critical to these same processes for maintenance, proliferation and quiescence in the CSC population (Miele, 2009). In our study, the comparison between tumor spheres and primary cell cultures derived from the bulk tumors represents a crucial step for understanding mechanisms regulating stem cell self-renewal that could be targeted by therapies. For this reason, the well-characterized primary RCC cultures, established in our laboratory and that have previously been shown to be able to maintain both the phenotypical characteristics (Perego, 2005; Bianchi, 2010) and the genetic alterations (Cifola, 2011) of primary samples, represent a useful model resembling the bulk tumor. The screening of molecular pathways involved in the self-renewal regulations in 786-0 spheres brought us to a preliminary identification of several genes, from diverse pathways upregulated respect to their corresponding monolayer cultures. The same pathways were upregulated in the spheres from RCC tissues, although we observed some differences in the differentially

expressed specific genes. Among these we evidenced the upregulation of some members of the Notch pathway in spheres from both 786-0 and RCC tissues compared with their corresponding monolayer cultures. Notch pathway has been shown to be involved in CSC population maintenance in breast cancer (Korkaya, 2007) and in the carcinogenesis of RCC (Liu, 2013). Although we did not observe the transcriptional upregulation of Notch target Hes1 and Hes2, we can still hypothesize its activation because of the upregulation of its targets Cyclin D1 (Cohen, 2010) and CDKN1A (Rangarajan, 2001) in spheres compared to their monolayer cultures. The upregulation of CDKN1A in both spheres from 786-0 and RCC tissues suggests that, similarly to the leukemia stem cell model (Viale, 2009), CDKN1A, by protecting CSCs from the accumulation of DNA damage, might prevent the exhaustion of their pool in RCC and could be targeted by therapy. Moreover, we observed the upregulation of STAT3 in both spheres from 786-0 and RCC tissues although its direct upstream activator, JAK2, was upregulated only in spheres from RCC tissues. We can thus hypothesize a JAK2 independent activation in 786-0, probably mediated by Notch (Kamakura, 2004). Since it has been shown that inhibition of STAT3 increases the sensitivity to therapy in RCC (Xin 2009), its upregulation in sphere population might suggest that spheres are enriched for a population resistant to the therapy that could be of clinical relevance. On the opposite, no specific roles for STAT5 in RCC have been identified yet, but several evidences from other models showed its involvment in CSCs maintenance (Kato, 2005; Bristschgi, 2013).

The identification in chronic myeloid leukemia (CML) of the Adenosine Deaminase Acting on RNA (ADAR1) as a new regulator of

self-renewal (Jiang, 2013) led us to investigate whether genes of the ADAR family were differentially expressed in spheres compared to the monolayer cultures representative of the bulk tumor. Although RNA editing is generally lower in tumors compared to normal tissues (Paz, 2007), tumor spheres from both 786-0 and RCC tissues showed a significant high expression of respectively both ADAR1 and ADAR2, or ADAR2 alone, thus suggesting that the activation of RNA editing might be a peculiar feature of stem cells within the whole tumor population. Moreover, the increase in the sphere forming efficiency of 786-0 spheres after lentiviral-enforced expression of ADAR1, suggests a role for this enzyme in the regulation of the self-renewal in this model. However, the fact that not ADAR1, but ADAR2 is upregulated in spheres from RCC tissues, might suggest that these enzymes act differently in liquid and solid tumor CSCs. Although no studies evaluated the expression of ADAR2 in CSCs population, it has been shown that ADAR2 leads to the upregulation of CDKN1A in glioblastoma (Galeano, 2012) thus suggesting a role for ADAR2 in the maintenance of a CSCs pool in RCC. Together with changes in the gene expression profile, we observed differentially expressed miRNA between 786-0 spheres and corresponding monolayers. Among them miR-7, that targets the pluripotency factor Kruppel-like factor 4 (Okuda, 2013), was statistically significant downregulated, suggesting that it might be responsible for enhanced pluripotency in the spheres. Emerging evidence shows that 20% of miRNA are edited, thus suggesting a role for ADARs in the regulation of microRNA expression and targeting mechanism. Interestingly, both miR-7 and miR-376a, that were downregulated in the spheres, have been described as ADAR2 targets (Heale, 2009), thus suggesting that

ADAR2 might regulate CSCs by affecting the expression of miRNA involved in pluripotency regulation. Further confirmation of enhanced pluripotency in the spheres came from array analysis showing the overexpression of the pluripotency genes NANOG and OCT4 in RCC tumor spheres. In particular, OCT4 overexpression, also observed at a protein level, might be driven by enhanced expression of HIF2α, which has been shown to be involved in the induction of a stem cell phenotype, by regulating OCT4 and Notch pathway (Gustaffson, 2005). A further functional characterization of these pathways will lead to the identification of targets for cancer stem cell-targeted therapies. A characterization of cell cycle properties and self-renewal capabilities of spheres came respectively from studies with the Fluorescent-ubiquitination based cell cycle indicator (FUCCI) and the PKH assay. By establishing a stable FUCCI cell line, that allows to monitor in real-time cell cycle progression (Sakaue-Sawano, 2007), we were indeed able to show for the first time in real time that most of the cells within the spheres were in G1, while only few cells were actually dividing and were localized on the outer side of the sphere. These observations suggested that, after a certain number of divisions, most of the cells stop dividing by blocking in G1, while only on the outer part few cells keep dividing, thus increasing the spheres size. Moreover, by Z-stack analysis we identified G0 quiescent cell in the inner part of the spheres. These observations suggest that within the spheres only few cells, localized in the middle of the spheres, are in G0 phase, while most of the cells after an unidentified number of divisions block in G1 phase. The necessity to undergo two rounds of transduction did not allow us to repeat this experiment in spheres from human RCC, but the establishment of a bicistronic vector will

allow us to monitor the cell cycle in spheres from primary samples too. However, we were still able to identify cells with different division properties within the spheres by the PKH assay. In this study we demonstrated that depending on the tumor grade, PKH^{high} population alone or both PKH^{high} and PKH^{low}were able to self-renew, while PKH^{neg} were not. It is interesting to highlight that in G1 grade tumors, where the cellular composition shows a high level of differentiation, only the PKH^{high} population has the ability to self-renew, while in G2 grade tumors, that are more de-differentiated at a cellular level, both PKH^{low} and PKH^{high} population give rise to spheres. This result led us to the hypothesis that a different balance between asymmetrical and symmetric division might be responsible for broader self-renewal ability in higher-grade tumors. Moreover, the phenotypic characterization of our spheres showed that PKH^{high} cells are enriched in both cells expressing CD105 and CD105/CD133. CD105 has already been described as a marker for renal CSC (Bussolati, 2008), while CD133 has been shown to characterize non-tumorigenic cells that can differentiate into endothelial or epithelial cell, thus supporting the tumor growth (Bruno, 2006). It is interesting to note that within the sphere population both $CD133^{+}$ and $CD105^{+}$ cells coexist, thus suggesting that spheres might represent a niche for the cancer stem cells, thus providing not only the tumorigenic cells, but also the supportive cells able to sustain the tumor growth. Moreover, thanks to the combination of PKH assay and surface markers, we were able to identify for the first time a $PKH^{high}/CD105^{+}/CD133^{+}$ population that have never been described before and might represent a previously unidentified tumorigenic population within the tumor, whose tumorigenicity has not been

defined yet. The experience with normal nephrospheres (Bombelli, 2013), where the combination of PKH assay and surface marker expression led to the identification of a pure population of renal stem cells, suggest to further investigate the tumorigenic potential of all the PKH/markers combination. Our preliminary xenograft data, showed that cells from spheres present a higher ability to engraft in vivo, compared to the corresponding primary cultures. However, the minimum number required to give rise to a mass is still too high to define them CSCs. This high number might be affected by the fact that cells from the whole sphere were injected.

Our study demonstrated the existence of cells with stem properties, able to self-renew, within spheres obtained from both RCC cell lines and tissues. Moreover we provided a series of putative candidate regulators of self-renewal that could represent targets for new CSCs targeted therapies. However, a further functional characterization of the mechanism and the role of these genes in RCC spheres will be necessary in order to define their role in the regulation of self-renewal. Moreover, the study with the PKH allowed us to show that the extent of cells with self-renewal ability within a tumor might depend on its grading. A further characterization of this aspect, together with the definition of the role of each PKH cell population in the spheres, will allow us to identify the CSC population, as well as to define the molecular mechanisms that could be responsible for therapeutic resistance and relapse. Finally, the establishment of stable FUCCI spheres from RCC tissues will represent a useful tool for the screening of new molecules and compounds that might be employed in the development of new therapies for RCC.

Figure legend

Figure 1: Sphere forming assay in RCC cell lines; A: Representative image of the spheres obtained from the RCC cell lines; B: All the three cell lines showed a similar SFE; C: Representative image of spheres obtained after staining the cells with PKH2 or PKH26 and plating mixing them together; D: Phase-contrast micrographs of spheres generated from single-cell cultures of CAKI-1, A498 and 786-0.

Figure 2: Sphere forming assay in human RCC samples. A: Representative phase contrast picture of RCC tumor spheres B: Proof of RCC tumor spherese clonality; Tumor spheres obtained from cells labeled with PKH26 alone, PKH2 alone and spheres obtained after plating a mix of cells previously stained with either PKH26 or PKH2; C: Growth properties of tumor spheres: the curve was obtained by plotting the number of spheres vs the passages in 3 different patient samples. At each passage tumor spheres were dissociated and replated at a density of 20000 cells/well. The continuous line represents the average.

Figure 3: Expression level of genes involved in the regulation of cell-cycle and self-renewal in spheres from 786-0 in comparison with their corresponding monolayer cultures. The data are plotted as $2^{-\Delta\Delta Ct}$ and represent the fold change between the spheres and the monolayer used as control and considered equal to 1. Statistically significant differences, are marked with a star. The error bars represent the standard error of the mean.

Figure 4: Expression levels of miRNA in 786-0 spheres compared to their corresponding primary cultures. The data are plotted as $2^{-\Delta\Delta Ct}$ and represent the fold change between the spheres and the monolayer used as control and considered equal to 1. Statistically significant differences are marked with a star. Error bars represent the standard error of the mean.

Figure 5: Stem cell TaqMan Low Density Array Panel and evaluation of self-renewal pathways; A: Statistically overexpressed genes in RCC spheres (RCCs) compared to their corresponding primary culture (RCCpc). B TMEV heat map showing the 42 genes analyzed; samples were clusterized on the basis of the ΔCt values: green genes correspond to lowest ΔCt values and the highest expression levels; red genes correspon to highest ΔCt values and lower expression levels; C: Expression levels of genes involved in the regulation of the self-renewal and cell-cycle. The data are plotted as $2^{-\Delta\Delta Ct}$ and represent the fold change between the spheres and the monolayer used as control and considered equal to 1. Statistically significant differences with $p<0.05$ are marked with a blue star, the one with $p<0.01$ with a red star. The error bars represent the standard error of the mean.

Figure 6: Western Blot analyses. Overexpression of HIF1α, HIF2α and OCT4 in spheres (RCCs) compared to their primary cultures (RCCpc). Protein expression level was calculated as OD vs OD of β-Actin used as housekeeping gene.

Figure 7: Effect of ADAR1 lentiviral overexpression on sphere forming efficiency. The difference in the SFE was considered significant when $p \leq 0.01$. Error bars represent the standar error of the mean, calculated on the basis of 3 experiments.

Figure 8: Cell cycle analyses by Fluorescent ubiquitination-based cell cycle indicator (FUCCI); A: Schematic representation of FUCCI mechanism: cells assume the same color of the fluorochrome associated to a specific phase of the cell cycle: red during G1 phase, orange during G1/S transition, greenin phases S/G2/M and colorless during G0 phase; B: comparison between abundance of populations in each phases of the cell cycle in spheres from 786-0 and corresponding monolayer culture: FACS data were expressed as % of cells per each cell cycle phase C: photograms of time lapse confocal analysis on FUCCI-RM spheres from 786-0: the first row of pictures shows the sequence of a cell division, the second row shows the switch of a cell from G2 phase (green) to cell division and finally G0 (colorless).

Figure 9: Identification of quiescent cells and evaluation of self-renewal potential of cells within the spheres; A: Distribution of PKH26 dye; B: Typical FACS plot obtained after dissociation of RCC tumor spheres: cells can be gated in three different population on the base of PKH26 fluorescence intensity. The PKH^{low} population ability to form filial spheres might correlate with the tumor grade.

Figure 10: Evaluation of ALDH activity in RCC tumor spehres. A: Representative FACS analyses of RCC tumor spheres (RCCs) and RCC primary cultures (RCCpc) after Aldefluor assay. Autofluorescent cells were gated out by adding the specific inhibitor DEAB (left column); B: There is no enrichment in ALDH+ cells in RCC tumor spheres compared to their corresponding primary cultures and the differences observed are not significant. The error bars represent the standard error of the mean.

Figure 11: Evaluation of expression of stem cell markers in RCC tumor spheres. A: Representative FACS analysis of the expression of stem cells markers CD133 and CD105 in RCC tumor spheres (RCCs) compared to their corresponding primary cultures (RCCpc). B: Representative FACS analysis of expression of stem cell markers in different PKH populations; C: Enrichment of cells expressing stem cell markers in the single PKH population: the percentage of cells expressing a specific combination of markers in each PKH population was normalized on the percentage of cells expressing the same specific markers combination in the total sphere.derived cells. P value lower or equal to 0.05 were considered statistically significant. The error bars represent the standard error of the mean.

Figure 12: Growth curve of tumors obtained from the xenografts of RCC primary cultures (RCCpc) and RCC spheres (RCCs).

Supplemental figure 1: Identification of quiescent cells and evaluation of self-renewal potential of cells within 786-0 spheres.

Typical FACS plot obtained after dissociation of RCC tumor spheres: cells can be gated in three different populations on the base of PKH26 fluorescence intensity and sorting of 786-0 PKH populations.

Supplemental figure 2: Expression of stem cell markers in 786-0. A: FACS analyses of marker expression in 786-0 monolayer and spheres. B: expression of stem cell markers in 786-0 monolayers and spheres C: FACS analyses of stem cell markers expression in PKH population D: Enrichment of cells expressing specific markers combination in different population PKH compared to the total population.

Figure 1

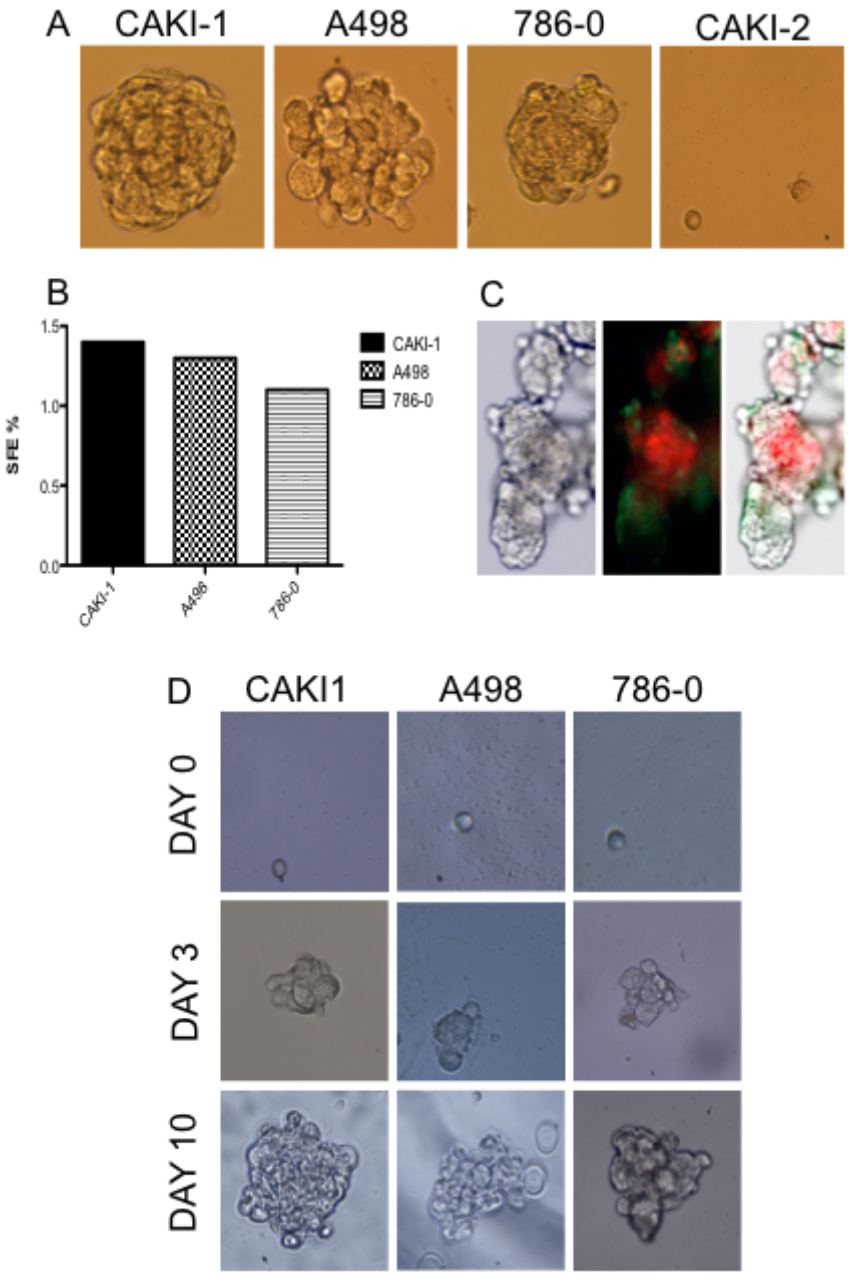
A
CAKI-1
A498
786-0
CAKI-2
B
SFE %
1.5
1.0
0.5
0.0
CAKI-1
A498
786-0
C
D
CAKI1
A498
786-0
DAY 0
DAY 3
DAY 10

Figure 2

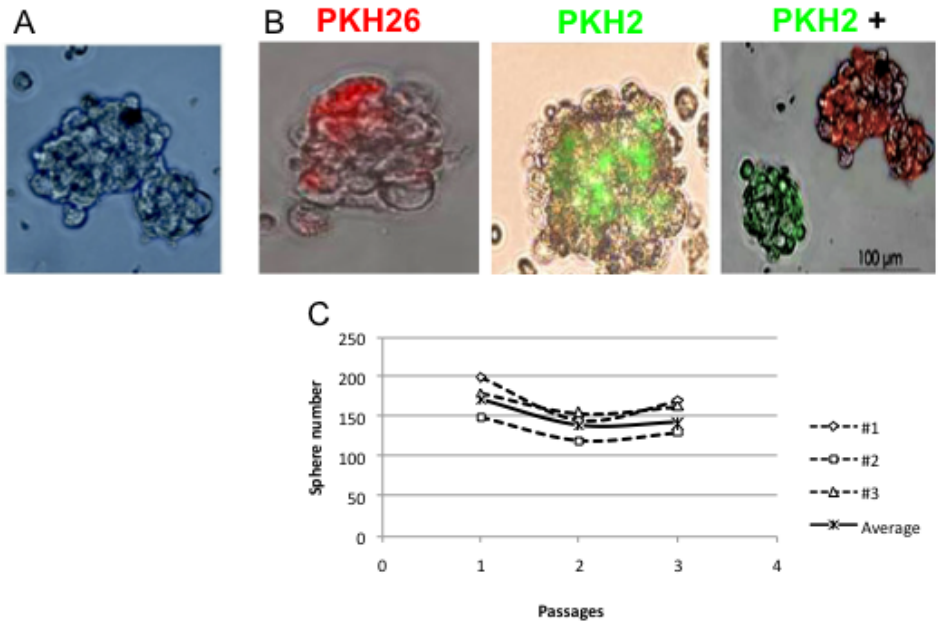

Figure 3

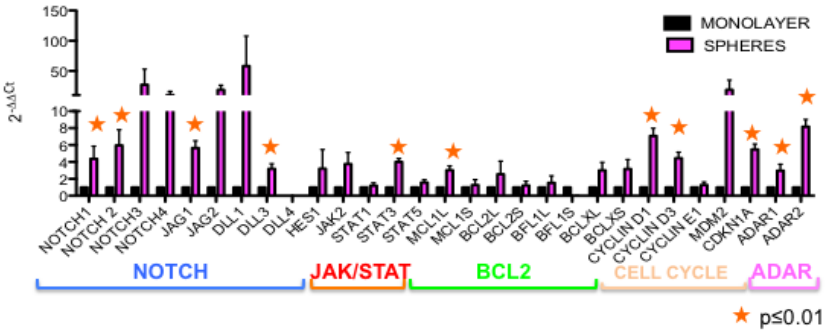

Figure 4

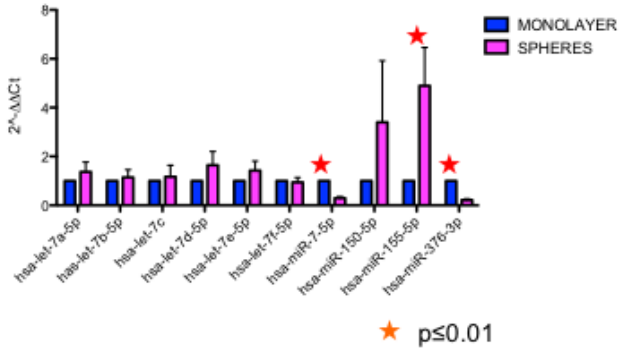

Figure 5

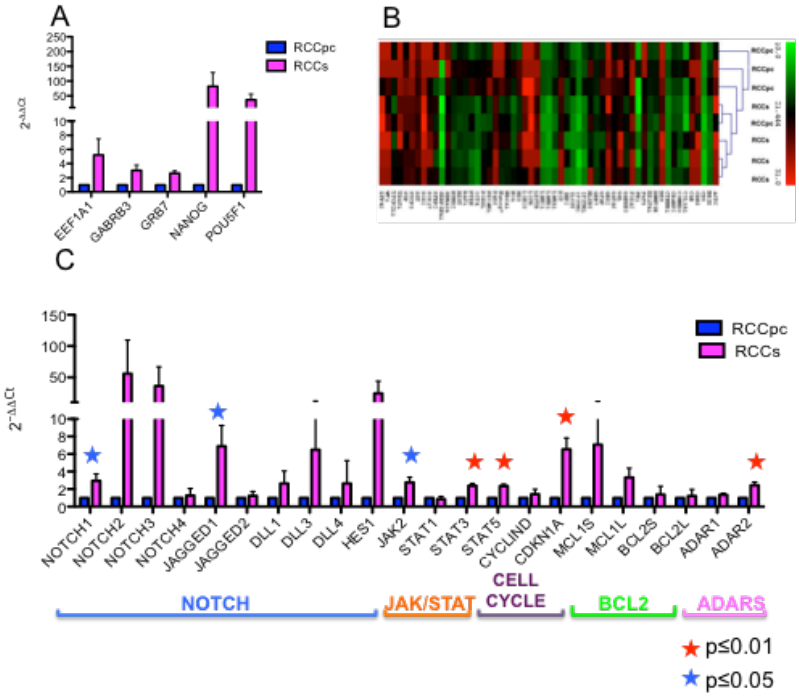

Figure 6

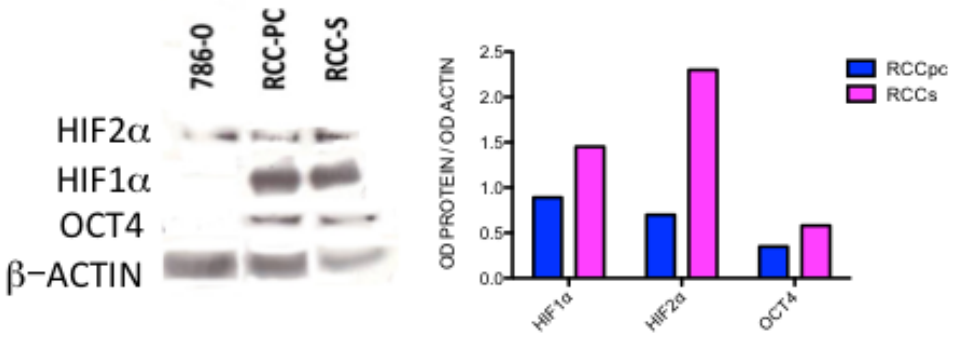

Figure 7

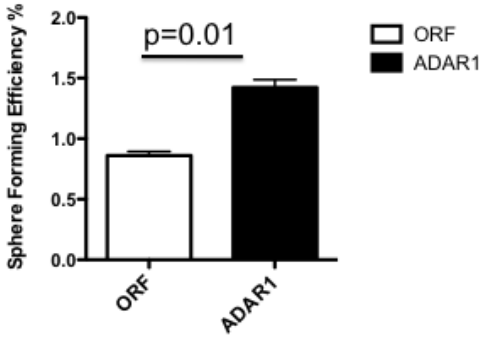

Figure 8

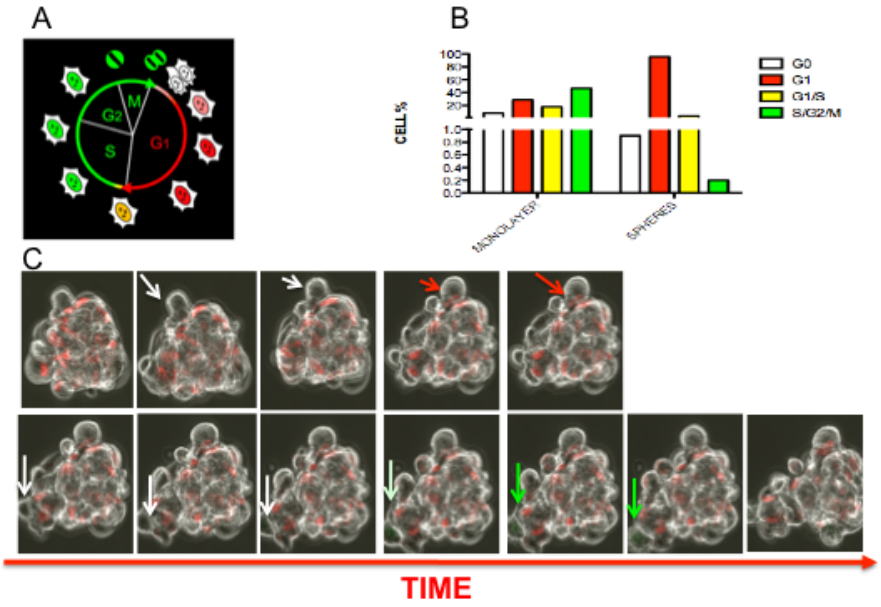

Figure 9

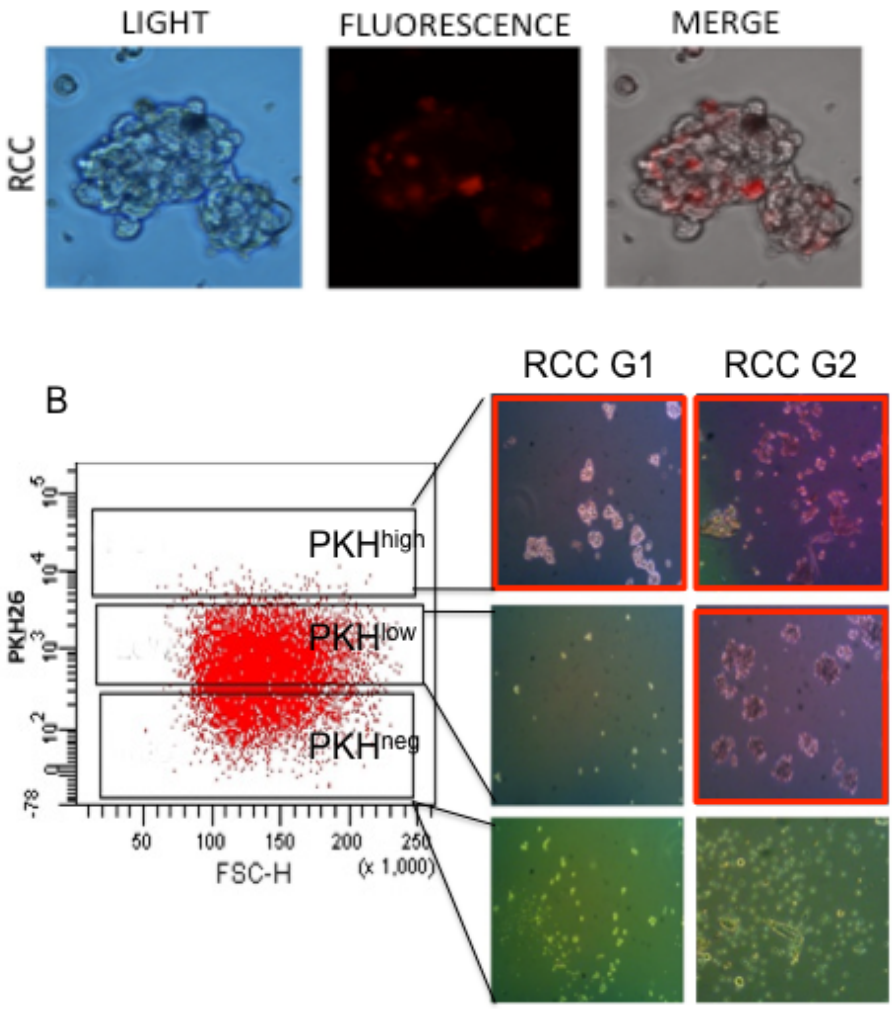
LIGHT
FLUORESCENCE
MERGE
RCC
B
RCC G1
RCC G2
PKH26
PKHhigh
PKHlow
PKHneg
FSC-H
(x 1,000)

Figure 10

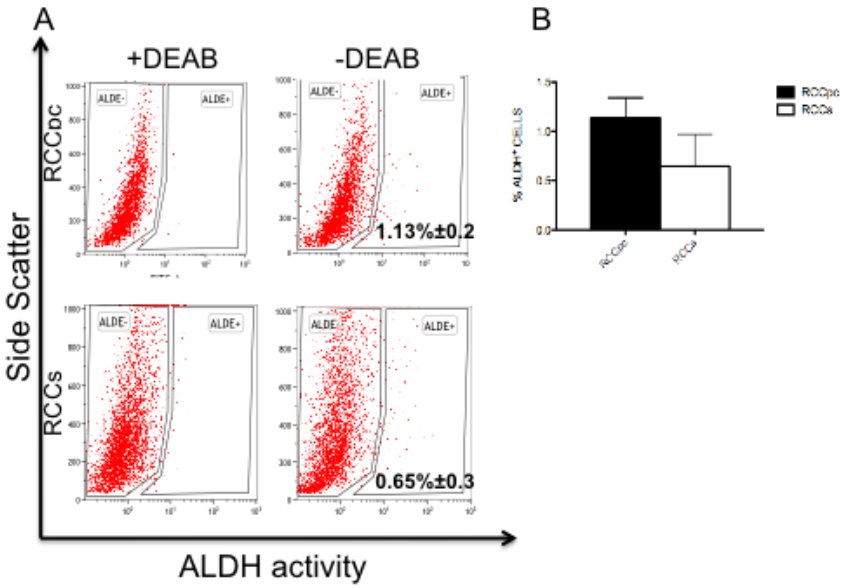
A
+DEAB
-DEAB
RCCpc
RCCs
ALDE-
ALDE+
1.13%±0.2
0.65%±0.3
Side Scatter
ALDH activity
B
RCCpc
RCCs

Figure 11

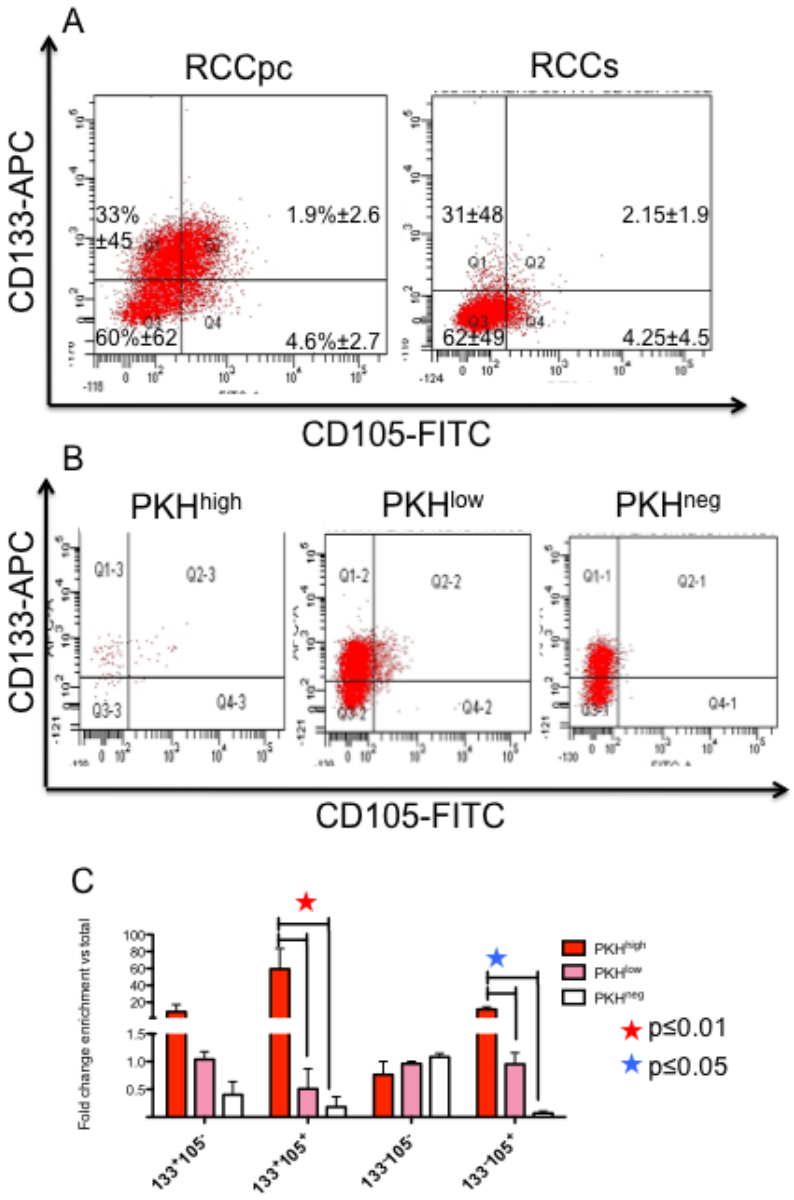
A
RCCpc
RCCs
CD133-APC
CD105-FITC
33%
±45
1.9%±2.6
60%±62
4.6%±2.7
31±48
2.15±1.9
62±49
4.25±4.5
B
PKHhigh
PKHlow
PKHneg
Q1-3
Q2-3
Q3-3
Q4-3
Q1-2
Q2-2
Q4-2
Q1-1
Q2-1
Q4-1
C
Fold change enrichment vs total
PKHhigh
PKHlow
PKHneg
p≤0.01
p≤0.05
133+105-
133+105+
133-105-
133-105+

Figure 12

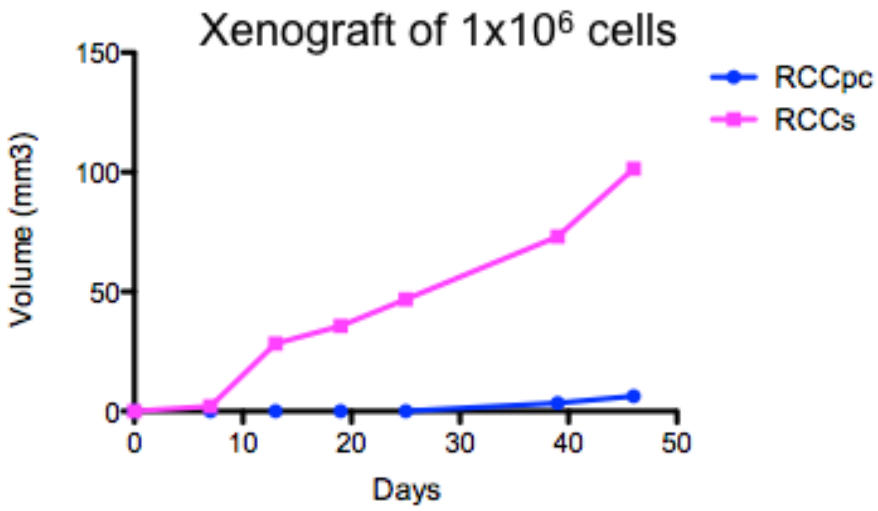

Supplemental Figure 1

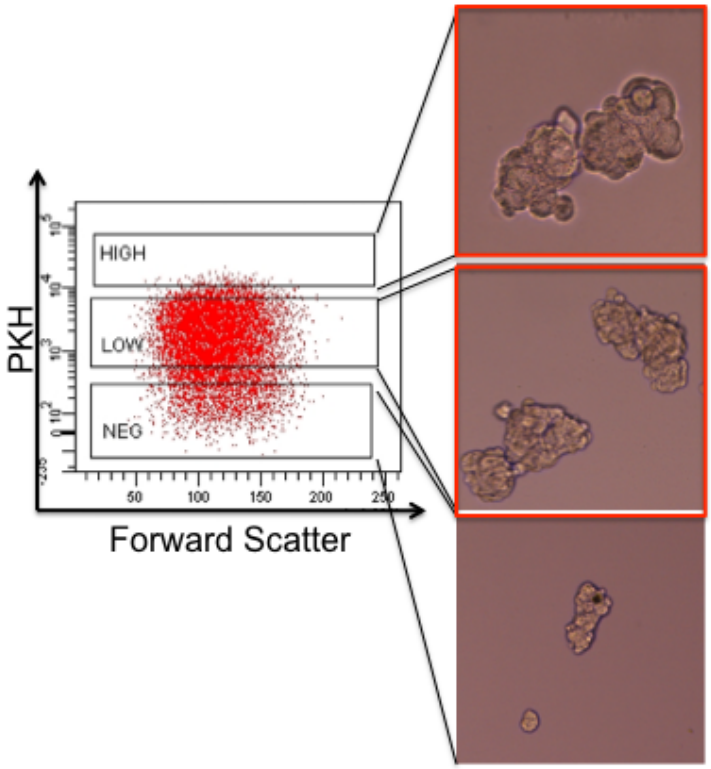

Supplemental Figure 2

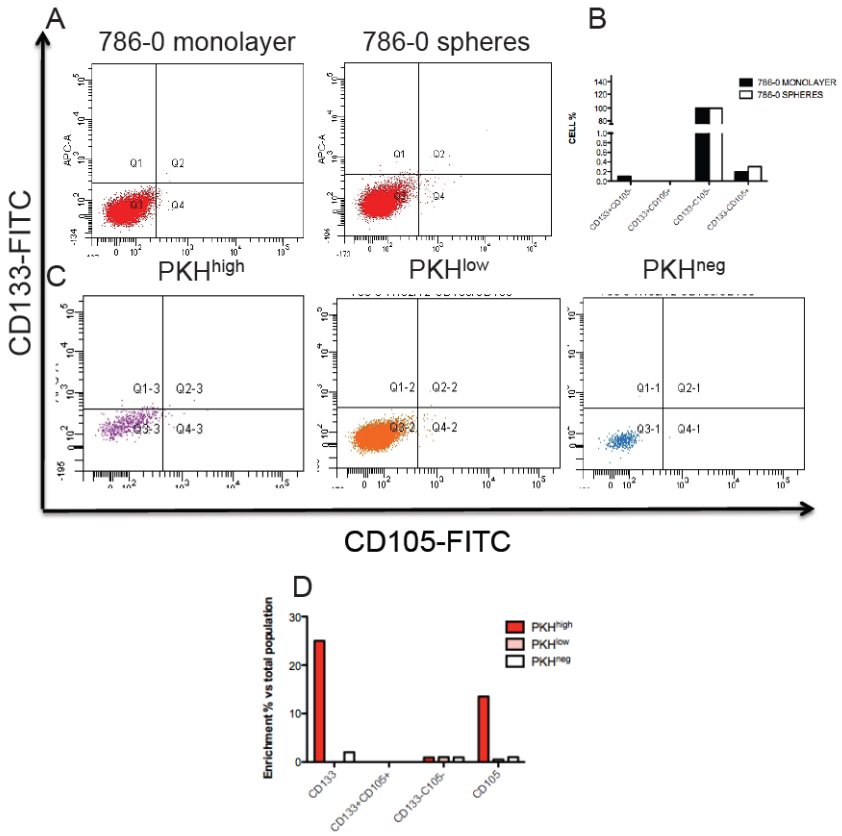

Supplemental Table 1-Primer list

GENE	FORWARD PRIMER 5'-3'	REVERSE PRIMER 5'-3'
ADAR1	TGCTGCTGAATTCAAGTTGG	TCGTTCTCCCCAATCAAGAC
ADAR2	TGTTCCGTGTGTGTCCAGTT	CGGCAGGTCAGAGTTTTCTC
β ACTIN	AGGCACCAGGGCGTGAT	GCCCACATAGGAATCCTTCTGAC
BCL2S	ATGTGTGTGGAGAGCGTCAA	CTCAGCCCAGACTCACATCA
BCL2L	ATGTGTGTGGAGAGCGTCAA	TTCAGAGACAGCCAGGAGAAA
BCLXS	CTTTGAACAGGATACTTTTGTGGAA	GGATGTGGTGGAGCAGAGAA
BCLXL	CATGGCAGCAGTAAAGCAAG	GAAGGAGAAAAAGGCCACAA
BFL1L	GCTGGGAAAATGGCTTTG	TCAGAAAAATTAGGCCGGTTT
BFL1S	CGGATGTGGATACCTATAAGGAGA	CTTCTTGTGGGCCACTGACT
CDKN1A	ATGAAATTCACCTTTCC	AGGTGAGGGGACTCCAAAGT
CYCLIN D1	TGTCCCACTCCTACGATAGC	CCATTAGAAAACTGCCCTCC
CYCLIN D3	AGTTGCGGGACTGGGAGG	GTGGCGATCATGGATGGC
CYCLIND	AACTACCTGGACGCGCTTCCT	CCACTTGAGCTTGTTCACCA
CYCLIN E1	GTTTCAGGGTATCAGTGGTG	GTGGGTCTGTATGTTGTGTG
DLL1	CGTCATAGCAACTGAGGTGTAA	CCTCTTCAGCAGCATTCGT
DLL3	GTCCGAGCTCGTCCGTA	TACCTCCCGAGCGTAGATG
DLL4	AACTGCCCTTCAATTTCACCT	GCTGGTTTGCTCATCCAATAA
HES1	ATGGAGAAAAATTCCTCGTCCC	TTCAGAGCATCCAAAATCAGTGT
HPRT1	TCAGGGATTTGAATCATGTTTGTG	CGATGTCAATAGGACTCCAGATG
JAGGED1	CCCGATCAAGGAAATCACTGAC	CTCAGCAAGGGAACAAGGAAA
JAGGED2	GGTGGTATCGTTGTCCCAGT	CATGGGCTATTTCGAGCTG
MCL1S	GAGGAGGACGAGTTGTACCG	ACTCCACAAACCCATCCTTG
MCL1L	AGACCTTACGACGGGTTGG	AATCCTGCCCCAGTTTGTTA
MDM2	GGTGGGAGTGATCAAAAGGA	ACACAGAGCCAGGCTTTCAT
NOTCH1	CCAGAGTGGACAGGTCAGTA	TGACACACACGCAGTTGTAG
NOTCH2	TGCCAGTACTCAACATCTCATC	TGGCACTCCTTACCTGTAAAC
NOTCH3	CAGGACATGGCGAGGAGTA	CTGGGAACAGACAAGGGAAG
NOTCH4	AACTCCTCCCCAGGAATCTG	CCTCCATCCAGCAGAGGTT
STAT1	AATAGAGTTGCTGAATGTCACT	AGCTGATCCAAGCAAGCATT
STAT3	CCGGAAGAGAGTGCAGGATC	TTCTGCCTGGTCACTGACTG
STAT5	CCTGTGGAACCTGAAACCAT	GGCGGTCAGGAAACACATAG

Supplemental Table 2-Growth characteristics of RCC tumor spheres.

	SFE : n° spheres/ n° plated cells (%)					
	Primary spheres	Secondary spheres	Tertiary spheres	n° cells/sphere	Maximum passages	% of success
RCC	1 ± 0,4	0,89 ± 0,61	0,59 ± 0,15	132 ± 33	5	35/45 (77%)

Supplemental Table 3-Tumor engraftment in nude mice

MOUSE		cell #	mm³ DAY 0	mm³ DAY 7	mm³ DAY 13	mm³ DAY 19	mm³ DAY 25	mm³ DAY 39	mm³ DAY 46
1	PCC	1000000	0	0	0	0	0	3,43	6,3
	NS	1000000	0	2	28,25	35,71	46,82	73,1	101,4
2	PCC	100000	0	0	0	0	0	0	0
	NS	100000	0	0	0	0	0	0	0
3	PCC	10000	0	0	0	0	0	0	0
	NS	10000	0	0	0	0	0	0	0
4	PCC	1000	0	0	0	0	0	0	0
	NS	1000	0	0	0	0	0	0	0
5	PCC	100	0	0	0	0	0	0	0
	NS	100	0	0	0	5,29	5,31	0	0

References

Addla, S. K., M. D. Brown, C. A. Hart, V. A. Ramani and N. W. Clarke (2008). "Characterization of the Hoechst 33342 side population from normal and malignant human renal epithelial cells." Am J Physiol Renal Physiol**295**(3): F680-687.

Al-Hajj, M., M. S. Wicha, A. Benito-Hernandez, S. J. Morrison and M. F. Clarke (2003). "Prospective identification of tumorigenic breast cancer cells." Proc Natl Acad Sci U S A**100**(7): 3983-3988.

Alison, M. R., W. R. Lin, S. M. Lim and L. J. Nicholson (2012). "Cancer stem cells: in the line of fire." Cancer Treat Rev**38**(6): 589-598.

Bianchi, C., S. Bombelli, F. Raimondo, B. Torsello, V. Angeloni, S. Ferrero, V. Di Stefano, C. Chinello, I. Cifola, L. Invernizzi, P. Brambilla, F. Magni, M. Pitto, G. Zanetti, P. Mocarelli and R. A. Perego (2010). "Primary cell cultures from human renal cortex and renal-cell carcinoma evidence a differential expression of two spliced isoforms of Annexin A3." Am J Pathol**176**(4): 1660-1670.

Bombelli, S., M. A. Zipeto, B. Torsello, G. Bovo, V. Di Stefano, C. Bugarin, P. Zordan, P. Vigano, G. Cattoretti, G. Strada, C. Bianchi and R. A. Perego (2013). "PKH(high) cells within clonal human nephrospheres provide a purified adult renal stem cell population." Stem Cell Res**11**(3): 1163-1177.

Borggrefe, T. and F. Oswald (2009). "The Notch signaling pathway: transcriptional regulation at Notch target genes." Cell Mol Life Sci**66**(10): 1631-1646.

Britschgi, A., T. Radimerski and M. Bentires-Alj (2013). "Targeting PI3K, HER2

and the IL-8/JAK2 axis in metastatic breast cancer: which combination makes the whole greater than the sum of its parts?" Drug Resist Updat**16**(3-5): 68-72.

Bruno, S., B. Bussolati, C. Grange, F. Collino, M. E. Graziano, U. Ferrando and G. Camussi (2006). "CD133+ renal progenitor cells contribute to tumor angiogenesis." Am J Pathol**169**(6): 2223-2235.

Bussolati, B., S. Bruno, C. Grange, U. Ferrando and G. Camussi (2008). "Identification of a tumor-initiating stem cell population in human renal carcinomas." FASEB J**22**(10): 3696-3705.

Cifola, I., C. Bianchi, E. Mangano, S. Bombelli, F. Frascati, E. Fasoli, S. Ferrero, V. Di Stefano, M. A. Zipeto, F. Magni, S. Signorini, C. Battaglia and R. A. Perego (2011). "Renal cell carcinoma primary cultures maintain genomic and phenotypic profile of parental tumor tissues." BMC Cancer**11**: 244.

Cohen, B., M. Shimizu, J. Izrailit, N. F. Ng, Y. Buchman, J. G. Pan, J. Dering and M. Reedijk (2010). "Cyclin D1 is a direct target of JAG1-mediated Notch signaling in breast cancer." Breast Cancer Res Treat**123**(1): 113-124.

Covello, K. L., J. Kehler, H. Yu, J. D. Gordan, A. M. Arsham, C. J. Hu, P. A. Labosky, M. C. Simon and B. Keith (2006). "HIF-2alpha regulates Oct-4: effects of hypoxia on stem cell function, embryonic development, and tumor growth." Genes Dev**20**(5): 557-570.

Dalerba, P., S. J. Dylla, I. K. Park, R. Liu, X. Wang, R. W. Cho, T. Hoey, A. Gurney, E. H. Huang, D. M. Simeone, A. A. Shelton, G. Parmiani, C. Castelli and M. F. Clarke (2007). "Phenotypic characterization of human colorectal cancer stem cells." Proc Natl Acad Sci U S A**104**(24): 10158-10163.

Dontu, G., W. M. Abdallah, J. M. Foley, K. W. Jackson, M. F. Clarke, M. J. Kawamura and M. S. Wicha (2003). "In vitro propagation and transcriptional profiling of human mammary stem/progenitor cells." Genes Dev**17**(10): 1253-1270.

Galeano, F., C. Rossetti, S. Tomaselli, L. Cifaldi, M. Lezzerini, M. Pezzullo, R. Boldrini, L. Massimi, C. M. Di Rocco, F. Locatelli and A. Gallo (2013). "ADAR2-editing activity inhibits glioblastoma growth through the modulation of the CDC14B/Skp2/p21/p27 axis." Oncogene**32**(8): 998-1009.

Gustafsson, M. V., X. Zheng, T. Pereira, K. Gradin, S. Jin, J. Lundkvist, J. L. Ruas, L. Poellinger, U. Lendahl and M. Bondesson (2005). "Hypoxia requires notch signaling to maintain the undifferentiated cell state." Dev Cell**9**(5): 617-628.

Heale, B. S., L. P. Keegan, L. McGurk, G. Michlewski, J. Brindle, C. M. Stanton, J. F. Caceres and M. A. O'Connell (2009). "Editing independent effects of ADARs on the miRNA/siRNA pathways." EMBO J**28**(20): 3145-3156.

Heale, B. S., L. P. Keegan, L. McGurk, G. Michlewski, J. Brindle, C. M. Stanton, J. F. Caceres and M. A. O'Connell (2009). "Editing independent effects of ADARs on the miRNA/siRNA pathways." EMBO J**28**(20): 3145-3156.

Hollingsworth, J. M., D. C. Miller, S. Daignault and B. K. Hollenbeck (2006). "Rising incidence of small renal masses: a need to reassess treatment effect." J Natl Cancer Inst**98**(18): 1331-1334.

Huang, B., Y. J. Huang, Z. J. Yao, X. Chen, S. J. Guo, X. P. Mao, D. H. Wang, J. X. Chen and S. P. Qiu (2013). "Cancer stem cell-like side population cells in clear cell renal cell carcinoma cell line 769P." PLoS One**8**(7): e68293.

Jiang, Q., L. A. Crews, C. L. Barrett, H. J. Chun, A. C. Court, J. M. Isquith, M. A.

Zipeto, D. J. Goff, M. Minden, A. Sadarangani, J. M. Rusert, K. H. Dao, S. R. Morris, L. S. Goldstein, M. A. Marra, K. A. Frazer and C. H. Jamieson (2013). "ADAR1 promotes malignant progenitor reprogramming in chronic myeloid leukemia." Proc Natl Acad Sci U S A**110**(3): 1041-1046.

Jiang, Y., W. Zhang, K. Kondo, J. M. Klco, T. B. St Martin, M. R. Dufault, S. L. Madden, W. G. Kaelin, Jr. and M. Nacht (2003). "Gene expression profiling in a renal cell carcinoma cell line: dissecting VHL and hypoxia-dependent pathways." Mol Cancer Res**1**(6): 453-462.

Kamakura, S., K. Oishi, T. Yoshimatsu, M. Nakafuku, N. Masuyama and Y. Gotoh (2004). "Hes binding to STAT3 mediates crosstalk between Notch and JAK-STAT signalling." Nat Cell Biol**6**(6): 547-554.

Kato, Y., A. Iwama, Y. Tadokoro, K. Shimoda, M. Minoguchi, S. Akira, M. Tanaka, A. Miyajima, T. Kitamura and H. Nakauchi (2005). "Selective activation of STAT5 unveils its role in stem cell self-renewal in normal and leukemic hematopoiesis." J Exp Med**202**(1): 169-179.

Korkaya, H. and M. S. Wicha (2007). "Selective targeting of cancer stem cells: a new concept in cancer therapeutics." BioDrugs**21**(5): 299-310.

Kovacs, G., M. Akhtar, B. J. Beckwith, P. Bugert, C. S. Cooper, B. Delahunt, J. N. Eble, S. Fleming, B. Ljungberg, L. J. Medeiros, H. Moch, V. E. Reuter, E. Ritz, G. Roos, D. Schmidt, J. R. Srigley, S. Storkel, E. van den Berg and B. Zbar (1997). "The Heidelberg classification of renal cell tumours." J Pathol**183**(2): 131-133.

Kovacs, G., M. Akhtar, B. J. Beckwith, P. Bugert, C. S. Cooper, B. Delahunt, J. N. Eble, S. Fleming, B. Ljungberg, L. J. Medeiros, H. Moch, V. E. Reuter, E. Ritz, G. Roos, D. Schmidt, J. R. Srigley, S. Storkel, E. van den Berg and B.

Zbar (1997). "The Heidelberg classification of renal cell tumours." J Pathol**183**(2): 131-133.

Liu, L., C. Gao, G. Chen, X. Li, J. Li, Q. Wan and Y. Xu (2013). "Notch Signaling Molecules Activate TGF- beta in Rat Mesangial Cells under High Glucose Conditions." J Diabetes Res**2013**: 979702.

Miele, L., Takebe N, Ivy P (2009). "The Cancer Stem Cell Hypothesis, Embryonic Signaling Pathways, and Therapeutics: Targeting and Elusive Concept."

Okuda, H., F. Xing, P. R. Pandey, S. Sharma, M. Watabe, S. K. Pai, Y. Y. Mo, M. Iiizumi-Gairani, S. Hirota, Y. Liu, K. Wu, R. Pochampally and K. Watabe (2013). "miR-7 suppresses brain metastasis of breast cancer stem-like cells by modulating KLF4." Cancer Res**73**(4): 1434-1444.

Paz, N., E. Y. Levanon, N. Amariglio, A. B. Heimberger, Z. Ram, S. Constantini, Z. S. Barbash, K. Adamsky, M. Safran, A. Hirschberg, M. Krupsky, I. Ben-Dov, S. Cazacu, T. Mikkelsen, C. Brodie, E. Eisenberg and G. Rechavi (2007). "Altered adenosine-to-inosine RNA editing in human cancer." Genome Res**17**(11): 1586-1595.

Perego, R. A., C. Bianchi, M. Corizzato, B. Eroini, B. Torsello, C. Valsecchi, A. Di Fonzo, N. Cordani, P. Favini, S. Ferrero, M. Pitto, C. Sarto, F. Magni, F. Rocco and P. Mocarelli (2005). "Primary cell cultures arising from normal kidney and renal cell carcinoma retain the proteomic profile of corresponding tissues." J Proteome Res**4**(5): 1503-1510.

Ponti, D., A. Costa, N. Zaffaroni, G. Pratesi, G. Petrangolini, D. Coradini, S. Pilotti, M. A. Pierotti and M. G. Daidone (2005). "Isolation and in vitro propagation of tumorigenic breast cancer cells with stem/progenitor cell

properties." Cancer Res**65**(13): 5506-5511.

Rangarajan, A., C. Talora, R. Okuyama, M. Nicolas, C. Mammucari, H. Oh, J. C. Aster, S. Krishna, D. Metzger, P. Chambon, L. Miele, M. Aguet, F. Radtke and G. P. Dotto (2001). "Notch signaling is a direct determinant of keratinocyte growth arrest and entry into differentiation." EMBO J**20**(13): 3427-3436.

Sakaue-Sawano A, K. H., Morimura T, Hanyu A, Hama H, Osawa H, Kashiwagi S, Fukami K, Miyata T, Miyoshi H, Imamura T, Ogawa M, Masai H, Miyawaki A (2007). "Visualizing Spatiotemporal Dynamics of Multicellular Cell-Cycle Progression." Cell**132**(3): 487-498.

Singh, S. K., C. Hawkins, I. D. Clarke, J. A. Squire, J. Bayani, T. Hide, R. M. Henkelman, M. D. Cusimano and P. B. Dirks (2004). "Identification of human brain tumour initiating cells." Nature**432**(7015): 396-401.

Viale, A., F. De Franco, A. Orleth, V. Cambiaghi, V. Giuliani, D. Bossi, C. Ronchini, S. Ronzoni, I. Muradore, S. Monestiroli, A. Gobbi, M. Alcalay, S. Minucci and P. G. Pelicci (2009). "Cell-cycle restriction limits DNA damage and maintains self-renewal of leukaemia stem cells." Nature**457**(7225): 51-56.

Xin, H., C. Zhang, A. Herrmann, Y. Du, R. Figlin and H. Yu (2009). "Sunitinib inhibition of Stat3 induces renal cell carcinoma tumor cell apoptosis and reduces immunosuppressive cells." Cancer Res**69**(6): 2506-2513.

Zhong, Y., K. Guan, S. Guo, C. Zhou, D. Wang, W. Ma, Y. Zhang, C. Li and S. Zhang (2010). "Spheres derived from the human SK-RC-42 renal cell carcinoma cell line are enriched in cancer stem cells." Cancer Lett**299**(2): 150-160.

Zhong, Y., K. Guan, S. Guo, C. Zhou, D. Wang, W. Ma, Y. Zhang, C. Li and S. Zhang (2010). "Spheres derived from the human SK-RC-42 renal cell carcinoma cell line are enriched in cancer stem cells." Cancer Lett**299**(2): 150-160.

Chapter 6

Summary, Conclusion and Future Perspectives

Summary

Cancer stem cells (CSC) are primary perpetrators driving disease progression, and are a major focus of current anti-cancer therapy development efforts. Renal cell carcinoma (RCC) accounts for 3.8 % of all malignancies in the adult and its incidency is annually increasing (Hollingsworth, 2006). As well as for other tumors, such as breast (Al Hajii, 2003) and colon cancer (Dalerba, 2007), CSCs, with their resistance to therapies and their tumor initiating ability may play a relevant role in the pathogenesis and prognosis of RCC. Although several studies have focused on the identification of CSC from RCC by exploiting different approaches (Bussolati, 2008: Addla, 2008, Zhong, 2010; Huang 2013) a definite marker for these cells is still lacking, thus suggesting the necessity to further investigate this field. During my PhD years, I focused on the identification of cells with stem properties within RCC by using the sphere-forming assay. This approach have already been described as an effective technique for the isolation of normal and cancer stem cells from various tissues, such as the brain (Reynolds, 1992), breast (Dontu, 2003; Pece, 2010), pancreas and prostate (Lawson, 2007). Moreover, during my PhD I have been involved in a project aimed to the isolation and characterization of adult stem cells from normal kidney, as described in chapter 2. This work has brought to a publication in 2013 (Bombelli, 2013), describing the identification, thanks to the combination of sphere forming assay, PKH assay and surface marker expression a more defined and homogeneous resident adult stem cell population in the kidney. This study set the bases for adapting the same assay to RCC human tissues, allowing optimizing the method and the steps for the identification of a stem cell population

by sphere forming assay in RCC too. Zhong and colleagues have already exploited this assay for the isolation of CSCs from a human RCC cell line, however we were the first group to use this method for human RCC tissues. The identification of markers that distinguish CSC from the bulk tumor might represent a crucial step toward the development of therapies based on antibodies able to target only the CSC population, as demonstrated by pancreatic cancer (Cioffi, 2012). However, surface markers can fall victim of their own promiscuity, thus suggesting the necessity to identify other features that distinguish CSC from the bulk tumor, such as pathways that make them acquire stemness hallmarks and therapeutic resistance. In order to identify differences between the bulk tumor and CSC population it is crucial to be able to study and characterize both the populations. During my PhD I had the opportunity to be involved in the establishment and molecular characterization of primary cultures from RCC, as described in chapter 3 (Cifola, 2011). This has not only allowed me to acquire technical skills, but has mainly provided a solid, well characterized and established model to use for the comparison between bulk tumor and stem cells within RCC, for both screening for surface markers and for identifying molecular regulator of self-renewal that might be targeted by therapies. The lack of studies on the characterization of molecular pathways responsible for CSCs maintenance and self-renewal in RCC brought us to refer to other models, where these pathways have extensively been characterized, such as for example Chronic Myeloid Leukemia Stem Cells. I spent the last year of my PhD in a laboratory highly specialized in cancer stem cell studies at Sanford Consortium for Regenerative Medicine, in San Diego (CA). I collaborated in the study on Chronic

Myeloid leukemia stem cells that represent a paradigm for distinguishing the cellular framework of genetic and epigenetic events involved in the CSCs production. This work, described in chapter 5, allowed the identification of a new role for RNA editing enzyme in the regulation of self-renewal in leukemia stem cells, most likely by regulation of microRNA. This suggested to evaluate this pathway in our model, in order to define whether it could be involved in the regulation of self-renewal in solid tumor as well.

The theoretical and technical knowledge acquired during my PhD led to the realization of my project, described in chapter 5, aimed towards the molecular and functional characterization of cells with stem properties, isolated by sphere forming assay, from human RCC tissues and cell line. We were able to obtain clonal tumor spheres from both human RCC cell line and tissues. These spheres were enriched in cells showing a stem molecular profile, as evidenced by the upregulation of genes involved in the regulation of self-renewal and pluripotency in the spheres compared to their corresponding bulk tumor cultures. Although we were not able to identify any surface marker able to distinguish the spheres from the bulk tumor, we were instead able to identify populations with different self-renewal capability within the spheres. Moreover, we showed that spheres enriched for both the already demonstrated putative CSC population expressing CD105 (Bussolati, 2008) and the sustaining CD133 progenitor cells (Bussolati, 2006) thus suggesting that it is able to re-create the niche necessary for CSC maintenance and tumor growth. Moreover, the use of PKH assay allowed us to identify, other than the $CD105^{+}$ population, also a $CD133^{+}CD105^{+}$ population that might have tumorigenic potential as well.

Conclusion and application to translational medicine

Cancer is the second leading cause of death for individuals younger than 85 (http://www.nimh.nih.gov/statistics/3AGES185.shtml) and thus represents the most life-threatening and challenging medical problem. While cancers are diverse in phenotype, they share essential functional properties frequently ascribed to stem cells such as the capacity to replicate themselves, differentiate into a number of lineages, survive and self-renew. For this reason, novel stem cell-based diagnostic and therapeutic strategies able to predict and prevent cancer progression and relapse represent compelling unmet medical needs (Damm, 2012). Identification and study of cancer stem cells have a clinical relevance when considering some of their features, such as resistance to conventional therapies. It has indeed been shown that eradication of non-cancer stem cell population might initially decrease tumor burden, but this treatment will have a long-term failure because of the inability of eradicating the CSC population, that might instead be selected by the treatment itself. Moreover, the CSC burden at the time of treatment is likely to predict clinical response and overall survival. Data from different tumors, such as CML, breast cancer (Mustjoki, 2013; Pece, 2010) suggest a correlation between the CSC burden and the prognosis. Starting from these observations, it becomes clear the necessity to further investigate the CSC field, in order to identify molecular prognostic marker as well as mechanism responsible for CSC phenotype that might be targeted by therapies. Our study on RCC brought to the identification of molecular pathways that distinguish cells within the spheres, most likely enriched in stem cells, from the bulk tumor. A

further functional characterization of these pathways and of their role in the regulation of self-renewal, might lead to the identification of new cancer stem cells targeted therapies that could be employed in the association of conventional chemotherapeutics. Moreover, our study identified two different subpopulations within the PKH^{high} self-renewing population that might equally represent putative candidate for tumorigenic cells. Among them one co-express both markers of the putative renal CSC and markers of renal progenitors that could be responsible for sustaining the tumor growth. These data, together with the finding that tumors with different grading show a different distribution of cells able to self-renew among the different PKH populations, highlight the necessity to further investigate the role of each population, in combination with the PKH assay, in order to define the population to target. Identifying RCC cancer stem cells and the molecular mechanisms driving their self-renewal and resistance to therapy, will allow to dramatically improve the outcome of this cancer by developing stem-cell based therapies.

Future perspectives

To better define the CSC population within RCC it becomes crucial to demonstrate their tumorigenicity by repeating the xenograft assay not only injecting the whole population deriving from the spheres, but also the cell populations identified by the combination of the PKH assay and the expression of surface markers.

The identification of the markers defining CSC in RCC will be crucial to evaluate their prognostic potential. It will indeed be neat to evaluate whether tumors with different grading, already demonstrated to generate spheres composed by cells with different self-renewing

abilities, present a diverse cellular composition, based on the expression of specific markers that could help to predict the outcome of the disease.

A functional characterization of the role of the genes resulted to be differentially expressed in the spheres compared to the bulk tumor will allow to identify the molecular targets of new therapies. Knockdown experiments, as well as inhibition with small molecules, will allow us to define not only their role in the regulation of self-renewal, but also to better clarify the eventual existence of cross-talk between different pathways.

A further characterization of miRNA expression profile in spheres from RCC will allow identifying new prognostic biomarkers. Moreover, we will evaluate any eventual correlations between increased RNA editing and microRNA expression, in order to evaluate whether the edited-miRNA expression profile might represent a biomarker of RCC CSCs.

Finally, the development of a bicistronic FUCCI vector will provide us a powerful tool for monitoring cell cycle changes and to test the effect of new molecules on the cell cycle of RCC CSCs in order to identify new therapeutic strategies against RCC.

References

Addla, S. K., M. D. Brown, C. A. Hart, V. A. Ramani and N. W. Clarke (2008). "Characterization of the Hoechst 33342 side population from normal and malignant human renal epithelial cells." Am J Physiol Renal Physiol**295**(3): F680-687.

Bombelli, S., M. A. Zipeto, B. Torsello, G. Bovo, V. Di Stefano, C. Bugarin, P. Zordan, P. Vigano, G. Cattoretti, G. Strada, C. Bianchi and R. A. Perego (2013). "PKH(high) cells within clonal human nephrospheres provide a purified adult renal stem cell population." Stem Cell Res**11**(3): 1163-1177.

Bussolati, B., B. Assenzio, M. C. Deregibus and G. Camussi (2006). "The proangiogenic phenotype of human tumor-derived endothelial cells depends on thrombospondin-1 downregulation via phosphatidylinositol 3-kinase/Akt pathway." J Mol Med (Berl)**84**(10): 852-863.

Cioffi, M., J. Dorado, P. A. Baeuerle and C. Heeschen (2012). "EpCAM/CD3-Bispecific T-cell engaging antibody MT110 eliminates primary human pancreatic cancer stem cells." Clin Cancer Res**18**(2): 465-474.

Damm, F., F. Nguyen-Khac, M. Fontenay and O. A. Bernard (2012). "Spliceosome and other novel mutations in chronic lymphocytic leukemia and myeloid malignancies." Leukemia**26**(9): 2027-2031.

Dontu, G., W. M. Abdallah, J. M. Foley, K. W. Jackson, M. F. Clarke, M. J. Kawamura and M. S. Wicha (2003). "In vitro propagation and transcriptional profiling of human mammary stem/progenitor cells."

Genes Dev**17**(10): 1253-1270.

Hollingsworth, J. M., D. C. Miller, S. Daignault and B. K. Hollenbeck (2006). "Rising incidence of small renal masses: a need to reassess treatment effect." J Natl Cancer Inst**98**(18): 1331-1334.

Huang, B., Y. J. Huang, Z. J. Yao, X. Chen, S. J. Guo, X. P. Mao, D. H. Wang, J. X. Chen and S. P. Qiu (2013). "Cancer stem cell-like side population cells in clear cell renal cell carcinoma cell line 769P." PLoS One**8**(7): e68293.

Lawson, D. A., L. Xin, R. U. Lukacs, D. Cheng and O. N. Witte (2007). "Isolation and functional characterization of murine prostate stem cells." Proc Natl Acad Sci U S A**104**(1): 181-186.

Mustjoki, S., J. Richter, G. Barbany, H. Ehrencrona, T. Fioretos, T. Gedde-Dahl, B. T. Gjertsen, R. Hovland, S. Hernesniemi, D. Josefsen, P. Koskenvesa, I. Dybedal, B. Markevarn, T. Olofsson, U. Olsson-Stromberg, K. Rapakko, S. Thunberg, L. Stenke, B. Simonsson, K. Porkka, H. Hjorth-Hansen and C. M. L. S. G. Nordic (2013). "Impact of malignant stem cell burden on therapy outcome in newly diagnosed chronic myeloid leukemia patients." Leukemia**27**(7): 1520-1526.

Pece, S., D. Tosoni, S. Confalonieri, G. Mazzarol, M. Vecchi, S. Ronzoni, L. Bernard, G. Viale, P. G. Pelicci and P. P. Di Fiore (2010). "Biological and molecular heterogeneity of breast cancers correlates with their cancer stem cell content." Cell**140**(1): 62-73.

Reynolds, B. A. and S. Weiss (1992). "Generation of neurons and astrocytes from isolated cells of the adult mammalian central nervous system." Science**255**(5052): 1707-1710.

Zhong, Y., K. Guan, S. Guo, C. Zhou, D. Wang, W. Ma, Y. Zhang, C. Li and S. Zhang (2010). "Spheres derived from the human SK-RC-42 renal cell carcinoma cell line are enriched in cancer stem cells." Cancer Lett**299**(2): 150-160.

Publications

Cifola, I., C. Bianchi, E. Mangano, S. Bombelli, F. Frascati, E. Fasoli, S. Ferrero, V. Di Stefano, M. A. **Zipeto**, F. Magni, S. Signorini, C. Battaglia and R. A. Perego (2011). "Renal cell carcinoma primary cultures maintain genomic and phenotypic profile of parental tumor tissues." BMC Cancer 11: 244.

Bianchi, C., B. Torsello, V. Di Stefano, M. A. **Zipeto**, R. Facchetti, S. Bombelli and R. A. Perego (2013). "One isoform of Arg/Abl2 tyrosine kinase is nuclear and the other seven cytosolic isoforms differently modulate cell morphology, motility and the cytoskeleton." Exp Cell Res 319(13): 2091-2102.

Bombelli, S., M. A. **Zipeto**, B. Torsello, G. Bovo, V. Di Stefano, C. Bugarin, P. Zordan, P. Vigano, G. Cattoretti, G. Strada, C. Bianchi and R. A. Perego (2013). "PKH(high) cells within clonal human nephrospheres provide a purified adult renal stem cell population." Stem Cell Res 11(3): 1163-1177.

Jiang, Q., L. A. Crews, C. L. Barrett, H. J. Chun, A. C. Court, J. M. Isquith, M. A. **Zipeto**, D. J. Goff, M. Minden, A. Sadarangani, J. M. Rusert, K. H. Dao, S. R. Morris, L. S. Goldstein, M. A. Marra, K. A. Frazer and C. H. Jamieson (2013). "ADAR1 promotes malignant progenitor reprogramming in chronic myeloid leukemia." Proc Natl Acad Sci U S A 110(3): 1041-1046.

Conference communications

BOMBELLI S, BIANCHI C, TORSELLO B, DI STEFANO V, **ZIPETO M.A**, PEREGO R.A, BOVO G, CATTORETTI G, VIGANO' P, STRADA G (2010). *"Identification and characterization of cells with stem/progenitor porperties in normal kidney and renal cell carcinoma."*83° National Congress of Italian Society of Urology, October 18-20, Milano, Italy. Abstract C5

BOMBELLI S, BIANCHI C, TORSELLO B, DI STEFANO V, **ZIPETO M.A**, BOVO G, CATTORETTI G, VIGANO' P, STRADA G, PEREGO R.A (2010*)* *" Identification and characterization of cells with stem/progenitor properties in normal kidney and Renal Cell Carcinoma*." Epigenetics and Stem Cells Conference. August 25-27, Copenaghen, Denmark. P 72

BOMBELLI S, BIANCHI C, TORSELLO B, DI STEFANO V, **ZIPETO M.A**, BOVO G, CATTORETTI G, VIGANO' P, STRADA G, PEREGO R. (2011) *"Identification and Characterization of cells with stem/progenitor properties in normal kidney".* 23rd ERCSG meeting, March 24-27 Desenzano del Garda, Italy

TORSELLO B, BIANCHI C, BOMBELLI S, DI STEFANO V, **ZIPETO M.A**, BOVO G, STRADA G, PEREGO R (2011)

"Molecular and functional characterization of Epithelial-Mesenchymal Transition induced in primary cultures of human tubular cells with high glucose concentration treatment". 23rd ERCSG meeting, March 24-27 Desenzano del Garda, Italy

BOMBELLI S, **ZIPETO M.A**, BIANCHI C, TORSELLO B, DI STEFANO V, MINNITI S, BUSCONE S, BOVO G, CATTORETTI G, VIGANO' P, STRADA G, PEREGO R. (2011)
"Molecular characterization of nephrospheres from normal kidney and renal cell carcinoma." 84° National Congress of Italian Society of Urology, October 23-26, Rome, Italy. Abstract P230

BOMBELLI S, **ZIPETO M.A**, BIANCHI C, TORSELLO B, DI STEFANO V, BOVO G, CATTORETTI G, VIGANO' P, STRADA G, PEREGO R. (2011)
"Identification and characterization of Cells with stem/progenitor properties in normal kidney and renal cell carcinoma." SIP YOUNG SCIENTISTS, October 24-25, Bologna, Italy.

BOMBELLI S, BIANCHI C, TORSELLO B, DI STEFANO V, **ZIPETO M.A**, BOVO G, VIGANO' P, STRADA G, CATTORETTI G, PEREGO R (2012)
"Nephrospheres as a model for the study of kidney development. "European Renal Cell Study Group March 22-25, Doorwerth (NL)

TORSELLO B, BIANCHI C, BOMBELLI S, DI STEFANO V, **ZIPETO M.A**, BOVO G, STRADA G, CATTORETTI C, PEREGO R (2012)

*"In human tubular primary cell cultures treated with high level of glucose there are cytoskeletal changes and the production of TGF-β1 related to Arg expression pattern."*European Renal Cell Study Group March 22-25, Doorwerth (NL)

ZIPETO M.A, BOMBELLI S, BIANCHI C, TORSELLO B, DI STEFANO V, BOVO G, VIGANO' P, STRADA G, CATTORETTI G, PEREGO R (2012)
"*Spheres from Human Renal Cell Carcinoma express pluripotency genes and contain different cell populations capable of self-renewal."*UniSR- CRG-DIMET Joint PhD Meeting, June 6-8, Presezzo, Italy. Abstract 47

ZIPETO M.A, BOMBELLI S, BIANCHI C, TORSELLO B, DI STEFANO V, VIGANO' P, BOVO G, STRADA G, CATTORETTI G, PEREGO R. (2012)
"Overexpression of pluripotency genes and presence of different cell populations with stem properties in Spheres from Human Renal Cell Carcinoma". 85° National Congress of Italian Society of Urology, October 21-24, Venice, Italy. Abstract P108

TORSELLO B, BIANCHI C, DI STEFANO V, BOMBELLI S, ZIPETO M.A., BOVO G, STRADA G, CATTORETTI G, PEREGO R. (2013)
"Molecular and functional characterization of human renal cortex and renal cell carcinoma primary cultures." 25th ERCSG meeting, Oxford, UK, 21st-24th March

JIANG Q, **ZIPETO M.A**, CREWS L, BARRETT C, CHUN H, COURT A, GOFF D, MINDEN M, SADARANGANI A, RUSERT J, DAO K, MORRIS S, GOLDSTEIN L, MARRA M, FRAZER K, JAMIESON C (2013)

"*The RNA Editase ADAR1 Promotes Malignant Progenitor Reprogramming in Chronic Myeloid Leukemia."*ESH - iCMLf International Conference on CML - Biology and Therapy. September 26-29, Estoril, Portugal

JIANG Q, **ZIPETO M**, COURT A, MORRIS S, CREWS L, JAMIESON C (2013)

"RNA Editing Enzyme Induces Accelerated Cell Cycle in Normal Hematopoietic. Stem Cells." Meeting on the Mesa. October 14-16, La Jolla, CA and CSHA/ISSCR Join Meeting On Stem Cells in Science and Medicine, October 14-17,Suzhou, China

BALAIN L, CREWS L, **ZIPETO M.A,** KULIDJIAN A, BALL E, BURKART M, JAMIESON C (2013).

*"A Highly selective SF_3B1-Targeted Splicing Inhibitor reduces human CD34+ Cell Survival and Self-Renewal In Acute Myeloid Leukemia." 55th*American Society of Hematology Annual Meeting, December 7-10, New Orleans (LA)

ZIPETO M.A., JIANG Q, CREWS L, JAMIESON C (2014)

"ADAR1-mediated microRNA regulation and blast crisis leukemia stem cell generation in chronic myeloid leukemia." AACR Annual meeting, San Diego (CA) Accepted for poster session

Congress proceedings published in peer-reviewed journals

BOMBELLI S, BIANCHI C, TORSELLO B, DI STEFANO V, **ZIPETO M.A**, BOVO G, CATTORETTI G, VIGANO' P, STRADA G, PEREGO R.A (2010). *"Identification and characterization of Cells with Stem/Progenitor Properties in Normal Kidney and Renal Cell Carcinoma."* XXX National Congress of Italian Society of Pathology, October 14-17, Salerno, Italy. Am J Pathol 177(Suppl):S30 Abstract SRC 01

BIANCHI C, TORSELLO B, BOMBELLI S, DI STEFANO V, **ZIPETO M.A,** BOVO G, STRADA *G, PEREGO R.A (2010).*
"Phenotypic and Molecular Study of Epithelial-Mesenchymal Transition Induced in Primary Cultures of Human Tubular Cells by High Glucose Concentration Treatment." XXX National Congress of Italian Society of Pathology, October 14-17, Salerno, Italy. Am J Pathol 177 (Suppl): S21 Abstract NBD 01

DI STEFANO V, BIANCHI C, BOMBELLI S, **ZIPETO M.A**, TORSELLO B, BATTAGLIA C, CIFOLA I, ZANETTI G, PEREGO R.A (2010).

"Expression Studies of Lysyl Oxidase and S100A4 Proteins in Normal Cortex and Renal Cell Carcinoma Primary Cultures." XXX National Congress of Italian Society of Pathology, October 14-17, Salerno, Italy. Am J Pathol 177 (Suppl):S25 Abstract NBO 12

TORSELLO B, BIANCHI C, DI STEFANO V, BOMBELLI S, **ZIPETO M.A**, PEREGO R.A (2010)
"*Cellular Localization and Cytoskeletric Effects of Eight Different Arg Isoforms Transfected in COS-7 Cells*." XXX National Congress of Italian Society of Pathology. October 14-17, Salerno, Italy. Am J Pathol 177 (Suppl):S12 Abstract CSA 05

TORSELLO B., BOMBELLI S., DI STEFANO V., MINNITI S., BUSCONE S., **ZIPETO M. A**., BOVO G., CATTORETTI G., PEREGO R., BIANCHI C. (2012)
"Study of molecular and functional effects induced in tubular primary cell cultures by high glucose treatment". 1st Joint Meeting of Pathology and Laboratory Diagnostics, Udine 12-15 Settembre 2012. Am J Pathol , 181 (Suppl): S15 Abstract KD1.

DI STEFANO V., BUSCONE S., BOMBELLI S., MINNITI S., TORSELLO B., **ZIPETO M.A**., FERRERO S., ALBO G., PEREGO R., BIANCHI C. (2012)
*"Molecular and functional characterization of annexin A3 in human normal cortex and renal cell carcinoma primary cultures".*1st Joint Meeting of Pathology and Laboratory Diagnostics, Udine 12-15 Settembre 2012. Am J Pathol , 181 (Suppl): S20 Abstract NBM1.

BOMBELLI S., **ZIPETO M.A**., BIANCHI C., TORSELLO B., DI STEFANO V., BOVO G., VIGANÒ P., STRADA G., CATTORETTI G., PEREGO R.(2012) *"Stem-like cells in nephrospheres tresent multilineage differentiative abilities"*.1st Joint Meeting of Pathology and Laboratory Diagnostics, Udine 12-15 Settembre 2012. Am J Pathol, 181 (Suppl): S29 Abstract SC2.

BOMBELLI S., **ZIPETO M.A.,** BIANCHI C., TORSELLO B., DI STEFANO V., VIGANÒ P., BOVO G., CATTORETTI G., STRADA G., PEREGO R. (2013) *"Cancer stem cell characteristics may be correlated to the renal cell carcinoma intratumoral heterogeneity"*.European Urol Suppl , 12:e769.